INFORMATION TO USERS

This manuscript has been reproduced from the microfilm master. UMI films the text directly from the original or copy submitted. Thus, some thesis and dissertation copies are in typewriter face, while others may be from any type of computer printer.

The quality of this reproduction is dependent upon the quality of the copy submitted. Broken or indistinct print, colored or poor quality illustrations and photographs, print bleedthrough, substandard margins, and improper alignment can adversely affect reproduction.

In the unlikely event that the author did not send UMI a complete manuscript and there are missing pages, these will be noted. Also, if unauthorized copyright material had to be removed, a note will indicate the deletion.

Oversize materials (e.g., maps, drawings, charts) are reproduced by sectioning the original, beginning at the upper left-hand corner and continuing from left to right in equal sections with small overlaps.

Photographs included in the original manuscript have been reproduced xerographically in this copy. Higher quality 6" x 9" black and white photographic prints are available for any photographs or illustrations appearing in this copy for an additional charge. Contact UMI directly to order.

Bell & Howell Information and Learning
300 North Zeeb Road, Ann Arbor, MI 48106-1346 USA
800-521-0600

STRAIN-DEPENDENT PHENOTYPES OF p130- AND p107-DEFICIENT MICE

By

JENNIFER E. LECOUTER, HONS. B.SC.

A Thesis
Submitted to the School of Graduate Studies
In Partial Fulfillment of the Requirements
for the Degree
Doctor of Philosophy

McMaster University

STRAIN-DEPENDENT PHENOTYPES OF p130- AND p107-DEFICIENT MICE

Doctorate of Philosophy (1998) McMaster University

(Medical Sciences) Hamilton, Ontario

TITLE: Strain-dependent phenotype of p130- and p107-deficient mice

AUTHOR: Jennifer E. LeCouter, Hons. B.Sc. (University of Waterloo)

SUPERVISOR: Dr. Michael A. Rudnicki

NUMBER OF PAGES: xv, 243

ABSTRACT

For the development of many cell types, terminal differentiation and continued cell cycle progression are incompatible processes. Rb, p107 and p130 comprise a gene family encoding transcriptional regulators that act within a complex network to control exit from, and progression through the cell cycle. The distinct requirements for p130 and p107 were assessed in vivo using homologous recombination in embryonic stem (ES) cells. p130 expression is ubiquitous, although the level of expression varies between tissues. As well, its induction during neuronal cell differentiation is consistent with p130 function accompanying terminal differentiation. p130 deficiency was incompatible with embryo survival in the hybrid 129Sv;Balb/c genetic background. The mutant embryos died between E11-13 and exhibited striking delays in growth and development at 10.5 dpc with specific deficits in neurogenesis, somitogenesis and cardiogenesis. p130 appears to be required for the maintenance and survival of specific cell types, most notably neuronal cells. The data indicate that the p130 gene is essential for normal development, but in a strain-specific manner. On a hybrid 129Sv;C57Bl/6 background, the p130 mutants exhibited no phenotype. The p107 mutants were viable and fertile, indicating that p107 function was adequately compensated by other proteins during development, potentially Rb and p130. The p107-/- mice did however exhibit a postnatal growth deficit and a diathetic myeloid proliferative disorder. The accelerated proliferation and cell-cycle kinetics of p107-/- EF indicated that p107 functions, in part, to regulate cyclin expression and cell cycle progression. p107-/- myoblasts also exhibited accelerated proliferation and aberrant in vitro differentiation. Lastly, the p107-/- phenotype was also dependent on the genetic strain, indicating the presence of modifying genes. The mice produced in these studies can be assessed for genes that modify the phenotypes in these different strains, potentially revealing epistatic relations to p107 and p130. Although both striking and

subtle cell-specific phenotypes were exhibited, these experiments strongly reconfirm that functional overlap and compensation exist within the Rb family. The overlapping expression patterns and apparent functional relations indicate that p130, p107 and Rb regulate transitions in a concerted manner during cell proliferation, and cell cycle exit and entrance.

Acknowledgments

I want to thank foremost Dr. Michael Rudnicki, my advisor, for his support and constructive criticism through the years. It's an honour being the first Ph.D. to graduate from the Rudnicki lab. Also, thank you to past and present members of the lab; in particular, Ying for her considerate manner and professionalism, Rod Hardy and Dr. Lynn Megeney for their support and valuable contributions to my work as well as Linda May and Dr. Boris Kablar. I must acknowledge my husband, David Dankort, for his (in)constant support, access to buffers I did not care to make, and ruthless criticism although it hardly compares to that of the Cell Cycle Mafia. Finally, thank you to my darling daughter Ainsley for providing the best diversion imaginable during my final two years in Hamilton. She's enriched my life; and its O.K. if she decides to go into science.

Contributions By Others

Preface to Results Prepared for Publication

The results presented in chapters 3, 4, and jointly 5 and 6 were prepared and submitted for publication (Oncogene, 1996, 12:1433-1440; Development, 1998, 125:4669-4679; Molecular and Cellular Biology, 1998, 18:7455-5465). I performed the majority of the work and experiments described in these chapters, prepared the data for publications and wrote first drafts and at times incorporated necessary revisions. Considerable advice and criticism, especially with regards to organization of results was given by my supervisor, Dr. M.A. Rudnicki. He also made a strong contribution to the final manuscripts. Other authors were included for their very valuable contributions of *p107* heterozygous mutant mice (Rod Hardy); the human p130 cDNA (Peter Whyte); technical assistance with regard to animal handling; sectioning and some staining of histological samples (Chuyan Ying and Linda May); excellent assistance in interpreting histology (Dr. Boris Kablar) and demonstrating methods (Linda May, Dr. Boris Kablar and Dr. Lynn Megeney).

TABLE OF CONTENTS

Title Page	ii
Abstract	iii
Acknowledgments	v
Contributions By Others	vi
Table of Contents	vii
List of Figures	xi
List of Tables	xiv
List of Used Abbreviations	xv
References	213

CHAPTER 1 Introduction

1.1 Overview 1

1.2 The cell cycle 2

1.3 Rb, p107 and p130 in Cell Cycle Control 6

1.4 Rb, p107 and p130 during embryogenesis 24

1.5 Roles for the Rb proteins during skeletal myogenesis 32

1.6 Gene targeting in ES cells and mice 39

1.7 Summary of intent 43

CHAPTER 2 Materials and methods

2.1 Bacteria and DNA 45

2.2 Cell culture 48

2.3 Analysis of gene expression 50

2.4 Embryo and animal manipulations 53

CHAPTER 3 Cloning and Characterization of the Mouse p130 mRNA

3.1 Introduction 55

3.2 Results 56

3.2.i Cloning of the mouse p130 cDNA 56

3.2.ii Northern analysis of p130 expression during P19 differentiation and in adult mouse tissues. 58

3.2.iii Overexpression of mouse p130 66

3.3 Discussion 73

CHAPTER 4 Strain-Dependent Embryonic Lethality in Mice Lacking p130

4.1 Introduction 76

4.2 Results 78

4.2.i Generation of the p130 null allele 78

4.2.ii The engineered mutation generates a null allele 78

4.2.iii Embryos lacking p130 display arrested growth 85

4.2.iv The p130 mutant heart 86

4.2.v Impaired neurogenesis and myogenesis in $p130^{-/-}$ embryos 93

4.2.vi Analysis of apoptosis 97

4.2.vii Analysis of in vivo proliferation 100

4.2.viii The p130 mutant phenotype is strain-dependent 105

4.3 Discussion 106

CHAPTER 5 Strain-Dependent Postnatal Growth Deficiency and Myeloid Hyperplasia in Mice Lacking p107

5.1 Introduction 113

5.2 Results 115

5.2.i p107 gene-targeting generates a null allele. 115

5.2.ii Postnatal growth deficit 123

5.2.iii p107 and Rb compound mutant embryos 124

5.2.iv Diathetic myeloid proliferative disorder in $p107^{-/-}$ mice. 125

5.2.v Perturbed architecture of the $p107^{-/-}$ mammary gland. 128

5.2.vi The p107 mutant phenotype is strain-dependent. 129

5.3 Discussion 152

CHAPTER 6 Growth and Cell-Cycle Kinetics of p107$^{-/-}$ Embryonic Fibroblasts

6.1 Introduction 156

6.2 Results 158

6.2.i Cell growth 158

6.2.ii Cyclin induction following synchronization 159

6.3 Discussion 170

CHAPTER 7 Enhanced Proliferation, Regeneration and Perturbed Differentiation of p107$^{-/-}$ Skeletal Myoblasts.

7.1 Introduction 172

7.2 Results 175

7.2.i Enhanced regeneration in p107$^{-/-}$ skeletal muscle 175

7.2.ii Characterization of p107$^{-/-}$ myoblast cultures 175

7.2.iii In vitro differentiation 178

7.3 Discussion 197

CHAPTER 8 Summary and Conclusions

8.1 Specific and overlapping roles for p130 and p107 in growth and development. 200

8.1.i Cell-type specific requirements 201

8.1.ii Functional compensation and overlap 202

8.2 Strain-dependence and modifier loci 205

8.2.i Mapping modifier genes 208

CHAPTER 9 References 213

List Of Figures

CHAPTER 1

Figure 1.1 The Cell Cycle 4

Figure 1.2 Rb family member contain conserved regions 10

CHAPTER 2 No Figures

CHAPTER 3

Figure 3.1 Mouse p130 cDNA sequence. 59

Figure 3.2 Comparison of mouse and human p130 amino acid sequences. 61

Figure 3.3 The cloned p130 cDNA does not represent the full-length mouse sequence. 63

Figure 3.4 Northern and immunoblot analysis of p130 expression during RA-induced P19 cell differentiation. 67

Figure 3.5 Northern blot analysis of p130 mRNA expression in a panel of adult tissues. 69

Figure 3.6 Expression of mouse p130 suppresses growth of P19 EC cells. 71

CHAPTER 4

Figure 4.1 Targeted disruption of the p130 gene. 80

Figure 4.2 The targeted mutation generates a null allele 82

Figure 4.3 Embryonic growth deficiency in the absence of p130 is strain-dependent 87

Figure 4.4 Normal placental cytomorphology and absence of apoptosis in p130-deficient placentas 89

Figure 4.5 Delayed cardiogenesis in $p130^{-/-}$ embryos. 91

Figure 4.6 Deficient neurogenesis and associated apoptosis in E10.5 $p130^{-/-}$ embryos 94

Figure 4.7 Deficient skeletal myogenesis and apoptosis in E10.5 $p130^{-/-}$ embryos 98

Figure 4.8 Increased apoptosis and poor differentiation of head neural structures in the absence of p130 101

CHAPTER 5

Figure 5.1 Targeted disruption of the p107 gene in ES cells and mice. 117

Figure 5.2 p107 gene-targeting generates a null mutation. 119

Figure 5.3 Expression of Rb-family members in p107-deficient mice 121

Figure 5.4 Severe postnatal growth deficiency in $p107^{-/-}$ mice 134

Figure 5.5 Sites of infection in $p107^{-/-}$ mice 136

Figure 5.6 $p107^{-/-}$ thymus contains a higher proportion of immature thymocytes 138

Figure 5.7 Myeloid hyperplasia in the bone marrow of $p107^{-/-}$ mice 141

Figure 5.8 Extramedullary hematopoiesis in $p107^{-/-}$ spleen and liver 143

Figure 5.9 Unusual sites of myeloid proliferation 145

Figure 5.10 Perturbed architecture of $p107^{-/-}$ virgin mammary gland 148

Figure 5.11 Targeting strategy for p107 conditional mutant allele 150

CHAPTER 6

Figure 6.1 Two-fold acceleration in cell-cycle kinetics in $p107^{-/-}$ fibroblasts 161

Figure 6.2 Flow cytometric analysis revealed no difference in the cell-cycle profile 163

Figure 6.3 Wildtype and $p107^{-/-}$ cultures contain an equivalent proportion of cycling cells 165

Figure 6.4 Immunoblot analysis of cyclin expression in $p107^{-/-}$ fibroblasts 167

Figure 6.5 Summary of cyclin induction in EF induced to reenter the cell cycle 169

CHAPTER 7

Figure 7.1 In vivo regeneration is enhanced in $p107^{-/-}$ skeletal muscle 182

Figure 7.2 Increased numbers of desmin-positive cells from $p107^{-/-}$ muscle 185

Figure 7.3 Two-fold acceleration in cell-cycle kinetics in $p107^{-/-}$ myoblasts 187

Figure 7.4 In vitro differentiation deficit in $p107^{-/-}$ myoblast cultures 189

Figure 7.5 Northern analysis of muscle actin isoforms 191

Figure 7.6 Northern analysis of secondary myogenic regulatory factors 193

Figure 7.7 Analysis of the induction of cdk inhibitor p21 and Rb 195

CHAPTER 8

Figure 8.1 Schematic representation of the chromosome 2 microsatellite linkage map. 211

CHAPTER 9 No Figures

List Of Tables

CHAPTER 1 No Tables

CHAPTER 2 No Tables

CHAPTER 3 No Tables

CHAPTER 4

Table 4.1 Viability of embryos derived from $p130^{+/-}$ interbreeding. 79

Table 4.2 Genetic background specifies the penetrance of the $p130^{-/-}$ phenotype. 84

Table 4.3 Variable percentages of PCNA-positive nuclei in wildtype versus $p130^{-/-}$ embryonic tissues at 10.5dpc. 104

CHAPTER 5

Table 5.1 The genetic background specifies the penetrance of the $p107^{-/-}$ phenotype. 132

Table 5.2 Reduced growth of p107-deficient micea. 133

Table 5.3 Peripheral blood cell counts in wildtype versus $p107^{-/-}$ mice. 140

Table 5.4 Granulocyte and macrophage colony-forming units from femurs and spleens of $p107^{-/-}$ and wildtype mice 147

CHAPTER 6 No Tables

CHAPTER 7

Table 7.1 $p107^{-/-}$ muscle cultures contain elevated numbers of myogenic cells 147

CHAPTER 8 No Tables

CHAPTER 9 No Tables

List of Used Abbreviations

aa	amino acid
bp	base pair
cdk	cyclin dependent kinase
cDNA	complementary DNA
CFU-GM	colony-forming unit /granulocyte, macrophage
dpc	days *post-coitum*
DMEM	Dulbecco's modified Eagle medium
DNA	deoxyribonucleic acid
EC	embyonal carcinoma cell line
ECL	enhanced chemiluminescence
EF	embryonic fibroblast cells
EMH	extramedullary hematopoiesis
ES	embryonic stem cell line
G418	Geneticin (neomycin) (GIBCO/BRL)
HAT	histone acetyl transferase
HDAC	histone deacetylase complex
HRP	horse radish peroxidase
kb	kilobase
kD	kilodalton
MRF	muscle regulatory factor
mRNA	messenger RNA
nt	nucleotide
PBS	phosphate buffered saline
PGK	phosphoglycerate kinase-1
RA	retinoic acid
RFLP	random fragment length polymorphism
RNA	ribonucleic acid
SDS-PAGE	sodium dodecyl sulphate polyacrylamide gel electrophoresis
TAD	transcriptional activation domain

CHAPTER 1

Introduction

1.1 Overview

Cells may proliferate, enter a quiescent state, die by programmed cell death (apoptosis), or become determined to a specific differentiation program. The gene expression profiles and subsequent fate of the cell (divide or arrest, remain pluripotent, become determined or terminally differentiated) are dictated by intrinsic and environmental signals or cues. Cellular differentiation involves commitment of a pluripotent stem cell to one particular lineage followed by terminal differentiation, development to become a functional, specialized cell. During differentiation the expression of cell-type specific genes is induced, and other genes including those required for cell cycle promotion, repressed. The cell program, and indeed proper development and maintenance of organ systems requires the accurate integration of combinatorial, growth-promoting and restrictive signals, both external and internal to the cell.

Several approaches have been used to identify and assess the requirement for factors that regulate or coordinate cell proliferation and arrest, including the terminal cell cycle arrest that accompanies differentiation. By analyzing genetic changes in tumour cells, principal factors in maintaining genetic stability and regulating normal growth control have been revealed. Processes controlling cell proliferation and arrest have also been studied by assessing the oncogenic activity of DNA tumour virus-derived proteins in mammalian cells. Other experiments, directed toward understanding how the gene

expression program is altered to orchestrate growth or differentiation of cells, within a tissue or organism, have also contributed by identifying cell-specific and ubiquitous regulatory factors and mechanisms. Combined, these approaches have defined the control nodes that dictate cell cycle progression or withdrawal, and induction or maintenance of quiescence, differentiation or apoptosis.

Recent advances in transgenic animal technologies have brought the study of cell cycle regulation to a novel level of manipulation, but also of complexity that is not attainable by cell or tissue culture. With the advent of ES cell technology as well as more traditional transgenic procedures and site-specific recombinases, investigators can manipulate gene expression in specific tissues or the entire organism to elucidate the function of a single gene in normal growth control and development (Gu, *et al.*, 1994a; Mansour and Capecchi, 1988; Orban, *et al.*, 1992).

With respect to cancer, a focus has been to assess the consequence of loss-of-function of genes implicated in genetic stability, oncogenesis and tumour suppression. Two predominant characteristics of malignantly transformed cells are uncontrolled proliferation and incomplete terminal differentiation. The retinoblastoma (Rb) proteins have been investigated, as these factors negatively regulate cell cycle progression, and impinge upon cellular differentiation.

1.2 The cell cycle

The foundation for mammalian cell cycle research is based in genetic and biochemical analyses of a variety of less complex organisms including budding and fission yeast. The cell division cycle proceeds in a temporally ordered series of events that involves both positive, and negative regulators, including the cyclin dependent kinases, and cyclin dependent kinase inhibitors and Rb proteins respectively (reviewed in Morgan, 1997; Nigg, 1995; Sherr and Roberts, 1995; Weinberg, 1995b). Basically, a cell

may exist in one of five states or phases (Figure 1.1A). Quiescent cells exist in the G_0 state, until receiving stimuli that activate a mitogenic switch. Specifically, quiescent cells may be multipotent, determined or terminally differentiated. The next four phases constitute the cell cycle proper, and they are termed G_1 for gap 1, the synthesis phase (S), G_2 for gap 2, and finally the mitosic phase (M). Following a mitogenic stimulus, cells enter the G_1 phase, and once beyond a point in G_1 referred to as the restriction point, continue through the remainder of the cycle (Pardee, 1974; Pardee, 1989). The S phase constitutes the DNA replicative period, and the M phase, cell division. Checkpoints in G_1 and G_2 preceding each S and M phase, respectively, ensure essential growth and complete replication. Today, the scaffold of factors and mechanisms that positively and negatively affect cell proliferation is clearly established.

Figure 1.1 The Cell Cycle

(A) The cell cycle proceeds in a temporally regulated fashion and is comprised of four phases, specifically G_1, S, G_2 and M. Following mitosis, a cell may continue to cycle, given sufficient stimulus, or proceed to a quiescent state (G_0). From G_0, a cell may reenter the cell cycle or continue along a determined path to become a fully differentiated, functional, specialized cell. Alternatively, the cell may die by apoptosis. (B) p130, Rb and p107 essentially function in overlapping phases of the cell cycle. p130 exerts its control in the G_0 state, Rb, in G_0 and G_1 prior to the restriction point (R), and p107 from late G_1 to S phase. Cyclins are expressed in distinct phases of the cycle and regulate specific cdk activity. Cyclin D1 associates with cdks 4 and 6; cyclin E and A expression follow and regulate cdk2 activity. Cyclin B1, a G_2 cyclin, and cyclin A are found in complexes with cdc2.

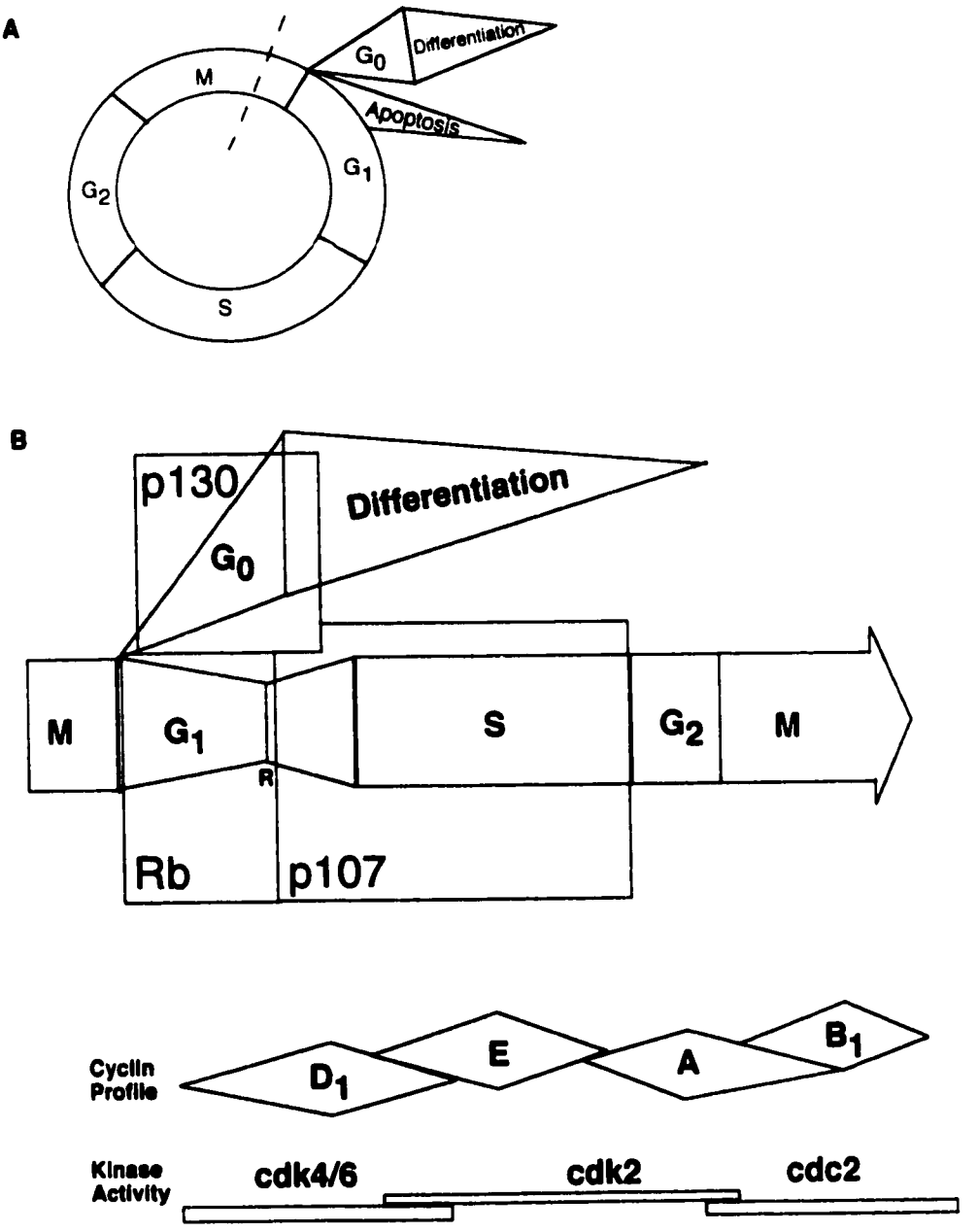
A
M
G0
Differentiation
Apoptosis
G1
G2
S
B
p130
G0
Differentiation
M
G1
R
S
G2
M
Rb
p107
Cyclin Profile
D1
E
A
B1
Kinase Activity
cdk4/6
cdk2
cdc2

Cell proliferation requires the actions of cyclins, proteins with oscillating levels corresponding to specific phases of the cell cycle. To date, there are 9 families of mammalian cyclins, designated A through I with subtypes (Bai, *et al.*, 1994; Fisher and Morgan, 1993; Nakamura, *et al.*, 1995; Tamira, *et al.*, 1993 reviewed in Grana and Reddy, 1995; Pines, 1995; Sherr, 1993). Cyclin expression is regulated at the level of transcription, and degradation via the ubiquitin-proteosome pathway. These small proteins serve as activators of their cognate cyclin-dependent, serine/threonine kinases (reviewed in Morgan, 1997; Pines, 1995; Sherr, 1993; Sherr, 1994) (Figure 1.1B). D and E type cyclins have been implicated in the entrance and progression through the restriction point in the G_1 phase (Ohtsubo, *et al.*, 1995; Quell, *et al.*, 1993; Resnitzky and Reed, 1995). G_1 cyclin accumulation is required for cell cycle entry and members of this family, particularly D-cyclins, have been identified as targets of growth factors (reviewed in Draetta, 1994; Pines, 1995; Sherr, 1994). More recently, the connection between Ras, a critical component of mitogenic-signaling pathways, and cyclin D expression and activity has been demonstrated (Leone, *et al.*, 1997; Peeper, *et al.*, 1997). Temporally, cyclins A and B, a G_2 cyclin, function after the G_1 to S transition (Girard, *et al.*, 1991; Pagano, *et al.*, 1992; Pines and Hunter, 1989; Pines and Hunter, 1991; Resnitzky, *et al.*, 1995). The Rb proteins appear to integrate cyclin-dependent kinase (cdk) activity and cell cycle progression, in part as mediated through the E2F transcription factors (see Section 1.3.iii). Specifically, p130, Rb and p107 negatively regulate transitions from the G_0, G_1 and S phases.

1.3 Rb, p107 and p130 in Cell Cycle Control

1.3.i. Cloning of Rb, p107 and p130

Rb is the prototypic member of the gene family that includes p107 and p130. The human Rb gene was identified and cloned through analyses of gene mutations linked to

the childhood ocular tumour, retinoblastoma (Friend, *et al.*, 1986; Friend, *et al.*, 1987; Fung, *et al.*, 1987; Lee, *et al.*, 1987). Both copies of the Rb gene are mutated in all retinoblatomas, and these mutations include gross structural alterations and point mutations. Rb loss-of-function mutations were revealed in a variety of other human cancers, for example 20-30% of breast and bladder carcinomas and 90% of small cell lung carcinomas, and others including prostate cancers and primary leukemia, suggesting that Rb functions as a general tumour suppressor in cells (Bookstein, *et al.*, 1990; Friend, *et al.*, 1986; Friend, *et al.*, 1987; Harbour, *et al.*, 1988; Horowitz, *et al.*, 1989; Mendoza, *et al.*, 1988; T'Ang, *et al.*, 1988; Toguchida, *et al.*, 1988; Weichselbaum, *et al.*, 1988). Unlike retinoblastomas, loss of Rb may not be a rate-limiting step in the development of these tumours. The prevalence of Rb gene mutations in cancers has established it is a tumour suppressor gene. Significantly, perturbations at each level of an epistatic pathway including the p16 cyclin-dependent kinase inhibitor, cdk4, cyclin D and Rb have been revealed in a great proportion of tumour types indicating that disruption of this pathway is a common event in cancer development (reviewed in Ruas and Peters, 1998; Sherr, 1996; Weinberg, 1995a).

The Rb gene encodes a ubiquitously expressed 105-110 kD nuclear phosphoprotein with cell-cycle dependent phosphorylation profiles (Buchkovich, *et al.*, 1989; Chen, *et al.*, 1989; DeCaprio, *et al.*, 1989; Furukawa, *et al.*, 1990; Ludlow, *et al.*, 1989; Mihara, *et al.*, 1989). The active protein is hypophosphorylated, and it is maintained in an otherwise inactive, hyperphosphorylated state by the coordinated, and presumably cooperative, actions of cdks (Dowdy, *et al.*, 1993; Ewen, *et al.*, 1993; Hinds, *et al.*, 1992; Hu, *et al.*, 1992; Lees, *et al.*, 1991; Lin, *et al.*, 1991; Matsushime, *et al.*, 1992).

Interest in the Rb, p107 and p130 proteins originated from the observations that DNA tumour virus oncoproteins, including adenovirus E1A, polyomavirus and SV40 T antigens, and human papillomavirus E7, specifically target and inactivate these and other

cell-cycle regulatory proteins to induce cell growth (Yee and Branton, 1985; Decaprio, *et al.*, 1988; Dyson, *et al.*, 1989; Harlow, *et al.*, 1986; Whyte, *et al*, 1988a; Whyte, *et al*, 1989). These associations with viral oncoproteins implicated the Rb family in cell cycle control. Subsequently, the p107 gene was isolated by virtue of its interaction with adenovirus E1A and displayed several regions of homology to Rb (Ewen, *et al*, 1991). p107 is not considered a *bona fide* tumour suppressor, as its specific loss in a tumour has not been demonstrated. Loss of p107, which resides on human chromosome 20q11.2, has been associated with a subset of human myeloid proliferative disorders, including a subgroup of neoplasias (Asimakopoulos, *et al*, 1994; Davis, *et al*, 1984; Green, 1996). The third member of the gene family, p130, was cloned independently by three groups using three different criterion: structural similarity with Rb, interaction with cdk2, and interaction with the adenovirus oncoprotein E1A (Hannon, *et al*, 1993; Mayol, *et al*, 1993; Li, *et al*, 1993). Loss of heterozygosity at the 16q12.2 locus for p130 is associated with hepatocellular carcinomas, breast, prostate and central nervous system primitive neuroectodermal tumours (Li, *et al*, 1993; Mayol, *et al*, 1993). Although p107 and p130 are localized in chromosomal regions that are frequently deleted in tumours, it is unclear whether mutations in these genes have significant roles in initiation or progression of human cancers. However, mutation of p130 has been recently reported for a small cell lung carcinoma cell line (Helin, *et al*, 1997). As well, overexpression of p130 inhibits specific tumour cell growth in nude mice (Howard, *et al*, 1998). For their relation to Rb, and specific targeting by DNA virus oncoproteins, the p107 and p130 proteins have received considerable attention.

1.3.ii. Structure

Rb, p107 and p130 are highly related both structurally and functionally. The three proteins have been generically termed "pocket" proteins, by virtue of non-contiguous regions of the proteins called domains A and B, interrupted by a spacer (S) region (Ewen,

et al, 1991; Kaelin, *et al*, 1992). These regions were initially identified for Rb, and subsequently for p107 and p130, as required for interactions with the oncoproteins of DNA tumour viruses (Davies, *et al*, 1993; Dyson, *et al*, 1992; Dyson, *et al*, 1989; Ewen, *et al*, 1991; Giordano, *et al*, 1991; Hannon, *et al*, 1993; Hu, *et al*, 1990; Huang, *et al*, 1990; Kaelin, *et al*, 1990; Mayol, *et al*, 1993; Whyte, *et al*, 1988b; Wolf, *et al*, 1995). Presumably, interaction between domains A and B form a binding surface, hence the term "pocket". Indeed, if domains A and B are expressed as separate peptides, they functionally interact to recreate an interaction surface/"pocket" for E1A and other proteins (Chow and Dean, 1996).

The amino acid sequences of the Rb proteins are similar or identical in several regions. An alignment of mouse Rb, p107 and p130 amino acid sequences is presented in Figure 1.2. Rb and p130 share approximately 25% homology, whereas p107 and p130 share approximately 50% (Hannon, *et al*, 1993; Li, *et al*, 1993; Mayol, *et al*, 1993; reviewed in Whyte, 1995). Not surprisingly, the most strongly conserved regions correspond to those that interact with E1A and T antigen. These regions reside in the C-terminal halves of the proteins. The amino-terminal sequences are less well-conserved, although p130 and Rb share a proline/alanine-rich sequence at the N-termini.

The sites required for E1A binding are contiguous with the regions required to interact with a family of cellular, heterodimeric transcription factors referred to as E2F. Domains A, S, B and additional carboxyl sequences are involved in binding these transcription factors (Bagchi, *et al*, 1991; Bandara and LaThangue, 1991; Chellappan, *et al*, 1991; Chittenden, *et al*, 1991; Stirdivant, *et al*, 1992; Zhu, *et al*, 1995).

Figure 1.2 Rb family member contain conserved regions

Alignment of the predicted amino acid sequences of mouse Rb (top), p107 (center) and p130 (bottom). The A and B subdomains are boxed and the spacer region is conspicuously absent from the Rb sequence. Amino acid positions are indicated at the left.

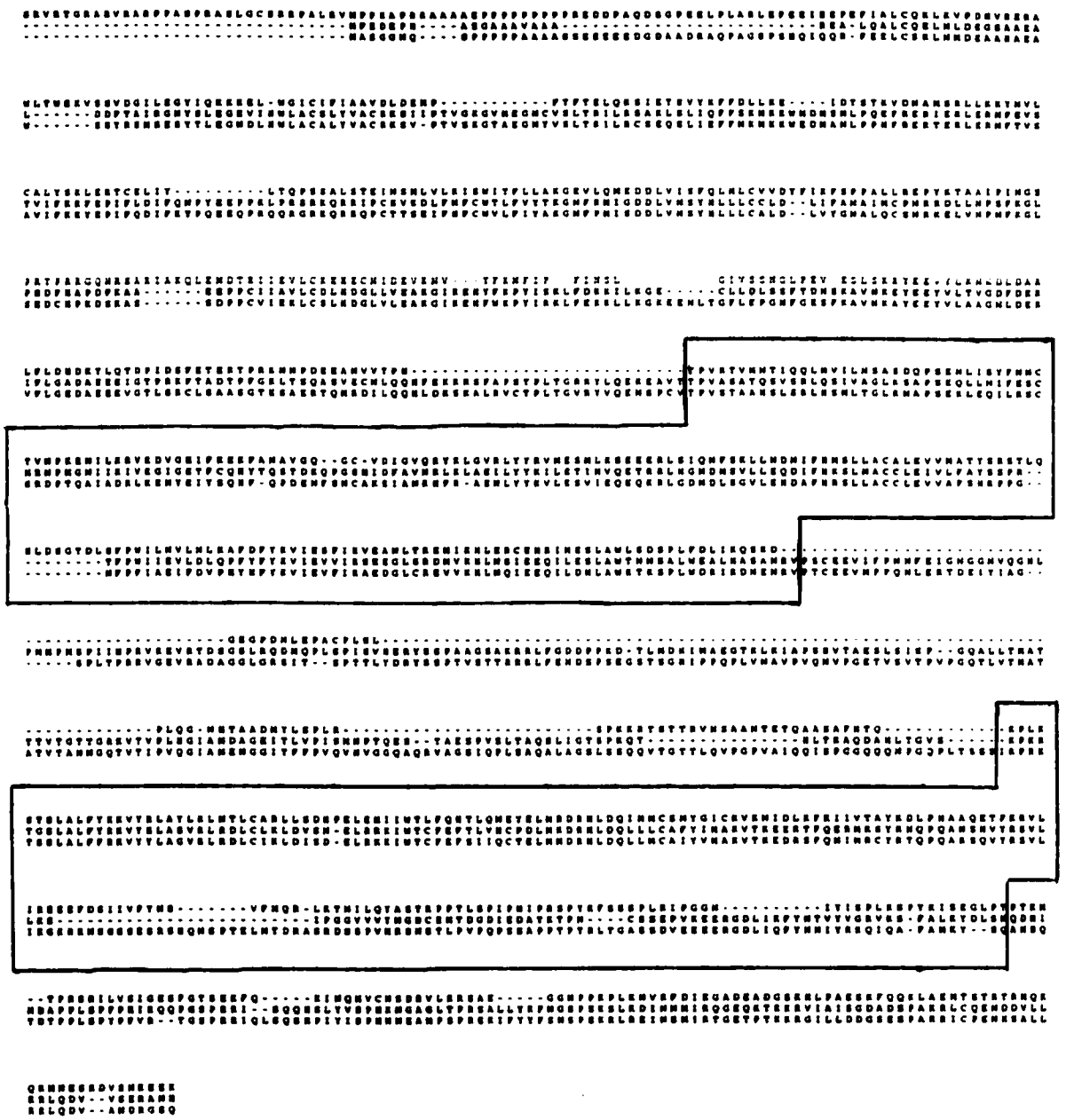

1.3.iii. The Rb proteins and E2F transcription factors

Overexpression of Rb, p107 or p130 can arrest cells in G_1 and repress transcription of genes that promote the cell cycle and S phase, signifying that these proteins normally function in G_1 to negatively regulate the G_1 to S transition (Claudio, *et al*, 1994; Goodrich and Lee, 1993; Qin, *et al*, 1992; Templeton, *et al*, 1991; Vairo, *et al*, 1995; Zhu, *et al*, 1995a). Accordingly, overexpression can also activate the transcription of genes that initiate or maintain cell cycle arrest. At least in part, the mechanism for negative cell-cycle control involves interactions with the ubiquitously-expressed, E2F transcription factors (Bandara and LaThangue, 1991; Beijersbergen, *et al*, 1994b; Cao, *et al*, 1992; Chellappan, *et al*, 1991; Chittenden, *et al*, 1991; Cobrinik, *et al*, 1993; Dynlacht, *et al*, 1994; Ginsberg, *et al*, 1994; Helin, *et al*, 1992; Lees, *et al*, 1993; Mudryj, *et al*, 1990; Smith and Nevins, 1995; Wolf, *et al*, 1995; Zhu, *et al*, 1995a; reviewed in Dyson, 1998; Muller, 1995; Nevins, *et al*, 1997)

Excepting specific viral proteins, the most extensively studied proteins that interact with Rb, p107 and p130 are the E2F transcription factors. E2F was originally described as a cellular activity that bound an early transcription region of adenovirus and activated transcription of the E2 genes (Kovesdi, *et al*, 1986a; Kovesdi, *et al*, 1986b). Actually, the ability of the viral oncoproteins to stimulate cell cycle progression is dependent on disrupting the Rb factors' interactions with E2F (Bagchi, *et al*, 1991; Bandara and LaThangue, 1991; Chellappan, *et al*, 1991; Mudryj, *et al*, 1990; Raychaudhuri, *et al*, 1991; Weintraub, *et al*, 1992). E2F binding sites are present in the promoters of many cellular genes induced during the G_1 to S phase transition. In cells, E2F transcriptional activity is necessary for the expression of genes that promote the cell cycle including cdc2, myc, myb, cyclins E and A; and genes required for S phase progression/DNA replication including dihydrofolate reductase (DHFR), ribonucleotide reductase, thymidine kinase, DNA polymerase α and PCNA (Blake and Azizkhan, 1989;

Dalton, 1992; DeGregori, *et al*, 1995; Geng, *et al*, 1996; Henglein, *et al*, 1994; Hiebert, *et al*, 1989; Ohanti, *et al*, 1995; Pearson, *et al*, 1991). The overexpression of specific E2F complexes in growth-arrested cells is sufficient to promote the cell cycle and DNA replication, but the resulting uncontrolled growth can induce apoptosis (Hiebert, *et al*, 1995; Johnson, *et al*, 1993; Wu and Levine, 1994). Taken together, E2F is central to cell cycle progression.

Great effort has contributed to our understanding of the E2F factors. To date, the E2F family is comprised of six E2F-like factors and two DP-type factors (Beijersbergen, *et al*, 1994b; Ginsberg, *et al*, 1994; Girling, *et al*, 1993; Halevy, *et al*, 1995; Helin, *et al*, 1993; Helin, *et al*, 1992; Hijmans, *et al*, 1995; Ivey-Hoyle, *et al*, 1993; Kaelin, *et al*, 1992; Lees, *et al*, 1993; Morkel, *et al*, 1997; Sardet, *et al*, 1995; Shan, *et al*, 1992; Trimarchi, 1998; Wu, *et al*, 1995; Zhang And Chellapan, 1995). The sequences of E2F 1-5 are conserved over DNA binding, heterodimerization, marked box and C-terminal transactivation domains (TADs); while E2F-6 lacks the C-terminal TAD and consequently does not associate with Rb proteins (reviewed in Dyson, 1998; Helin, 1998). The DP-type proteins have limited homology to E2F-like proteins in the DNA-binding and heterodimerization domains. E2F/DP association is essential for high-affinity DNA binding, transcriptional activity and high-affinity interaction with Rb, p107 or p130 (Bandara, *et al*, 1993; Helin, *et al*, 1993; Huber, *et al*, 1993; Krek, *et al*, 1993). The mechanistic distinction between specific E2F-type/DP-type complexes remains unresolved. Presumably, each E2F/DP heterodimer controls the expression or repression of specific target genes. Alternatively, these complexes may act in a temporally-specific, but coordinated manner. The latter model is most relevant, considering that specific E2F factors and specific Rb proteins have overlapping phases of activity during cell cycle progression. The cyclic activation and repression of E2F-target genes presumably controls progression through the cell cycle.

E2F activity is regulated at several levels, consistent with essential control of E2F activity (or free E2F) in normal cells. The expression and activity of these factors is cell-cycle position-dependent, for example E2F-4 is predominant in G_0, and E2F-1,2 and 3 are induced at G_0 to G_1 transition (Ginsberg, *et al*, 1994; Johnson, *et al*, 1994; Kaelin, *et al*, 1992; Moberg, *et al*, 1996; Sardet, *et al*, 1995; Slansky, *et al*, 1993). E2F also is regulated transcriptionally. E2F-1 for example, contains E2F-binding sites in its promoter (Johnson, *et al*, 1994; Neuman, *et al*, 1994). As well, expression studies in mice demonstrated that specific E2F factors are expressed in several proliferating and post-mitotic cells (Dagnino, *et al*, 1997a; Dagnino, *et al*, 1997b). Post-translational modifications of E2F activity include differential E2F-type subcellular localization, phosphorylation, and degradation via the ubiquitin-proteosome pathway (Fagan, *et al*, 1994; Haetboer, *et al*, 1996; Hofmann, *et al*, 1996; Lindeman, *et al*, 1997; Peeper, *et al*, 1995; Verona, *et al*, 1997; reviewed in Cobrinik, 1996). Finally, by associating with Rb proteins, E2F is rendered transcriptionally inactive (reviewed in Dyson, 1998). Interestingly, in addition to functions described below, association with Rb, p107 or p130 can protect specific E2F factors from ubiquitin-mediated degradation (Haetboer, *et al*, 1996; Hofmann, *et al*, 1996).

A central function of the Rb proteins is to negatively regulate the activity of E2F transcription (Beijersbergen, *et al*, 1994b; Cress, *et al*, 1993; Flemington, *et al*, 1993; Ginsberg, *et al*, 1994; Hamel, *et al*, 1992; Helin, *et al*, 1993; Hiebert, *et al*, 1992; Hijmans, *et al*, 1995; Johnson, 1995; Schwarz, *et al*, 1993; Smith and Nevins, 1995; Vairo, *et al*, 1995; Weintraub, *et al*, 1992; Welsh and Wang, 1995; Zamanian and Thangue, 1992; Zhu, *et al*, 1993). Essentially, appreciation for the unique functions of Rb, p130 and p107 came partly from the analyses of the specificity displayed by the Rb proteins in their E2F interactions. The Rb protein/E2F protein interactions are both cell-cycle position-dependent and E2F-type specific (Figure 1.1). Rb/E2F complexes are a

minor component of G_0 E2F DNA-binding activity (Chittenden, *et al*, 1993; Cobrinik, *et al*, 1993; Schwarz, *et al*, 1993). Rb interacts with E2F-1,2,3 specifically and appears to exert control in the early G_1 phase (Helin, *et al*, 1992; Kaelin, *et al*, 1992; Lees, *et al*, 1993; Wu, *et al*, 1995). The p130/E2F interaction is a major element of E2F control in G_0 and G_1 cells. p130 interacts with E2F-4, the major G_0 E2F activity; and although isolated through its interaction with p107, E2F-5 also interacts preferentially with p130 (Helin, *et al*, 1992; Hijmans, *et al*, 1995; Kaelin, *et al*, 1992; Lees, *et al*, 1993; Sardet, *et al*, 1995; Vairo, *et al*, 1995; Wu, *et al*, 1995). Presumably, during cell cycle exit and quiescence, p130 negatively regulates the expression of factors that promote the cell cycle progression (reviewed by Mayol and Grana, 1998). Consistent with specific interactions, overexpression of E2F-4 or E2F-1 more efficiently overcomes p130-induced or Rb-induced G_1 blocks, respectively (Vairo, *et al*, 1995). Together, this work indicates that p130 and Rb use distinct mechanisms to arrest the cell cycle, involving unique E2F family members. p107 preferentially interacts with E2F-4 and 5, and these complexes appear late in G_1 and S phase (Beijersbergen, *et al*, 1994b; Ginsberg, *et al*, 1994). Combined, the diversity of potential interactions between these protein families allow for a high degree of coordinated control in regulating E2F function and subsequently, cell-cycle progression. Dependent on whether E2F:DP or an Rb protein/E2F:DP complex is bound to the promoter, different E2F-regulated genes can be activated or repressed, controlling cell-cycle progression (Weintraub, *et al*, 1992; Zamanian and LaThangue, 1992; reviewed in Dyson, 1998).

The importance of the interactions between the Rb proteins and E2F is revealed by the predominance of mutations in the Rb pathway in human cancers, and experiments that disrupt Rb, p107 or p130 and E2F interactions (Hiebert *et al*, 1993; Hu, *et al*, 1990; Huang, *et al*, 1990; Kaelin, *et al*, 1990; Ruas and Peters, 1998; Weinberg, 1995a). Mutations in the Rb or p107 pocket which disrupt binding to E2F/DP prevent

transcriptional repression and cell cycle arrest. As well, the previously mentioned interactions with DNA virus oncoproteins disrupt Rb protein/E2F interactions (Bandara and LaThangue, 1991; Chelleppan, *et al*, 1992; Flemington, *et al*, 1993; Weintraub, *et al*, 1992; Zamanian and LaThangue, 1992). Interestingly, targeted loss of E2F-1 function in mice results in quite diverse phenotypes. Dependent on the tissue context, the result is tumourigenesis, suppressed apoptosis or reduced cell proliferation (Field, *et al*, 1996; Yamasaki, *et al*, 1996). These results indicate that the major function imposed by E2F is cell-type dependent. Essentially by removing E2F-1, an effector of Rb, the deregulated expression of E2F-dependent genes may result in uncontrolled cell growth, and apoptosis or oncogenesis. The compound *E2F/Rb* mutation in mice results in survival beyond that of the *R*b homozygous mutants, again revealing the functional connection between these factors (Tsai, *et al*, 1998).

In Rb-deficient primary embryonic fibroblasts (EF), cells progress through the G_1 phase faster, although the overall length of cell cycle is unaltered (Herrara, *et al*, 1996). These cells also inappropriately entered S phase in the presence of specific inhibitors or mitogen-poor conditions for growth. Deregulated expression of several E2F-regulated genes, including cyclin E, DHFR and thymidylate synthase, accompanied the altered cell cycle kinetics (Almasan *et al*, 1995; Herrara, *et al*, 1996). Hurford and colleagues (1997) demonstrated that Rb and p107/p130 are required for the regulated expression of different sets of E2F-responsive genes in mouse EF. In Rb-deficient EF the expression of p107 and cyclin E were perturbed. By contrast, in doubly mutant *p107/p130* EF, myb, cdc2 rrm2 and cyclin A2 expression were perturbed. Therefore, these proteins repress transcription in the context of specific E2F-regulated genes. Work is ongoing to categorize specific E2F:DP heterodimer targets and E2F:DP/Rb protein regulated genes.

1.3.iv. Ras, Rb and E2F

The connections between positive or negative growth effectors and the cell-cycle machinery have been clearly appreciated but largely unresolved. Growth factors were known to induce cyclin D1 and growth inhibitors, to repress cyclin D1-linked activity (Ewen, *et al*, 1993; Polyak, *et al*, 1994; Sewing, *et al*, 1993; Winston and Pledger, 1993; Won, *et al*, 1992). Ras is a proto-oncogene that is central in mitogenic signal transduction, to cell cycle entrance and G_1 to S transitions (reviewed in Downward, 1997; Lloyd, 1998). Ras inactivation results in a G_1 arrest, decreased cyclin D1 levels and the consequent accumulation of active Rb (Peeper, *et al*, 1997). G_1 arrest was rescued by the expression of E2F:DP1 supporting that cyclin D1, Rb and E2F are components of the Ras-effector pathway. Additionally, Ras and myc (also a proto-oncogene) or a second positive growth effector, induced G_1 cyclin/cdk and E2F activities and subsequently S phase (Leone, *et al*, 1997). Therefore, recent work indicates that Rb along with cyclin D and E2F are important in linking Ras-dependent mitogenic signals to cell-cycle regulation.

1.3.v. Mechanisms for Rb protein-mediated transcriptional repression

Rb-family/E2F(1-5):DP complexes formed at different phases of the cell cycle are believed to bind promoters at E2F sites and repress transcription. The mechanisms whereby Rb, p107 and p130 accomplish this are two-fold: 1) by interfering with basal transcription machinery contacts and 2) through chromatin remodeling.

Transcriptional activation by enhancer-binding proteins appears to involve direct, or indirect, contact between one or more TADs and one or more of the transcription factors required for basal transcription (Hampsey, 1998; Tijan and Maniatus, 1994). The Rb binding domain on E2F is embedded within the TAD, overlapping with the TATA-binding protein (TBP) binding site. Therefore, Rb may physically interfere with the ability of E2F's TAD to contact components of the basal machinery, i.e. TFIID (Hamel, *et*

al, 1992; Helin, *et al*, 1993; Weinberg, 1995b; Weintraub, *et al*, 1992; reviewed in Kouzarides, 1995) Additionally, Rb, p107 and p130 are capable of interacting with the largest subunit of TFIID, TATA-binding protein associated factor TAF(II) 250 (Shao, *et al*, 1995). Once tethered through E2F, Rb can bind adjacent transcription factors (domains A and B share significant homology with TBP and TFIID) also blocking their interaction with the basal complex to inhibit the activity of promoters with enhancers in addition to E2F (Bremner, *et al*, 1995; Hagemeier, *et al*, 1993; Weintraub, *et al*, 1995). p107, like Rb, also acts as a general repressor that blocks transcription when it is tethered to a promoter through E2F or other DNA binding domain (Starostik, *et al*, 1996).

Rb can also repress RNA polymerase I by inhibiting the DNA binding of a factor, UBF, and polymerase III transcription by interacting with both TFIIIB and TFIIIC2 (Cavanaugh, *et al*, 1995; Chu, *et al*, 1997; Voit, *et al*, 1997; White, *et al*, 1996). If Rb normally inhibits the synthesis of both rRNA and tRNA by polymerases I and III, it has evolved a potent mechanism for restraining cell growth.

A second mechanism for Rb protein transcriptional repression involves altering chromatin structure. Chromatin is the highly organized, packaged form of DNA in eukaryotic cells, functioning to condense chromosomes and regulate gene expression. The basic structural unit of chromatin is referred to as the nucleosome, consisting of approximately 146 bp of DNA wrapped around a histone octamer containing two molecules each of histones H2A, H2B, H3 and H4. Chromatin structure is dynamic, existing in transcriptionally active and inactive configurations (reviewed in Davie, 1998; Gregory and Horz, 1998). One mechanism to increase the accessibility of DNA to proteins that regulate transcription is the enzymatic modification of histones. Hyperacetylation of specific lysine residues in the N-terminal histone tails is accomplished by histone acetyltransferases (HAT). Conversely, histone deacetylation (HDA) is associated with transcriptional inactivity/repressed chromatin configuration.

Rb, p107 and p130 are each capable of binding HDAC-1 and E2F, thereby recruiting histone deacetylase activity to E2F-containing promoters to repress transcription (Brehm, *et al*, 1998; Ferreira, *et al*, 1998; Luo, *et al*, 1998; Magaghi-Jaulin, *et al*, 1998; Stiegler, *et al*, 1998). Interestingly, relaxed chromatin structure was reported in Rb-deficient cells (Herrara, *et al*, 1996). E2F can also bind the Creb binding protein, CBP, a transcriptional cofator, which has intrinsic histone acetylase activity and may recruit additional HATs to the complex . This work suggests that E2F binding partners influence the chromatin structure to activate or repress transcription. Rb may also interact with transcriptional activators that function within an ATP-driven chromatin-remodeling complex in mammalian cells (Dunaief, *et al*, 1994; Strober, *et al*, 1996).

1.3.vi. p107 and p130 interact with other regulatory proteins

In addition to interacting with E2F, p107 and p130 are capable of binding specific cyclins, cyclins E and A, and cdk2 through their spacer region (Ewen, *et al*, 1992; Li, *et al*, 1993; Hannon, *et al*, 1993; Lacy and Whyte, 1997; DeLuca, *et al*, 1997). p130 interacts with cyclin A in a cdk2-dependent manner, however, it can interact with cyclin E even without cdk2 (Lacy and Whyte, 1997). The overexpression of the p107 cyclin-binding domain can cause growth arrest in G_1 dependent on the cell line, and this arrest can be rescued by co-expression of cyclins A and E (Ewen, *et al*, 1992). Activation of p107-bound cyclin/cdk kinases leads to dissociation of p107 from E2F (Lees, *et al*, 1992). Actually, both p107 and p130 are *in vitro* substrates of their bound kinases. As the dissociation of p130 from cdk complexes leads to significantly increased kinase activity, p130 functions to inhibit activity. Consistent with this, cyclin A in complex with p107 or p130 is unable to phosphorylate all substrates commonly used in cdk assays. It was suggested that the p107 and p130 associated activity may represent a distinct pool with a distinct substrate specificity, for instance preferentially targeting Rb family members (Hauser, *et al*, 1997). However, stoichometric association of p107 or p130 with

either cyclin E/cdk2 or cyclin A/cdk2 inhibits the activities of these kinases. (Woo, *et al*, 1997). Mechanistically, the data suggest that p107 or p130 complex with and inhibit the central cell-cycle kinases to suppress cell growth.

There are two families of mammalian cdk inhibitors, low molecular weight proteins classified by sequence homology and the kinases inhibited by each (reviewed in Sherr and Roberts, 1995). The p16, p15, p18 and p19 proteins all contain four ankyrin repeats and exclusively inhibit cyclin D/ckd4 and cyclin D/cdk6 kinases. Their primary mechanism of action is to prevent cyclin D association with cdk4 and cdk6 (Guan, *et al*, 1994; Hannon and Beach, 1994; Serrano, *et al*, 1993; Toyoshima and Hunter, 1994). The second family of cdk inhibitors include p21, p27 and p57, which share high sequence identity in the amino terminal halves of the proteins, and have a broader range of cyclin/cdk targets, including kinases associated with cyclins D, E and A (Gu, *et al*, 1993b; Harper, *et al*, 1993; Harper, *et al*, 1995; Polyak, *et al*, 1994). These cdk inhibitors act primarily to induce a conformational change in the cdk to affect the ATP binding site. p107, like the p21 family of cdk inhibitors, inhibited the phosphorylation of target substrates by cyclin A/cdk and cyclin E/cdk and the associations of p107 and p21 were mutually exclusive (Woo, *et al*, 1997; Zhu, *et al*, 1995b). The inhibition was dependent on a sequence in p107 pocket that is a p21-related domain. p130 also inhibits cdk2 activity through a domain in the spacer (DeLuca, *et al*, 1997; Lacy and Whyte, 1997). Recent work demonstrated that a second amino-terminal region exists in p107 and p130 for cyclin binding and cdk inhibition (Castano, *et al*, 1998). It appears that p107 and p130 use a dual cyclin-binding domain, analogous to p21.

p107 also regulates the activity of the *myc* proto-oncogene. The activity of Myc is tightly regulated at transcriptional, translational and post-translational levels. *myc* transcription is repressed in quiescent or terminally differentiated cells and is induced rapidly and transiently following mitogenic stimulation, maintained through G_1 and

remains at a basal level for the remainder of the cell cycle (reviewed in Bouchard, *et al*, 1998; Rabbitts, *et al*, 1985; Zou, *et al*, 1997). Transcription from the human *myc* promoter is efficiently induced by E2F and repressed by Rb (Hiebert, *et al*, 1989; Thalmeiere, *et al*, 1989). Additionally, both cyclin D1 and cyclin A promote transcription of myc, dependent on an E2F site in the promoter (Oswald, 1994; Watanabe, *et al*, 1995). Taken together, the data indicate that the active Rb proteins inhibit *myc* transcription by an E2F-dependent mechanism. *In vivo*, p107 also associates with the Myc protein through the TAD and represses its transcriptional activity, presumably through mechanisms mentioned above (section 1.2.iv) (Beijersbergen, *et al*, 1994a; Gu, *et al*, 1994b). Mutant forms of Myc incapable of forming complexes with p107 were isolated from lymphoma patients, suggesting that the p107/Myc interaction represents an important regulatory mechanism (Hoang, *et al*, 1995).

p107 is also capable of binding the Sp1 transcription factor. p107 associates with Sp-1, independent of the 'pocket' region, through its amino-terminus and negatively regulates Sp1 activity (Datta, *et al*, 1995). Sp1 and E2F sites are found together in the promoters of several replication-specific genes (Azizhan, *et al*, 1993). Additionally, Sp1 sites are also prevalent in the promoters of myeloid-specific genes (Clarke and Gordon, 1998). Interestingly, Rb has been demonstrated to affect Sp-1 activity in a positive manner, although it does not directly complex with Sp1 on DNA. Rather it appears to sequester an Sp1 inhibitory factor (Sp1-I) (Chen, *et al*, 1994).

Interactions between p107 and transcription factors coupled to cell cycle promotion are consistent with this protein functioning to ensure proper cell cycle progression, and implicate p107 in initiating cell cycle arrest. p107 does not appear to function in permanently arrested cells, as its expression is extinguished in quiescent cells over time (Chittenden, *et al*, 1993; Cobrinik, *et al*, 1993; Smith, *et al*, 1998).

Conversely, p130 is implicated in the initiation and maintenance of cell cycle arrest. In addition to binding E2F-4, the major G_0 E2F species, p130 also associates with proteins that are induced in differentiating cells, including HBP-1 and paired homeodomain-containing proteins. HBP-1 is a sequence-specific high mobility group box transcription factor. HBP-1 interactions with Rb and p130 are up-regulated during differentiation and associations with p130, Rb or p107 repress HBP-1-mediated transactivation. It was proposed that HBP-1 is a transcriptional repressor that, in part, initiates and maintains cell cycle arrest during differentiation (Lavender, *et al*, 1997; Tevosian, *et al*, 1997). p130 can also associate with paired-like homeodomain-containing proteins. These transcription factors control determination of cell fate and differentiation. The association between Rb proteins and the homeodomain-containing proteins repressed their transcriptional activity also (Wiggan, *et al*, 1997).

1.3.vii. Regulation of Rb, p107 and p130 Function

Rb, p130 and p107 are not equivalently expressed in all phases of the cell cycle in all cell types. Rather, p130 expression can be highly induced in G_0, and decreases in growing cells prior to mitosis. Rb expression is relatively constant throughout the cell cycle and is induced during terminal cell cycle withdrawal; and p107 is depleted from G_0 cells and expression is not detected in the early G_1 phase following re-entrance into the cell cycle (Chittenden, *et al*, 1993; Cobrinik, *et al*, 1993; Smith, *et al*, 1998). p130 protein levels appear to be controlled post-transcriptionally, potentially by a proteosome-based mechanism; and p107 expression appears to be controlled at the level of transcription (Smith, *et al*, 1998). As p107 is depleted from G_0 cells and later during terminal differentiation, E2F/p130 potentially inhibits *p107* transcription. The levels of Rb protein change little during cellular growth, as do Rb/E2F complexes. However, levels of both p107/E2F and p130/E2F complexes are determined by the levels of p107 and p130 proteins (Corbeil, *et al*, 1995). In addition to their expression profiles, other

post-translational modification is required to relieve the negative regulation imposed by Rb, p107 and p130. The major mechanism for inactivation is cell cycle position-dependent phosphorylation.

Rb, p107 and p130 are phosphoproteins that can be prominently phosphorylated at specific serine and threonine residues. Negative regulation of E2F by Rb, p107 and p130 is dynamic, as blocks to E2F function and cell cycle arrest induced by Rb, p107 or p130 can be overcome by cyclin expression (Beijersbergen, *et al*, 1995; Buchkovich, *et al*, 1989; Chen, *et al*, 1989; DeCaprio, *et al*, 1989; Ewen, *et al*, 1992; Ewen, *et al*, 1993; Faha, *et al*, 1992; Hinds, *et al*, 1992; Mayol, *et al*, 1995). As well, transcriptional activation by E2F is more sensitive to repression by a mutant Rb molecule that is constitutively hypophosphorylated, and consequently active (Hamel, *et al*, 1992). Phosphorylation that relieves Rb-mediated repression and potentially p107 and p130, is accomplished by one or more of the cell cycle-dependent kinases (Weinberg *et al*, 1994). D-type cyclins can rescue Rb-mediated cell cycle arrest (Hinds, *et al*, 1992). p130 exists in multiple phosphorylated forms. Two forms of these appear at early G_1 to give way to a third, highly phosphorylated form which is the only form in mid G_1 to S and to G_2/Mphases (Mayol, *et al*, 1995). *In vivo* , release of a p130/E2F complex from the promoter correlated with the induction of cdc2 expression, indicating that gene repression is dependent on p130 (Tommasi and Pfeifer, 1995). Phosphorylation of p107 accompanies the loss of its ability to associate with E2F-4, and p107 induced cell-cycle block can be released by cyclin D/cdk4 but not cyclin E/cdk2 (Beijersbergen *et al*, 1995). p107 also associates with and blocks transactivation by E2F, independent of cyclin/cdk complex binding (Schwarz, *et al*, 1993; Zamanian and LaThangue, 1993; Zhu, *et al*, 1993). All Rb proteins are highly phosphorylated on multiple serine and threonine residues during S phase when E2F activity is highest, and hypophosphorylated in arrested cells when E2F activity is low. The E2F complex therefore serves a dual regulatory role:

association with Rb proteins, represses transcription, while phosphorylation and subsequent release of the Rb proteins induces E2F-mediated transcription (reviewed in Dyson, 1998; Weinberg, 1995b).

1.4. Rb, p107 and p130 during embryogenesis

Cellular determination and subsequent terminal differentiation require the transcriptional induction of cell-type specific genes and the arrest of cell proliferation for complete differentiation (reviewed in Sidle, *et al*, 1996; Wiman, 1993). Particularly, cell cycle promoting factors are inactivated or transcriptionally repressed in many terminally differentiated cells as these have irreversibly withdrawn from the cell cycle. Multiple and overlapping mechanisms may control terminal differentiation and cell cycle arrest. A central feature of arrest however is inactivation of cdks and activation of mediators of negative cell cycle control including the cdk inhibitors and the Rb and p130 proteins (Corbeil, *et al*, 1995; Halevy, *et al*, 1995; Kiess, *et al*, 1995; Parker, *et al*, 1995; Slack, *et al*, 1993; Slack, *et al*, 1995). Specifically, in differentiating cells the Rb proteins are implicated in the integration of cell cycle repression and induction of terminal differentiation, as well as maintenance or survival of these cells.

1.4.i. Expression profiles during development

Rb, p107 and p130 are differentially expressed during embryogenesis, indicating distinct as well as overlapping roles (Jiang, *et al*, 1997). The Rb protein is detected in mouse embryos as early as 9.5 dpc, with highest expression in brain, spinal cord and liver at 12.5-14.5 dpc (Bernards, *et al*, 1989). Rb is highly expressed during neurogenesis, hematopoiesis, skeletal myogenesis and lens development. Rb expression is detected in both proliferating and post-mitotic neurons and glial cells in the CNS, and the ganglion layer of the retina. However, the appearance of hypophosphorylated Rb protein at 12.5-14.5 dpc coincides with the time most neurons in the mid- and hindbrain have left the cell

cycle (Lee, *et al*, 1994). In epithelial tissues, Rb protein is only expressed in the more differentiated layers (Szekely, *et al*, 1992). There is a high level of protein expression in blood-forming cells of fetal liver, osteoblasts, and skeletal muscle, but otherwise a high degree of heterogeneity exists.

p130 is expressed as early as 8.5 dpc, and then throughout embryogenesis. It appears to be ubiquitously expressed, reaching a peak at 13.5 dpc (Chen, *et al*, 1996a; Jiang, *et al*, 1997; Pertile, *et al*, 1995). The low levels of detectable expression may have precluded a clear analysis of its specific expression profile. High levels of p130 are detected in all adult tissues.

p107 is expressed prominently in heart, lung, kidney and intestine during development, with levels peaking at 13.5 dpc. In the developing liver and CNS, p107 expression overlaps that of Rb. In most other tissues examined and in the newborn, only very low levels of p107 are present (Jiang, *et al*, 1997). A second 2.4 kb transcript is observed in addition to the wildtype 4.8 kb, and both are virtually undetected in adult tissues (Kim, *et al*, 1995). This 2.4 transcript appears to arise by alternate splicing of a common precursor and lacks the sequences encoding the spacer and B subdomain.

1.4.ii. Inactivation by viral oncoproteins

The expression of viral oncoproteins during the development of specific tissues has demonstrated the importance of the Rb proteins in normal growth control, cell differentiation and survival. The human papillomavirus-16 E6 and E7 oncoproteins inactivate cellular p53 and Rb, p107 and p130, respectively. Expression of E7 in the developing eye resulted in microphthalmia and cataracts, inhibition of lens fiber cell differentiation, inappropriate proliferation in regions of the lens and apoptosis (Pan and Griep, 1994). Expression of an E7 protein that is defective for binding the Rb proteins, did not affect eye development. This result indicates that the Rb proteins regulate exit from the normal cell division cycle in differentiating lens fiber cells. If E6 was expressed

with E7, lens tumours resulted, indicating that p53 function was required to protect from uncontrolled growth. Likewise, in embryos that are genotypically $Rb^{-/-}$ $p53^{-/-}$, lens fibre cells continued to proliferate and apoptosis was markedly reduced (Morgenbesser, *et al*, 1994). Significantly, loss of function of Rb is not the rate-limiting step to development of retinoblastomas in mice.

Mice expressing SV40 T antigen also develop retinoblastomas at high frequency suggesting that Rb, p107 and p130 function in a concerted manner to suppress tumourigenesis (Windle, *et al*, 1990). Consistent with these results, mice harbouring Rb, p107 and p53 functionally null proteins, through a combination of gene targeting and transgene expression, also develop retinoblastomas (Robanus-Maandag, *et al*, 1998). Taken together, the Rb proteins function in concert to control cell cycle progression and exit. p107 appears to functionally compensate for Rb-deficiency in the mouse eye and p53 protects the tissue from uncontrolled or inappropriate cell growth.

1.4.iii. Gene-targeted inactivation

Embryos that are Rb-deficient, due to homozygous loss-of-function mutations (designated $^{-/-}$) in the gene, die *in utero* between day 13.5 and 15.5 of gestation, and exhibit defects in erythropoiesis and extensive cell death in the CNS (Clarke, *et al*, 1992; Jacks, *et al*, 1992; Lee, *et al*, 1992; see comment Harlow, 1992). The $Rb^{-/-}$ fetal liver displayed reduced cellularity and immature, nucleated red blood cells were predominant in the circulation. Interestingly, during the *in vitro* differentiation of erythroleukemia cells, the majority of Rb is hypophosphorylated and the levels of Rb mRNA and protein increase 3-5 fold (Richon, *et al*, 1992). Rb appears to be intimately involved in the control of the terminal cell division of erythroid cells.

The $Rb^{-/-}$ retina appeared normal in the mutant mice, but the eye lens structure was highly disorganized and displayed improper fibre cell differentiation, ectopic mitoses and increased apoptosis and cellular degeneration (Maandag, *et al*, 1994). There was

massive cell death in the CNS, apoptosis was detected in the post-mitotic layers of the brain and the spinal cord, and furthermore, the spinal ganglia were completely degenerated in embryos surviving beyond 14.5 dpc (Lee, *et al*, 1994; Lee, *et al*, 1992). FACS analysis revealed that cells from the $Rb^{-/-}$ hindbrain region at E13.5 contained an inappropriately high proportion of proliferating cells. Although the central and peripheral nervous systems exhibited ectopic proliferation and marked apoptosis, the expression patterns of some differentiation markers were normal. When cultured from the $Rb^{-/-}$ embryos, the morphology of primary dorsal root ganglia cells was aberrant and there were decreases in neuronal cell survival and in neurite outgrowth (Lee, *et al*, 1994). Significantly, the expression level of p130 was appreciably higher in the $Rb^{-/-}$ brains, indicating that p130 may partially compensate for the loss of Rb in neuronal cell types (Slack, *et al*, 1998). These observations indicated that neuronal maturation was deficient or blocked, and supported that Rb plays a major role in establishing the post-mitotic state of neuronal cells.

The *Rb* heterozygous mice are viable but are predisposed to neuroendocrine tumours, specifically pituitary and thyroid tumours. Additionally, sites of thyroid C cell metastases were found in the lungs of the heterozygous mice. By genotyping the pituitary tumours that developed, somatic mutation of the remaining wildtype Rb allele was demonstrated (Hu, *et al*, 1994; Jacks, *et al*, 1992).

As Rb-deficiency during embryonic development affects the normal differentiation of a number of different cell types and results in early lethality, to assess postnatal effects of loss-of-function mutation in *Rb* (for example, on tumourigenesis) a series of rescue experiments have been performed. Overexpression of human Rb in transgenic mice leads to a dwarf phenotype, however, transgene expression in an Rb-null background resulted in normal healthy mice (Bignon, *et al*, 1993). This result indicated

that the phenotype described previously is attributable to loss of Rb and not secondary affects. A similar approach was employed using an Rb minitransgene (Zacksenhaus, *et al*, 1996). This weak allele permitted survival of $Rb^{-/-}$ embryos to term, and revealed a role for Rb in skeletal muscle terminal differentiation (section 1.4).

A second series of experiments has examined the ability of $Rb^{-/-}$ ES cells to contribute to tissue development in chimeric embryos (Maandag, *et al*, 1994; Williams, *et al*, 1994). There are several drawbacks to these chimeric analyses, including the variable contribution of mutant cells to the tissues, adaptive processes during early development that may modify the effects of the mutation and the work involved, as each chimeric mouse is generated by embryo manipulation. However, these experiments do enable investigators to generate mice composed of mutant ($Rb^{-/-}$) and wildtype cells. Chimeric embryos and mice with high (80%) $Rb^{-/-}$ ES contribution to the retinal pigment and tail were viable, and showed no abnormalities in the developing brain, spinal cord and adult CNS. The $Rb^{-/-}$ cell contribution to the CNS however, was variable, and low. In the retina, ectopic mitoses and substantial cell degeneration was detected, and the formation of lens fibre cells was disturbed. In addition to being highly disorganized, chimeric lenses exhibited cataracts. Rb appears to be absolutely required for proper lens development, as revealed by cell death and disorganization in the chimeras and in the transgenic mice expressing the weak Rb allele (Zacksenhaus, *et al*, 1996). Nearly all chimeric animals died with pituitary gland tumours, derived exclusively from $Rb^{-/-}$ cells (Maandag, *et al*, 1994). An increase of nucleated red blood cells occurred prenatally during fetal liver erythropoiesis in the chimeras, however in mice, mature Rb-deficient erythrocytes were present. This data indicated that the deficit previously observed in $Rb^{-/-}$ embryos resulted from a delay rather than a block in erythroid differentiation. The presence of nucleated erythrocytes in the peripheral blood and extensive extramedullary erythropoiesis indicated that the $Rb^{-/-}$ erythrocytes were not completely normal. These

experiments also revealed that the erythrocyte phenotype was cell-autonomous (Hu, *et al*, 1997). As well, the proliferation rates in spleen colony-forming assays of $Rb^{-/-}$ cells were higher than wildtype, suggesting that highly proliferative $Rb^{-/-}$ erythrocytes may be delayed in exiting the cell cycle. Significantly, in transplantation experiments, the transferred $Rb^{-/-}$ fetal liver cells displayed characteristics in short and long term hematopoietic cultures that indicated most blood cell lineages matured normally.

So despite its ubiquitous expression, loss of Rb function results in tissue and cell-type specific effects indicating specific requirements for Rb during development. Disruption of the Rb pathway results in a variety of cell-type dependent phenotypes, that include inappropriate proliferation, inappropriate entry into S phase leading to apoptosis, delayed differentiation or endoreduplication without mitosis (Clarke, *et al*, 1992; Jacks, *et al*, 1992; Lee, *et al*, 1994; Lee, *et al*, 1992; MacLeod, *et al*, 1996; Zacksenhaus, *et al*, 1996). Analysis of mice lacking genes that regulate Rb, and Rb effectors demonstrated that other genes in this epistatic pathway also have tissue-specific effects during development and affect specific tumor susceptibility in mice (Fantl, *et al*, 1995; Field, *et al*, 1996; Yamasaki, *et al*, 1996)

Mice lacking either p107 or p130 in a mixed 129/Sv:C57BL/6J genetic background exhibited no overt phenotype, were viable and fertile, and embryonic fibroblasts derived from the mutants displayed normal cell-cycle kinetics (Cobrinik, *et al.*, 1996; Hurford, *et al.*, 1997; Lee, *et al.*, 1996). Functional compensation in the p130 mutant mice was suggested by the presence of p107/E2F-4 complexes in mature $p130^{-/-}$ thymocytes. Furthermore, in *p107/p130* compound mutants, Rb was found in complexes with E2F-4 (Mulligan, *et al.*, 1998). This finding was particularly significant since Rb does not preferentially associate with E2F-4, and therefore indicated the extent of compensation between the p130 and Rb proteins. Embryos lacking both Rb and p107 in

the 129Sv:C57Bl/6J hybrid background died *in utero* two days earlier than Rb-deficient embryos, and exhibited extensive apoptosis in the liver and CNS suggesting some redundancy (overlap) in the function of these proteins (Lee, *et al.*, 1996). Mice that lack both p130 and p107 died soon after birth due to a rib defect and exhibited defective endochondral bone development (Cobrinik, *et al.*, 1996). These data suggested that p107 and p130 have relatively subtle roles in regulating the cell cycle and again, that a significant degree of overlap in function exists between the proteins. As well, consistent with the Rb proteins specifically regulating E2F activity, different patterns of inappropriate cell proliferation were observed in $Rb^{-/-}$ and the compound $p107^{-/-};p130^{-/-}$ embryos. Recall that E2F-dependent transcription was perturbed in distinct sets of genes in $Rb^{-/-}$ and $p107^{-/-};p130^{-/-}$ EFs (Hurford, *et al*, 1997).

1.4.iv. E2F during development

E2F genes are also differentially expressed during the development of distinct tissues. During mouse nervous system development, for example, E2F-1, 2 and 5, first detected at 9.5 dpc, are expressed in the forebrain by E11.5, and throughout the CNS by 12.5 dpc (Dagnino, *et al.*, 1997a). Essentially, these E2F factors are expressed in proliferating, undifferentiated neuronal precursors and are down-regulated as neurons differentiate. In the retina, E2F-3 expression is up-regulated as retinoblasts differentiate in the ganglion cell layer. In non-neuronal tissue, E2F-2 and -4 are associated with proliferative regions including chondrocytes and the thymic cortex. During epithelial development, E2F-2 and 4 appear to particitpate in maintaining epithelial cells in a proliferative, undifferentiated state. Subsequently, E2F-5 appears in quiescent cells and may function to maintain the differentiated state (Dagnino, *et al.*, 1997b).

The phenotype of *E2F-1* gene-targeting in mice also varies, dependent on the tissue context, and ranges from inappropriate cell proliferation, tumourigenesis in the reproductive tract and lung; reduced apoptosis in immature thymocytes; to reduced cell

proliferation in the testis (Field, *et al.*, 1996; Yamasaki, *et al.*, 1996). These results indicate that the major function imposed by E2F-1 is cell-type dependent, and also that in many tissues, functionally overlapping factors, potentially E2F-2 and 3, are present and compensating. By removing E2F-1 and consequently Rb-dependent transcriptional repression, the deregulated expression of E2F-dependent genes may result in uncontrolled cell growth and oncogenesis. Interestingly, the homozygous loss of DP-1 in mice results in embryonic lethality, presumably since loss of DP-1 would affect the function of all E2F-type factors (Yamasaki, unpublished observation). Taken together, E2F factors, known effectors of Rb, functionally overlap to an extent; and are absolutely required in cell-specific contexts.

1.4.v. Differentiation in inducible cell lines

The levels of Rb, p107 and p130, their state of phosphorylation and their interactions with specific E2F factors have been analyzed in a variety of cell lines that can be induced to differentiate. For example, the P19 embryonic carcinoma cell line can be induced to differentiate to neuroectodermal cell types with retinoic acid treatment or mesodermal cell types with DMSO treatment (Jones-Villeneuve, *et al.*, 1982; Rudnicki and McBurney, 1987a). A dramatic 10-fold induction of Rb levels accompanies the induction of neuroectoderm in mouse embryos and in differentiating cultures of P19 (Slack, *et al.*, 1993; Slack, *et al.*, 1995). Cells transfected prior to induction with adenovirus E1A mutants able to bind Rb, p107 and p130 exhibited extensive cell death, specifically neurons and astrocytes were lost. E1A expression precluded P19 differentiation into mesodermal lineages, cardiac or skeletal muscle, however no apoptosis was observed. Recent work also supports that although the induction of differentiation does not require Rb, p107 and p130, the cell cycle exit and survival of determined neurons is dependent upon functional Rb proteins (Slack, *et al.*, 1998). During the course of P19 neuronal differentiation, the composition of E2F-containing

complexes proceeds from free E2F, Rb or p107-containing complexes to those fully-complexed with Rb and p130 (Corbeil, *et al.*, 1995).

As found in P19 cells, during the differentiation of the neuroblastoma cell line, LAN-5, p130 levels increase. p130 was detected as the major component of the E2F complex on the E2F site of the B-myb promoter, repressing transcription in differentiating cells. E2F-4 expression was also up-regulated and underwent changes in cellular localization (Garriga, *et al.*, 1998).

During the induced differentiation of a myeloid cell line, p107 levels remain high for the first four days and then decrease dramatically, concomitant with an increase in p130 levels and the accumulation of post-mitotic granulocytes (Garriga, *et al.*, 1998). This change in expression may reflect p130-mediated repression of p107 transcription. Although these experiments are correlative, they strongly suggest that Rb protein/E2F complexes coordinate cell cycle exit and terminal differentiation.

1.5. Roles for the Rb proteins during skeletal myogenesis

The interdependence between skeletal muscle terminal differentiation and cell-cycle control has been long appreciated (reviewed Lassar, *et al.*, 1994; Mainone and Amati, 1997). Skeletal muscle is derived from segmented paraxial mesoderm, somites, arranged on either side of the neural tube. Specifically, skeletal muscle originates from the dermomyotomal compartment of the somite (reviewed in Buckingham, 1994; Cossu, *et al.*, 1996; Hauschka, 1994). Vertebrate skeletal muscle development is characterized by irreversible withdrawal of undifferentiated precursors into a G_0/G_1 arrested state (reviewed Lassar, *et al.*, 1994; Olson, 1992). Environmental signals that promote cell cycle progression through G_1 effectively suppress myogenic differentiation in cell culture models (Clegg, *et al.*, 1987; Massague, *et al.*, 1986; Olson, *et al.*, 1986). Once terminally differentiated cells are established, they cannot be re-induced to enter the cell cycle but

remain resilient to further mitogenic stimulus. Skeletal muscle terminal differentiation is an appropriate system for examining the involvement of the Rb factors and molecular mechanisms of differentiation for several reasons. The endogenous muscle-specific gene activation profile is very well-characterized. Secondly, the differentiated cells become unresponsive to further mitogen stimulation, so they initiate and maintain a permanent cell-cycle withdrawal. Finally, the phenotypic changes that accompany terminal differentiation are very distinct, involving a transition from rapidly growing, mono-nucleated cells called myoblasts to multi-nucleated and tubular myotubes.

1.5.i. The muscle regulatory factors

The muscle regulatory factors (MRFs) constitute a gene family of basic helix-loop-helix (HLH) transcription factors that are central to the determination and differentiation of skeletal muscle (reviewed in Weintraub, *et al.*, 1991; Weintraub, 1993; Rudnicki and Jaenisch, 1995). These were identified on the basis of their capacity to convert non-muscle cells into skeletal muscle. The four MRFs each contain a basic domain involved in DNA binding and an HLH domain involved in homo- or heterodimerization with other HLH proteins that enhance or inhibit MRF activity (E proteins and Id proteins, respectively) (Benezra, *et al.*, 1990; Murre, *et al.*, 1989). At least one of these factors, MyoD, participates in the cell's withdrawal from the cycle and in G_0 maintenance by activating mechanisms that are not directly related to their tissue-specific function. MyoD and Myf5 are primary factors that together play an essential role in muscle fate determination (Braun, *et al.*, 1992; Rudnicki, *et al.*, 1992; Rudnicki, *et al.*, 1993). Expression of MyoD and/or Myf 5 can precede cell cycle arrest and differentiation (Braun, *et al.*, 1989; Davis, *et al.*, 1987). Myogenin, in contrast, is essential for differentiation of most skeletal muscle *in vivo* and its expression is typically up-regulated at the onset of differentiation in inducible cell lines (Edmondson and Olson, 1989; Hasty, *et al.*, 1993; Nabashima, *et al.*, 1993; Thayer, *et al.*, 1989). Myogenin and

MRF4 represent factors that act later in muscle development, and are referred to as secondary or differentiation factors. Interplay between the MRFs and members of the Rb family is implicated in the irreversible withdrawal from the cell cycle, the elaboration of late and terminal skeletal muscle differentiation and survival.

1.5.ii. Viral oncoproteins block myogenesis

Terminal differentiation has been referred to as a process integrated with cell cycle arrest that requires continuous, active control. DNA tumor virus oncoproteins that were known to disrupt growth control can also inhibit differentiation. The expression of adenovirus E1A, SV40 or polyomavirus large T antigens blocked muscle differentiation (Braun, *et al.*, 1992; Caruso, *et al.*, 1993; Fimia, *et al.*, 1998; Maione, *et al.*, 1994; Slack, *et al.*, 1995; Tedesco, *et al.*, 1995). Expression of E1A in terminally differentiated muscle cells reactivated the cell cycle and suppressed tissue-specific genes (Tiainen, *et al.*, 1996). These studies have indicated a critical role for the Rb proteins as suppressors of cell proliferation in the differentiation pathway.

1.5.iii. Cyclins and cdks in muscle differentiation

The MRFs' negative effect on cell growth could be partly mediated by inactivation of growth-response genes and induction of growth inhibitors, including the cdk inhibitors. Accumulating evidence points to a significant functional interaction between the G_1 cdk inhibitors and regulators of muscle differentiation. p21 mRNA, protein and activity are significantly up-regulated during MyoD-induced differentiation of both myogenic and non-myogenic cells (Guo, *et al.*, 1995; Halevy, *et al.*, 1995 Missaro *et al*, 1995). Actually, p21 expression is sustained in myotubes re-exposed to high concentration of mitogens, indicating that expression of p21 is central in promoting terminal cell cycle arrest during myocyte differentiation (Guo and Walsh, 1997; Guo, *et al.*, 1995). Consistent with this, during mouse embryogenesis, the p21 expression pattern correlates with the terminal differentiation of multiple cell lineages including skeletal

muscle, cartilage, and skin (Parker, *et al.*, 1995). Generally, p21 appears to function during development as an inducible inhibitor that arrests cell proliferation and promotes differentiation.

Ectopic expression of the cdk inhibitors p16, p21 or p27 augmented muscle-specific gene expression in cells maintained in high concentrations of serum, and enhanced myogenic differentiation initiated by MyoD in muscle cell culture (Guo and Walsh, 1997; Guo, *et al.*, 1995; Skapek, *et al.*, 1995; Zabludoff, *et al.*, 1998,). The data indicate that active cyclin/cdk complexes suppress MyoD function in proliferating cells. Mice deficient for p21, p27, or p16 function do not however exhibit skeletal muscle phenotypes, likely reflecting functional compensation within these families of proteins (Deng, *et al.*, 1995; Fero, *et al.*, 1996; Franklin, *et al.*, 1998; Kiyokawa, *et al.*, 1996; Nakayama, *et al.*, 1996).

Mitogens or factors that inhibit myogenesis induce cyclin D1 expression in myoblasts, and ectopic cyclin D1 or E2F-1 expression inhibits C2C12 myoblast differentiation (Skapek, *et al.*, 1995; Wang, *et al.*, 1995). These results indicate that this pathway functions to inhibit myoblast differentiation . Overexpression of cyclin E and cdk2 rescued the proliferative block initiated by MyoD, and repressed MyoD and myogenin expression. As well, ectopic expression of cyclin A (and E) inhibited muscle gene expression, and correlated with Rb hyperphosphorylation (Skapek, *et al.*, 1996). Cyclin D1 can also inhibit muscle gene expression, even in the presence of a mutant, phosphorylation site-deficient, form of Rb. Therefore G_1 cyclin/cdk activity blocks the initiation of skeletal muscle differentiation by distinct Rb-dependent and independent mechanisms. As alluded to, cyclin D1 expression and inhibition of MyoD transactivation of muscle-specific genes correlate with phosphorylation (inactivity) of MyoD. Taken together, cell cycle promoting factors including cyclins, cdks and E2F inhibit terminal differentiation of skeletal muscle cells.

The MRFs' abilities to activate differentiation-specific genes and induce cell-cycle arrest are negatively regulated by members of the Id family of HLH proteins (reviewed Norton, *et al.*, 1998). These antagonists are induced during mitogenic signaling, and function by sequestering thier basic domain-HLH (bHLH) targets to inactive heterodimers, unable to bind to muscle-specific gene regulatory sequences. Surprisingly, cyclin/cdk complexes can phosphorylate Id2 and Id3 to neutralize their function (Deed, *et al.*, 1997; Hara, *et al.*, 1997). Therefore, specific cdk activity, induced during differentiation, may inhibit Id-mediated repression of myogenesis and contribute to enhanced MRF activity. Indeed, specific cyclin expression (cyclin D3) and cdk activity correlate with skeletal muscle differentiation (Kiess, *et al.*, 1995; Lazaro, *et al.*, 1997)

1.5.iv. E2F

Multiple changes in E2F function and regulation occur upon muscle differentiation. In undifferentiated cells the p107/E2F complex predominates; whereas, the p130/E2F complex is most prominent during cell cycle exit and terminal differentiation of myotubes (Corbeil, *et al.*, 1995; Garriga, *et al.*, 1998; Kiess, *et al.*, 1995; Shin, *et al.*, 1995). A striking 8-fold increase in 130 protein levels accompanied differentiation, concomitant with decrease in p107 expression. This data suggests that p130 may directly regulate p107 transcription. Rb levels also increased significantly during induced cell cycle exit. Potentially, the induction of permanent cell cycle arrest by MyoD is dependent upon cdk inhibition and suppression of E2F-regulated genes required for cell-cycle promotion (Puri, *et al.*, 1997).

The composition of E2F complexes in proliferating and differentiated muscle cell lines indicate that Rb and p130 function in maintenance of terminal cell cycle arrest, and that p107 functions to negatively control cell cycle progression during the proliferative phase. p107 may also contribute to initializing cell cycle arrest.

1.5.v. Phenotypes of *Rb*$^{-/-}$ myoblasts

Schneider and colleagues (1994) demonstrated that Rb is essential in maintaining the post-mitotic state of differentiated myocytes, as Rb-deficient myotubes can be induced by serum to reenter the cell cycle. During the differentiation of the *Rb*$^{-/-}$ cells, p107 expression increased, in contrast to the down-regulation that normally accompanies differentiation. Although p107 appeared to initiate the cell-cycle arrest and functionally substitute for Rb during differentiation, it could not maintain the terminally differentiated state. Further evidence implicating Rb in skeletal myocyte differentiation include the requirement for ectopic expression of Rb to induce MyoD-mediated affects in Rb-deficient cell lines, and that antisense Rb inhibits terminal differentiation of myoblast cells (Gu, *et al.*, 1993a; Kobayashi, *et al.*, 1998; Novitch, *et al.*, 1996). Additionally, in *Rb*$^{-/-}$ fibroblasts, ectopically-expressed MyoD induced aberrant skeletal muscle differentiation. The expression of early differentiation markers was normal but expression of late markers, including myosin heavy chain (MHC) and muscle creatine kinase (MCK), was perturbed. These *Rb*$^{-/-}$ 'differentiated' myocytes accumulated in S and G_2 phases of the cell cycle, and accordingly, expressed high levels of cyclins A, B and cdk2 (Novitch, *et al.*, 1996). These observations indicate that Rb is required for the expression of late skeletal muscle differentiation markers, for the inhibition of DNA synthesis and exit into the G_0 state.

MyoD and myogenin were reported to bind Rb via its pocket domain, and a direct interaction between these factors was suggested to mediate MRF-induced cell-cycle exit and expression of differentiation-specific genes (Gu, *et al.*, 1993a). This work is quite controversial, rather, the heavily supported hypothesis is an indirect interplay between these factors (reviewed in Lassar, *et al.*, 1994).

In addition to promoting cell cycle exit, Rb also appears to inhibit apoptosis during *in vitro* differentiation. Compared with wildtype, Rb-deficient myocytes undergo higher frequencies of apoptosis during differentiation. In the differentiating *Rb* null myocytes, cdk inhibitors were induced and cdk activities were suppressed. These results suggested that an Rb-dependent mechanism(s), and not a cdk inhibitor-mediated activity, normally suppresses apoptosis. Consequently, ectopic Rb expression suppressed programmed cell death during myocyte differentiation (Wang, *et al.*, 1997). Recall that inactivation of Rb in the germline, or Rb, p130 and p107 via expression of specific viral oncoproteins in neuronal cell types, also has serious consequences to survival of this cell type. Deregulated E2F activity is implicated to promote p53-dependent apoptosis in these settings (Wang, *et al.*, 1995).

Evidence from *in vivo* experiments also implicate Rb function in skeletal muscle differentiation. During embryogenesis, Rb is expressed at high level in myogenic cells. $Rb^{-/-}$ mice expressing a weak Rb allele survived to birth and exhibited a generally reduced muscle mass, reduced expression of late muscle-specific genes including MRF4, ectopic DNA synthesis (consistent with *in vitro* experiments) and high levels of apoptosis (Jiang, *et al.*, 1997; Zacksenhaus, *et al.*, 1996). The marked apoptosis indicated a requirement for Rb in myocyte survival *in vivo*. Analysis of $Rb^{-/-}$; wildtype chimeric mice did not reveal a skeletal muscle phenotype, as fusion of $Rb^{-/-}$ and wildtype myoblasts into multi-nucleated myotubes presumably rescued Rb-deficient nuclei (Maandag, *et al.*, 1994; Williams, *et al.*, 1994).

Taken together, the data indicate that in the absence of functional Rb, p107 (and p130) can compensate to an extent to initiate cell cycle arrest, but the differentiation program is not successfully integrated with maintenance of a G_1/G_0 state. Deregulation of Rb effectors then promote apoptosis. That p130 functions later during skeletal muscle development is suggested by the existence of p130/E2F complexes and high levels of

expression in post-mitotic myocytes (Corbeil, *et al.*, 1995; Garriga, *et al.*, 1998; Kiess, *et al.*, 1995; Shin, *et al.*, 1995).

1.6. Gene targeting in ES cells and mice

The development of cultured ES cells and the ability to target these cell lines by homologous recombination has revolutionized the approach to assessing gene function (Evans and Kaufman, 1981; Martin, 1981). Because ES cells are pluripotent, genome modifications (*i.e.* null mutations) generated in ES cells can be introduced into the developing mouse. The basic design of the gene-targeting vector incorporates expression cassettes to select for integration and select against random integration, thereby enriching for targeted-integration of the construct (reviewed in Capecchi, 1989). In the vast majority of gene-targeting experiments, the PGK-neomycin selectable marker disrupts an exon and is flanked by several kb of genomic sequence derived from the locus to be targeted. Following selection and confirmation, the gene-targeted ES cells are injected into recipient blastocyst-staged embryos. Given that the ES cells contribute to the development of this embryo, chimeric mice are generated. The chimera is then mated to wildtype mice, most commonly of a different genetic background than the ES cells are derived. If the cells harbouring the mutation have developed into germ cells (i.e. sperm) in the chimera, the ES cell mutation will be transmitted through the germline, and some progeny (referred to as the F_1 generation) of this breeding will be heterozygous for the introduced mutation. Interbreeding these heterozygous mice produces F_2 mice with wildtype, heterozygous or homozygous mutant genotypes.

1.6.1. Functional overlap and compensation

Functional overlap and functional compensation have been irrefutably demonstrated through numerous gene targeting experiments. Many of the genes that have been mutated in ES cells and mice are members of gene families with overlapping

expression profiles and functions. The reason that investigators undertake gene-targeting experiments is to address the unique, non-overlapping functions of a specific gene *in vivo*. However, when a gene is disrupted, a cascade of changes can be initiated from the earliest stages of development (reviewed in Gerlai, 1996). Therefore, although the initial focus is the phenotype that results from removing this gene function; investigators must consider whether removing the gene function altered the expression or activity of related or unrelated gene products in an attempt to maintain proper growth, development or function of the cell and tissue in general. Functional overlap (sometimes referred to as redundancy) would not be an issue if the gene's function is absolutely unique or expression is stringently restricted to specific, non-overlapping tissues. Unexpected, often subtle phenotypes do result, especially when closely related genes act in a concerted or equivalent manner; and expression patterns are overlapping, perhaps even identical. Functional compensation was clearly demonstrated in the mouse by an elegant experiment in which the expression of one gene of a gene family, engrailed-2, was dependent on the endogenous promoter and locus of the related gene, engrailed-1 (Hanks, *et al.*, 1995). This study revealed that although one gene could fully compensate for the related gene, temporally distinct expression resulted in the specific functions and phenotypes displayed in the individual mutants. Therefore, when considering the roles of ubiquitously expressed factors such as p107 and p130 that function in basic cell cycle control, in the final analysis of the phenotype, functional overlap and potential compensation are anticipated.

1.6.2. Concept of modifier genes

In addition to being a vehicle for basic genetic experimentation, there is outstanding interest in the development and use of mouse models, for a variety of reasons, of human genetic disease. Mice have a short gestational period, have large litter sizes, inbred strains are available, and controlled breeding can be performed. The

differences in penetrance and expressivity of human dominant diseases may be caused by environmental factors, locus or allelic heterogeneity or genetic modification. In mice, strain-specific effects involving the identical allele (or transgene) have clearly defined a role for modifier genes (reviewed in Erickson, 1996; Gerlai, 1996). Modifiers are allelic variants at loci other than the one being modified. Simply stated, the allele for a gene X in the Balb/c inbred strain may be different from the allele for gene X in C57Bl/6. Allelic variation is predominant among inbred strains, and even between substrains. A recent analysis of 129SV mice revealed a 45% polymorphism between some substrains, which is quite astounding (Simpson, *et al.*, 1997).

There are several strains of inbred mice utilized in genetic experiments. The most commonly inbred mouse strain in use is C57Bl/6, and the second or third most common is Balb/c. C57Bl/6 usually has good breeding performance, and Balb/c is referred to as a general-purpose strain with good breeding performance and a long reproductive life (Jackson Laboratories). These strains originated from a common ancestry, but have been separated for approximately 100 years (Hogan, *et al.*, 1986). Given that the average lifespan of a mouse is 2-3 years, 100 years represents 30-50 inbred "lifetimes". The allelic variation between these strains is presumably very high.

In almost all gene-targeting experiments, embryonic stem cells derived from 129 mouse substrains have been utilized. For reasons that remain unresolved, 129 mice are particularly amenable for the derivation of ES cells. Consequently, the targeted mutations are usually derived within the 129 mouse genome, and the chimeras are mated in the inbred strain or to a different strain than 129, for example C57Bl/6 or Balb/c. The progeny of these matings are not only heterozygous for the mutant/targeted allele, but have one set of chromosomes from strain 129 and another from i.e. Balb/c. Subsequently, deriving a homozygous mutant strain on a mixed genetic background will

establish a new combination of alleles from the two original strains that may produce phenotypes independent of, or interacting with, the targeted alleles.

Several investigators have reported that one mutation can have striking variation in phenotype on a different genetic background. This variation is due to different alleles at modifying loci in various inbred strains. For example, a mutation in the epidermal growth factor receptor (EGFR) resulted in perimplantation lethality on a CF-1 background, on a 129Sv background mutants died at mid-gestation and on a CD-1 background, the mutants lived for up to three weeks (Sibilia and Wagner, 1995; Threadgill, *et al.*, 1995).

In keeping with the theme of genetic variation, a mutation in the homologous gene in mice does not always lead to the same phenotype as is found in man. Ironically, probably the best known example of this is the *Rb* gene-targeting experiments. Homozygous mutation of *Rb* in mice does not result in retinoblastoma (reviewed in Harlow, 1992).

The modifier gene(s) implicated in phenotypic variation may interact directly with the gene being modified, in an epistatic pathway, or in similar/parallel pathways, or very much indirectly. Although the cost (time and financial commitment) is considerable, many investigators, including those in the cancer field, are exploiting strain-differences to assess and identify genes that influence phenotype. For example, both tumour susceptibility and progression to a metastatic phenotype have been analyzed to identify modifying genes (Fineman, *et al.*, 1998; Lifsted, *et al.*, 1998). The analysis of modifying genes is one example of the phenotype-driven approaches in mice that are coming into practice. Importantly, these genetic strain differences in mice represent a valuable resource to the study of human disease initiation and progression. By identifying modifier genes in the mouse, we may uncover how these same genes in man modify development, growth and pathophysiology.

1.7 Summary of intent

The cloning and biochemical analyses of Rb-related p130 and p107 have elucidated important interactions of these proteins with critical components of the cell cycle machinery. Experiments documented in this introduction have also revealed cell-type specific and differentiation-specific interactions, and functions to some extent.

As these genes are not directly associated with human pathology, such as tumourigenesis, and other *in vivo* analyses of their functions are confounded by the inactivation of all three family members, the specific functions of these individual proteins during cellular proliferation and differentiation are unresolved. The purposes of the work presented here were to assess the requirements for p130 and p107 in the developing mouse by targeting these genes for inactivation in ES cells and mice. By assessing the mutants' development, roles for these factors in proliferation, apoptosis and differentiation of all cell types can be assessed.

Chapter 3 of this thesis describes the cloning and expression analysis of the mouse p130 cDNA. Chapters 4 through 7 present the generation and characterization of embryos, mice and primary cells carrying the individual *p130* and *p107* null mutations. Embryos deficient for p130 displayed arrested growth and development and died between E11-13. Histological analysis revealed varying degrees of deficiencies in neural, dermomyotomal and cardiac structures. The results indicated an essential role for p130 in normal development, that was strain-dependent. Notably, p130 was required for the survival of specific tissues, particularly neuronal cell types. Mice lacking p107 were viable and fertile, suggesting functional compensation by related factors. The $p107^{-/-}$ mice did exhibit a growth deficit and developed a myeloproliferative disorder. Data from the analysis of primary fibroblasts and myoblasts from the p107-deficient embryos and adults support that p107 plays a central role in negatively regulating cell cycle progression. Taken together, this thesis contains several novel observations concerning

the unique *in vivo* functions of p130 and p107. As well it confirms different extents of functional overlap within the Rb family and contributes to the overall understanding of p130 and p107 as cell cycle, and cellular differentiation regulators. Additionally, the work demonstrates strain-dependent phenotypes for both *p130* and *p107* null mutations, and provides a reservoir of mice and cell-types to be analyzed in future experiments that evaluate modifier genes and mechanistic details.

CHAPTER 2

Materials and methods

2.1 Bacteria and DNA

2.1.i. Bacterial culture

All recombinant plasmids were amplified and maintained in *Escherichia coli* strain DH5α. DH5α was cultured in Lauria-Bertani (LB) medium or agar (1% w/v bacto-tryptone, 0.5% w/v yeast extract, 1% w/v NaCl, pH7.0 and for agar also containing 1.5% w/v bacto agar, 0.2% w/v glucose) (Sambrook, *et al.*, 1989) . DH5α transformed with recombinant plasmid were cultured in LB or on LB agar plates both containing 50 ug/ml of ampicillin. Stocks of bacterial cultures were stored at –70°C in 20% glycerol.

2.1.ii. Transformation of bacteria

Electrocompetent DH5α bacteria were prepared by standard procedure. 1 µl (2-4 ng DNA) of a ligation reaction was added to 40 µl of electrocompetent bacteria in a Gene Pulser/E. coli Pulser cuvette (Bio-Rad) and subsequently electroporated at 2.25-2.50 kV using a Bio-Rad *E. coli* Pulser. This culture was transferred to 800 µl of SOC media and agitated at 37°C for 30 minutes prior to plating on LB ampicillin plates. Plates were incubated at 37°C for 12-16 hours to visualize colonies.

2.1.iii. DNA manipulations and cloning

All DNA manipulations required for cloning, including small scale preparation of plasmid DNA, determination of DNA concentration, restriction enzyme digests (GIBCO/BRL or Boehringer Mannheim), techniques to remove 5' and 3' overhangs, ligations, phenol:chloroform extractions, ethanol precipitations and agarose gel

electrophoresis are described by Sambrook et al (1989). All DNA fragments for cloning were isolated in low melting point agarose (GIBCO/BRL). PCR-based mutagenesis to create a restriction enzyme site in an exon of p130 (codon 106) was performed as described in PCR primer: a laboratory manual (Dieffenbach and Dveksler, 1995). All oligos were synthesized at the Central Facility of the Institute for Molecular Biology and Biotechnology, McMaster University.

2.1.iv. Large scale isolation of phage and phagemid DNA

The phage SV129J genomic library was plated and screened by standard methods (Sambrook, *et al.*, 1989) using a 720 bp XbaI fragment from the 5' end of the human p130 cDNA (supplied by P. Whyte). The method used to purify phage DNA from the SV129J genomic library was a mid-scale preparation as previously described (Sambrook, *et al.*, 1989). The p130 cDNA was cloned from a λZAP Balb/c thymus cDNA library using a 500 bp EcoRI/HindIII fragment of the mouse p130 genomic clone containing 200 bp of exon sequence. Three phagemids were purified from the library as per the manufacturer's instructions (Stratagene).

2.1.v. Isolation of mouse genomic DNA

At 3-4 weeks of age, approximately 1 cm of the mouse's tail was clipped and incubated in 500 µl of DNA lysis buffer (100 mM Tris HCl pH 8.5, 0.2% SDS, 200 mM NaCl and 1 ug/ml Proteinase K) in an eppendorf tube at 55°C for 8-16 hours (Laird, *et al.*, 1991). The tube was centrifuged for 2 min at 14000 g and the supernatant decanted into a second eppendorf containing 500 µl of isopropanol. Following vortexing, the DNA precipitate was removed with a pipette tip and subsequently dissolved in 200 µl of TE (10 mM Tris HCl, 1 mM EDTA pH 8.0).

2.1.vi. Screening of targeted cell lines and mice by Southern blotting

DNA was isolated from ES cells essentially as described above for tail DNA, with the modification that the ES clones in 24-well dishes were incubated in 500 µl of DNA

lysis buffer at 37°C for 1-4 days, depending on the confluency of the cells in each group of wells. Isopropanol was added to each well and the plates were vigorously shaken on a platform for 1-3 hours. The DNA from each well was then transferred to an eppendorf containing 200 µl TE. A 5-10 µg sample of DNA was used for Southern blotting. DNA fragments, generated by cleavage with appropriate restriction enzymes (GIBCO-BRL or Boehringer Mannheim) and resolved on 0.7-1% agarose gels, were transferred to Hybond N (Amersham) using standard techniques (Sambrook, *et al.*, 1989). Specific RFLPs were detected by hybridization to particular radiolabeled probes, including those derived from 5' and 3' sequences external or internal to the targeting vectors and *neo* sequences.

Blots were prehybridized at 65°C for 2 hours in hybridization solution (Denhardts, 1 mM NaP, 100 µg/ml sonicated salmon sperm DNA, 5 x SSC, 1% SDS and 0.5% dextran sulphate) prior to adding the radiolabelled probe. For random priming, 25-50 ng of the designated probe (in low melting point agarose) was denatured by boiling in buffer containing 2 µl of pd(N6) primers (Pharmacia) and then quickly cooled to 4°C. The polymerization reaction was initiated by adding 2 µl Klenow fragment and 5 µl (50uCi) of α-^{32}P-dCTP (Amersham, 3000 uCi/mM). This mixture was incubated at 37°C for 2 hours. Alternatively, probes were generated using the rediprime II random prime labeling system (Amersham Life Sciences). Unincorporated dNTP's were removed from the mixture using a G-50 Sephadex spin column (Pharmacia), the probe was denatured by boiling and added to the prehybridized blot. Blots were hybridized at 65°C overnight. After hybridization, filters were washed in several changes of 2 x SSC, 0.1% SDS at RT for 40 min, followed by a final wash in 0.2 x SSC, 0.1% SDS at 65°C for 1 hr. Hybridization was visualized by autoradiography in the presence of intensifying screens at -80°C, using Kodak X-OMAT/AR or BIOMAX/MS.

2.1.vii. Sequencing

Sequencing was performed at MOBIX Central Facility with the exception of the p130 cDNA which was sequenced by Stephen Baird at the Canadian Genetic Disease Network's Automated DNA sequencing facility.

2.2 Cell culture

2.2.i. P19 cell culture and differentiation

P19 mouse embryonic carcinoma (EC) cells were cultured in DMEM supplemented with 10% fetal calf serum (GIBCO), 100 U/ml penicillin G and streptomycin sulphate (GIBCO) (Teratomas and Embryonic Stem Cells: A Practical Approach, E.J. Robertson, ed (Oxord: IRL Press), 1987). Differentiation was induced following 2 days in suspension culture with 0.2 υM retinoic acid as previously described (Rudnicki and McBurney, 1987b). P19 transfections were carried out using Lipofectamine reagent (GIBCO) with 2 μg of total DNA and 2 μl of reagent for 4 hrs as per the manufacturer's instructions with optimization. Cells recovered for 24 hrs following transfection prior to the addition of 2 μg/ml puromycin to the media.

2.2.ii. ES cell culture and transfection

J1 ES cells (Li, *et al.*, 1992) were cultured on γ-irradiated (3000 rads) EF in DMEM, 15% FCS, 500 U/ml LIF , 10^{-6} M β-mercaptoethanol (Sigma), 0.1mM non-essential amino acids , 2 mM L-glutamine , 50 μg/ml penicillin and streptomycin sulphate (all GIBCO/BRL) (Gene Targeting: A Practical Approach, A.L. Joyner, ed (Oxford: IRL Press), 1993). Tissue culture plates were coated with 0.1% gelatin approximately 1 hour before plating cells. 5 x 10^7 ES cells were electroporated with 75 μg of linearized targeting vector in electroporation buffer (Thomas and Capecchi, 1987) using the Bio-Rad Cell Pulser at settings of 400 mV, 25 μF. 24 hours after plating, 200 μg/ml of active G418 (GIBCO/BRL) was added to select for transfectants over 8-10 days.

2.2.iii. Primary EF isolation and culture

To isolate 14.5 days *post-coitum* (dpc) EF, timed matings were performed with the morning following plugging designated as 0.5 dpc. Fibroblasts were isolated and cultured as described by Robertson (Teratomas and Embryonic Stem Cells: A Practical Approach, E.J. Robertson, ed (Oxford: IRL Press), 1987). The mitotic index was assessed by ^{3}H-thymidine incorporation. 5 x 10^4 cells were plated and the following day were incubated for 2 hours in 1 μCi/ml (methyl-^{3}H)thymidine (Amersham, @90 Ci/mmol). For FACS analysis of asynchronous (subconfluent) cultures, cells were trypsinized, rinsed twice in PBS and incubated for 30 minutes on ice with 50 μg/ml propidium iodide (Sigma) and 66 units/ml RNase (GIBCO/BRL) in PBS. 10^4 cells were sorted using an Epics-Profile II (Coulter Electronics, Inc., USA). Quantitation of cell cycle distribution was performed using MCYCLE software. EF cultures were synchronized by culturing in 0.1% FCS in DMEM for 72 hours. Cells were restimulated with 10% FCS.

2.2.iv. Primary myoblast culture and differentiation

Myoblasts were isolated from the hindlimbs of adult (>2 months) mice, to avoid isolating fetal myoblasts, as previously described by Rando and Blau (1994). Cultures were maintained in subconfluent monolayer on rat tail collagen-coated plates in Ham's F12 nutrient media supplemented with 20% FCS, 2.5ng/ml bFGF, 50 ug/ml penicilllin/streptomycin and 0.002% fungizone (all from GIBCO/BRL) (Megeney, *et al.*, 1996). To induce differentiation, cells were washed several times in PBS and transferred to DMEM with 5% horse serum (GIBCO/BRL).

2.2.v. Immunocytochemistry

Cells were rinsed twice with PBS and fixed in wells or on plates for 4 minutes at -20°C in cold 90% methanol. Cells were blocked at 37°C with 5% skim milk powder in PBS, and afterward incubated at RT with 1/50 desmin antibody (DAKO) or 1/10 MF20

hybridoma supernatant, washed for 15 min in PBS, and incubated for 1 hr at RT with 1/1000 goat anti-mouse HRP-conjugated secondary antibody (Bio-Rad). Cells were then washed for 15 min with PBS and reacted with 0.6 mg/ml DAB (3,3'-diaminobenzidine tetrahydrochloride) and 0.03% H_2O_2 in 50 mM Tris HCl (pH 7.6). 15-30 min later, when staining was visualized, the plates were rinsed several times in PBS and cover slips were applied prior to photography.

2.3 Analysis of gene expression

2.3.i. Isolation of RNA and mRNA

Total RNA was isolated from tissue by placing approximately 3 cc of tissue in 2 ml 3 M LiCl and 6 M urea and homogenizing for 10 sec (Auffray and Rougeon, 1980). To isolate RNA from cultured cells, RES-1 method was used as previously described (Birnboim, 1988). PolyA+ RNA was selected on oligo-dT cellulose beads as per the manufacturer's instructions (Pharmacia). RNA was quantified by UV absorbance using a Beckman spectrophotometer. The OD260 was used to calculate concentration of diluted RNA samples (1 OD= 42 μg RNA/ml). All solutions used in these procedures, with the exception of Tris, were treated with 0.1% DEPC (Sigma) for at least 12 h at 37°C, followed by autoclaving.

2.3.ii. RT-PCR analysis

Reverse transcriptase (Superscript, GibcoBRL) was reacted in the supplied reaction buffer with approximately 2 μg of total RNA and 50 pmoles oligo-dT primer. PCR was performed using appropriate conditions (denaturation 94°C, annealing at 60°C and extension at 72°C for 1 min each for 30 cycles) and 10 pmol of each oligo specific for p130 cDNA sequence spanning the apparent deletion in the cloned species (forward primer 5'-GCTACCGCAGCATGAGCGAG-3' and reverse primer 5'-CAGCTTCTC-AATGACACACGG-3'). PCR fragments were separated on 2% agarose gels.

2.3.iii. Northern blot analysis

10-20 μg of total RNA or 2-4 μg of polyA+ RNA were electrophoresed in denaturing gels and transferred using standard techniques (Sambrook, *et al.*, 1989). Probes were prepared as previously described (see section 2.1.vii)

2.3.iv. Isolation of protein

To isolate total cellular protein, cultured cells were rinsed twice in PBS and scraped in 500 μl of modified TNE lysis buffer (50 mM Tris pH8.0, 150 mM NaCl, 1% NP40, 2mM EDTA, 100 mM NaF, 10 mM sodium pyrophosphate with 1 mM sodium vanadate, with protease inhibitors 10ug/ml phenylmethylsulfonyl fluoride, aprotinin, leupeptin and pepstatin A (all from Sigma). After incubation on ice for 20-30 minutes, lysates were cleared by a 10 min centrifugation at 4°C, 14000 rpm. A 5 μl aliquot of the lysate was used to determine concentration by the Bradford assay (manufacturer's instructions, Bio-Rad) with bovine serum albumin (Bio-Rad) used to construct a standard curve for each individual experiment.

Tissue protein lysates were prepared by homogenizing tissue approximately 5 sec in EBC lysis buffer (50 mM Tris HCl, 150 mM NaCl, 0.5% NP40, 100 mM NaF, 200 μM NaV with protease inhibitors 10ug/ml phenylmethylsulfonyl fluoride, aprotinin, leupeptin and pepstatin A), or passing embryos twice through an 18G needle. Note, protease inhibitors were added after the tissues were disrupted. Thereafter, lysates were treated as above.

2.3.v. Immunoblot analysis

30-300 μg of total protein was electrophoresed on 7 -12% SDS-PAGE gels and transferred in the Bio-Rad Trans-Blot Cell in transfer buffer (25 mM Tris, 150 mM glycine and 20% methanol) as described in Laboratory Guide to Antibodies (harlow and lane, 1988). Blots were stained with Ponceau S (Sigma) prior to blocking to confirm

equivalent loading/transfer of protein. PVDF membranes (Millipore) were blocked in 5% skim milk powder in TBST (10 mM Tris base, 150 mM NaCl, 0.5% Tween 20) for 30 min at RT prior to incubating for 1 hr with primary antibody. Following five 5 min washes with TBST, blots were incubated with 1/1000 secondary antibody (appropriately goat anti-mouse or goat anti-rabbit HRP-conjugated, Bio-Rad). Following five washes in TBST, immune complexes were visualized using ECL (Amersham) or Supersignal Ultra (Pierce) as per the manufacturer's instructions. Several exposures of each immunoblot were accumulated.

Antibodies used for immunoblotting were specific for p130 (1/1000, C20 Santa Cruz), p107 (1/500, C-18 Santa Cruz), Rb (1/500, G3-245 Pharmingen), cyclin D1 (1/1000, C-20 Santa Cruz), cyclin E (1/1000, M20 Santa Cruz), cyclin A (1/1000, H432 Santa Cruz) and cyclin B1 (1/1000, GNS1 Santa Cruz).

2.3.vi. Immunohistochemistry

Standard methods for processing and sectioning were applied. Antibodies used were specific for Islet-1/2 (1:50, 39.4D5, Developmental Studies Hybridoma Bank), PCNA (1:500, PC10, DAKO), BrdU (1:100, Amersham Cell Proliferation Kit), MF20 supernatant (prepared by R. Perry, hybrioma from Developmental Studies Hybridoma Bank), desmin (1:50, D33, DAKO) and myeloperoxidase (1:200, DAKO). For antigen retrieval, slides were briefly boiled in citrate buffer (10mM citric acid, pH6.0) over 10 min and then cooled for approximately 30 min. Slides were quenched of endogenous peroxidases in 3% H_2O_2 in methanol for 30 min. Peroxidase-conjugated secondary antibodies were detected with AEC (3-amino-9-ethyl-carbazole) chromagen solution for 30 minutes. Slides were lightly counter-stained with hematoxylin.

Apoptosis assays were performed as per the manufacturers' instructions (Oncor and Genzyme)

2.4 Embryo and animal manipulations

2.4.i. Embryo isolation and genotyping

All animal handling was in accordance with institutional guidelines. In order to assess embryonic development, embryos were isolated following timed matings. For 9.5-16.5 dpc, pregnant mice were sacrificed and the uterine horns were removed to 10 cm plates containing PBS. Following this wash, the horns were transferred to a new plate, and a single incision running the length of the horn was made to reveal the embryos and placentas. Embryos were observed for a heart beat and either fixed in 4% PFA/glutaraldehyde or photographed at the dissecting scope prior to fixation. The embryo-derived portion of each placenta was teased away from the maternal portion and placed in 500 µl of DNA lysis buffer (section 2.1.iv) for subsequent genotyping by Southern blot.

2.4.ii. Muscle injury and BrdU *in vivo* labeling

Male animals used to assess skeletal muscle repair were between 2 and 4 months of age. Mice were anaesthetized by intraperitoneal injection with 2.5% avertin. A small incision was made below the knee of the hind limb, revealing the *tibialis anterior* muscle. Using large, blunt-ended tweezers, the instrument was clamped with full force in the mid-section of the muscle. The *TA* was chosen for its ease of identification using clear landmarks and surface location. Then at 4.5 days post-injury, 6 and 3 h prior to collecting the regenerating muscle, BrdU (30 ul/g body weight) was injected IP and the manufacturer's instructions were thereafter followed (Cell Proliferation Kit, Amersham). The crushed and contralateral control muscles were fixed in 10% formalin for 12 h and further processed as described (section 2.3.vi).

Preface to Results Prepared for Publication

The results presented in chapters 3, 4, and jointly 5 and 6 were prepared and submitted for publication (Oncogene, 1996, 12:1433-1440; Development, 1998, 125:4669-4679; Molecular and Cellular Biology, 1998, 18:7455-5465). I performed the majority of the work and experiments described in these chapters, prepared the data for publications and wrote first drafts and at times incorporated necessary revisions. Considerable advice and criticism, especially with regards to organization of results was given by my supervisor, Dr. M.A. Rudnicki. He also made a strong contribution to the final manuscripts. Other authors were included for their very valuable contributions of *p107* heterozygous mutant mice (Rod Hardy); the human p130 cDNA (Peter Whyte); technical assistance with regard to animal handling: sectioning and some staining of histological samples (Chuyan Ying and Linda May); excellent assistance in interpreting histology (Dr. Boris Kablar) and demonstrating methods (Linda May, Dr. Boris Kablar and Dr. Lynn Megeney).

CHAPTER 3

Cloning and Characterization of the Mouse p130 mRNA

3.1. Introduction

The p130 gene is the third member of the retinoblastoma susceptibility gene family to be identified. The human p130-specific cDNA was independently cloned by three groups by virtue of homology to Rb, and the abilities to associate with adenovirus E1A and cellular cdk2 (Hannon, *et al.*, 1993; Li, *et al.*, 1993; Mayol, *et al.*, 1993). The p130 protein more closely resembles p107 outside of the pocket domain, additionally both of these proteins contain intervening sequences between the two domains comprising the "pocket" (Ewen, *et al.*, 1991). This spacer region of p107 and p130 confers the ability to associate with the cell cycle regulatory proteins, cyclins A, E and cdk2 (DeLuca, *et al.*, 1997; Hannon, *et al.*, 1993; Lacy and Whyte, 1997; Li, *et al.*, 1993; Mayol, *et al.*, 1993). The structural differences among the three proteins reflect the unique functions of Rb, p107 and p130.

Several recent studies have addressed the functional differences among these three proteins. A major focus has been the interactions with specific E2F/DP transcription factors. The presence of Rb, p107 or p130 in complexes with the E2F transcription factors is dependent on cell-cycle position. In addition to these specific associations with E2F, Rb, p107 and p130 interact with distinct E2F family members (reviewed Dyson, 1998). Clearly, differences exist in the abilities of, and mechanisms employed by these factors to suppress cell growth (Claudio, *et al.*, 1994; Vairo, *et al.*, 1995). Gene targeting studies have revealed that endogenously expressed p107 or p130 proteins are not capable

of fully substituting for Rb function during embryogenesis. These data support that the members of this gene family are not redundant, although their activities appear to overlap, but do have specific functions (Clarke, *et al.*, 1992; Jacks, *et al.*, 1992; Lee, *et al.*, 1992).

To facilitate the molecular genetic investigation of p130 function during mouse embryonic development, I cloned the full length mouse p130 cDNA from a thymus-derived library using a 5' portion of the human cDNA as a probe. The 4515 bp mouse cDNA encodes a putative 1092 amino acid protein with predicted molecular mass of 123 kD. Northern analysis of P19 EC and retinoic acid (RA)-induced P19 cultures indicates p130 mRNA is not expressed at detectable levels in undifferentiated stem cells and is strongly up-regulated after post-mitotic neurons begin to accumulate in the cultures. Northern analysis of adult tissues indicated that the 4.8 kb p130 mRNA is expressed ubiquitously, however, a putative 5'-truncated 1.7 kb isoform is detected solely in the testis and prostate, and is the abundant form expressed. Overexpression of mouse p130 induced growth suppression of P19 cells and immunoblot analysis of transfected P19 cells suggested the cloned cDNA encodes the fully functional p130 protein.

3.2. Results

3.2.i. Cloning of the mouse p130 cDNA

The mouse p130 cDNA was isolated from a B6/CBAF1J thymus λ ZAP library (Stratagene) using the first 1031 bp from the human p130 cDNA as a probe (Li, *et al.*, 1993). Four clones were identified by this screen and one clone, with the largest insert of about 4.5 kb, was chosen for further study. DNA sequencing revealed that the 4515 bp cDNA contains a 3276 bp open reading frame, with a consensus Kozak translation initiation sequence (Kozak, 1986), encoding a predicted 1092 amino acid protein with a molecular mass of 123 kD (Figure 3.1). The open reading frame is preceded by a 5'-

untranslated region (UTR) of 61 nt containing one in-frame stop codon and is followed by a 3'-UTR of 1178 nt.

The mouse p130 cDNA is highly homologous to the human p130 cDNA (Hannon, *et al.*, 1993; Li, *et al.*, 1993; Mayol, *et al.*, 1993) with an overall 66.4% similarity at the nucleotide level (not shown) and 88.9% identity at the protein level (Figure 3.2). Interestingly, the mouse p130 cDNA clone I isolated contains a number of alterations relative to human p130 notably, within the coding region, an in-frame deletion of 129 bp between nt 691 and 692 (analogous to nt 708-837 of the human sequence) removing 43 aa of conserved potential coding sequence. The open reading frame also contains, relative to the human sequence, two point deletions (nts 115 and 163), three 2 nt deletions (nts 111, 151, 162), and a 6 nt (nts 3005-3012) insertion. In addition, the mouse 5' UTR contains a 2 nt deletion relative to the human sequence.

cDNA sequencing of both strands revealed an open reading frame that consists of 3276 nucleotides which potentially encode 1092 aa of the p130 protein. Most striking in the alignment of the mouse and human deduced amino acid sequence is the lack of 43 aa of conserved sequences following position 211 of the mouse, relative to the human sequence. This appears to be the major difference between the two orthologs. In addition, the mouse p130 contains a single aa deletion at residue 637, a 2 aa deletion at residue 889, a 3 aa deletion at residue 913 and a 2 aa insertion between residues 979 and 982 relative to the human sequence. To determine whether the 43 aa deletion was an alternative splice variant or a cloning artifact, I performed RT-PCR with primers flanking the deletion on total RNA isolated from mouse thymus, muscle, liver and heart tissues (Figure 3.3). Although the preliminary data indicated that the mouse p130 mRNAs uniformly contained this deletion, further analysis (P. Seale) was performed with a new primer set and tissue extracts to conclusively demonstrate that the deletion at position 211

actually does not represent the normal sequence of the mouse p130 protein. Interestingly, two other groups cloned mouse p130 cDNAs, and both of these groups reported slight sequence variations (Chen, *et al.*, 1996a; Pertile, *et al.*, 1995). As this alteration following amino acid position 211 does not remove sequences with a defined activity, for example domains A and B of the "pocket" region, this cDNA was used in all subsequent experiments described below.

3.2.ii. Northern analysis of p130 expression during P19 differentiation and in adult mouse tissues.

To examine the expression of p130 mRNA during cell proliferation and differentiation as well as in adult tissues, Northern blot experiments were performed using the mouse p130 cDNA as a probe, and total RNA isolated from cultured P19 cells and from a panel of mouse tissues. To evaluate p130 function during proliferation and differentiation, embryonic carcinoma (EC) or stem (ES) cell lines were used as a model system, since these otherwise continuous cell lines can be induced to differentiate into a variety or cell types. The multipotent P19 EC cell line was derived from a murine teratocarcinoma. EC cells share several characteristics with ES cells including rapid proliferation with a very short to near absent G_1 cell cycle stage, and the ability to differentiate into a variety of cell types *in vitro*. P19 EC cells differentiate into neurons, glia, and fibroblast-like cells when aggregated and exposed to 0.5 μM RA (Jones-Villeneuve, *et al.*, 1982; Rudnicki and McBurney, 1987a). Rb expression has been reported to increase during the differentiation of mouse P19 EC cells and ES cells during RA-induced differentiation and become almost totally hypophosphorylated (Savatier, *et al.*, 1994; Slack, *et al.*, 1993). Rb expression is associated with reduced apoptosis in these cultures. Total RNA was isolated at 0, 2, 4, 6, 8, 10, 12, and 14 days following the initiation of differentiation as described in Chapter 2.

Figure 3.1. Mouse p130 cDNA sequence.

Nucleotide sequence of the mouse p130 cDNA and the deduced amino acid sequence of the open reading frame with high homology to human p130.

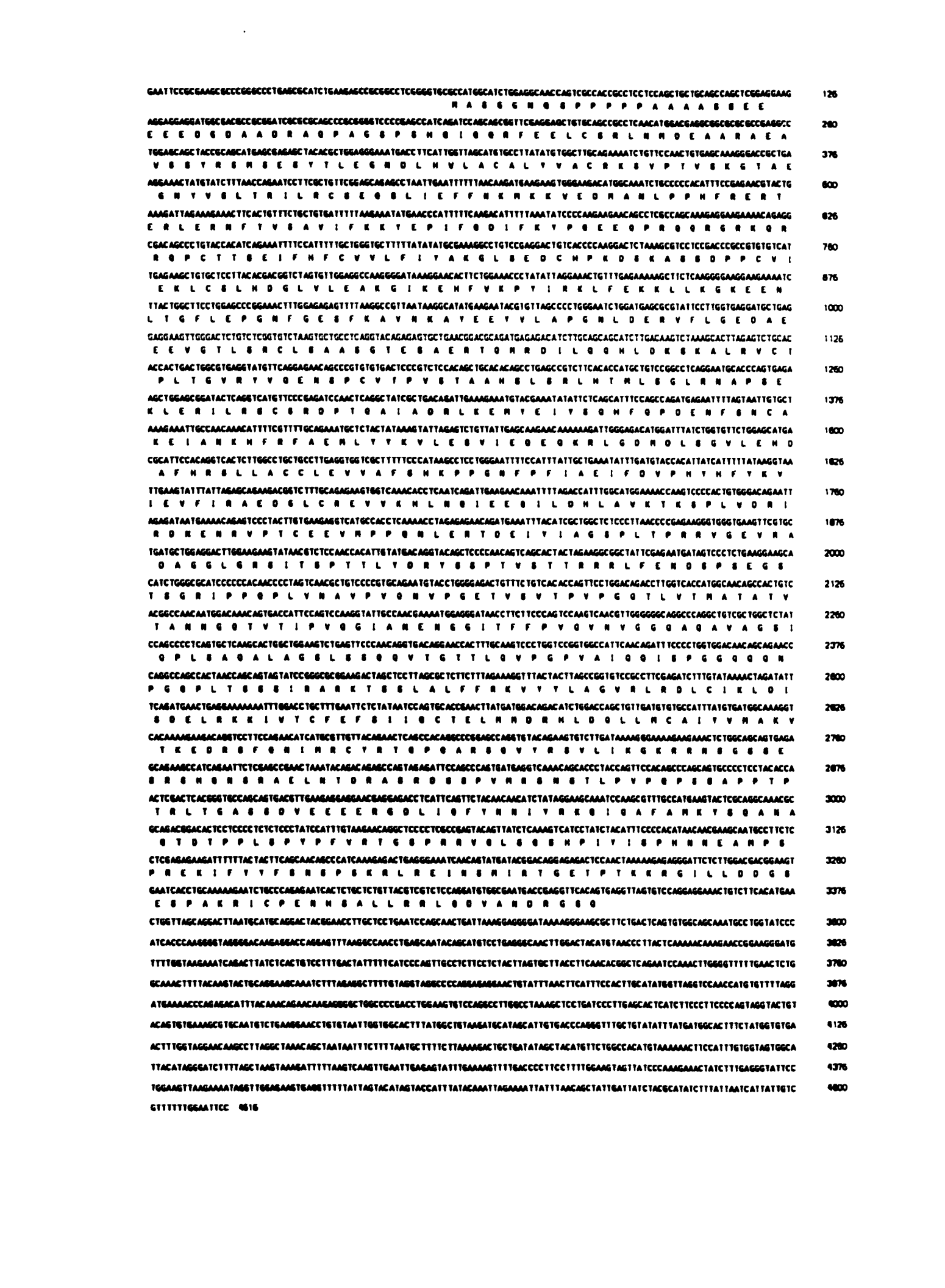

Figure 3.2. Comparison of mouse and human p130 amino acid sequences.

Residues that are identical to the mouse p130 sequence are boxed. While the protein sequences show an overall similarity of 88.4%, the mouse p130 sequence at residue 211 contains a 43 aa deletion in a conserved region relative to the human sequence located upstream of domains A and B of the pocket region.

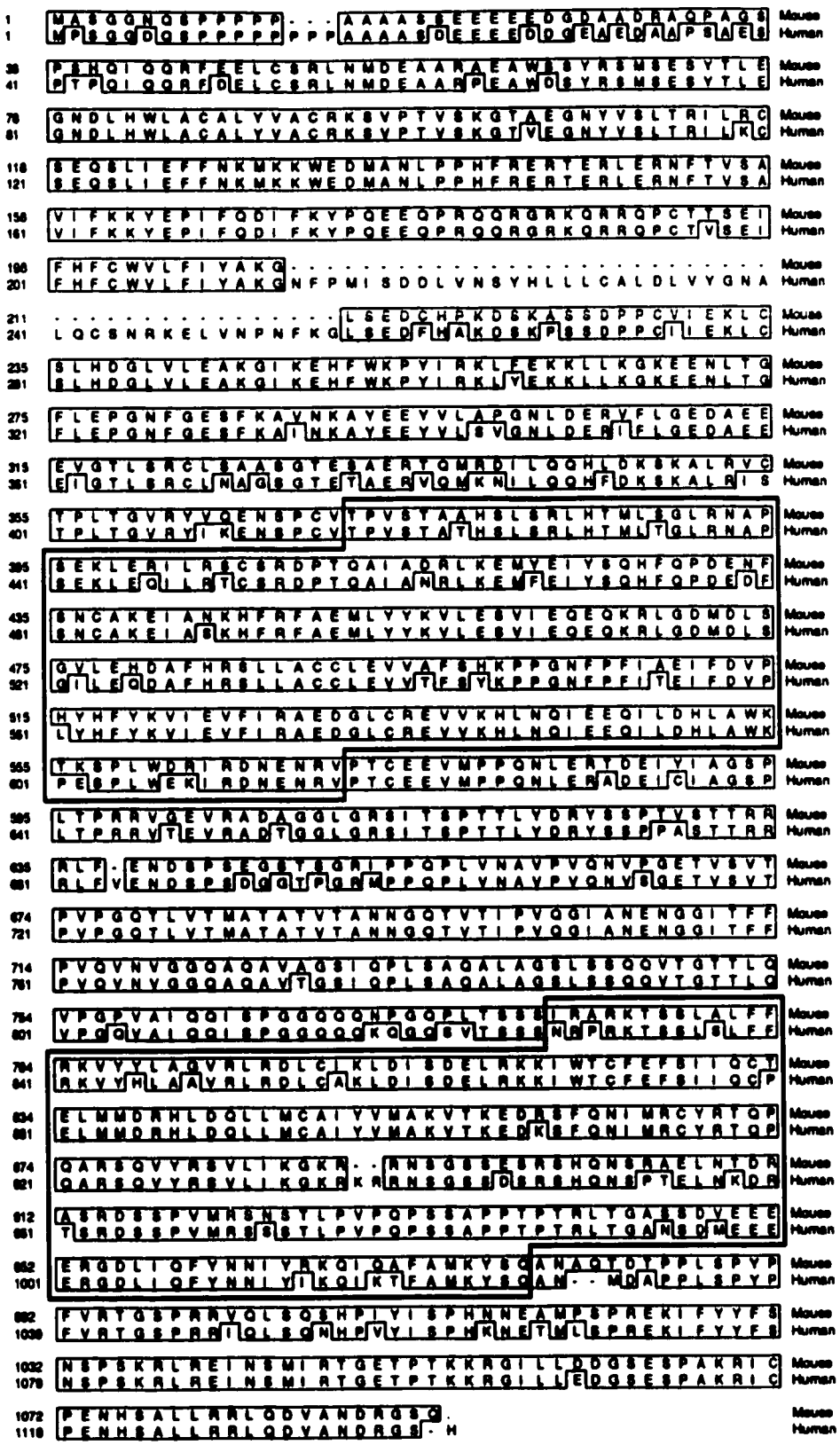
A
B

Figure 3.3 The cloned p130 cDNA does not represent the full-length mouse sequence.

(A) Amplification of the mouse p130 mRNA indicated uniformity of structure. RT-PCR was performed on mouse-derived RNA with primers located on either side of residue 211 of mouse p130 to determine whether the 129 nt deletion is a general feature of the mouse p130 mRNA sequence. The 455 bp fragment amplified from the cDNA is representative of the p130 RT-PCR product from thymus, skeletal muscle, liver or heart as detected by Southern blot analysis using the cloned p130 cDNA as a probe. The predicted size of the product representing a 129 nt insertion in this amplified region is 580 bp. Further analysis with a new primer set and newly isolated tissue RNA indicated that the cloned cDNA does not represent the genuine structure of the full-length p130 cDNA, in contrast to the initial result that may have been the consequence of contamination of the RT-PCR samples. (B) Comparison of the region with 2 clones isolated and reported independently by two other groups is presented.

A

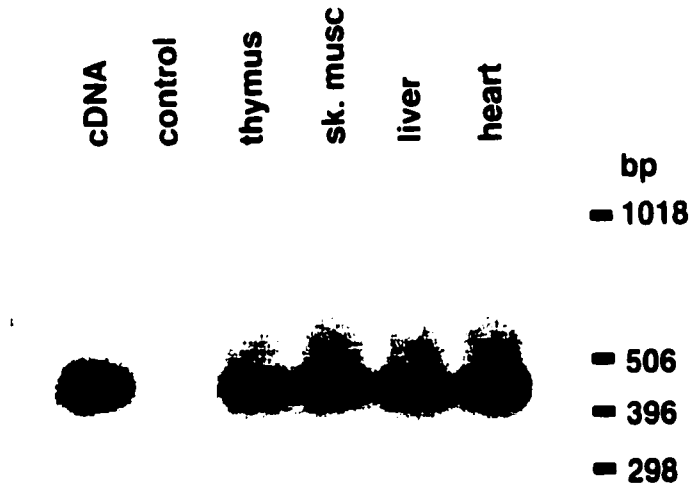

B

AKG----------L
AKGNFPMISDDLVNSYHLLLCALDLVYGNALQCSNRKELVNPNFKGL
AKGNFPMISDDLVNSYHLLLCALDLVYGNALQCSNRKELVNPNFKGL

Northern blot analysis indicated that while the 4.8 kb mouse p130 mRNA was below the limit of detection in undifferentiated EC cells, it was up-regulated to readily detectable levels between the 4th and 6th day of differentiation (Figure 3.4A). This time-frame corresponds to accumulating post-mitotic neurons in RA-treated P19 cultures, and may be considered analogous to the *in vivo* differentiation which occurs around 12.5 dpc in the mouse embryo (Lee, *et al.*, 1994). In addition, Northern analysis of J1 (Li, *et al.*, 1992) and D3 (Gossler, *et al.*, 1986) embryonic stem (ES) cell lines revealed that like P19 EC cells, p130 mRNA was not detectable (data not shown) suggesting that p130 is not expressed or, alternatively, it is expressed at a very low level in pluripotential embryonic stem cells. P19 and ES cells are rapidly proliferating lines that double approximately every 15 h, and presumably very low proportions of these cells in asynchronous cultures are in the G_0 or G_1 phases. FACS analysis of one ES cell line revealed that less than 18% of cells in proliferating cultures are in the G_0/G_1 compartment (Savatier, *et al.*, 1994). Presumably, the cell-cycle kinetics of these cells would exclude the analysis of any G_0 or cell-cycle entry molecules in these proliferating, asynchronous cultures. RNA loading was assessed by hybridization to a probe derived from the mouse phosphoglycerate kinase-1 cDNA (Figure 3.4B), and by ethidium bromide staining of the agarose gels (not shown) (Adra, *et al.*, 1988). Immunoblot analysis of extracts, isolated in parallel with the RNA above, with rabbit polyclonal antibody reactive to p130 (C-20, Santa Cruz Biotechnology Inc.) confirmed the induction of expression of p130 protein on day 6, which increased to a maximum by day 10 and decreased somewhat by day 14 (Figure 3.4C).

Total RNA was isolated from a panel of adult mouse organs for Northern blot analysis with the "full-length" mouse p130 cDNA as probe. RNA loading was assessed by hybridization to a probe derived from the ribosomal protein L32 cDNA (Figure 3.5C) and by ethidium bromide staining of the agarose gel (not shown) (Dudov and Perry,

1984). Expression of the 4.8 kb p130 mRNA was found in all tissues examined and its level appears to moderately vary between tissue types (Figure 3.5A). In addition, Northern blot analysis indicated a putative second species of p130 mRNA of about 1.7 kb in mouse testis. Interestingly, an 800 bp probe generated from the 5'-end of the cDNA did not hybridize this species (data not shown), whereas a full-length cDNA probe did hybridize (Figure 3.5A). Although the structure of the testis p130 mRNA remains to be determined, these experiments suggest that a tissue-specific isoform of p130 is expressed in adult testis, perhaps due to a second internal promoter or by alternative splicing from internal or upstream sequences to generate a 5'-truncated RNA species. Alternatively, a testis-specific gene is closely linked to the p130 gene generating an mRNA which contains some portion of p130 sequence. Further work by Chen *et al* (1996a) examined the appearance of p130 expression in the testis. p130 was induced between 15 and 25 days of age, coincident with the maturation of this tissue. The highest expression was in Leydig cells, the source of testosterone.

3.2.iii. Overexpression of mouse p130

A possible result of p130 overexpression is cell cycle arrest in early G_1 on the basis of negative E2F regulation. To confirm that the mouse p130 cDNA encodes a biologically active protein, this cDNA was cloned into an expression cassette between the PGK-1 promoter and polyadenylation signals in a plasmid that also contains PGK-puromycin, a selectable marker (designated PGKp130/puro). This plasmid was transfected into P19 EC cells as they do not express detectable p130 mRNA or protein (Figure 3.4 A, C), and cultures were selected in 2 μg/ml puromycin for 7 days. Growth suppression induced by p130 expression was assessed by the ability of transfected cells to form colonies. Figure 3.6 (A) clearly demonstrates that colony formation of P19 EC cells is markedly reduced by expression of mouse p130. Light microscopic examination of

Figure 3.4. Northern and immunoblot analysis of p130 expression during RA-induced P19 cell differentiation.

p130 is induced several days following initiation of differentiation. (A) Northern blot analysis with the mouse p130 cDNA as a probe of total RNA isolated from undifferentiated EC cells and cultures treated with RA for 2, 4, 6, 8, 10, 12 and 14 days. (B) The filter from (A) was stripped and rehybridized with the PGK-1 cDNA to assess loading between lanes. (C) Immunoblot analysis with specific anti-p130 C-20 antibody (Santa Cruz Biotechnology Inc.) of protein extracts isolated during P19 RA-induced differentiation.

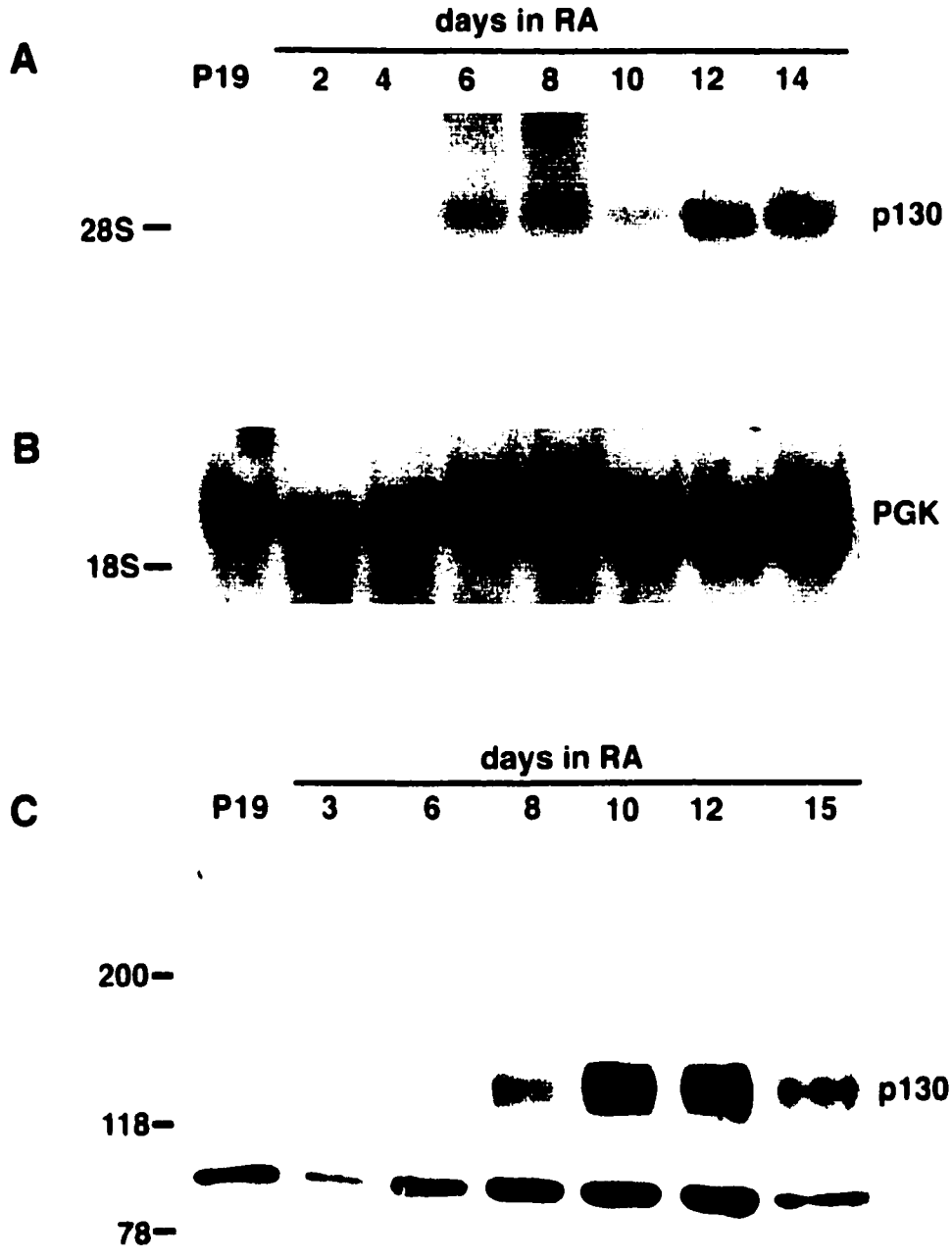
A
days in RA
P19
2
4
6
8
10
12
14
28S
p130
B
18S
PGK
C
days in RA
P19
3
6
8
10
12
15
200
118
78
p130

Figure 3.5. Northern blot analysis of p130 mRNA expression in a panel of adult tissues.

(A) The 4.8 kb p130 full-length mRNA is expressed ubiquitously in all mouse tissues examined. Interestingly, in testis a putative 5'-truncated 1.7 kb isoform (*) was expressed as assessed by probing with the first 800 bp of the p130 cDNA. (B) The filter was subsequently stripped and hybridized with the L32 cDNA to assess loading between lanes.

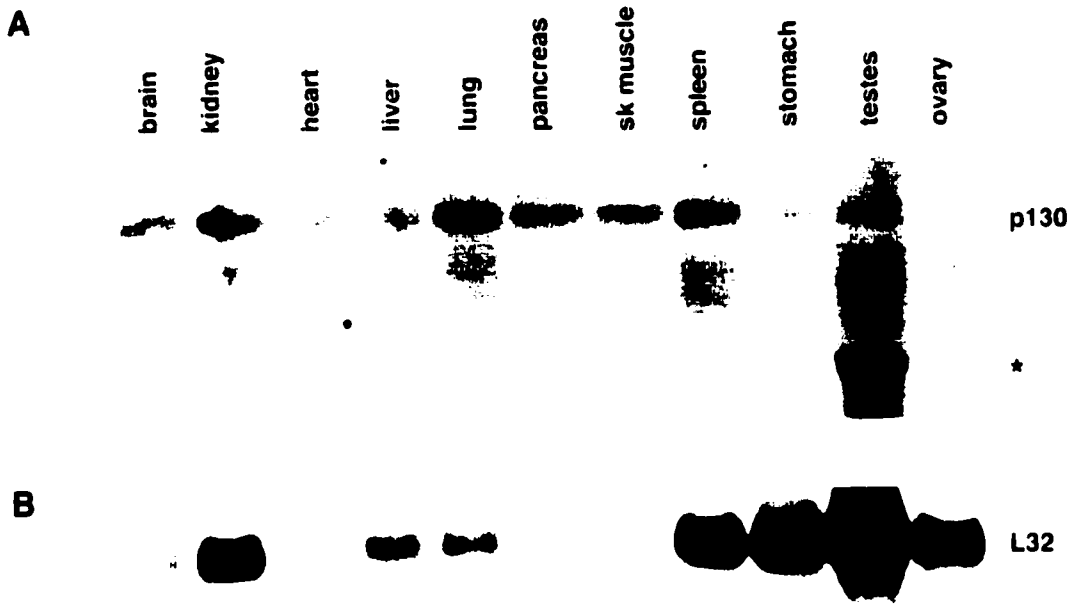
A
brain
kidney
heart
liver
lung
pancreas
sk muscle
spleen
stomach
testes
ovary
p130
B
L32

Figure 3.6. Expression of mouse p130 suppresses growth of P19 EC cells.

(A) P19 EC colonies 7 days following electroporation with PGK-puro alone and a plate of P19 EC colonies 7 days following electroporation with PGK-p130/puro and selection. Each 10 cm plate was seeded with 10^6 electroporated P19 cells, selected in 2 μg/ml puromycin for 7 days and the resulting colonies were fixed and stained with 0.1% methylene blue in ethanol. (B) Immunoblot for p130 protein with anti-p130 specific antisera of protein extracts isolated from Chago cells, a cell line considered to express p130 at a high level, differentiated cells or following electroporation of PGK-puro or PGK-p130/puro and puromycin selection.

A

PGKpuro PGK130/puro

B

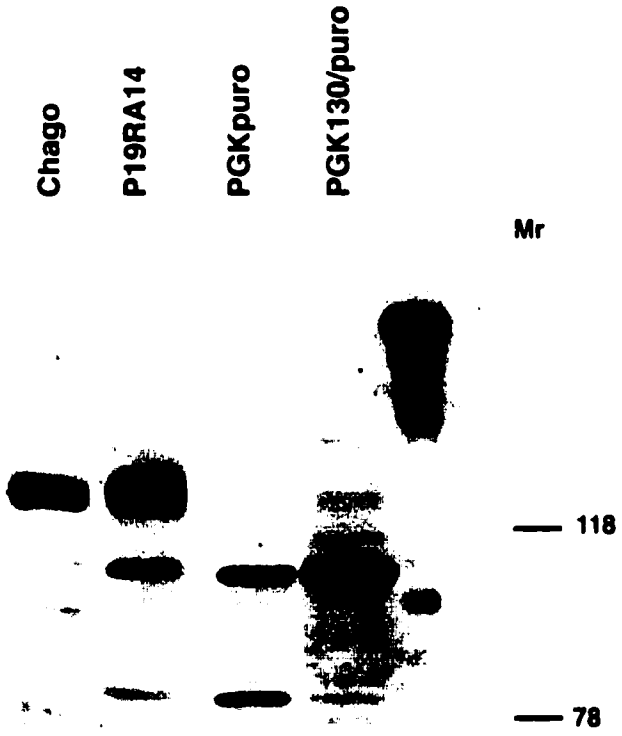

p130 transfected cells indicated that the cells retained a compact phase-dark EC cytomorphology and had not differentiated into neurons or fibroblasts (not shown).

Protein extracts were isolated from puromycin-selected P19 cells transfected with PGK-p130/puro and immunoblot analysis performed with rabbit polyclonal antibody C-20 reactive to p130. In contrast to untransfected cells, or cells transfected with PGKpuro, the P19 cells transfected with PGK-p130/puro expressed a moderate level of p130 protein, migrating with apparently normal mobility (Figure 3.6B). These data indicate the mouse cDNA described here encodes a mouse p130 polypeptide that is biologically active with growth suppressive properties similar to that observed following overexpression of the human p130 (Claudio, *et al.*, 1994).

3.3. Discussion

Undifferentiated P19 cells are analogous to ES cells, the totipotential stem cell of the embryo. P19 EC cells express very low levels of Rb mRNA which after 4-6 days of RA-induced differentiation increases by approximately 15-fold. The very low level of Rb in undifferentiated P19 EC cells is mostly hyperphosphorylated, whereas the increase in Rb levels that accompanies differentiation is coincident with an almost complete shift to the hypophosphorylated form (Slack, *et al.*, 1993). In contrast, ES cells express similar amounts of Rb before and after differentiation, but analogous to P19 cells, Rb is entirely hyperphosphorylated in undifferentiated cells and hypophorphorylated in differentiated cells (Savatier, *et al.*, 1994). Therefore, undifferentiated EC and ES cells both express low amounts of active Rb whereas their differentiated derivatives express significant levels of the active, hypophosphorylated Rb. Significantly, a low proportion of ES cells and presumably EC cells are in the G_1 phase, consistent with hyperphosphorylation of essentially all Rb protein.

Northern blot analyses suggest that p130 mRNA is not expressed in undifferentiated P19 EC cells, or in J1 and D3 ES cells. The levels of p130 mRNA and protein were not markedly up-regulated until post-mitotic neurons accumulated in RA-treated P19 cultures between 4 and 6 days after initiation of differentiation. Immunoblot analysis confirmed that the pattern of induction of p130 protein correlated with the expression of p130 mRNA. By contrast, Corbeil et al (Corbeil, *et al.*, 1995) reported the presence of similar levels of p130 protein in both undifferentiated and differentiated P19 cells. The basis for this variation is not clear. In agreement with results presented here, others also do not detect p130 protein in the undifferentiated P19 cells (R.M. Gill, personal communication). Differences between P19 sublines may account for the discrepancy. In cycling (non-stem) cells, p130/E2F complexes are predominant in G_0 and early G_1, while Rb/E2F complexes form in mid-G_1 and p107/E2F complexes form mainly in late G_1 (Chittenden, *et al.*, 1993; Cobrinik, 1996). Very low levels of Rb and p130 and the normal levels of p107 suggest that in proliferating P19 cultures, a very low percentage of cells exist in a G_0 state and that P19 cells exhibit a truncated G_1, resulting in a seemingly shortened cell cycle.

Northern blot analysis of total RNA revealed the presence of a putative 5'-truncated 1.7 kb isoform of mouse p130 mRNA expressed solely in testis. By contrast, Northern blot analysis of human tissues failed to reveal the presence of such a testis-specific form (Claudio, *et al.*, 1994). However, a 2.8 kb variant of the mouse 4.8 kb Rb mRNA is expressed in the testis, likely in the spermatids (Bernards, *et al.*, 1989). Alternate splicing has also been suggested to generate a 2.4 kb variant of the mouse p107 mRNA, the full-length version of which is 4.8 kb (Kim, *et al.*, 1995). The predicted amino acid sequence from the alternative p107 splice variant predicts a carboxyl-terminal truncation beginning after subdomain A in the spacer region. This product lacking subdomain B of the pocket region potentially affects the biological activity of p107. The

1.7 kb testis-specific isoform of mouse p130 appears to contain a 5'-truncation as probes generated from the 5-end of the 4.5 kb cDNA did not hybridize this species whereas full-length probes did. Molecular cloning of the 1.7 kb p130 mRNA should clarify the structure of this isoform and allow characterization of the function of this variant (putative) protein. Interestingly, expression of an amino-terminal mutant protein in Rb-deficient embryos demonstrated that this region of Rb is necessary for late embryonic development and survival, and delayed tumour progression in heterozygous mice (Riley, *et al.*, 1997). Potentially, an amino-terminal mutant p130 protein could affect p130 function in the testis.

The overexpression of human p130 can induce growth arrest of many cell types, including cell lines in which proliferation is not inhibited by overexpression of either p107 or Rb (Claudio, *et al.*, 1994; Vairo, *et al.*, 1995). The data presented in this chapter indicated that overexpression of mouse p130 inhibits proliferation of P19 EC cells, but does not induce morphological differentiation. However, cell cycle arrest may be due to cytotoxic effects of ectopic p130 expression. Overexpression of human p130 induced growth arrest of sarcoma cells and in a glioblastoma cell line in G_1 and this block could be overcome by overexpression of E2F-4 but not by E2F-1 (Vairo, *et al.*, 1995). Potentially, co-transfection of E2F-4 would rescue the growth arrest induced by mouse p130 in P19 cells, and provide insight into the mechanism evoked.

Finally, the cloning of the mouse p130 cDNA should facilitate the molecular genetic investigation of p130 function during mouse embryogenesis. Clearly, the generation of transgenic mice expressing mutant versions of Rb, p107 and p130, and the incorporation of wildtype or mutant cDNAs in the context of the heterologous promoters will also be valuable approaches to determine the unique and overlapping roles of these factors in cell growth and differentiation.

CHAPTER 4

Strain-Dependent Embryonic Lethality in Mice Lacking p130

4.1. Introduction

In the developing embryo, combinatorial signals and complex regulatory networks elicit appropriate patterning and morphogenesis by controlling cell determination, proliferation, differentiation, and programmed cell death (reviewed in Slack, 1992). The Rb family, including *Rb*, *p107*, and *p130*, play integral roles in the regulatory pathways controlling cell cycle progression and differentiation, in part by negatively regulating E2F-dependent transcription (reviewed by Dyson, 1998; Muller, 1995; Nevins, 1992; Weinberg, 1995b). Rb, p107 and p130 associate with cyclins and their cognate cdks resulting in the differential phosphorylation of Rb proteins during cell-cycle progression. The Rb family similarly regulates the activity of other developmentally important transcription factors, for example specific Rb proteins can interact with paired homeodomain-containing proteins that specify cell type, as well as C/EBP and other important regulatory proteins like c-Myc and c-Abl (Chen, *et al.*, 1996b; Wiggan, *et al.*, 1997; reviewed in Weinberg, 1995b; Whyte, 1995). An important role for p130 in cellular differentiation is also supported by the observation that p130:E2F complexes are predominant in differentiated cells (Chittenden, *et al.*, 1993; Corbeil, *et al.*, 1995; Garriga, *et al.*, 1998; Kiess, *et al.*, 1995; Shin, *et al.*, 1995).

Mice deficient for Rb die *in utero* between days 13.5 and 15.5 of gestation and exhibit delayed erythropoiesis and extensive cell death in the CNS (Clarke, *et al.*, 1992; Jacks, *et al.*, 1992; Lee, *et al.*, 1992; Maandag, *et al.*, 1994; MacLeod, *et al.*, 1996;

Williams, *et al.*, 1994). Embryonic fibroblasts derived from the Rb mutants displayed a shortened G_1 cell-cycle phase and expression of E2F-regulated genes, p107 and cyclin E were perturbed (Herrara, *et al.*, 1996; Hurford, *et al.*, 1997). Mice lacking either p107 or p130 in the hybrid 129Sv;C57Bl/6J genetic background exhibited no overt phenotypes, were viable and fertile, and EF derived from the mutants displayed normal cell-cycle kinetics and appropriately regulated E2F-dependent genes (Cobrinik, *et al.*, 1996; Hurford, *et al.*, 1997; Lee, *et al.*, 1996). Embryos deficient for Rb and p107 died two days earlier than Rb-deficient embryos and exhibited apoptosis in the liver and CNS suggesting that p107 partially compensated for the loss of Rb. The p130 and p107 compound mutant mice died perinatally and exhibited defective endochondral bone development.

To investigate potential roles of p130 in development, a targeted disruption in p130 was independently-derived in ES cells and the germline of mice. The null allele was bred onto Balb/cJ and C57BL/6J genetic backgrounds. In a hybrid 129Sv;Balb/cJ genetic background, $p130^{-/-}$ embryos displayed arrested growth and died between embryonic days 11 and 13. Histological analysis revealed varying degrees of disorganization in neural and dermomyotomal structures; variably, interruptions in the notochord in central-axial regions; deficiencies in neurogenesis, cardiac and skeletal myogenesis; and apoptosis in some but not all tissues. However, the placentas of $p130^{-/-}$ embryos did not display elevated apoptosis and were indistinguishable from wildtype. Following a single backcross with the C57BL/6 mice, B2$p130^{-/-}$ animals were derived that were viable and fertile. These results indicate that p130 in a Balb/cJ or the hybrid genetic background plays an essential role that is required for normal development. Moreover, these experiments establish that second-site modifier genes exist that have potentially epistatic relationships with p130.

4.2. Results

4.2.i. Generation of the p130 null allele

The *p130* gene was disrupted using the targeting strategy outlined in figure 4.1. Chimeras were generated following the microinjection of targeted ES cells into Balb/cJ blastocysts. Two independent mutant p130 mouse lines were generated. The observed homozygous phenotype was completely identical so the lines are discussed together. Interbreeding of $p130^{+/-}$ mice generated no viable $p130^{-/-}$ mice, as assessed at weaning (3-4 weeks of age). In addition, the absence of viable newborn pups suggested that $p130^{-/-}$ embryos were dying *in utero*. To delineate the gestational stage that $p130^{-/-}$ embryos were dying, cesarean sections were performed at successive dpc following timed matings (Table 4.1). At 9.5 dpc and 10.5 dpc, I observed an approximate Mendelian frequency of 1:2:1 of wildtype, $p130^{+/-}$ and $p130^{-/-}$ genotypes. However, about 50% of the expected numbers of $p130^{-/-}$ embryos were observed on 11.5 dpc, about 15% on 12.5, and no viable $p130^{-/-}$ embryos after this stage. In addition, I observed that approximately 25% of conceptuses were non-viable and were being absorbed on and after 13.5.

4.2.ii. The engineered mutation generates a null allele

To demonstrate whether the targeted mutation created a null allele, Northern blots and immunoblots were performed. Northern blots, using full-length p130 cDNA as probe, revealed reduced levels of p130 mRNA in $p130^{+/-}$ embryos and no detectable p130 mRNA in $p130^{-/-}$ embryos (Figure 4.2). By contrast, the previously reported mutation reduced the level of p130 mRNA five-fold (Cobrinik, *et al.*, 1996). Immunoblot analysis with antibody C20 reactive with p130 revealed reduced levels of p130 in $p130^{+/-}$ tissue and no p130 in lysates from $p130^{-/-}$ tissue. Therefore, a null mutation in *p130* in a Balb/c (129Sv hybrid) genetic background resulted in an embryonic lethal phenotype with embryos dying between day 11 and 13 of gestation.

Table 4.1 Viability of embryos derived from *p130*$^{+/-}$ interbreeding.

	Days *post coitum*					
Genotype	9.5	10.5	11.5	12.5	13.5	14.5
Wildtype	6	17	15	13	9	5
p130$^{+/-}$	15	31	23	23	13	14
p130$^{-/-}$	4	14	9	2	0	0

The F1 *p130*$^{+/-}$ offspring of chimeras bred with Balb/cJ mice were interbred and cesarean sections performed at different gestational ages. Note, the morning following mating is considered 0.5 days post coitum.

Figure 4.1 Targeted disruption of the p130 gene.

(A) Genomic locus, targeting vector and structure of the disrupted p130 locus with exons depicted as filled boxes. The targeting vector contained 3 kb of 5'- and 7.2 kb of 3'-homologous sequence. The PGKneo expression cassette was inserted in the opposite transcriptional orientation to p130 disrupting the aa 106 codon and replacing the remaining 16 aa codons in this exon and 0.5 kb of intron sequence. (B) Southern analysis of EcoRV-digested DNA isolated from E11.5 embryos derived from a heterozygous intercross resulted in the predicted RFLP. Genotypes are indicated above the lanes. Abbreviations: E, EcoRV; X, XbaI; H, HindIII; B, BamHI. Sizes of EcoRV fragments that hybridize the probe illustrated, are indicated below the genomic locus (WT) and targeted locus (T).

A

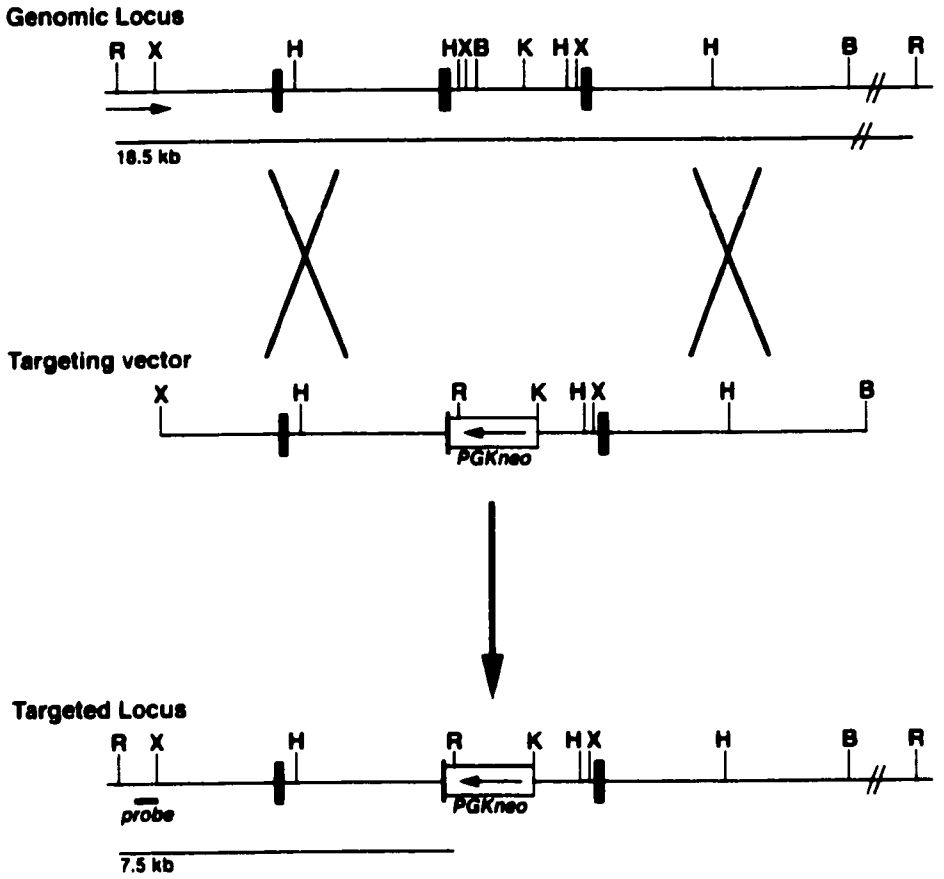
Genomic Locus
R X H HXB K HX H B R
18.5 kb
Targeting vector
X H R K HX H B
PGKneo
Targeted Locus
R X H R K HX H B R
probe
PGKneo
7.5 kb

B

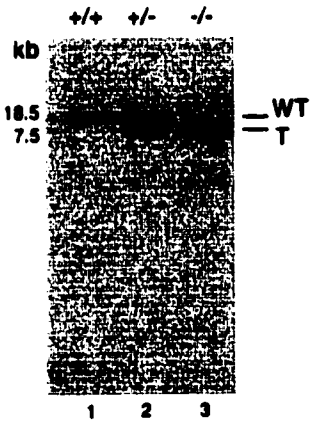
+/+ +/- -/-
kb
18.5
7.5
WT
T
1 2 3

Figure 4.2 The targeted mutation generates a null allele

(A) Northern blot analysis of total RNA probed with the full-length mouse cDNA revealed a complete absence of a transcript from the targeted p130 alleles. Presumably, any transcript being produced from the targeted locus is unstable and/or below the limit of detection. (B) Immunoblot analysis with antibody C20 reactive with p130 (Santa Cruz Biotechnology Inc.) against tissue lysates indicated that no protein was expressed from the targeted allele. Taken together, the targeted mutation generates a null allele. Genotypes are indicated above the lanes. Abbreviation: M^r, relative mobility in kD. Arrows indicate bands corresponding to p130.

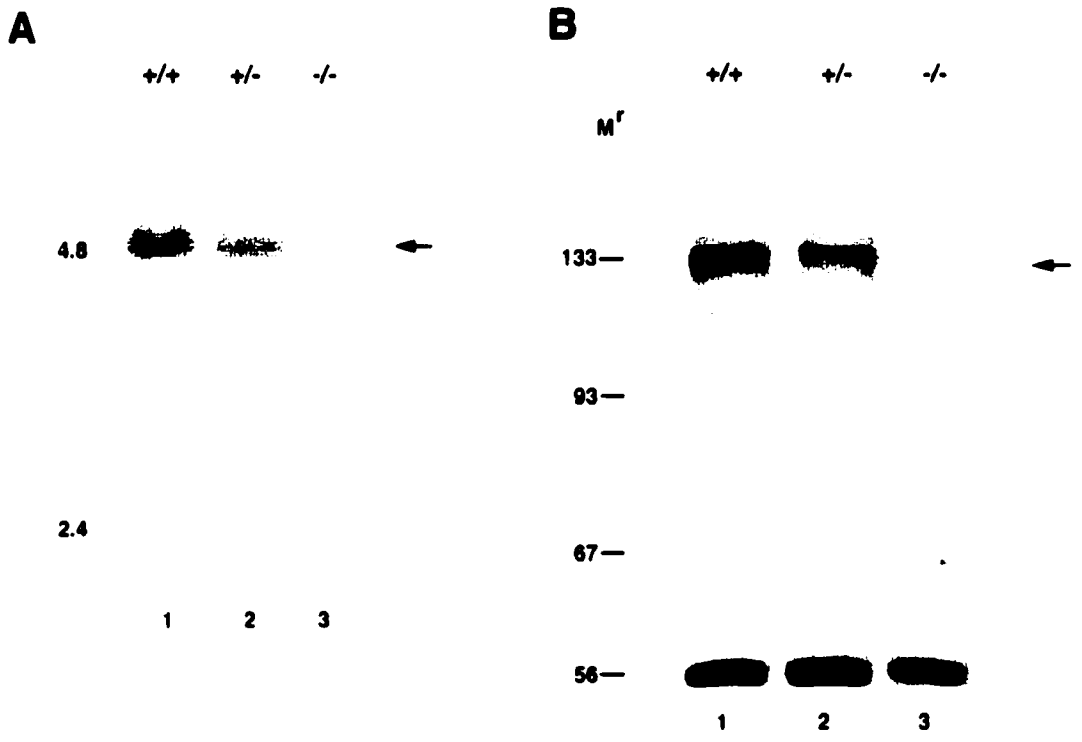
A
+/+
+/-
-/-
4.8
2.4
1
2
3
B
+/+
+/-
-/-
Mr
133—
93—
67—
56—
1
2
3

Table 4.2 Genetic background specifies the penetrance of the *p130*$^{-/-}$ phenotype.

	Intercross		
	Chimera X Balb/cJ ↓	F1$^{+/-}$ X Balb/cJ ↓	F1$^{+/-}$ X C57Bl/6J ↓
Genotype	F1$^{+/-}$ X F1$^{+/-}$[a]	B1$^{+/-}$ X B1$^{+/-}$[b]	B1$^{+/-}$ X B1$^{+/-}$[c]
Wildtype	42	12	21
p130$^{+/-}$	78	28	39
p130$^{-/-}$	0	0	24

[a] The F1 *p130*$^{+/-}$ progeny of the founding chimeras bred with Balb/cJ mice when interbred yielded no viable *p130*$^{-/-}$ pups. [b] The B1 *p130*$^{+/-}$ mice derived from an F1 *p130*$^{+/-}$ X Balb/cJ mating when interbred also failed to produce B2 *p130*$^{-/-}$ mice. [c] The B1 *p130*$^{+/-}$ mice, derived from a F1 *p130*$^{+/-}$ X C57Bl/6J mating, when interbred generated litters that contained viable and fertile B2 *p130*$^{-/-}$ mice that displayed an apparently normal phenotype.

4.2.iii. Embryos lacking p130 display arrested growth

Inspection of *p130*$^{-/-}$ embryos revealed a disparity in growth that increased with gestational age until 11.5 dpc when the mutant embryos attained approximately 25% of the normal size (Figure 4.3). Mutant embryos at 10.5 dpc displayed beating hearts with an abnormal dilated morphology, but with seemingly normal vascularization and distribution of blood. The embryonic membranes also appeared to be appropriately vascularized (data not shown). Although 10.5 dpc *p130*$^{-/-}$ embryos exhibited normal brain segmentation and the neural tube had completely closed, the embryos exhibited markedly reduced posterior growth, failure to form hindlimb buds and generally the number of somites in the embryo were indicative of earlier stages. So although the head structures closely resembled those of 10.5 wildtype embryos, a significant proportion of *p130*$^{-/-}$ 10.5 dpc embryos resembled much earlier, 8.5-9.0 dpc, embryos. By 11.5 dpc, mutant embryos had progressed little in development and appeared similar in size to 10.5 *p130*$^{-/-}$ embryos.

A possible cause of death at mid-gestation may be the result of placental failure. Placenta function is required as the yolk sac circulation becomes limiting once the embryo has attained a certain size. In the mouse, this corresponds to about E9.5. Failure of the chorioallantoic placenta to form, via fusion of the allantois and the chorion, leads to death around E10.5 (Kaufman, 1992; Rossant, 1996). Importantly, the *p130*$^{-/-}$ placentas exhibited normal anatomy and arrangement of extraembryonic blood vessels and membranes. Histological analysis indicated a normal cytomorphology at the ectoplacental plate. Giant cells have several functions including phagocytosing maternal red blood cells to transfer iron to the conceptus and producing steroid hormones. This cell type may also function to facilitate normal implantation. No apoptosis is detected in the giant cells or the placental labyrinth, (Figure 4.4). Apoptosis was assessed by TUNEL (terminal deoxynucleotide transferase (TdT)-mediated dUTP-biotin nick end

labeling) staining (Gavrieli, *et al.*, 1992). Taken together, these data support the conclusion that the growth deficit and mortality of *p130*$^{-/-}$ embryos was not due to placental failure.

4.2.iv. The p130 mutant heart

The vertebrate heart originates from paired mesodermal progenitor populations that ingress through the primitive streak at gastrulation and migrate to the anterior-lateral aspect of the embryo (7 dpc, pre-somite embryo). There, the cells begin differentiation, fuse at the midline and initially form a simple tube (initiated at 8 dpc) comprised of an outer myocardial epithelium separated from the inner endocardial layer. This contractile tube (8.5 dpc) is patterned into atrial and ventricular portions and is then transformed by elongation, looping, and spatially distinct patterns of differentiation (8.5-10.5) into the mature, multi-chambered heart. After E9 there is evidence of an outer compact layer of the myocardium and an inner, spongy zone. The spongy zone becomes trabeculated. The trabaculae eventually coalesce to become the septa. The basic morphological changes that accompany cardiac development are outlined in Figure 4.5G (reviewed in Fishman and Chien, 1997).

Upon dissection, the *p130*$^{-/-}$ embryos revealed a somewhat dilated myocardium and abnormal cardiac morphology suggestive of a defect in chamber formation (Figure 4.3D). To characterize the cardiac structures of *p130*$^{-/-}$ embryos, serial sections through the hearts were immunostained with desmin-specific antibody. The myocardium of *p130*$^{-/-}$ embryos was poorly developed with a thin wall, the compact layer lacked trabeculae (projections of myocardium and endocardium) in the ventricular chamber, and development of the interventricular septum was defective. Examination of serial sections through the heart revealed a failure to loop and form the four chambers (Figure 4.5). Instead, the mutant heart was similar to the two chambered E8.5 heart consisting of the

Figure 4.3 Embryonic growth deficiency in the absence of p130 is strain-dependent

(A) Wildtype embryos at 9.5 dpc have turned whereas (B) *p130*$^{-/-}$ embryos were observed in the lordotic position and displayed reduced numbers of somites (average of 10 pairs of somites versus 25-30 in wildtype embryos). By 10.5 dpc, (D) *p130*$^{-/-}$ embryos were about half the normal size of (C) wildtype embryos, and displayed normal development of brain structures. By contrast, more posterior structures, including the heart and the hindlimb bud, were underdeveloped. The mutant embryo at (F) 11.5 dpc was strikingly smaller than (E) wildtype and appeared arrested at the E10.5 stage. (G,H) In the C57Bl/6J (129Sv hybrid) genetic background, *p130*$^{-/-}$ mice were viable, fertile and displayed no overt phenotype (see Table 4.3). Note, 9.5 dpc and 10.5 dpc embryos were photographed before fixation, whereas 11.5 dpc embryos were photographed post-fixation.

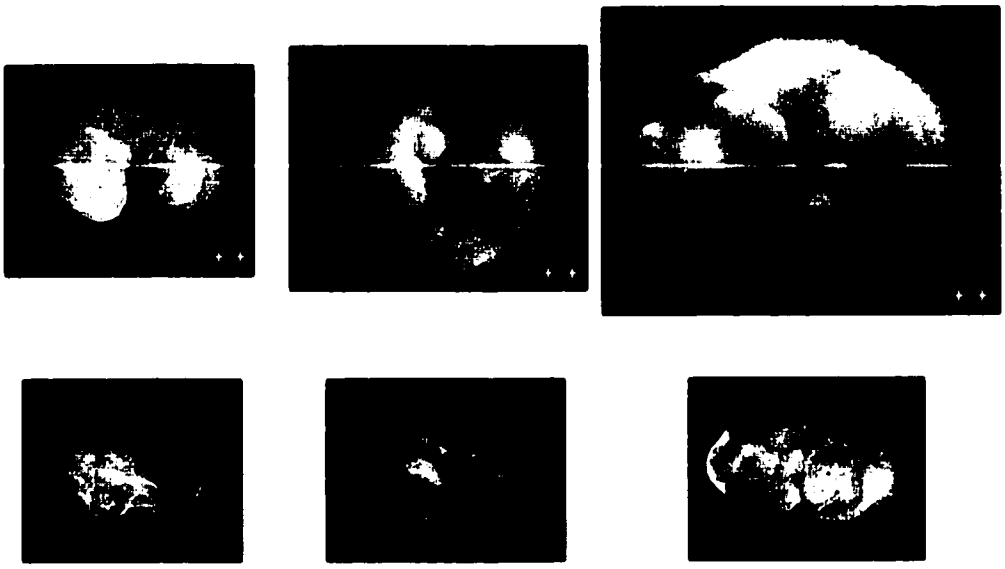

G

+/+

H

-/-

Figure 4.4 Normal placental cytomorphology and absence of apoptosis in p130-deficient placentas

The placentas of wildtype (A) and *p130*$^{-/-}$ (B) embryos were identical in appearance and both contained very few apoptotic nuclei as assessed by TUNEL assay. Abbreviations: gc, giant cells; la, labyrinth. Panels were photographed at a magnification of 400X.

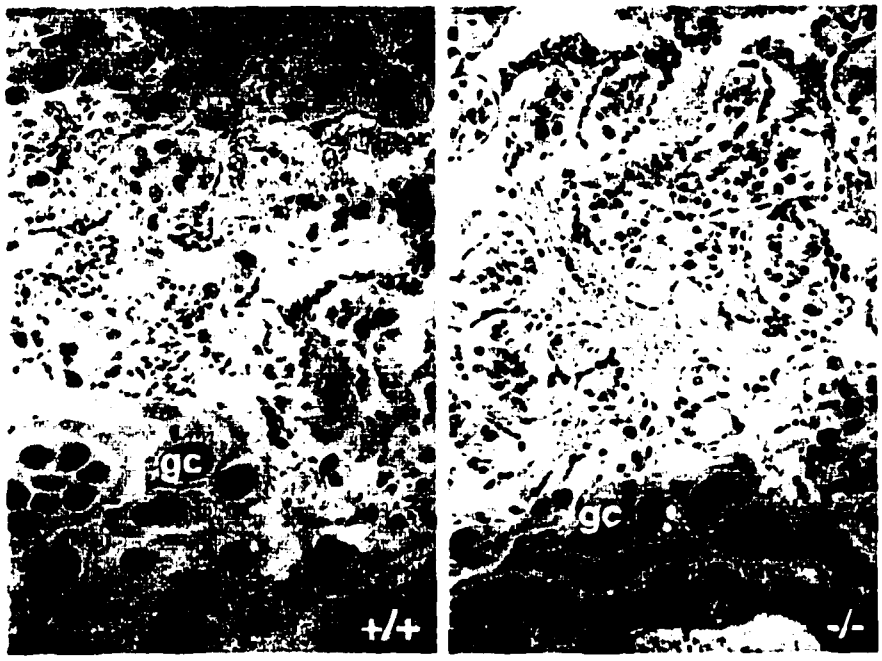
gc
+/+
gc
-/-

Figure 4.5. Delayed cardiogenesis in p130$^{-/-}$ embryos.

Immunohistochemistry with antibody reactive with desmin revealed the four-chambered myocardium of wildtype embryos (A,C). By contrast, the myocardium of *p130*$^{-/-}$ embryos (B,D) was poorly developed and serial sections indicated the presence of a two-chambered heart, consisting of the bulbus cordis and a common ventricular chamber. TUNEL analysis did not reveal any significant apoptosis in wildtype (E) or mutant (F) hearts. (G) Outline of the morphological changes that accompany cardiac development (adapted from Gilbert, 1994) Abbreviations: m, myocardium; pc, pericardium; ra, right atrium; la, left atrium; rv, right ventricle; lv, left ventricle; bc, bulbus cordis; v, ventricle; a, atrium ; ar, aortic roots; sv, sinus venosus; bs, bulboventricular sulcus. Panels were photographed at magnification of 100X (A,B) and 400X (C, D,E, F).

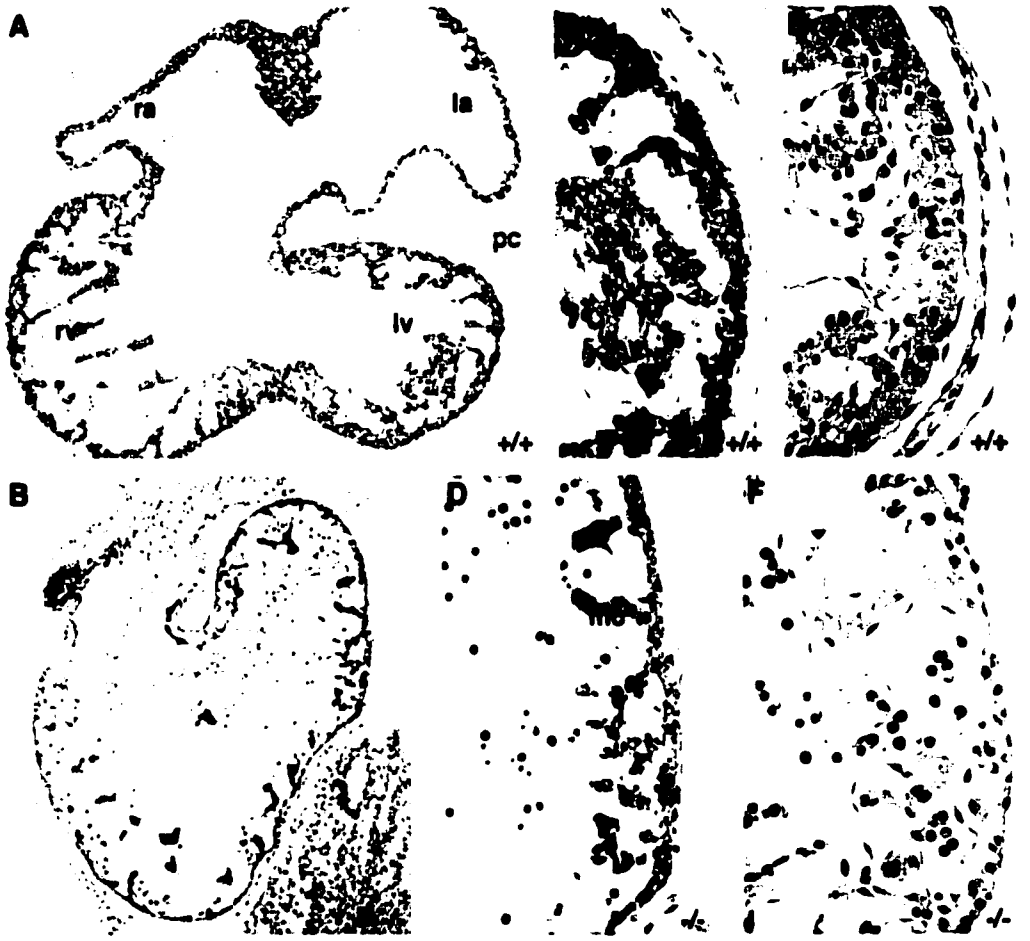
A
ra
la
pc
lv
+/+
+/+
+/+
B
D
mc
+/-
+/-

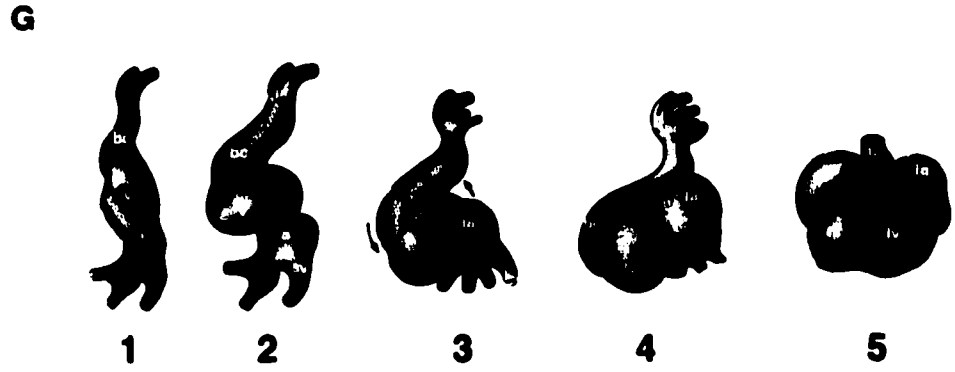
G
1
2
3
4
5

bulbus cordis and ventricular chamber. The pericardium and endocardium appeared normal. Apoptosis was not detected in the wildtype or mutant hearts.

Histological examination of sections of 10.5 dpc *p130*$^{-/-}$ embryos revealed some variability in the appearance of embryos, presumably reflecting their overall viability. This variability is potentially attributed to the hybrid genetic background (129Sv;Balb/cJ) of these animals which may affect the penetrance of the phenotype. The typical 10.5 dpc p130$^{-/-}$ embryo exhibited a beating heart while being delivered; and upon histological examination, a poorly developed neural tube, dermomyotome, myocardium and the presence of high numbers of apoptotic nuclei. The neural epithelium in the neural tube failed to elaborate a basement membrane and cells were not organized into layers as in the wildtype neural tube (Figure 4.6).

4.2.v. Impaired neurogenesis and myogenesis in p130$^{-/-}$ embryos

Neuroepithelial cells within the ventral neural tube are the progenitors of motor neurons that differentiate in response to signals from the notochord and floor plate of the neural tube (Yamada, *et al.*, 1993; Yamada, *et al.*, 1991). To assess neurogenesis, immunohistochemistry was performed with antibody reactive against the LIM-domain transcription factors Islet-1 and Islet-2 that are expressed in newly born motor and sensory neurons (Ericson, *et al.*, 1992; Tsuchida, *et al.*, 1994). Decreased numbers of Isl-1 expressing motor neurons were detected within the ventral horn of a somewhat disorganized neural tube. Additionally, decreased numbers of sensory neurons within a poorly demarcated dorsal root ganglia were present (Figure 4.6). The dorsal root ganglia are actually derivatives of neural crest cells which migrate from regions of the dorsal neural tube. So although ventral and dorsal-derivatives were developing, the reduced numbers of these neurons suggested that these cells were being lost. The neuroepithelia in the neural tube also entirely failed to elaborate a basement membrane and cells were not organized into layers as in the wildtype neural tube. Loss of the notochord in mutant

Figure 4.6. Deficient neurogenesis and associated apoptosis in E10.5 *p130*$^{-/-}$ embryos

(A) Wildtype embryos contained numerous motor and sensory neurons in the neural tube and dorsal root ganglia, respectively, as detected with antibody reactive to Islet-1/2. (B) Embryos lacking p130 were reduced in size, displayed a disorganized morphology, and contained severely reduced numbers of Islet-1/2 expressing motor and sensory neurons. TUNEL analysis revealed low levels of apoptosis in wildtype (C) and markedly increased numbers of apoptotic bodies (arrowheads) in the neural tube and dorsal root ganglia of the *p130*$^{-/-}$ embryos (D). Note the absence of the notochord, the disorganized neural floor plate, and absence of a basement membrane in the neural tubes of p130$^{-/-}$ embryos (B,D). Note, the tissue that normally surrounds the notochord is also markedly perturbed. Abbreviations: nt, neural tube; nc, notochord; mn, motor neurons; drg, dorsal root ganglion. Panels were photographed at 200X magnification (A,B) and 400X (C,D). Arrowheads indicate immunoreactive cells.

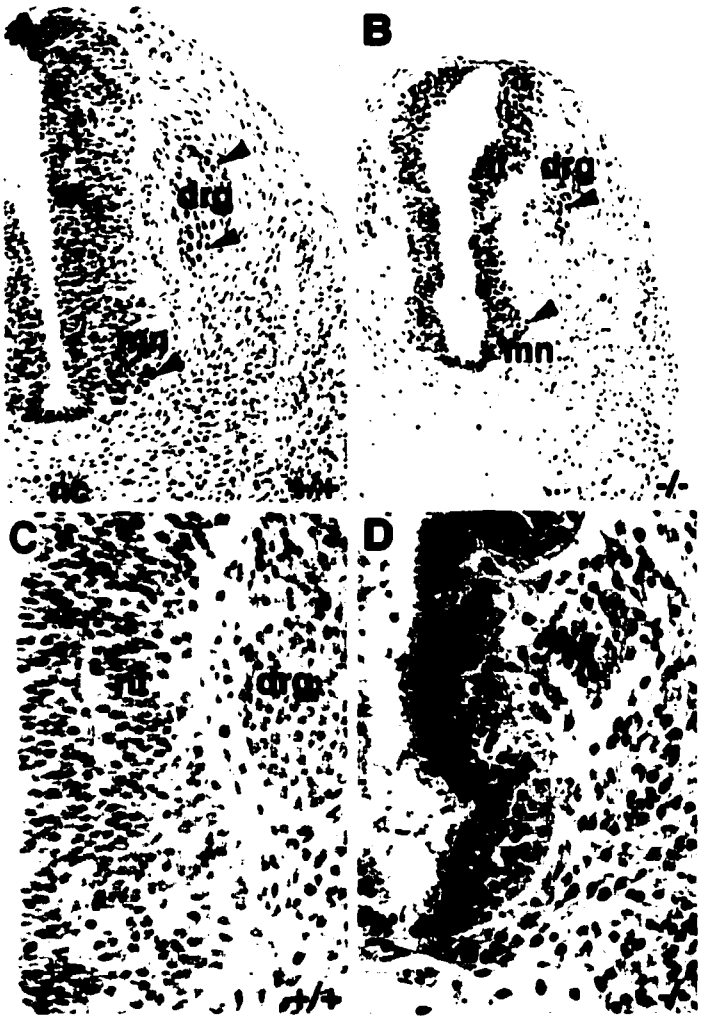
B
drg
mn
drg
C
D

sections was usually accompanied by a reduced or complete absence of neural floor plate. Interestingly, there is evidence to suggest that motor neurons may begin to differentiate prior to the induction of floor plate cells in response to Shh signaling (reviewed in Placzek, 1995).

One striking feature of a number of *p130*$^{-/-}$ embryos was loss of the notochord in the central axis region. The notochord is an organizing node in the embryo, signaling for formation of the floor plate and motor neurons in the ventral neural tube. The notochord was observed to be completely lost at thoracic and lumbar levels but not in the most cranial or caudal region. The notochord does mediate induction of ventral cell types, and the final pattern of ventral cells may also depend on the ability of the notochord to provide a mitogenic stimulus for neuroepithelial and paraxial mesodermal. One hypothesis to explain the loss of the notochord is that after growth arrest, without the proper p130-dependent mechanisms in place, the notochord degenerated and an excess of cell death occurred. Alternatively, the notochord and surrounding mesenchyme, drastically affected in the *p130*$^{-/-}$ embryos, may represent tissues that are most sensitive to reduced circulation/ ischemia that occurred due to cardiac insufficiency.

In the paraxial mesoderm, segmentation, growth and differentiation give rise to the somites, structures segmentally arranged on either side of the neural tube. Recent evidence indicates that somite patterning and differentiation are governed by a complex network of signals. The notochord and floor plate express the Shh secreted glycoprotein, the N-terminal fragment of which appears to coordinate cell patterning and proliferation. Shh signaling by the floor plate and notochord induces sclerotome formation in the lateral portion of the somite. The myotome, the first differentiated skeletal muscle of the embryo, is induced by Shh and dorsally-derived Wnt proteins, also secreted glycoproteins (Munsterberg, *et al.*, 1995; reviewed in Hauschka, 1994). Myogenic differentiation was assessed in the *p130* mutants with antisera reactive to desmin, an intermediate filament

Figure 4.7. Deficient skeletal myogenesis and apoptosis in E10.5 *p130*$^{-/-}$ embryos

(A) The normal myotome of wildtype embryos was reduced to a small rudiment in *p130*$^{-/-}$ embryos (B) as revealed by staining with antibody reactive to desmin. TUNEL analysis demonstrated low levels of apoptosis in wildtype embryos (C) versus increased numbers of apoptotic bodies in the dermamyotome of *p130*$^{-/-}$ embryos (D). Abbreviation: dm, dermamyotome. Panels were photographed at 200X and 400X magnification, arrowheads indicate desmin-positive (A,B), and TUNEL-positive cells (C,D).

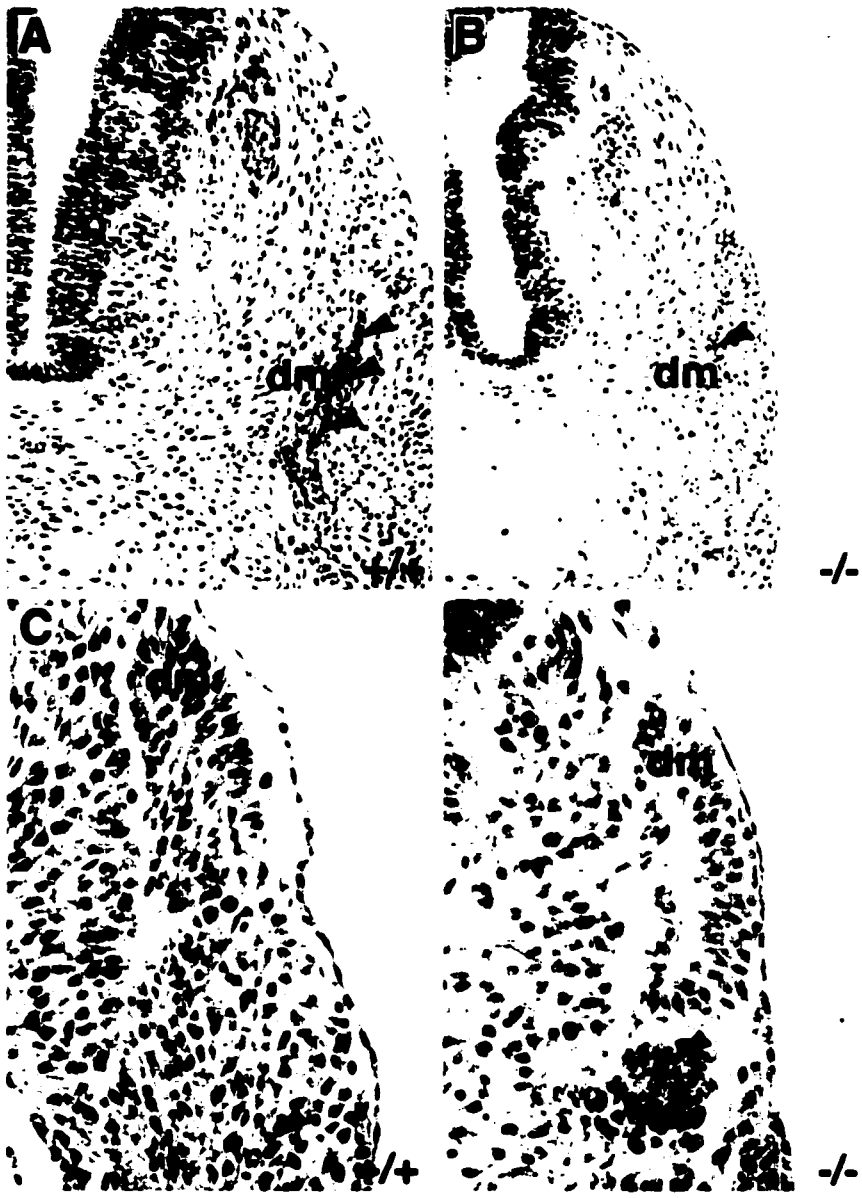
A
dm
+/+
B
dm
-/-
C
dm
+/+
dm
-/-

cell cycle and developmentally regulated genes could be lost in G_0 cells, acting to initiate the apoptotic programme.

Examination of neural structures in the heads of *p130*$^{-/-}$ embryos suggested that neuronal differentiation was severely perturbed in the absence of p130 in the developing CNS. Histological and TUNEL analyses of 10.5 dpc *p130*$^{-/-}$ embryos revealed reduced size and extensive apoptosis in the optic vesicle (Figure 4.8), optic stalk, *facio acoustica* neural crest complex (pre-ganglia VIII and IX), and otic vesicle. By contrast, wildtype embryos displayed only moderate numbers of apoptotic bodies in head neural structures. Interestingly, Rb-deficient embryos displayed elevated apoptosis and inappropriate proliferation in neurons in the brain and retina at relatively later embryonic stages (Clarke, *et al.*, 1992; Jacks, *et al.*, 1992; Lee, *et al.*, 1994; Lee, *et al.*, 1992; Maandag, *et al.*, 1994; MacLeod, *et al.*, 1996). These data suggest that Rb and p130 play important and unique (non-redundant) functions in coupling cellular differentiation to maintained cell cycle control. These factors appear to be central to the survival of differentiating cells, specifically in the context of neural development.

By contrast, the myocardium of *p130*$^{-/-}$ embryos, like the wildtype myocardium, contained very few apoptotic nuclei (Figure 4.5). Although this data may indicate that p130 functions differently in cardiac muscle than skeletal muscle or neural tissue for example, at 10.5 dpc the majority of cardiomyocytes are not post-mitotic. Further analysis of cardiomyocytes in culture, may also reveal loss of the post-mitotic compartment via apoptosis.

4.2.vii Analysis of *in vivo* proliferation

p130 is considered a negative regulator of cell cycle progression so the high levels of apoptosis observed in the mutants may be a mechanism to compensate for uncontrolled or inappropriately maintained cell cycle arrest and E2F regulation in 10.5 dpc embryos.

Figure 4.8. Increased apoptosis and poor differentiation of head neural structures in the absence of p130

TUNEL analysis of 10.5 dpc wildtype embryos (A) revealed moderate numbers of apoptotic bodies in the optic vesicles (D), optic stalks (F), *facio acoustica* neural crest complexes (H), and otic vesicles (J). The head neural structures of *p130*$^{-/-}$ embryos (B,C) displayed reduced size and extensive apoptosis in the optic vesicle (E), stalks (G) *facio acoustica* neural crest complexes (I), and otic vesicles (K). Note the absence of a basement membrane lining the neural structures of *p130*$^{-/-}$ embryos. In A-C, long arrow denotes optic vesicle and stalk, and short arrow denotes otic vesicle. In the remainder of the panels, arrowheads indicate TUNEL-positive cells. Abbreviations: oc, optic cup; os, optic stalk; fa, facio-acoustica pre-ganglia complex; ov, otic vesicle. Panels were photographed at 400X magnification with the exception of A-C, at 25X.

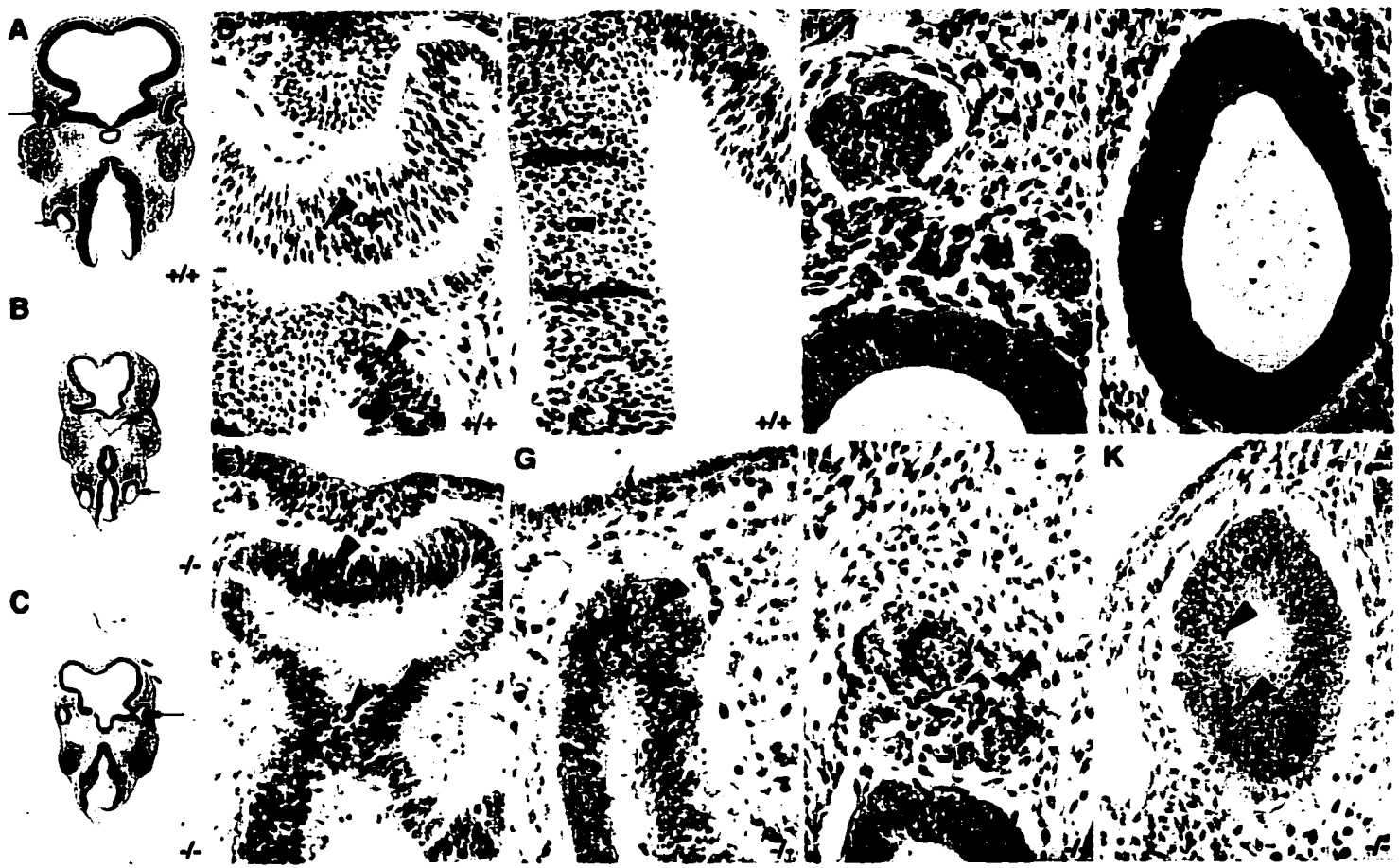
A
+/+
B
+/-
C
+/-
+/+
+/+
G
K

The mutant embryos are smaller, so potentially, high levels of apoptosis may contribute to this phenotype. Alternatively, there may be relatively lower levels of proliferation in the mutants. To address the issue of differential rates of proliferation, the expression of proliferating cell nuclear antigen (PCNA), a cell-cycle regulated factor that functions to enhance the processivity of DNA polymerase α, was analyzed. Sections from wildtype (n=3) and p130 mutant embryos (n=3) were subjected to immunostaining with antisera reactive to PCNA, specific for nuclei in or recently in S phase. PCNA-positive cells in lung, neural tube, forebrain, branchial arches and heart were assessed. The forebrain and neural tube of mutant embryos contained 4- and 1.5-fold higher frequency of proliferating cells, respectively. The mutant heart contained a lower percentage of PCNA-positive cells relative to wildtype, and other mutant tissues were comparable to wildtype (Table 4.3). A direct interpretation of this data is confounded by differences, some slight, in the discrepancies in stages of development of various tissues and structures in the mutant embryos relative to the controls. For instance, from E9.5-10 there is an elaboration of the telencephalic vesicles and high levels of proliferation in this tissue that dramatically increase the volume of the structures at this stage of embryogenesis (Kaufman, 1992). I have not directly assessed the growth rate of cells cultured from mutant versus wildtype 10.5 dpc embryos, therefore the cell-autonomy of decreased or increased growth rates are not addressed. It is clear from the data, and expected, that the rate of growth as assessed here by PCNA reactivity, is highly dependent of the tissue context. There appears to be cell-type specific changes in the percentages of PCNA-reactive cells, indicating that p130-deficiency does not affect all tissues equally, dependent on cell context or stage of development.

Table 4.3 Variable percentages of PCNA-positive nuclei in wildtype versus p130$^{-/-}$ embryonic tissues at 10.5dpc.

Tissue	Number of PCNA -positive cells [a]
Forebrain	
wildtype	$9.7^{+/-}1.0$
p130$^{-/-}$	$38.5^{+/-}13.1$
Heart	
wildtype	$23.2^{+/-}2.1$
p130$^{-/-}$	$13.7^{+/-}1.5$
Neural tube	
wildtype	$16.1^{+/-}0.5$
p130$^{-/-}$	$24.2^{+/-}0.8$
Branchial arch	
wildtype	$22.1^{+/-}2.6$
p130$^{-/-}$	$20.5^{+/-}3.0$
Lung	
wildtype	12
p130$^{-/-}$	13

[a] 500-1000 nuclei were counted from 2 or 3 mutant and wildtype embryos, except for lung (1 embryo for each genotype was analyzed). Errors are presented as standard deviations.

4.2.viii. The p130 mutant phenotype is strain-dependent

The relatively normal phenotype of the *p130* $^{-/-}$ mice previously described in a 129Sv;C57Bl/6J hybrid genetic background, and the embryonic lethal phenotype of the *p130*$^{-/-}$ mice in a 129Sv;Balb/cJ background suggested that the penetrance of the *p130*$^{-/-}$ phenotype was dependent on second site modifier genes. To test this hypothesis, F1 *p130*$^{+/-}$ mice, the progeny of the founding chimeras and Balb/c mice were bred with either C57Bl/6J or Balb/cJ mice. The B1 (for backcross 1) *p130*$^{+/-}$ mice were then interbred to generate B2 *p130*$^{-/-}$ mice. The B1 *p130*$^{+/-}$ mice derived from the C57 cross have one set of C57 chromosomes and a second set composed of a mixture of Balb/c and 129Sv chromosomes. 129Sv is the strain of the ES cells. The B1 *p130*$^{+/-}$ mice derived from the F1 *p130*$^{+/-}$ X Balb/c cross have one set of Balb/c chromosomes and a second set composed of an undefined mixture of Balb/c and 129Sv. These breeding experiments allow an assessment of the contribution of Balb/cJ and C57BL/6J genetic backgrounds to the penetrance of the phenotype. However, these experiments do not directly assess the contribution of the 129/Sv genetic background to the penetrance of the phenotype. Backcrosses to 129Sv mice have been initiated.

As described above, *p130*$^{-/-}$ animals derived from an F1 *p130*$^{+/-}$ X F1*p130*$^{+/-}$ mating displayed 100% penetrance of the lethal phenotype (Table 4.2 1st column). Interbreeding of B1 *p130*$^{+/-}$ mice derived from a F1 *p130*$^{+/-}$ X Balb/c mating gave rise to B2 mice that also exhibited the phenotype (Table 4.2 2nd column). By contrast, the B2 mice derived from a F1 *p130*$^{+/-}$ X C57BL/6J mating gave rise to *p130*$^{-/-}$ mice that were viable and fertile indicating that the C57BL/6J background suppressed the phenotype (Table 4.2, 3rd column).

I have also derived a targeted *p107* mutant allele into either Balb/cJ or C57BL/6J genetic backgrounds. The *p107*$^{-/-}$ embryos in a hybrid 129Sv;Balb/cJ background are viable and fertile but exhibit diathetic myeloid metaplasia, a severe postnatal growth

deficiency, and an accelerated cell cycle (Chapters 5 and 6). By contrast, the majority of *p107*$^{-/-}$ mice in a hybrid 129Sv;C57BL/6J background display no apparent phenotype (Chapter 5; Lee, *et al.*, 1996). These data strongly support the interpretation that second-site modifier genes exist that effect the penetrance of null mutations in both *p130* and *p107*, although there is no indication that these are the same genes.

4.3. Discussion

The data presented in this chapter clearly indicate that p130 plays an essential role in development, but in a strain-dependent manner. Although not fully able to compensate for p130 function in the 129Sv;Balb/c genetic background, potentially other factors can partially fulfill the general and tissue-specific roles of p130 during development. The expression of related Rb and p107 have not been assessed in the mutant embryos. In order to address functional overlap, the interbreeding of the p130 mutants with Rb and p107 mutant mice has been initiated.

There are very clear distinctions between cardiac and skeletal muscle development including their distinct progenitors, splanchic mesoderm versus dermomyotome and the fact that cardiac muscle terminally differentiates postnatally. In the embryo, fully functioning cardiac myocytes are not post-mitotic nor do these cell fuse. During embryogenesis, increases in cardiac mass are the result of proliferative mononucleated cardiomyocytes (Litvin, *et al.*, 1992). As development progresses, an increasing proportion of cardiac myocytes withdraw from the cell cycle so that shortly (@ 2 weeks) after birth in mice, cardiomyocytes terminally differentiate and irreversibly withdraw from the cell cycle.

At the molecular level, in contrast to skeletal myogenesis, the regulation of cardiomycyte terminal differentiation remains unresolved; although genetic experiments in zebrafish and mice have implicated specific transcription factors and signal

transduction pathways (reviewed in Fishman and Chien, 1997; Rossant, 1996). Expression of SV40 T antigen in the heart can block terminal differentiation and permit *in vivo* (limited) proliferation in differentiated cardiomocytes (Kim, *et al.*, 1994). Interestingly, E1A expressed in post-mitotic cardiac myocyctes, promotes apoptosis. (Liu and Kitsis, 1996). p130 may be relevant in terms of maintenance or survival at later stages of cardiomyogenesis. It is possible that Rb (or p107) can functionally compensate, in terms of suppressing apoptosis during early stages development.

Cardiac insufficiency is potentially the cause of death round E11 in the p130-deficient embryos. It is possible that expressing the p130 cDNA under the control of a heart-specific promoter will rescue the defective cardiac phenotype and permit survival beyond E11. This approach would not only address the cardiac phenotype, but could permit an extended look to the consequence of loss of p130 beyond this point of development.

The p130 mutant embryos contained low numbers of Islet1/2 expressing motor and sensory neurons in the neural tube and DRG and low numbers of desmin-expressing myocytes in the dermomytome. This deficiency was correlated with loss of the notochord and perturbed floor plate structures in the trunk, together with increased levels of apoptosis throughout these regions. Several contributing mechanisms can be proposed to functionally explain the embryogenic phenotypes and lethality in the absence of p130 in the hybrid or Balb/C-enriched genetic backgrounds. For example, patterning, morphogenesis and proliferation may be perturbed following the loss of key structures during development. Also, cellular differentiation and survival may be detrimentally affected because of a unique function of p130 in withdrawal from the cell cycle or in enforcing terminal differentiation.

Apoptotic loss of structures like the notochord during development of $p130^{-/-}$ embryos could contribute significantly to the embryonic phenotype. For example, the

determination of progenitors of motor neurons is regulated in part by signals from the notochord and the neural tube floor plate (Yamada, *et al.*, 1993; Yamada, *et al.*, 1991). Signals generated from the node, notochord and dorsal neural tube function in patterning mesodermal (notochord, somite) and neural tissues (Placzek, *et al.*, 1993 reviewed in (Placzek and Furley, 1996). Specifically, Shh, expressed in notochord and floor plate, induces motor neuron progenitors (Ericson, *et al.*, 1996; Marti, *et al.*, 1995; Roelink, *et al.*, 1994; Roelink, *et al.*, 1995). These progenitors, situated in the ventricular epithelium of the ventral neural tube, are induced to migrate laterally and settle in a single continuous primary motor column (Tanabe, *et al.*, 1995). Additionally, combinatorial signals including Shh expressed in the floor plate and notochord, and Wnt family members, expressed in the dorsal neural tube, have been suggested to activate myogenesis in the somite (Dietrich, *et al.*, 1997; Munsterberg, *et al.*, 1995; Rong, *et al.*, 1992; Teillet, *et al.*, 1998). Wnts positively stimulate myogenesis in the somite, whereas Shh is believed to indirectly inhibit lateral plate-derived repressive signals (Hirsinger, *et al.*, 1997; Marcelle, *et al.*, 1997; McMahon, *et al.*, 1998; Reshef, *et al.*, 1998)). Presumably, loss of structures such as the notochord in *p130*$^{-/-}$ embryos would severely affect regional development, exemplified by the phenotype in the notochord-less HNF-3β gene-targeted mouse (Ang and Rossant, 1994; Weinstein, *et al.*, 1994). As well, when the notochord and neural tube are removed, muscle derivatives fail to develop (Rong, *et al.*, 1992). As all these structures were initially induced and present, the perturbations or losses exhibited in the *p130*$^{-/-}$ embryos suggest that p130 functions later in their differentiation programme or survival. Expression of differentiation-specific markers and TUNEL reactivity of these same terminally differentiated cells would confirm the hypothesis that p130-deficient differentiated cells are dying via apoptosis.

Loss-of-function mutation in *p130* may result in cell-autonomous deficits in cellular differentiation. For example, the reduced neurogenesis and myogenesis observed in $p130^{-/-}$ embryos may reflect a global perturbation of patterning due to specific requirements for p130 in directly negatively regulating proteins with paired-like homeodomains that have central developmental roles (Wiggan, *et al.*, 1997). Alternatively, appropriate withdrawal from the cell cycle and terminal differentiation may be affected due to an important regulatory role played by the formation of specific E2F/p130 complexes (Dyson, 1998; Muller, 1995; Weinberg, 1995b). For example skeletal myoblasts and neuronal cells contain free E2F as well as E2F complexed with p107 and Rb, whereas their differentiated derivatives primarily contain E2F complexed with p130 (Corbeil, *et al.*, 1995; Kiess, *et al.*, 1995; Shin, *et al.*, 1995). In differentiated myocytes, E2F complexes are primarily composed of E2F-4/p130 and formation of this complex has been suggested to be a necessary event in terminal differentiation. Similarly, formation of analogous E2F/p130 complexes has been observed during both myeloid and cardiomyocyte differentiation (Flink, *et al.*, 1998; Garriga, *et al.*, 1998; Raschella, *et al.*, 1997). Therefore, it is interesting to speculate that the low numbers of cells expressing Islet-1 or desmin in $p130^{-/-}$ embryos may reflect an important and unique role for p130 in withdrawing from the cell cycle or enforcing terminal differentiation. Interestingly, inactivation of Rb, p107 and p130 during neuronal induction *in vitro*, results in aberrant cell cycle exit and apoptosis (Slack, *et al.*, 1998).

The neuronal phenotype of the p130-deficient mice is reminiscent of that exhibited by Rb gene-targeted embryos (Clarke, *et al.*, 1992; Jacks, *et al.*, 1992; Lee, *et al.*, 1994; Lee, *et al.*, 1992). In Rb-deficient embryos, cells continue to proliferate in regions of the central and peripheral nervous system that normally contain only post-mitotic cells with many of the neurons undergoing apoptosis shortly after entering an ectopic S-phase. Apoptosis in the nervous system of $Rb^{-/-}$ embryos is p53-dependent and

correlates with increased levels of E2F, cyclin E and p21 (MacLeod, *et al.*, 1996). The expression pattern of several genes in cells undergoing apoptosis actually mirrors those of G_1 cells. Interestingly, p130 levels are increased in $Rb^{-/-}$ brains, suggesting that p130 may partially compensate for Rb in the mutant brain (Slack, *et al.*, 1998). As well, in the absence of Rb, determined neurons expressed early neuronal genes but then underwent programmed cell death (Lee, *et al.*, 1994). By contrast, in $Rb^{-/-}$skeletal muscle cells. p107 appears to partially compensate for Rb (Schneider, *et al.*, 1994). Rb-deficiency resulted in apoptotic-loss of inappropriately proliferating cells that failed to undergo terminal differentiation (Riley, *et al.*, 1997; Wang, *et al.*, 1997; Zacksenhaus, *et al.*, 1996). Taken together, Rb and potentially p130 functions to initiate or enforce cell cycle exit and loss of p130-dependent regulation can result in apoptosis.

Heterozygous *Rb* mice developed lens cataracts due to loss of the other allele. *Rb* $^{-/-}$ lens cells were poorly differentiated, highly proliferative and displayed very high rates of apoptosis. By contrast, heterozygous *Rb* mice bred into a *p53* homozygous mutant background exhibited overt lens hyperplasia with no associated apoptosis (Morgenbesser, *et al.*, 1994). Similarly, transgenic mice expressing HPV-16 E7 in retinal cells exhibited very high rates of retinal apoptosis. However, expression of both E7 and E6 which targets p53, or E7 in p53 mutant background induced retinal tumours with a reduction or absence of associated apoptosis (Pan and Griep, 1994). Inactivation of Rb, p107 and p53 also resulted in the development of retinoblastoma in mice (Robanus-Maandag, *et al.*, 1998). Interestingly, homozygous loss of *E2F-1* in the *Rb* null backgound, improved the survival of the Rb-deficient embryos, and reduces apoptosis in some tissues (Tsai, *et al.*, 1998). Several relevant points are raised by these experiments. The failure of retinoblastomas to form in targeted *Rb*-mutant mice is a consequence of functionally overlapping p107 and perhaps p130. Secondly, loss of Rb function can signal an apoptotic response that is E2F- and p53-dependent. Inappropriate activation of E2F in a

wide variety of cell types leads to p53-enhanced apoptosis (Hiebert, *et al.*, 1995; Phillips, *et al.*, 1997; Qin, *et al.*, 1994; Shan and Lee, 1994). Indeed, p53 functions to guard cells against hyperproliferative signals, and $p19^{ARF}$ appears to promote this response (Destanchina, *et al.*, 1998; Zhang, *et al.*, 1998 reviewed in Sherr, 1998). Therefore, generation of compound *p130*$^{-/-}$ *p53*$^{-/-}$ embryos in a Balb/cJ genetic background may elucidate whether the observed widespread apoptosis is p53-dependent. Rb and p130 appear to induce G_1 arrest via biochemically distinct mechanisms involving E2F-1 or E2F-4, respectively (Vairo, *et al.*, 1995). It would be interesting to generate compound mutant *p130/E2F-4* mice, to assess whether the *E2F-4* mutation would suppress the phenotype. The gene targeting of *E2F-4* has not been reported.

Cells are being derived from mutant embryos in order to address cell autonomous phenotypes, with a specific focus on consequences to cell cycle exit, re-entrance and survival of post-mitotic cells. Also, rescue experiments using *p130*$^{-/-}$ ES cell / wildtype chimeras can be employed to assess the cell autonomy of the p130$^{-/-}$ phenotypes. The drawbacks of these experiments include labour-intensive embryo manipulation and variable mutant ES cell contribution to tissues. Alternatively, transgene-derived p130 expression in the heart may permit a partial rescue of mutant embryos, permitting an analysis of p130 function beyond 10.5 dpc. A more informative and directed approach is to develop a strain of mice in which p130 can be conditionally mutated by virtue of sites for recombinase-specific disruption of required gene sequences. Work is ongoing to develop these ES cell lines.

An analysis of *p130*$^{-/-}$ EF cells, similar to that undertaken for the p107 mutant cells, can also be performed. The focus should be the processes of cell cycle exit and re-entrance and survival of quiescent cells. Additionally, it would be interesting to assess the expression of putative E2F-target genes in these cells, as well as *p107*$^{-/-}$ EF, using the

identical approach as Hurford et al (hurford, *et al.*, 1997). Further work could assess the expression of E2F-reporter genes in these cells, or derived cell lines.

The penetrance of the phenotypes of mice carrying targeted null mutations in *IGF-1*, *EGF*, *CFTR*, *TGFβ1*, *TGFβ3*, and *β1-adrenergic receptor*, vary in different genetic backgrounds indicating the importance of second-site modifier genes when characterizing null mutations (Bonyadi, *et al.*, 1997; Liu, *et al.*, 1993; Rohrer, *et al.*, 1996; Rozmahel, 1996; Sibilia and Wagner, 1995; Threadgill, *et al.*, 1995). The molecular basis for the penetrance of the *p130/-* phenotype on C57BL/6J versus Balb/cJ backgrounds remains to be established. However, the breeding data is consistent with the existence of few modifier alleles representing either recessive loss-of-function mutations in the C57BL/6J background, dominant gain-of function mutations in the Balb/cJ background, or a mixture of both (Table 4.2). Subsequent genetic analysis may reveal whether heterozygosity at a modifying locus i.e. one 129Sv allele and the second Balb/cJ, is required to elaborate this phenotype. By performing microsatellite analysis, the number of modifying genes and their approximate locations may be accurately determined. Clearly, the molecular identification of genes potentially epistatically interacting with p130 will further our understanding of the regulatory pathways within which p130 functions.

CHAPTER 5

Strain-Dependent Postnatal Growth Deficiency andMyeloid Hyperplasia in Mice Lacking p107

5.1. Introduction

Mouse embryonic development represents a model system to genetically assess the requirements for a gene product during cell proliferation, terminal differentiation, and apoptosis. During embryogenesis, p107 expression is most prominent in the heart and intestine and overlaps with Rb expression in the developing CNS and liver. Generally, in other tissues as well as post-mitotic tissues p107 expression is very low or undetectable (Jiang, *et al.*, 1997; Kim, *et al.*, 1995). This expression pattern implicates p107 functions in the proliferative phase and potentially in initiating cell cycle withdraw during differentiation.

As a cell cycle regulator, p107 functions in the G_1 and S phases (Chittenden, *et al.*, 1993; Cobrinik, *et al.*, 1993; reviewed in Cobrinik, 1996; Dyson, 1998). Although all indications point to Rb and p130 in the G_0 maintenance of differentiated cells, p107 negatively regulates cell cycle progression and may participate to varying extents in cell cycle withdrawal during the development of several cell types (Zamanian and LaThangue, 1993; Zhu, *et al.*, 1995a). For example, although not completely restored in their ability to differentiate, p107 overexpression in Rb-deficient myocytes, permitted cell cycle withdraw, fusion and the expression of differentiation-specific genes (Schneider, *et al.*, 1994).

p107, like Rb and p130, can inhibit E2F-dependent transcription and cell growth in the context of specific cell lines (Zhu, *et al.*, 1993). Generally, p107/E2F complexes are not a major component of G_0 arrested cells, but appear to exert control on E2F activity at late G_1 and early S phase transitions. The identity of genes regulated by p107/E2F complexes versus Rb and p130 complexes are unresolved, although the rather discrete functional domains (cell cycle phases) of these proteins are overlapping and indicate that these factors coordinately regulate E2F-dependent transcription. It is proposed that genes regulated by p130/E2F complexes may be controlled by p107/E2F after re-entrance into the cell cycle (Smith, *et al.*, 1998). Additionally, p107 is capable of associating with factors distinct from those for Rb and p130 indicating that p107 has specific functions not shared by the related proteins. In addition to interactions with the cyclin/cdk complexes, p107 can associate with myc, B-myb and Sp-1 transcription factors (Beijersbergen, *et al.*, 1994a; Datta, *et al.*, 1995; Gu, *et al.*, 1994b; Sala, *et al.*, 1996). As well, p107 is capable of interacting with paired-like homeodomain containing proteins and C/EBP (CATT/enhancer binding proteins) transcription factors that function during cell differentiation (Chen, *et al.*, 1996b; Wiggan, *et al.*, 1997). Therefore, to assess the specific *in vivo* functions, *p107* was targeted for mutation in ES cells, and p107-deficient mice were generated.

p107$^{-/-}$ mice in the hybrid 129Sv;Balb/c genetic background are viable and fertile, indicating that functionally overlapping factor(s) are compensating for its loss during development. However, during the immediate postnatal period a growth deficit is exhibited by the mutant mice. There is also significant early mortality with signs of acute or chronic inflammation apparent in selected and unselected animals. Interestingly, the p107 mutants exhibited extramedullary hematopoiesis (EMH) and a myeloproliferative disorder that had an increasing penetrance with age. This indicated that secondary events were required to manifest the disorder. These phenotypes were also strain-dependent, as

in a mixed 129Sv;C57Bl/6 genetic background, the majority of *p107*$^{-/-}$ mice were indistinguishable from their wildtype and heterozygous littermates. Second-site modifiers, as is the case with the p130 mutants, affect the phenotypes in these distinct genetic backgrounds.

5.2 Results

5.2.i. p107 gene-targeting generates a null allele.

The p107 gene (Figure 5.1) was disrupted by homologous recombination in J1 embryonic stem cells (R. Hardy) by standard techniques. Two independent p107 mutant mouse lines were derived into the germline and, as the observed homozygous phenotype was completely identical in all experiments, these are discussed together. Interbreeding of heterozygous mice yielded an approximate Mendelian ratio of 1:2:1 between wildtype, heterozygous and homozygous mutant mice, respectively. As summarized in Table 5.1, the genotypes of the first 265 mice were 71 wildtype (26.8%), 136 *p107*$^{+/-}$ (51.3%) and 58 *p107*$^{-/-}$ (21.9%). Therefore, the absence of p107 appeared not to significantly affect embryonic development or postnatal survival. However, *p107*$^{-/-}$ mice did exhibit a profound difference in growth rate in the immediate postnatal period as described below.

To confirm that the disruption of p107 with the PGK-neo cassette had generated a null mutation, Northern and immunoblot analyses were performed with RNA and protein isolated from 14.5 dpc embryos. Northern analysis with polyA+ RNA isolated from EF revealed the mature 4.8 kb p107 mRNA and a truncated product previously characterized, at 2.4 kb in wildtype EFs (Kim, *et al.*, 1995). However, *p107*$^{+/-}$ EF cells also expressed transcripts about 300 nt smaller than the full-length or truncated species, and *p107*$^{-/-}$ cells only expressed the smaller RNAs (Figure 5.2A). The 'targeted' RNA did not hybridize a *neomycin* cDNA probe rather a 0.8 kb fragment was detected with a *neomycin* probe

(Figure 5.2B). S1 nuclease protection assays (Figure 5.2C, D) indicated that the smaller RNA expressed from the mutant *p107* allele was initiated from the PGK-1 promoter but in the opposite direction to the normal PGK-1 transcriptional initiation. This generated a truncated sense p107 transcript. The exact structure of this transcript is unknown at present.

Immunoblot analysis was performed with antiserum specific to the carboxy-terminus of p107. The p107 protein was readily detected in extracts from 14.5 dpc wildtype embryos, and reduced levels were observed in extracts from $p107^{+/-}$ embryos (Figure 5.3A). No detectable product was observed in lysates from $p107^{-/-}$ embryos. As heterozygous mice or embryonic fibroblasts do not exhibit a phenotype distinguishable from wildtype, if a protein product is produced it does not appear to interfere with the product of the wildtype allele. Unfortunately, there are no commercially available antibodies that recognize a p107 amino-terminal epitope. Taken together, the data indicate that the disruption of p107 exon 4 with the *PGK-neo* cassette generated a null mutation at the protein level.

Experiments with gene targeted mice have demonstrated that functional overlap and compensation are prevalent within gene families. To analyze the expression of related proteins, immunoblots were performed for p130 and Rb on identical extracts as for the p107 blots. The levels of p130 were similar in extracts prepared from wildtype, $p107^{+/-}$ and $p107^{-/-}$ embryos (Figure 5.3B). By contrast, Rb levels were reproducibly increased about 2-fold in extracts prepared from $p107^{-/-}$ embryos (n=5), and were unaltered in extracts prepared from $p107^{+/-}$ embryos (Figure 5.3C). Therefore, the data is consistent with p107 indirectly or directly negatively regulating Rb expression. This overexpression of Rb in the $p107^{-/-}$ embryos suggests that Rb is functionally compensating/substituting for p107 at this stage of development. Evidence for direct, reciprocal regulation between members of the Rb family exists (see Discussion).

Figure 5.1. Targeted disruption of the *p107* gene in ES cells and mice.

(A) Structure of the targeting vector (generated by W.R. Hardy), restriction map of the mouse *p107* gene, and structure of the targeted locus following homologous recombination. Exons are depicted as numbered closed boxes. Genomic fragments (probe-A and probe-B) used as probes for Southern blotting are shown as speckled boxes. The targeting vector contains PGK-neo in a reverse orientation relative to the *p107* gene. (B) Southern blot analysis of genomic DNA isolated from mouse tails. The DNA was digested with HindIII and hybridized with probe-B. Abbreviations: B, BamHI; E, EcoRI; RV, EcoRV; H, HindIII; WT, wildtype allele; T, targeted allele. Sizes in kb of the WT and T alleles are indicated at the right, and below the genomic and targeted loci (A).

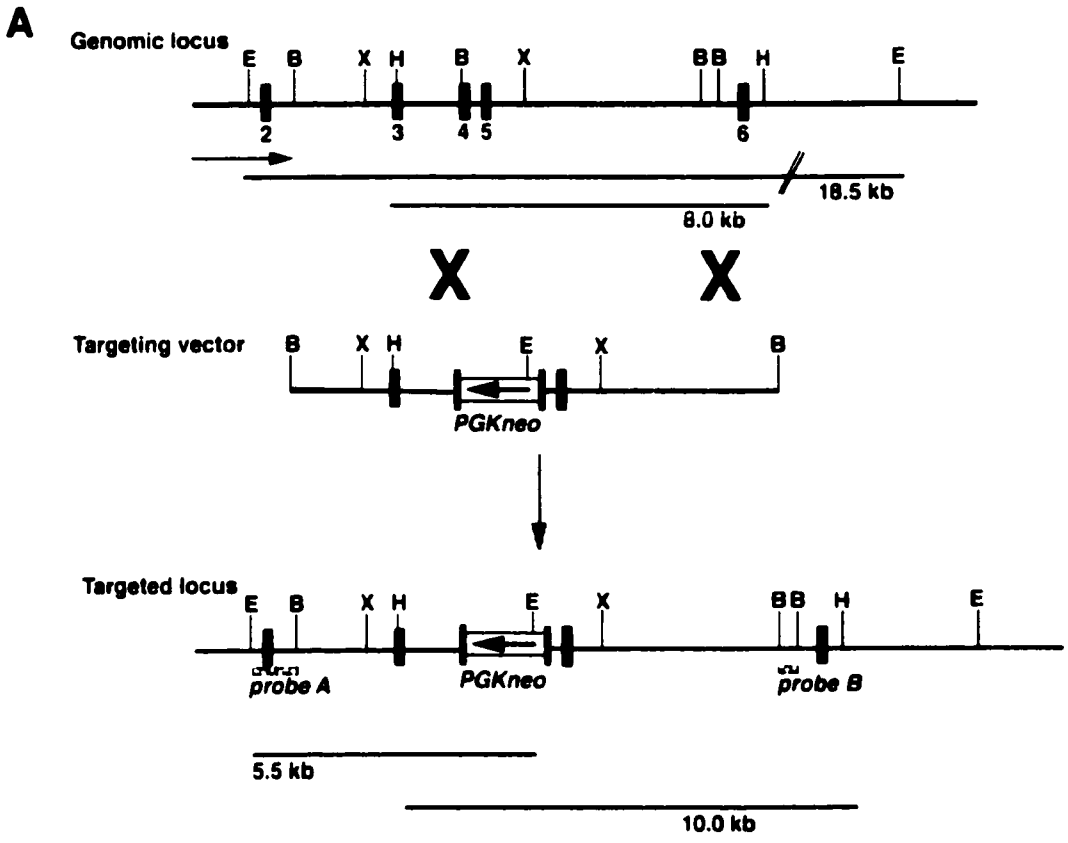
A
Genomic locus
E B X H B X B B H E
2 3 4 5 6
18.5 kb
8.0 kb
X X
Targeting vector
B X H E X B
PGKneo
Targeted locus
E B X H E X B B H E
probe A
PGKneo
probe B
5.5 kb
10.0 kb

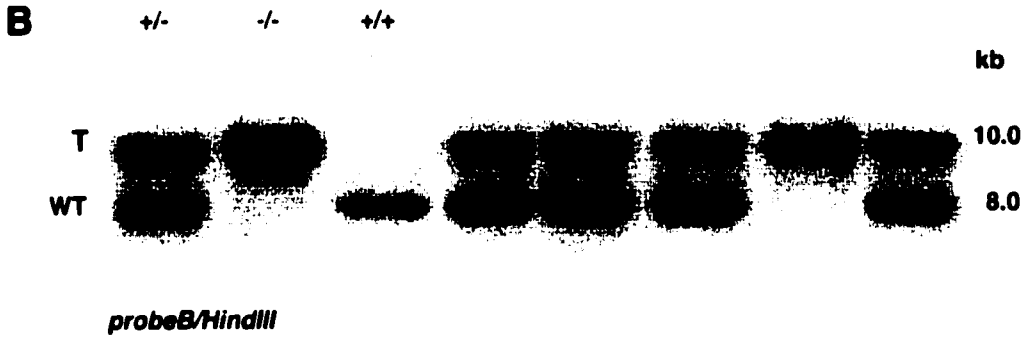
B
+/-
-/-
+/+
kb
T
WT
10.0
8.0
probeB/HindIII

Figure 5.2. *p107* gene-targeting generates a null mutation.

(A) Northern analysis of poly-A+ selected RNA prepared from wildtype ($^{+/+}$), p107$^{+/-}$ and p107$^{-/-}$ EF subconfluent cultures using the full-length p107 cDNA as probe. The targeted allele (T) gave rise to a truncated sense transcript that likely originated from within the PGK-1 promoter. The 2.4-kb p107 transcript (*) was also detected. (B) Northern blot analysis using full-length *neo* gene as probe indicated that *neo* coding sequence is not contained within the p107 transcripts from the targeted allele. (C) Immunoblot analysis with anti-p107 antibody revealed no detectable p107 protein or truncated version of the protein in extracts prepared from *p107*$^{-/-}$ 14.5 dpc embryos. (D) S1 nuclease protection assay using the antisense probe, illustrated below the blot (red), indicated that the sequences 5' of the *neo* site of integration are not expressed at a detectable level. (E,F) S1 nuclease protection assay using the antisense probe, illustrated below the blot, indicate that sequences 3' of the *neo* integration are expressed to a low level relative to wildtype or *p107*$^{+/-}$. The variation in size of the protected fragments indicates that the 5' end of the transcript is not fixed. These are two exposures of the same blot. Abbreviations: WT, wildtype p107 transcript; T, truncated p107 transcript; M^r, apparent relative mobility in kD.

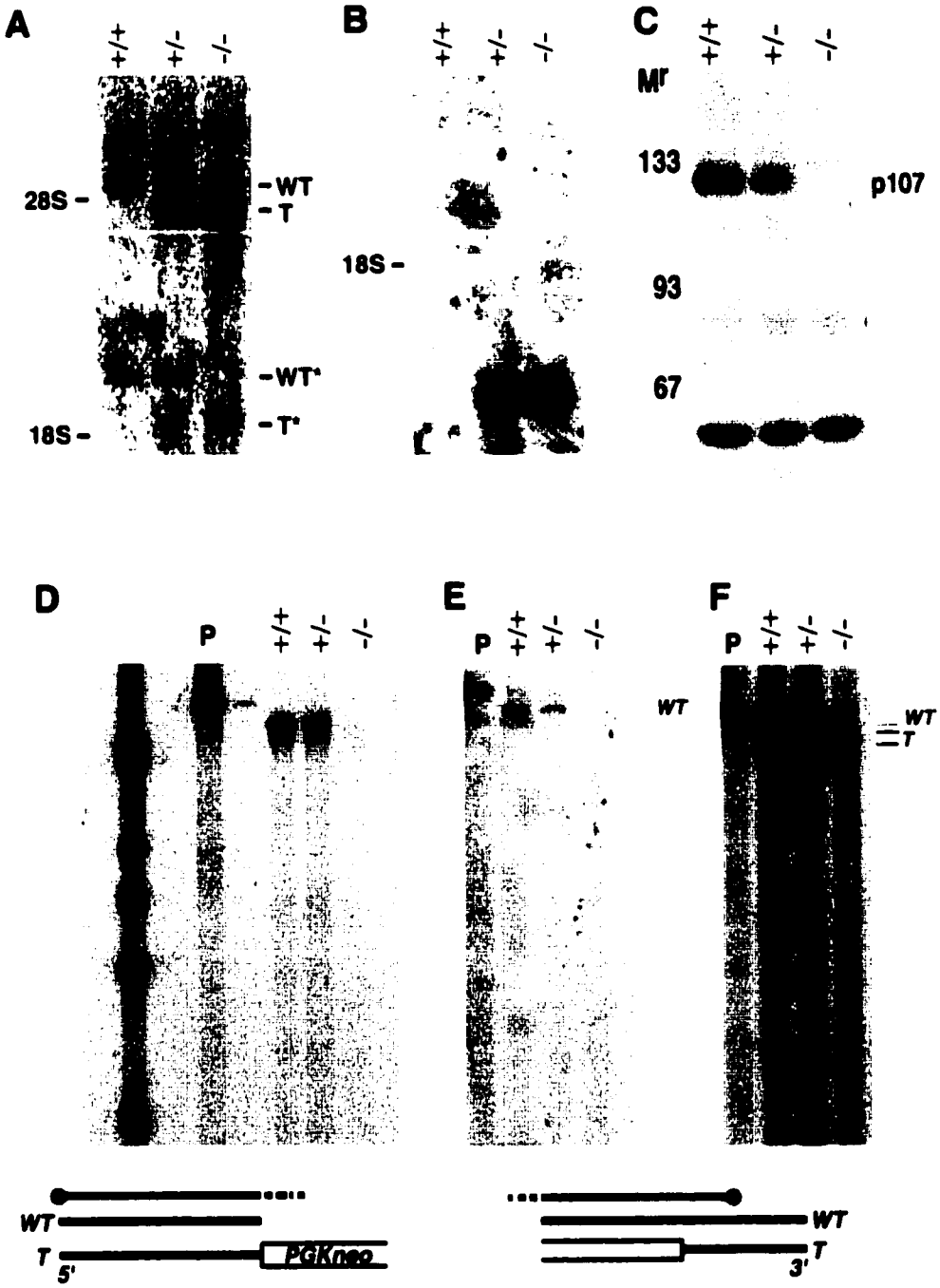
A
+/+
+/-
-/-
28S -
18S -
WT
T
WT*
T*
B
+/+
+/-
-/-
18S -
C
+/+
+/-
-/-
Mr
133
93
67
p107
D
P
+/+
+/-
-/-
WT
T
5'
PGKneo
E
P
+/+
+/-
-/-
WT
F
P
+/+
+/-
-/-
WT
T
WT
T
3'

Figure 5.3. Expression of Rb-family members in p107-deficient mice

(A) Immunoblot analysis with anti-p130 antibody revealed approximately similar levels of p130 in extracts from wildtype, *p107*$^{+/-}$ and *p107*$^{-/-}$ 14.5 dpc embryos. (B) Immunoblot analysis with anti-Rb antibody revealed about a 2-fold increase in levels of Rb in extracts prepared from *p107*$^{-/-}$ 14.5 dpc embryos, relative to extracts prepared from wildtype and *p107*$^{+/-}$ siblings. For lanes 7, 8 and 9, 50%, 25%, and 10% of lysate loaded in lane 5 were assessed. The Rb protein was not detectable when ^{125}I-conjugated secondary antibody was applied for quantitating levels of protein. However, it appears that the level of expression in mutant embryos is 2-fold higher than controls. Abbreviations M^r, apparent relative mobility in kD. Genotypes of extracts are indicated above the lanes.

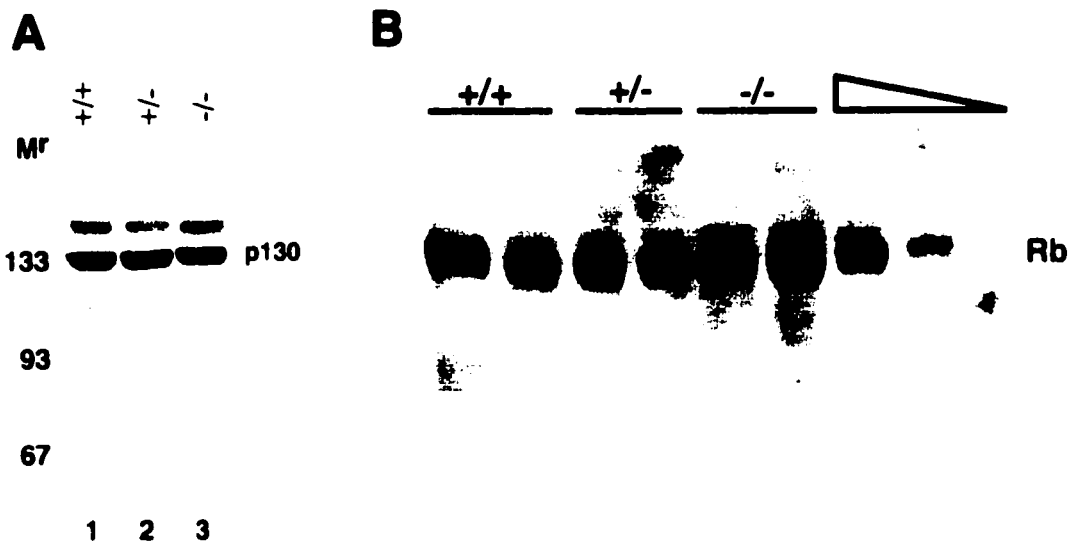
A
+/+
+/-
-/-
Mr
133
93
67
p130
1
2
3
B
+/+
+/-
-/-
Rb

Interestingly, transgenic mice overexpressing Rb display a runted appearance and altered growth kinetics reminiscent to that observed in *p107*$^{-/-}$ mice (Bignon, *et al.*, 1993). Although the growth of Rb transgenic mice was not as severely affected as the p107 mutants, the levels of Rb protein expressed in the transgenic mice was low (<2-fold increase over wildtype). It is interesting to speculate that the reduced growth of *p107*$^{-/-}$ mice is simply a consequence of the elevated Rb levels, however I am unable to determine whether *p107*$^{-/-}$ mice in a *Rb*$^{+/-}$ background would display normal postnatal growth. This compound mutant in a hybrid Balb/cJ strain displays embryonic lethality (see below).

5.2.ii. Postnatal growth deficit

Mutant embryos at 14.5 dpc and newborn pups were indistinguishable from their siblings in both size and morphology. Strikingly, by three weeks of age, *p107*$^{-/-}$ pups were uniformly about half the normal weight of their heterozygous and wildtype littermates (Figure 5.4). However, by 12 weeks of age *p107*$^{-/-}$ mice reached about 80% the weight of *p107*$^{+/-}$ and wildtype animals. In addition, the mutant animals displayed normal physical appearance and exhibited no notable abnormal behavioural traits. Histological inspection of organs throughout the *p107*$^{-/-}$ mice revealed no apparent anatomical abnormalities. Moreover, TUNEL analysis revealed no appreciable increase in apoptotic cells.

To examine the growth kinetics of *p107*$^{-/-}$ mice, animals were weighed at regular intervals for 60 days following birth (Figure 5.4C and D). This data suggested that newborn *p107*$^{-/-}$ mice failed to grow at the same rate as their wildtype and heterozygous littermates in the immediate postnatal period. However, mutant mice were weaned at 4 weeks postpartum and reached sexual maturity at the normal time, females at 6 weeks and males at 8. Taken together, these data suggest that mice deficient for p107 are not delayed in postnatal development but rather, exhibit a reduced rate of postnatal growth.

Newborn mutant pups exhibited normal suckling behaviour with milk evident in their stomachs within a few hours after birth. In 3 week old pups, histological examination of the pancreas revealed a normal appearance with an absence of zymogen particles, indicating that p107 mutant animals were likely absorbing nutrients in a normal manner. However, consistent with the reduced overall size of the mutant animals and proportionately smaller organs, reduced cellularity was observed in many tissues, for example the retina, gut epithelium and spleen (data not shown).

The normal birth size and reduced postnatal growth of newborn animals lacking p107 suggested that this phenotype was due to endocrine deficiencies. The anterior lobe of the pituitary is the major secretory portion of this neuroendocrine gland and five of its cell types produce the six major trophic hormones, including growth hormone. Significantly, lack of growth hormone causes symmetric retardation of growth. Serum levels of growth hormone, which acts postnatally, appeared to be completely normal in 4 week old $p107^{-/-}$ mice (Wt n=2, $p107^{-/-}$ n=2). Further analysis from younger mice (3 weeks) has been complicated due to insufficient volumes of serum samples. Northern blots were performed to assess the expression of insulin-like growth factor-1 using the mouse IGF-1 cDNA (gift of A. Musaro) as probe for RNA isolated from the liver, spleen and skeletal muscle of wildtype and $p107^{-/-}$ mice. Importantly, IGF-1 acts postnatally, and downstream of growth hormone (reviewed in Baker, *et al.*, 1993; Han and Hill, 1992). However, IGF-1 mRNA levels appeared normal (Figure 5.4). As sexual development, lactation and fertility are not affected in the mutants, and the growth deficit is transient in nature, general pituitary insufficiency is not evident. Therefore, the basis of the growth deficiency remains unresolved.

5.2.iii. p107 and Rb compound mutant embryos

In order to address functional compensation between Rb and p107, I attempted to derive compound mutant mice and characterize the resulting phenotype. Rb gene-

targeted mice were purchased from Jackson laboratories and backcrossed into the Balb/c genetic strain. *p107*$^{-/-}$ and *Rb*$^{+/-}$ mice were intercrossed to generate the compound heterozygotes, and these *p107*$^{+/-}$*Rb*$^{+/-}$ mice were subsequently intercrossed. From previous reports, Rb$^{-/-}$ embryos die *in utero* between 13.5-15.5 days (Clarke, *et al.*, 1992; Jacks, *et al.*, 1992; Lee, *et al.*, 1992) and *Rb*$^{+/-}$*p107*$^{-/-}$ mice (Lee, *et al.*, 1996) were viable and fertile but exhibited a postnatal growth deficit reminiscent of that I observed in our *p107*$^{-/-}$ mice. The expected frequency of *Rb*$^{+/-}$*p107*$^{-/-}$ mice derived from *Rb*$^{+/-}$ *p107*$^{+/-}$ X *Rb*$^{+/-}$*p107*$^{+/-}$ was 2 of 13 progeny. In 108 progeny from such matings, no viable *Rb*$^{+/-}$*p107*$^{-/-}$ mice were generated. Matings between the compound *Rb*$^{+/-}$*p107*$^{+/-}$ and *p107*$^{-/-}$, predicted to generate *Rb*$^{+/-}$*p107*$^{-/-}$ 1 in 4 also did not result in any mice of the desired genotype. Timed matings were set to determine when these embryos were dying. The data indicated that *Rb*$^{+/-}$*p107*$^{-/-}$ embryos are dying around 12.5 dpc, and *Rb*$^{-/-}$*p107*$^{-/-}$ around 9.5 dpc. These embryos exhibited a severe growth arrest (data not shown). The reduced survival and delayed appearance of these embryos support functional overlap between Rb and p107. Further histological analysis will potentially reveal the cause of lethality and allow a more thorough description of the phenotype.

5.2.iv. Diathetic myeloid proliferative disorder in *p107*$^{-/-}$ mice.

Although all animals were housed in a specific pathogen-free barrier facility, a high incidence of morbidity was observed in mice lacking p107, often in mice between 2 and 4 months of age. Approximately 10% of *p107*$^{-/-}$ mice suffered unexpected death, or displayed symptoms suggestive of opportunistic infections of a severity that warranted euthanasia. Histological analyses of these animals revealed the presence of inflammatory responses suggestive of acute lung and intestinal infections (Figure 5.5 and data not shown). Furthermore, histological analysis of unselected *p107*$^{-/-}$ animals at 10 months of age (n=9) revealed that 70% exhibited signs of either acute or chronic inflammation with tissues containing extensive infiltration of either neutrophils, or of macrophages, mast

and plasma cells. In some of these *p107*$^{-/-}$ mice, the inflammation was manifested as skin ulcers and abscesses (not shown). Importantly, no infections, sudden death or histological evidence of inflammation was observed in wildtype or *p107*$^{+/-}$ mice. Taken together, these data suggested that the immune response of *p107*$^{-/-}$ mice was compromised.

Thymocyte development was assessed in 4-6 week old wildtype and *p107*$^{-/-}$ mice. Thymocytes are lymphocytic derivatives that are central to cell-based immunity. Analysis of thymocytes from mutant mice did not reveal a consistent difference. Initially, FACS analysis of thymocytes from *p107*$^{-/-}$ spleens and thymii had a profile of CD4 and CD8 antibody reactivity that was characteristic of an earlier stage of development than controls. The higher levels of surface CD4 and CD8 co-receptors indicated that the p107$^{-/-}$ thymocytes were more immature than those found in wildtype or littermates (Figure 5.6) (reviewed in rodewald and fehlling, 1998; zuniga-pflucker and lenardo, 1998). However, further analysis did not corroborate initial results, perhaps due to the hybrid genetic background of the mice. This analysis may be revisited when the *p107* mutation has been successfully derived on a congenic background.

Blood analysis was also performed to assess the development and distribution of leukocytes, erythrocytes and platelets (Table 5.2). Leukocyte counts were consistently higher in unselected mutant mice compared to their wildtype and heterozygous counterparts. However, the white blood cell differential counts for p107-deficient mice was not apparently affected and there was no indication of defects in erythropoiesis.

Further analysis of *p107*$^{-/-}$ mice revealed a high proportion of animals that displayed a pattern of changes consistent with the presence of a myeloproliferative disorder. In the marrow of the sternum, a hypercellularity was observed that consisted of a strong shift to myeloid lineages. More specifically, in wildtype mice the ratio of myeloid to erythroid cells was 3:1 (similar to human), in contrast to the mutant, where the

observed ratio was 10:1 (Figure 5.7). Examination of spleens revealed extensive EMH within the red pulp that was predominantly myeloid in composition (Figures 5.8, 5.9). However, the most striking change was the presence of EMH in liver consisting of well-developed islands, some actually located in the walls of blood vessels (Figures 5.8, 5.9). The EMH in the spleen and liver was almost completely myeloid as confirmed by cytomorphology and immunohistochemistry with anti-myeloperoxidase antibody (Figure 5.9).

Myeloid cell progenitors (colony-forming units granulocyte/macrophage, CFU-GM) were enumerated following culture of marrow isolated from the femurs of 5-6 week old mice (Olga Gan with Dr. John Dick). Significantly increased numbers of myeloid progenitors were obtained from the femurs of 2 of 3 *p107*$^{-/-}$ mice, even at this young age. The numbers of CFU-GM in the two elevated p107$^{-/-}$ samples were increased 2.7 fold and 12 fold relative to 3 wildtype siblings (Table 5.3).

Sites of predominantly myeloid EMH were also noted at extremely unusual sites, including the pancreas, kidneys, and skeletal muscles of some mutant animals (Figure 5.9). In affected mutant animals, the lymph nodes from the pulmonary hilus were found to be unaltered. Fibrosis of the bone marrow results from fibroblast proliferation and is secondary to progression to the myeloproliferative disorder. However, marrow and sites of EMH had not undergone fibrosis as revealed by reticulin staining (data not shown). As well, in keeping with the lack of fibrosis, there were no teardrop-shaped erythrocytes in the circulation. Moreover, the proportion of blast cells relative to their differentiated derivatives appeared normal. Therefore, the disorder resembles a hyperplasia of the myeloid compartment rather than an overt neoplasia. As described above, although the mutant mice developed myeloid hyperplasia, there was no evidence of this condition

from peripheral blood analysis. However, neutrophils and granulocytes are resident in tissue, and would not be detectably increased in peripheral blood samples.

The proportion of the mutant animals that displayed the disorder increased with age. Mice lacking p107 between 2 and 6 months of age (n=8), often exhibited evidence of metaplastic myeloid proliferation in the spleen, but not liver. However, 54% of *p107*$^{-/-}$ mice over the age of 6 months (n=13) exhibited metaplasia in the liver and spleen ranging from mild to severe. By contrast, only a small number of well-dispersed individual myeloid cells were detected in livers of wildtype (1 of 10) and *p107*$^{+/-}$ mice (1 of 8). That the penetrance of the myeloproliferative disorder increased with age, suggested secondary events were required for progression to the disorder. The secondary events leading to the disorder could be mutations in other genes, for example activating mutations in oncogenes or inactivation of other tumour suppressors that would result in clonal hyperplasia. Alternatively, conditions leading to constitutive stimulation of the myeloid lineage, for example recurring opportunistic infections leading to polyclonal hyperplasia. The molecular basis for this disorder in the p107$^{-/-}$ mice remains to be resolved although the favoured hypothesis is that recurring infections lead to development of a polyclonal myeloid hyperplasia.

No hyperplastic or neoplastic changes were noted in a histological survey of a variety of other tissues. Together, the data indicate that p107$^{-/-}$ mice develop a diathetic myeloproliferative disorder that possibly predisposed animals to opportunistic infections.

5.2.v. Perturbed architecture of the p107$^{-/-}$ mammary gland.

In preliminary work, whole-mount mammary gland preparations were made from virgin animals, 2 months and 1 year of age (Figure 5.10). Strikingly, at 2 months of age, the primary ducts appeared wider in the *p107*$^{-/-}$ gland; and secondary and tertiary branching was markedly reduced. At 1 year, the glands of *p107*$^{-/-}$ mice (n=2) exhibited the appearance of multiparous animals, as the end buds had an extremely stellate

appearance. Again, the primary ducts appeared wider. Cross-sectional views of the glands will permit further characterization of this phenotype. These observations obligate a more complete analysis of this tissue, including an analysis of the developing lactating gland. Notably, mutants in the mixed genetic background do successful lactate and nurse their young.

Recently, p107 and Rb have been demonstrated to affect cyclin D1 expression (Watanabe, *et al.*, 1998). Cyclin D1-deficient mice displayed a mammary phenotype and the deficit necessitated fostering litters to other lactating females (Fantl, *et al.*, 1995). In humans, overexpression of cyclin D1 has been revealed in mammary tumours (reviewed in Hosokawa and Arnold, 1998). Therefore, cyclin D1 levels may be higher in the *p107* mutant mammary gland. Levels could be assessed by immunoblotting lysates prepared from the glands, and by immunohistochemistry.

5.2.vi. The p107 mutant phenotype is strain-dependent.

The normal phenotype of the p107 mice previously reported in the 129Sv;C57Bl/6J genetic background (lee, *et al.*, 1996), and the striking phenotype of p107 mutant mice crossed into a Balb/cJ background suggested that the penetrance of the mutant phenotype was dependent on the mouse genetic strain. To test this hypothesis, we bred male and female F1 $p107^{+/-}$ mice, that were progeny of the founding chimeras and Balb/cJ mice, with either C57Bl/6J or Balb/cJ mice. The resulting B1 $p107^{+/-}$ mice were then interbred to generate B2 $p107^{-/-}$ mice. Importantly, the B1 mice derived in the backcross have one set of C57Bl/6 chromosomes and a second set composed of an undefined mixture of Balb/c and 129Sv chromosomes. The B1 mice derived from the F1 X Balb/c cross have one set of Balb/c chromosomes and a second undefined mixed set, composed of Balb/c and 129Sv. Therefore, the interbreeding of B1 $p107^{+/-}$ mice derived from such backcrosses allows the assessment of the contribution of Balb/c and C57Bl/6 genetic backgrounds to the penetrance of the phenotype. The contribution of 129Sv to

the phenotype is not formally tested, however, genetic analysis should allow resolution of these issues.

As described above, *p107*$^{-/-}$ animals derived from an F1 X F1 mating displayed 100% penetrance of the growth phenotype (Table 5.1). In a small proportion of F2 *p107*$^{-/-}$ X F2 *p107*$^{-/-}$ matings, I observed litters that contained a mixture of runted and normal-sized F3 *p107*$^{-/-}$ mice, suggesting that second-site modifier genes were segregating in the population. Interbreeding of B1 *p107*$^{+/-}$ mice in the Balb/c mating series also resulted in B2 *p107*$^{-/-}$ with 100% penetrance of the growth phenotype indicating that the Balb/c background was permissive for penetrance. Additionally, the *p107*$^{-/-}$ mice were only 35% the size of heterozygous and wildtype littermates at 3 weeks indicating that the growth phenotype was more severe in the Balb/c-enriched genetic background. In subsequent generations, reduced numbers of 3 week old mice in a more pure Balb/c genetic background indicate that the mutants die perinatally and potentially *in utero* (C. Ying). By contrast, the interbreeding in the C57Bl/6 series gave rise to a high proportion of B2 *p107*$^{-/-}$ mice that did not exhibit the growth deficit, suggestive of the C57Bl/6 background suppressing the phenotype (Table 5.1). Importantly, as the *p107*$^{-/-}$ mice segregated discreetly into two weight groups, the trait does not appear quantitative in nature. Moreover, while primary myoblasts derived from runted *p107*$^{-/-}$ mice, C57Bl/6 B2, displayed a 2-fold acceleration in cell-cycle kinetics, primary myoblasts isolated from the normal sized *p107*$^{-/-}$ C57Bl/6 B2 mice exhibited normal growth. In addition, the reduced number of viable *p107*$^{-/-}$ offspring in mice derived from the Balb/c backcross supports the assertion that the severity of the *p107*$^{-/-}$ phenotype in increased in a Balb/C genetic background, and potentially a 129/Sv modifier gene reduces the penetrance of lethality. Taken together, these data support the hypothesis that multiple second-site modifier genes exist that may act in pathways impinging on p107 activity. The requirement for heterozygosity at specific modifying loci is possible. If this is the case,

interbreeding of B1 C57Bl/6 and B1 Balb/C or breeding these mice with 129/Sv mice may be informative, and may reveal the nature and number of the modifying gene(s).

Table 5.1 The genetic background specifies the penetrance of the p107$^{-/-}$ phenotype.

	Intercross		
	Chimera X Balb/cJ ↓	F1$^{+/-}$ X Balb/cJ ↓	F1$^{+/-}$ X C57Bl/6J ↓
Genotype	F1$^{+/-}$ X F1$^{+/-}$[a]	B1$^{+/-}$ X B1$^{+/-}$[b]	B1$^{+/-}$ X B1$^{+/-}$[c]
Wildtype	71	24	21
P107$^{+/-}$	136	46	39
p107$^{-/-}$ runted	58	15	7
normal	0	0	23

[a] The F1 *p107*$^{+/-}$ progeny of the founding chimeras bred with Balb/cJ mice when interbred yielded *p107*$^{-/-}$ pups that exhibited the runted phenotype. [b] The B1 *p107*$^{+/-}$ mice derived from an F1 *p107*$^{+/-}$ X Balb/cJ mating when interbred also produced B2 *p107*$^{-/-}$ runted mice. [c] The B1 *p107*$^{+/-}$ mice, derived from a F1 *p107*$^{+/-}$ X C57BL/6J mating, when interbred generated litters that contained both runted and normal B2 *p107*$^{-/-}$ mice.

Table 5.2 Reduced growth of *p107*-deficient mice[a].

Mouse	Weight (g)	Sample size (n)
Male		
Wildtype	$12.4^{+/-}1.5$	18
$p107^{+/-}$	$12.1^{+/-}0.81$	16
$p107^{-/-}$	$6.5^{+/-}0.6$	14
Female		
Wildtype	$10.8^{+/-}1.6$	15
$p107^{+/-}$	10.4+-/0.71	16
$p107^{-/-}$	$4.5^{+/-}1.3$	12

[a] Offspring from F1$p107^{+/-}$ X $p107^{+/-}$ breeding were weighed at 21 days post- partum. Male $p107^{-/-}$ mice were 52% of the normal weight, whereas $p107^{-/-}$ females were 42% of the normal weight. Errors are expressed as standard deviations.

Figure 5.4. Severe postnatal growth deficiency in p107$^{-/-}$ mice

Wildtype (A) and p107-deficient (B) littermates at 12 days of age derived from an F1 *p107*$^{+/-}$ X *p107*$^{+/-}$ intercross. Note the severe postnatal growth deficiency evident in *p107*$^{-/-}$ pups (see Table 5.2). (C) Growth curve of male wildtype (n=7, blue) and *p107*$^{-/-}$ (n=7, red) mice derived from heterozygous mutant matings. Male mice lacking p107 by 21 days of age were about 53% the normal weight. (D) Growth curves of female *p107*$^{+/-}$ (n=9, blue) and *p107*$^{-/-}$ (n=8, red) mice derived from heterozygous mutant matings. Female mice by 21 days of age were about 42% the normal weight. Errors are expressed as standard deviations.

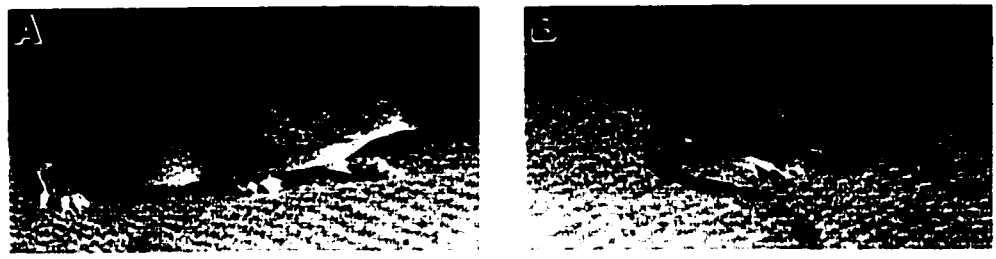
A
B

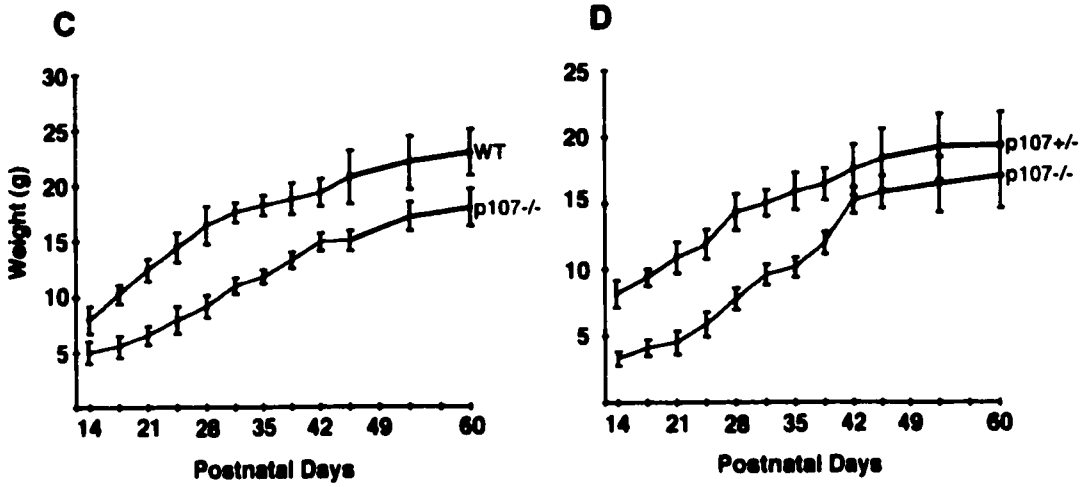
C
D
Weight (g)
30
25
20
15
10
5
14
21
28
35
42
49
60
Postnatal Days
WT
p107-/-
p107+/-
p107-/-

Figure 5.5 Sites of infection in p107$^{-/-}$ mice

Histological analysis of a great proportion of p107-deficient mice revealed sites of infection including infiltrated lungs (B). Compare the mutant consolidated tissue to (A) lung tissue from a wildtype age-matched animal. Panels were photographed at 200X magnification.

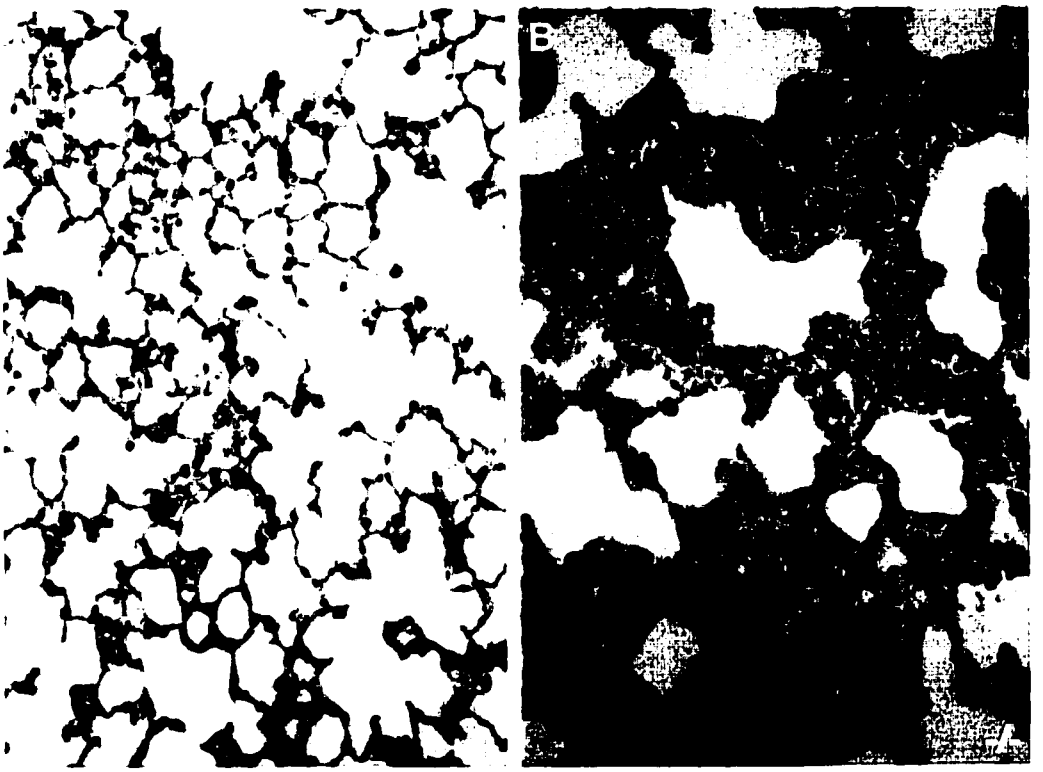
B

Figure 5.6. *p107*$^{-/-}$ thymus contains a higher proportion of immature thymocytes

Thymocytes from (A) wildtype (n=3) and (B) p107-deficient (n=3) 6-week old mice were immunostained with anti-CD8 and anti-CD4 antibodies and sorted by flow cytometry. The proportion of double positive thymocytes (immature) in mutant tissue was 94.9% versus 79% in the wildtype thymus. Also, note that the intensity of staining was greater in the mutant, indicating that the *p107*$^{-/-}$ thymocytes are at an early stage of development. There was a decrease in the proportion of peripheral (mature) T cells in these mutants (data not shown).

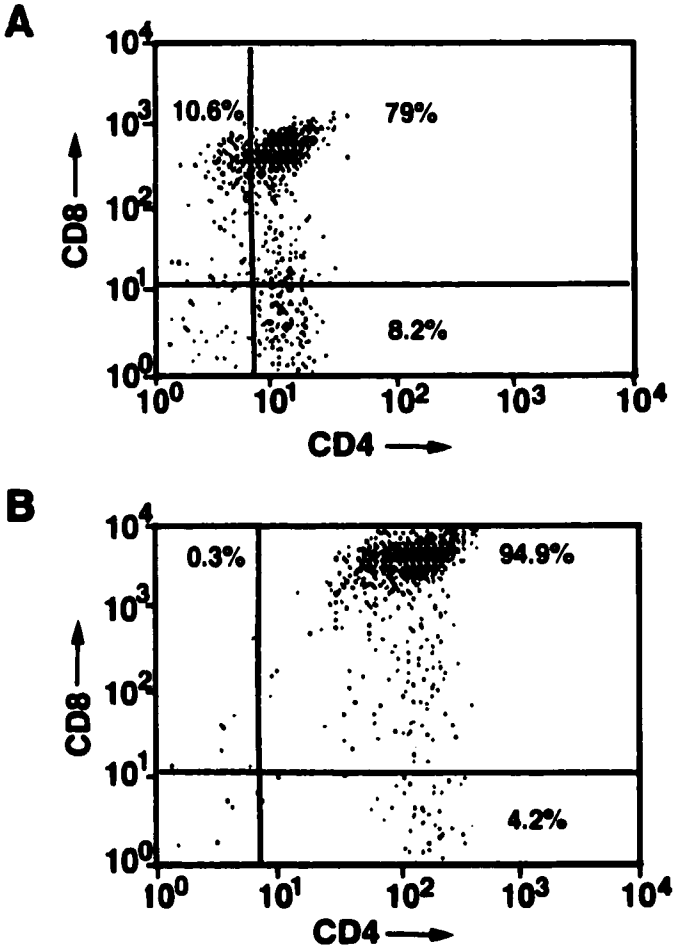
A
10^4
10^3
10^2
10^1
10^0
CD8
10.6%
79%
8.2%
10^0
10^1
10^2
10^3
10^4
CD4
B
10^4
10^3
10^2
10^1
10^0
CD8
0.3%
94.9%
4.2%
10^0
10^1
10^2
10^3
10^4
CD4

Table 5.3. Peripheral blood cell counts in wildtype versus *p107*$^{-/-}$ mice.

	Leukocytes X 10^9/L	Erythrocytes X 10^{12}/L
Wt-1	1.8	8.75
Wt-2	1.4	9.67
Wt-3	1.4	8.79
Wt-4	2.3	8.92
Wt-5	2.1	N/D
Wt-6	2.3	8.92
Wt-7	2.9	8.54
Wt-8	2.3	8.91
Wt-9	1.6	9.36
Wt-10	2.6	9.24
Wt-11	2.3	9.64
Wt-12	2.8	N/D
Wt-13	3.2	N/D
Mean	$2.23^{+/-}0.57$	$9.07^{+/-}0.38$
p107$^{-/-}$1	5.7	9.64
p107$^{-/-}$2	5.5	9.25
p107$^{-/-}$3	3.4	8.87
p107$^{-/-}$4	7.5	9.46
p107$^{-/-}$5	5.2	9.71
p107$^{-/-}$6	5.8	N/D
p107$^{-/-}$7	3.9	8.78
p107$^{-/-}$8	3.8	8.69
p107$^{-/-}$9	3.8	8.97
p107$^{-/-}$10	6.7	N/D
p107$^{-/-}$11	6.2	N/D
p107$^{-/-}$12	7.1	8.54
p107$^{-/-}$13	9.5	9.11
Mean	$5.7^{+/-}1.75$	$9.10^{+/-}0.40$

Note: Errors are expressed as standard deviations.

Figure 5.7. Myeloid hyperplasia in the bone marrow of *p107*$^{-/-}$ mice

Histological analysis of hematoxylin and eosin stained sections revealed a hypercellularity with a strong shift to myeloid lineages in the marrow of *p107*$^{-/-}$ mice (B) relative to wildtype mice (A). Antibody specific for myeloperoxidase, expressed in granulocytes, confirmed the histological identification of these myeloid cells (Figure 5.9). Abbreviations: M, megakaryocyte; RP, red pulp; GC germinal center. Panels A and B were photographed at 400X magnification.

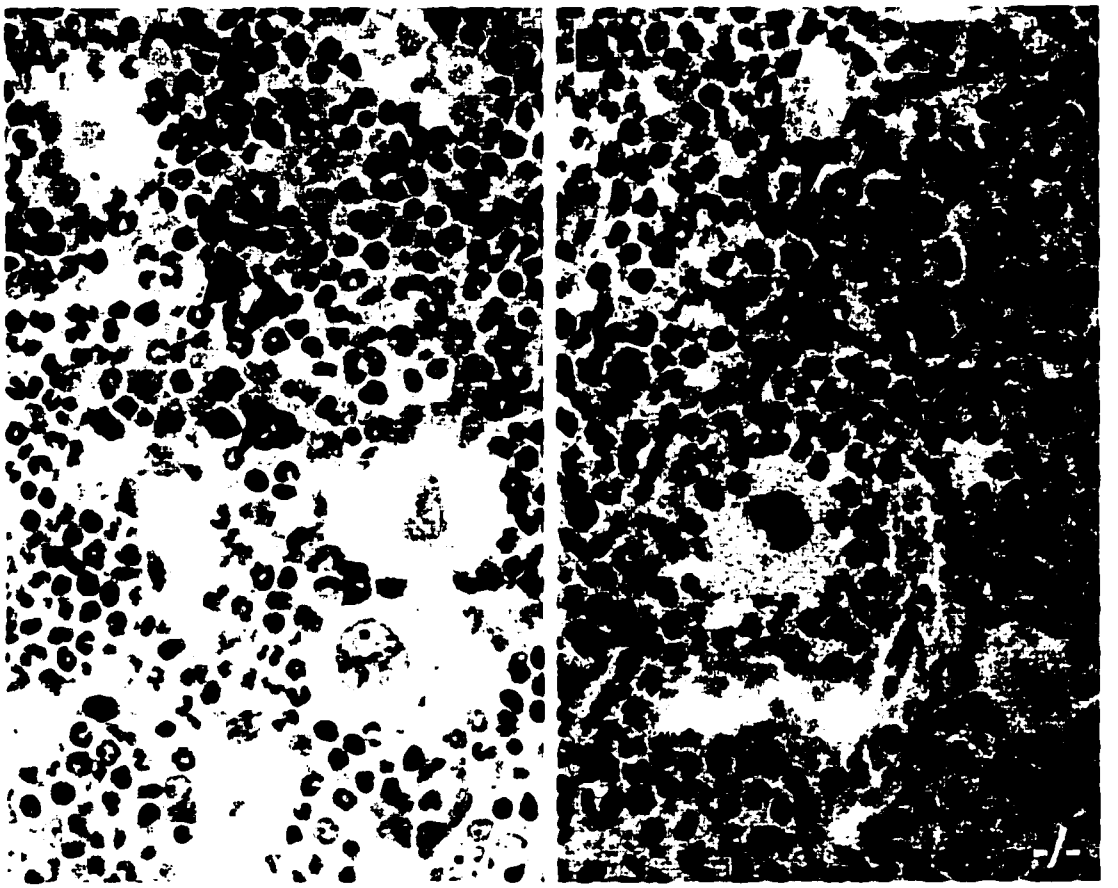
-1-

Figure 5.8. Extramedullary hematopoiesis in *p107*$^{-/-}$ spleen and liver

Examination of mutant spleens (D,E) revealed extensive EMH within the red pulp that was predominantly myeloid in composition. Normal spleen from a wildtype littermate (A,B). A high proportion of *p107*$^{-/-}$ livers contained extensive infiltration of well-developed hematopoetic islands that were also mostly myeloid in composition (F). (E) Normal liver from a wildtype littermate. Samples shown are from 12 month old mice. Arrowheads denote myeloid cells and arrows, sites of myeloid metaplasia. Panels A and D were photographed at 50X magnification and B,C,E, and F at 200X.

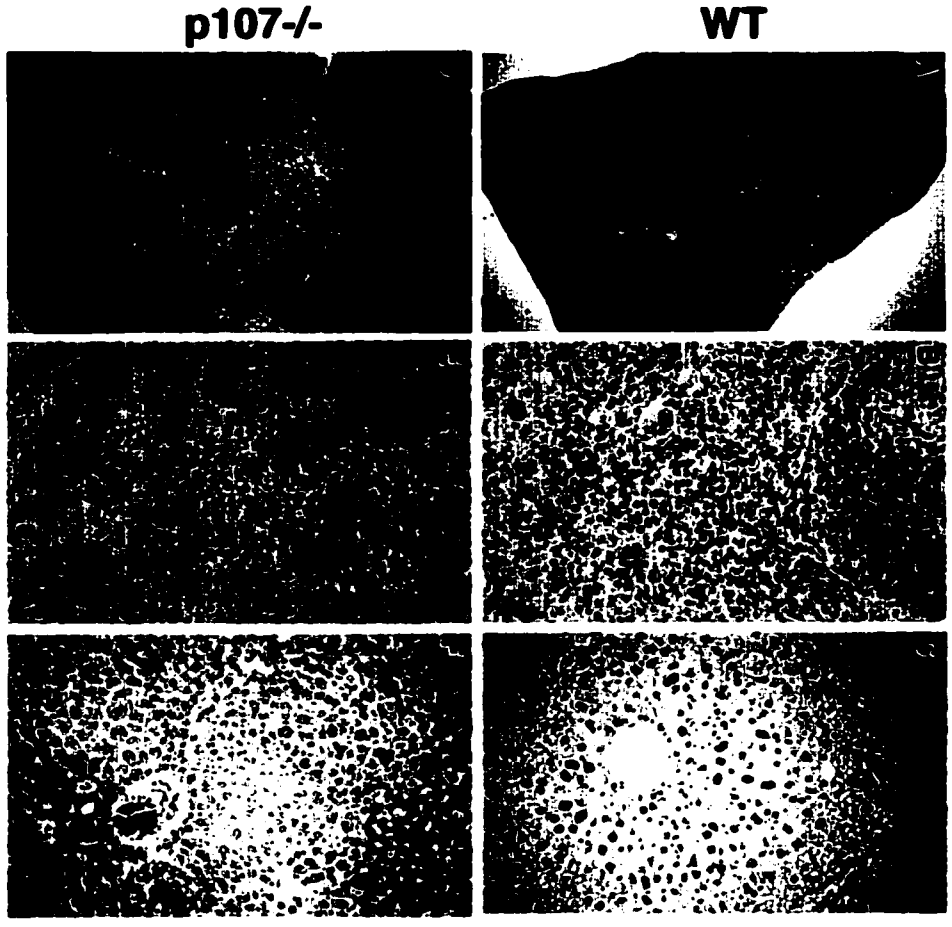
p107-/-
WT

Figure 5.9. Unusual sites of myeloid proliferation

In addition to the sites in (A) liver (B) spleen and (C) bone marrow, anti-myeloperoxidase immunostaining indicated sites of myeloid metaplasia in (D) thymus and (E) skeletal muscle. Myeloproliferation was also detected in the (F) kidneys of some mutant animals. Panels were photographed at 400X magnification.

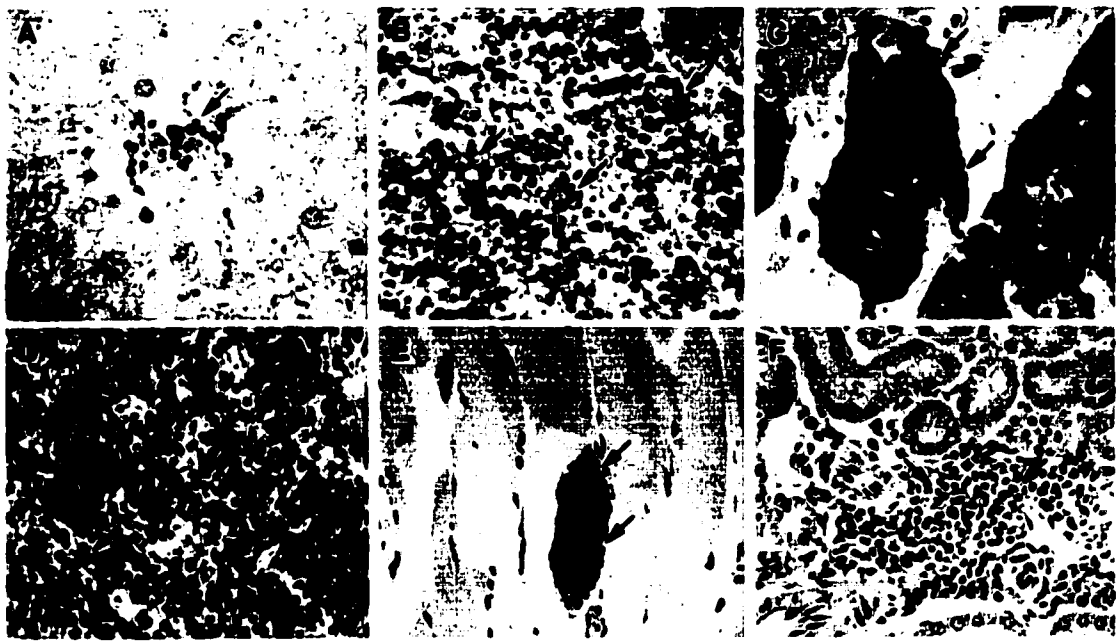

Table 5.4 Granulocyte and macrophage colony-forming units from femurs and spleens of *p107*$^{-/-}$ and wildtype mice.

	Cells per femur ($x10^6$)	CFU-GM per femur	Cells per spleen ($x10^6$)	CFU-GM per 10^5 spleen cells	CFU-GM per spleen
Wt-1	7.5	$14800^{+/-}2261$	88	$5.3^{+/-}1.1$	$4635^{+/-}939$
Wt-2	6.3	$13104^{+/-}525$	44	$8.5^{+/-}1.2$	$3740^{+/-}508$
Wt-3	8.3	$18371^{+/-}586$	96	$11.3^{+/-}2.2$	$10880^{+/-}2098$
MEAN	$7.4^{+/-}0.6$	$15425^{+/-}1039$	$76^{+/-}16$		$6418^{+/-}1312$
p107$^{-/-}$1	8.8	$41647^{+/-}3974$	76	$23.2^{+/-}3.3$	$17607^{+/-}2543$
p107$^{-/-}$2	7.1	$17513^{+/-}1550$	42	$7.8^{+/-}0.4$	$4290^{+/-}185$
p107$^{-/-}$3	5.7	$185040^{+/-}1135$	190	$41.0^{+/-}5.8$	$77900^{+/-}11011$
MEAN	$7.2^{+/-}0.9$	$19837^{+/-}2553$	$59^{+/-}17$*		$10448^{+/-}3398$*

The data from p107$^{-/-}$3 was excluded from the calculation (*).

Note, errors are expressed as standard deviations.

Figure 5.10. Perturbed architecture of *p107*$^{-/-}$ virgin mammary gland

Mammary gland whole-mount analysis of 2 month old mice revealed that in contrast to (A) wildtype and (B) *p107*$^{+/-}$ glands, the (C) *p107*$^{-/-}$ gland exhibited reduced numbers and extent of side branching. Additionally the primary ducts appeared wider. Arrowheads indicate primary and secondary ducts. Analysis of 1 year old virgin tissue revealed that the mutant glands (E,F) (n=2) had the appearance of multiparous tissue. The primary ducts were wider and the end buds exhibited a stellate form compared to the (D) *p107*$^{+/-}$ mammary gland. Arrowheads indicate end buds.

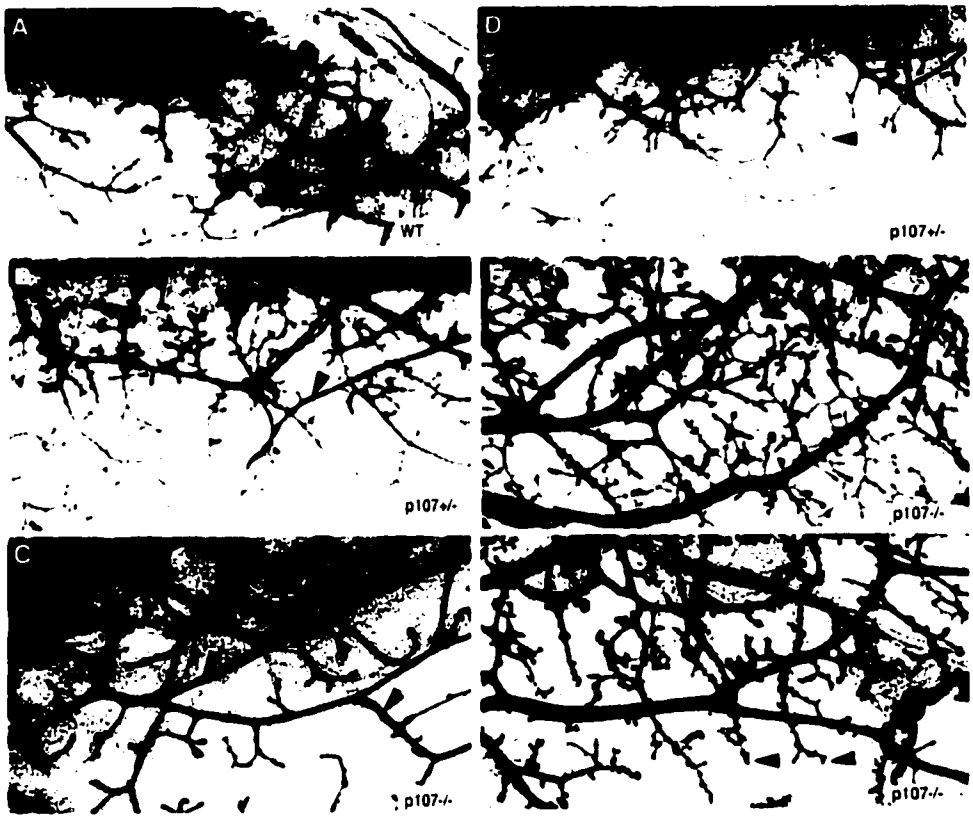
A
WT
D
p107+/-
B
p107+/-
E
p107-/-
C
p107-/-
F
p107-/-

Figure 5.11. Targeting strategy for *p107* conditional mutant allele

(A) A portion of the genomic locus of the *p107* gene is illustrated along with a targeting vector that contains the *PGK-neo* expression cassette flanked by CRE recombinase recognition (loxP) sequences in intron 5, and a third loxP site in intron 3. Following expression of the bacteriophageP1 Cre recombinase protein, sequences flanked by direct repeats of the LoxP sites will be deleted. The possible configurations of the targeted allele following Cre expression are illustrated. ES cells harbouring the allele I will be used to generate chimeric mice. The homozygous mice generated can be bred to CRE transgenic mice for transgene-specific mutation of the 'floxed' *p107* alleles (configuration II).

A

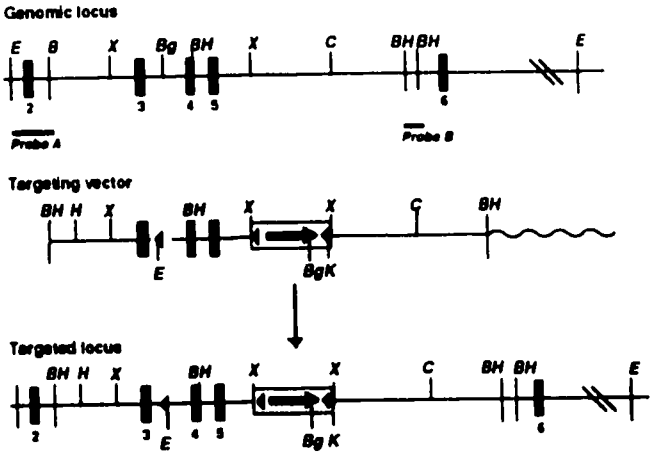
Genomic locus
E
B
X
Bg
BH
X
C
BH BH
E
2
3
4
5
6
Probe A
Probe B
Targeting vector
BH H X
BH
X
X
C
BH
E
BgK
Targeted locus
BH H X
BH
X
X
C
BH BH
E
2
3
E
4
5
Bg K
6

B

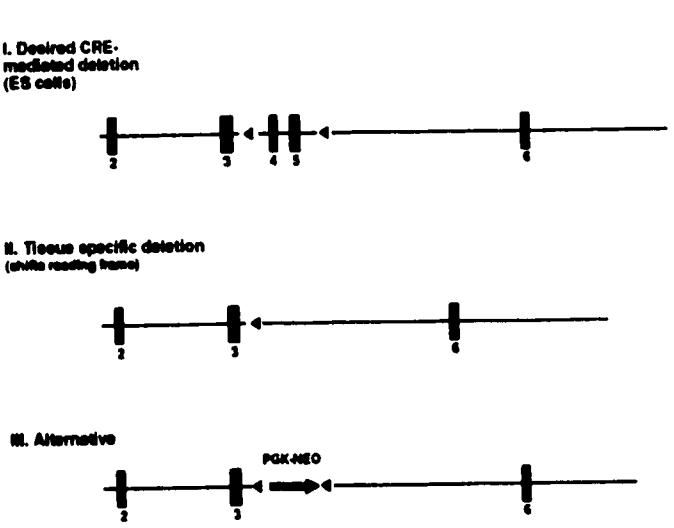
I. Desired CRE-mediated deletion (ES cells)
2
3
4
5
6
II. Tissue specific deletion
(shifts reading frame)
2
3
6
III. Alternative
PGK-NEO
2
3
6

5.3. Discussion

The data presented in this chapter and elsewhere indicate p107 is not required during mouse development (Lee, *et al.*, 1996). Given that the p107 mutants are viable and fertile, functionally overlapping factor(s) are presumably capable of fulfilling p107 roles in most cell types. Of course, the related factors, Rb and p130 are implicated to functionally compensate for p107. There is evidence that increased expression of related factors contributes to compensation. In $Rb^{-/-}$ fibroblasts, p107 is expressed at higher levels than found in wildtype cells (Hurford, *et al.*, 1997). In $Rb^{-/-}$ embryos, p130 appears to partially compensate (expressed higher) in the brain, and p107 partially compensates (expression high and sustained) in cultured $Rb^{-/-}$ differentiating myoblasts. Repression of p107 transcription is ascribed to E2F sites in its promoter, which may interact with Rb/E2F or p130/E2F complexes (Smith, *et al.*, 1998; Zhu, *et al.*, 1995c). Conversely, in the p107-deficient embryos, Rb expression is approximately 2-fold higher than in control embryos. The Rb promoter contains an E2F site, and Rb expression is activated or repressed when E2F or Rb, respectively are overexpressed. Additionally, the overexpression of p107 represses the Rb promoter by virtue of the E2F site (Zacksenhaus, *et al.*, 1993). The Rb promoter also contains an Sp1 site that appears critical for activity of the gene. As p107 negatively regulates E2F and Sp1 activities, loss of p107 could directly lead to increased expression from the Rb locus. Alternatively, the increase in Rb expression may be accomplished through an indirect mechanism. Further evidence to support functional compensation by Rb is that even heterozygous loss of Rb function in the p107-null background is incompatible with embryo survival. There is biochemical evidence that indicates Rb proteins can substitute for each other in complex with E2F in thymocytes *in vivo*, and presumably fully functional compensation (Cobrinik, *et al.*, 1996; Mulligan, *et al.*, 1998). Taken together, the data suggest that these proteins can regulate the expression of related factors, and regulate the effectors of related factors.

The extent of the overlap within the Rb family is being investigated through the generation of chimeric mice harbouring the compound mutant ES cells, and the generation of conditional mutations in the three genes.

The most apparent phenotype of the *p107*$^{-/-}$ mice was the postnatal growth deficit exhibited. Although the basis of the growth phenotype is unresolved, given that cells cultured from mutant embryos or adult tissue actually displayed enhanced proliferation, this runting phenotype is not apparently cell autonomous (Chapter 6 and 7). Hormone dysfunction is therefore strongly implicated. Pituitary function, specifically GH, and the expression of IGF-1 mRNA have been investigated. No discrepancies have been revealed between wildtype and mutant mice. Therefore, the basis of the reduced growth is unresolved.

The loss-of-function of *p107* had a dramatic effect specifically in myeloid cells. In humans, the *p107* gene maps to the long arm of chromosome 20, and 20q deletions are highly prevalent in myeloproliferative disorders, myelodysplastic syndromes, and acute myeloid leukemia (Asimakopoulos, *et al.*, 1994; Davis, *et al.*, 1984; Green, 1996). However, loss of p107 occurs only in a small subgroup of myeloid neoplasias associated with loss of 20q. Nevertheless, the observations of hyperplastic changes in the myeloid lineage of *p107*$^{-/-}$ mice suggests that homozygous loss-of-function of *p107* can contribute to the development of myeloid proliferative disease.

It is possible that p107 functions to regulate factors that have myeloid-specific expression or alternatively, factors common to other cells that are selectively more relevant to myeloid cell development. Members of the C/EBP (α, β and ε) family of leucine zipper transcription factors appear critical for myeloid-specific expression of genes, including neutrophil elastase, and receptors for macrophage, granulocyte and granulocyte/macrophage colony stimulating factor (reviewed in Clarke and Gordon, 1998) C/EBPε is a myeloid-specific family member. Interactions between Rb and

C/EBP have been reported, and p107 is also capable of associating with these factors (Chen, *et al.*, 1996b). As well, p107 is highly expressed in myeloid cell types and is down-regulated 4 days post-induction of differentiation *in vitro* by G-CSF (Garriga, *et al.*, 1998). In myeloid cell lines, p107 appears to be required for TGFβ1 inhibition of IL-3-dependent growth via suppression of c-Myc activity and E2F transcription (Bang, *et al.*, 1996). As well, mutations in the amino-terminal portion of Myc in lymphoma patients abrogates interactions with p107 leading or contributing to inappropriately increased c-Myc activity (Hoang, *et al.*, 1995). p107 regulation of Sp1-mediated transcription may also be important for myeloid-restricted, and controlled expression of target genes (i.e. expression of Myb). Sp1 sites are prevalent in the promoters of myeloid-specific genes.

The nature of the myeloid disorder in the p107 mutants was not directly analyzed. Further examination of the aforementioned pathways in myeloid cells derived from *p107*$^{-/-}$ mice in a Balb/c genetic background should elucidate the molecular basis of this phenotype. To address the cell-autonomy of this myeloid phenotype, bone marrow or fetal liver transplantation experiments can be performed.

Therefore, the disruption of p107, a ubiquitously expressed factor, gave rise to relatively subtle phenotypes, indicating that functionally overlapping factors were compensating. It is not possible to examine the consequence of loss of more than one of the Rb proteins, in a specific tissue context because either the single or compound mutants die *in utero*. In order to generate mice with compound mutations in the Rb family of genes, I have subsequently constructed a *p107* gene targeting vector which permits expression of the wildtype protein unless the CRE recombinase is co-expressed in cells harbouring the *p107* modified allele (Figure 5.11). By generating mice with such conditional 'knock-out' vectors, the combined or overlapping functions of these factors can be assessed.

The existence of second-site modifier loci affecting the penetrance of the phenotypes of mice carrying targeted null mutations has been reported by several laboratories. The breeding data is consistent with the existence of multiple modifying alleles representing either recessive loss-of-function mutations in the C57Bl/6 background, dominant gain-of-function mutations in the Balb/c background or a mixture of both. That heterozygosity at some modifier loci contributes to the observed phenotype remains a possibility. The 129Sv genetic contribution is not directly assessed in the breeding experiments described in this chapter. Future experiments will include backcrossing the null allele into the 129Sv genetic background. Pooling DNA samples from normal $p107^{-/-}$ C57Bl/6 B2 mice versus non-revertant (exhibiting the phenotype) $p107^{-/-}$ B2 C57Bl/6 mice, may reveal distinct differences with a large PCR primer set for genotyping microsatellites (Chapter 8). Software and services, offered by Research Genetics Inc., are available to map modifier loci. Clearly, understanding the identity of the modifier genes having potentially epistatic relationships with p107 will provide important insights into the regulatory networks within which p107 operates.

CHAPTER 6

Growth and Cell-Cycle Kinetics of *p107*$^{-/-}$ Embryonic Fibroblasts.

6.1. Introduction

p107 interacts with critical cell cycle regulatory factors including cyclins A, E, cdk2 and E2F (Cao, *et al.*, 1992; Ewen, *et al.*, 1992; Faha, *et al.*, 1992; Ginsberg, *et al.*, 1994; Shirodkar, *et al.*, 1992). E2F activity and cdk activity are central nodes of control for positive regulation of cell-cycle promotion (reviewed in Bernards, 1997; Morgan, 1997). Loss of p107-mediated inhibition of cyclin A/ and E/cdk2 complexes may perturb the cell-cycle kinetics by altering the progression through the G_1 and S phases. As well, the derepression or transactivation of genes normally regulated by p107/E2F complexes may also have significant consequences to cell cycle progression (reviewed in Dyson, 1998).

Rb-deficient embryonic fibroblasts displayed altered cell-cycle kinetics, and the expression of cyclins E and A were deregulated. Furthermore, p107 expression was up-regulated in these mutant cells (Hurford, *et al.*, 1997). The data indicated that Rb-deficient fibroblasts transit the G_1 phase faster than wildtype cells from an arrested state.

To examine the cell autonomous phenotype of p107-deficient cells, embryonic fibroblasts were isolated from wildtype, heterozygous and homozygous mutant 14.5 dpc embryos. Primary EF cells are technically amicable to isolation and manipulation in short-term cultures. All experiments described in this chapter were performed in early passage (2-4) EF cell populations. The doubling time of the mutant cells was reduced 2-fold in comparison to wildtype cells. Intriguingly, FACS analysis of the mutant EF

revealed no significant change in the cell-cycle profile when compared with wildtype or heterozygous cells. This data indicated that the time to transit each phase of the cell cycle was reduced by a common factor. Furthermore, there was no significant difference in the proportion of apoptotic cells, or non-dividing cells in these cultures. Analysis of cyclin induction in synchronized cultures revealed that the expression of cyclins E and A preceded cyclin D1 induction; and cyclin D1 and the G_2 cyclin, B1, were induced with accelerated kinetics compared to wildtype cells. Taken together, the data suggest an unappreciated role for p107 in cyclin expression and timing of cell-cycle progression.

6.2. Results

6.2.i. Cell growth

To facilitate the characterization of cell-cycle kinetics of cells lacking p107, primary cultures of wildtype, *p107*$^{+/-}$ and *p107*$^{-/-}$ EF cells were derived from 14.5 dpc sibling embryos following timed matings of heterozygous mutant mice. Notably, *p107*$^{-/-}$ embryos at 14.5 dpc were indistinguishable from littermates. Cell growth was monitored by counting the increase in the number of early passage, viable EF cells in subconfluent replicate cultures. Wildtype and *p107*$^{+/-}$ EF cells (14.5 dpc) doubled in number about every 60 hours (Figure 6.1A), comparable to that previously reported (Fantl, *et al.*, 1995). By contrast, *p107*$^{-/-}$ EF cultures displayed a markedly increased growth rate, and doubled in number about every 35 h. Moreover, *p107*$^{-/-}$ EF cultures incorporated 2-fold more ^{3}H-thymidine per hour than wildtype and *p107*$^{+/-}$ EF cultures (n=5 cultures of each genotype, normalized to cell number) (Figure 6.1B). Significantly, the observed accelerated cell-cycle kinetics in p107-deficient cells is not limited to embryonic fibroblasts, but is also displayed by adult myoblasts (see Chapter 7).

Flow cytometry of independently isolated EF cultures (n=6) in exponential growth indicated that the proportion of cells in G_1, S and G_2 was unaltered in the absence of p107. The proportion of wildtype and mutant EF cells in G_1 was approximately 54%, S was 30% and G_2, 16% (Figure 6.2). However, forward- versus side-scatter during flow cytometry indicated no detectable difference in cell size between *p107*$^{-/-}$ and wildtype EF cells. Intriguingly, these data indicate that the length of the different phases of the cell cycle were proportionately reduced by about a factor of 2 in EF cells (and myoblasts, Chapter 7) lacking p107.

The discrepancies between growth rate and the unaltered cell cycle profile could be the result of differences in cell survival or in the percentages of non-cycling cells between the mutant and wildtype cell populations. In order to address potential

differences in cell survival, apoptosis was assessed in asynchronous cultures by several approaches. FACS analysis did not reveal any significant sub-G_1 cell population, which would represent cells undergoing apoptosis in either genotype (Figure 6.2B). Annexin-V immunoreactivity was also assessed, and again no cells exhibited evidence of membrane inversion, a hallmark of apoptosis. Finally, TUNEL assays revealed that both wildtype and *p107*$^{-/-}$ cultures were essentially free of apoptotic cells (data not shown). To assess the presence of non-proliferating cells, BrdU was continually supplied in the media. Importantly, non-proliferating cells would be represented by lack of BrdU-positive nuclei. Following 15, 30 and 60 hours, cells were fixed and immunostained with anti-BrdU specific monoclonal antibody. Greater than 97% of cells in wildtype (n=2) and *p107*$^{-/-}$ (n=3) were BrdU-positive following the 60 h incubation. Also, at 30 h, almost 96% of p107$^{-/-}$ EF were BrdU-positive; in contrast to wildtype cultures, which were approximately 43% BrdU-positive (Figure 6.3). The data supports that p107$^{-/-}$ cell cycling time is reduced.

6.2.ii. Cyclin induction following synchronization

The absence of p107 in EF cells clearly resulted in about a 2-fold acceleration in cell-cycle kinetics. p107 is known to associate with and negatively regulate cyclin E and A/cdk activity, and these genes are potential targets for E2F-dependent transcription (Botz, *et al.*, 1996; Ewen, *et al.*, 1992; Faha, *et al.*, 1992; Geng, *et al.*, 1996; Henglein, *et al.*, 1994; Huet, *et al.*, 1996; Ohanti, *et al.*, 1995; Schulze, *et al.*, 1995). Additionally, overexpression of specific cyclins can be sufficient for cell cycle progression, and can inhibit cell cycle exit (Cardoso, *et al.*, 1993; Quell, *et al.*, 1993; Rao, *et al.*, 1994; Resnitzky, *et al.*, 1995; Skapek, *et al.*, 1995). To investigate the consequence of these altered kinetics on cyclin expression, immunoblot analyses with a panel of antibodies reactive with cyclins D1, E, A and B1 were performed on extracts isolated from synchronized cultures of EF cells. Immunoblots were performed on 3 independently

isolated cultures of each genotype, all in duplicate. Cultures were serum starved (0.1% FCS for 3 days) to arrest cells in G_0, then stimulated with 10% serum to initiate entry into the cell cycle. Cell-synchronization was assessed by ^{3}H-thymidine incorporation (Figure 6.4I) and flow cytometry (not shown). Consistent with accelerated in cell-cycle kinetics, *p107*$^{-/-}$ fibroblasts exhibited a more rapid transit through S-phase in serum-stimulated cultures as assayed by ^{3}H-thymidine-incorporation. ^{3}H-thymidine incorporation peaked at 24h and started to decline by 30h in p107 mutant cultures, versus peak incorporation at or beyond 30h in wildtype cultures, corresponding to the end of the experiment time course. However, the transit from the G_0 phase to S, was only slightly attenuated. Taken together, this data indicates that the loss of p107 did not apparently accelerate entry into the G_1 phase from an arrested state. Consequently, mutation of Rb (or potentially p130) would affect entrance and progression in the G_1 phase (Herrara, *et al.*, 1996). In G_0/G_1 arrested cells, p107 expression is not induced until approximately 8 hours following mitogen-induction into the cell cycle (Cobrinik, *et al.*, 1993).

As shown in Figure 6.4 and summarized in Figure 6.5, cyclin D1 and cyclin E were up-regulated in synchronized wildtype EF cells about 12h after serum stimulation. Cyclin A was up-regulated about 18h after stimulation, and cyclin B1 about 24 h. By contrast, *p107*$^{-/-}$ cells displayed constitutive high level expression of cyclin E that continued to increase throughout the time interval investigated. In addition, cyclins A and D1 were up-regulated about 6 h following stimulation. Lastly, the G_2 cyclin B1 was up-regulated about 6h following stimulation of the mutant EF cells. The data indicate that p107 is required for the appropriate regulation of cyclin expression and plays an important role in regulating the overall length of the cell cycle, but in a strain-dependent manner. Others have reported that *p107*$^{-/-}$ EF cells derived in a hybrid 129Sv;C57Bl/6J genetic background exhibit no phenotypic differences to wildtype (Hurford, *et al.*, 1997; Lee, *et al.*, 1996).

Figure 6.1. Two-fold acceleration in cell-cycle kinetics in *p107*$^{-/-}$ fibroblasts

(A) Growth curves for cultured wildtype and *p107*$^{-/-}$ embryonic fibroblasts (EF) isolated from 14.5 dpc embryos (n=3 for each genotype). Heterozygous EF cells displayed the same growth kinetics as wildtype EF cells (not shown). Growth of *p107*$^{-/-}$ EF cells plotted in blue. (B) Growth rate of wildtype, *p107*$^{+/-}$ and *p107*$^{-/-}$ EF cells as revealed by ^{3}H-thymidine incorporation following 2 h exposure in exponential growth (n=5 for each genotype).

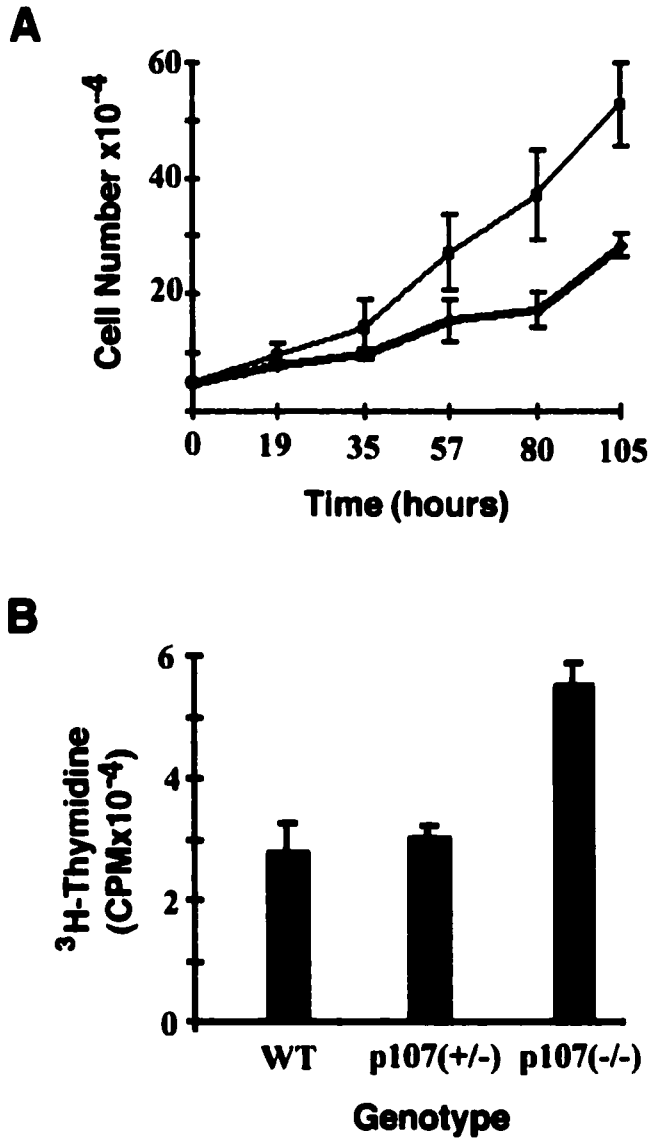
A
Cell Number x10^{-4}
60
40
20
0
19
35
57
80
105
Time (hours)
B
^{3}H-Thymidine (CPMx10^{-4})
6
4
2
0
WT
p107(+/-)
p107(-/-)
Genotype

Figure 6.2. Flow cytometric analysis revealed no difference in the cell-cycle profile

(A) Flow cytometry of EF cultures in exponential growth indicated that the proportion of mutant EF cells (n=6) in G_1, S and G_2 phases was similar to wildtype (n=4) and $p107^{+/-}$ (n=6) fibroblasts. Wildtype EF cells plotted in blue, $p107^{+/-}$ in green and $p107^{-/-}$ in red. (B) Histograms from wildtype and $p107^{-/-}$ sorts. Errors are expressed as standard deviations. Note, n = the number of independently-derived cell cultures analyzed.

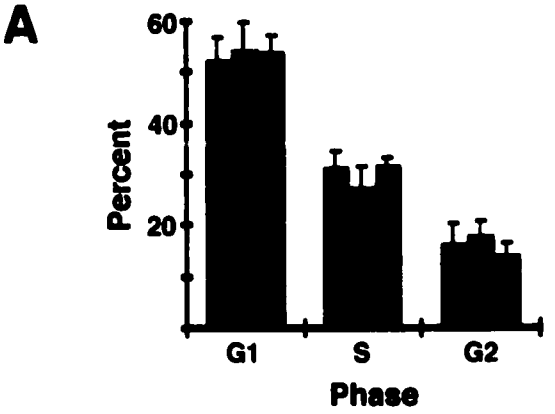
A
60
40
20
Percent
G1
S
G2
Phase

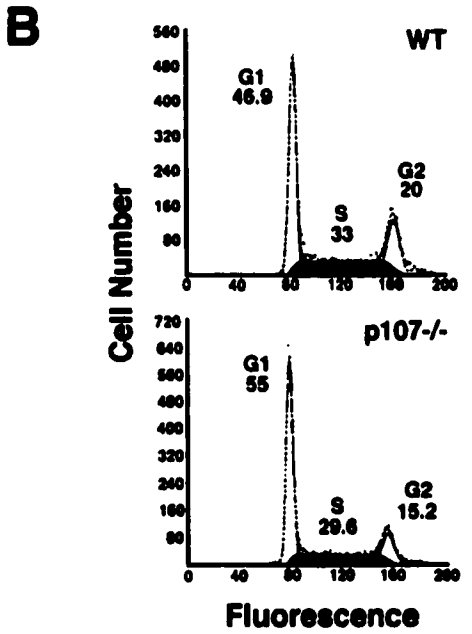
B
WT
G1
46.9
S
33
G2
20
p107-/-
G1
55
S
29.6
G2
15.2
Cell Number
Fluorescence

Figure 6.3 Wildtype and *p107*$^{-/-}$ cultures contain an equivalent proportion of cycling cells

(A) Wildtype and (B) *p107*$^{-/-}$ cells were pulsed with BrdU for 30h and processed for anti-BrdU immunostaining. 1000 nuclei were counted for each of 3 EF cultures for each genotype. Approximately 96% of the *p107*$^{-/-}$ cells have incorporated BrdU at 30h versus about 43% in wildtype cultures. By 60h, almost 97% of wildtype cells are BrdU-positive (data not shown).


A
WT
B

Figure 6.4. Immunoblot analysis of cyclin expression in *p107*$^{-/-}$ fibroblasts

Protein lysates were prepared at the indicated times after addition of serum to EF cells synchronized by serum starvation (n=3). (A-H) Cyclin proteins were detected by polyclonal (cyclins D1, E and A) or monoclonal (cyclin B1) antibodies. Note the dysregulated induction of cyclin expression in *p107*$^{-/-}$ cells with cyclin E constitutively expressed, and cyclins A and B1 expressed about 12 h and 18 h earlier than wildtype, respectively. (I) Incorporation of ^{3}H-thymidine at intervals following serum stimulation support that *p107*$^{-/-}$ EF cells transit S phase about twice as fast as normal. Note, n = the number of independently derived cell populations each characterized twice by immunoblot analysis.

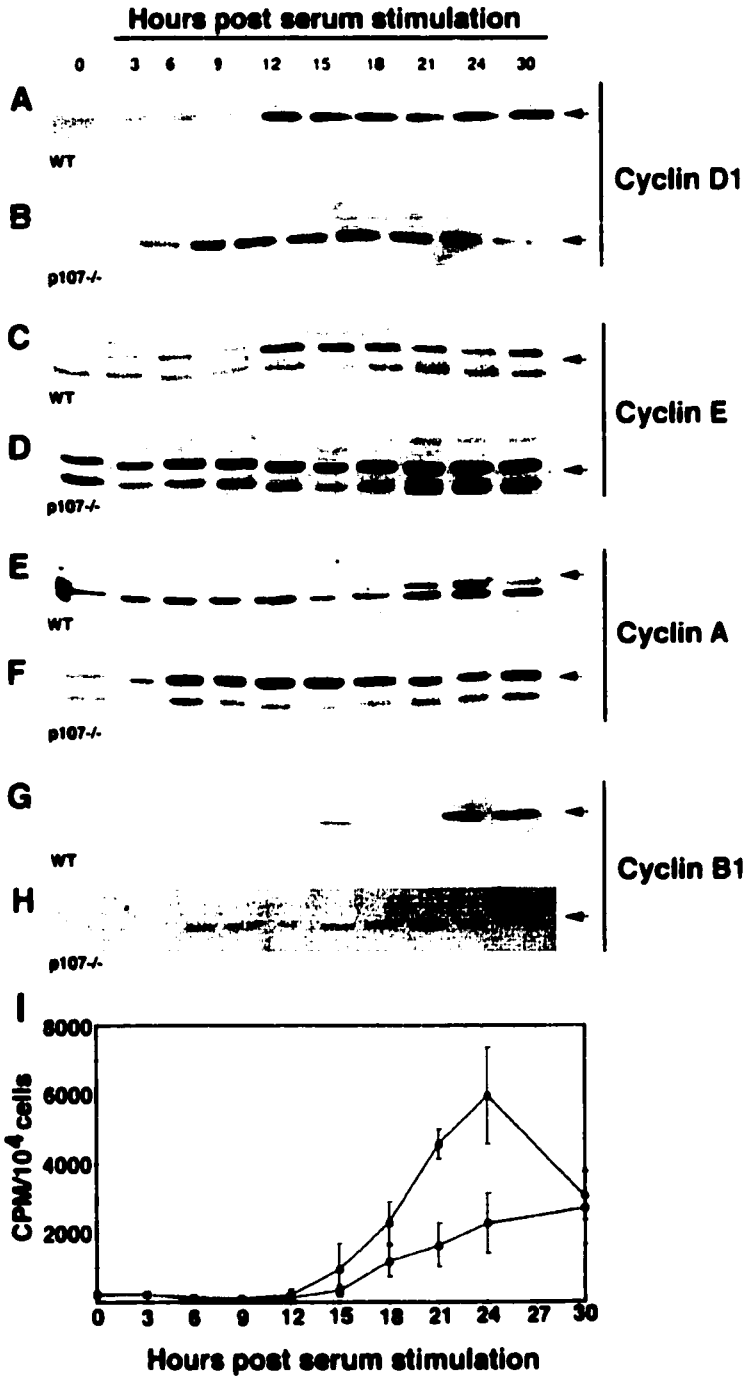
Hours post serum stimulation
0 3 6 9 12 15 18 21 24 30
A
WT
B
p107-/-
Cyclin D1
C
WT
D
p107-/-
Cyclin E
E
WT
F
p107-/-
Cyclin A
G
WT
H
p107-/-
Cyclin B1
I
8000
6000
4000
2000
CPM/10^4 cells
0 3 6 9 12 15 18 21 24 27 30
Hours post serum stimulation

Figure 6.5 Summary of cyclin induction in EF induced to reenter the cell cycle

Cyclins D1 and E were up-regulated in wildtype EF cells about 12h after serum stimulation. Cyclin A was up-regulated about 18h after stimulation, and cyclin B1 about 24 h. By contrast, *p107*$^{-/-}$ cells displayed constitutive high-level expression of cyclin E that continued to increase throughout the time interval investigated. Cyclins A and D1 were up-regulated about 6 h following stimulation. Lastly, the G_2 cyclin B1 was up-regulated about 6h following stimulation of the mutant EF cells. Abbreviation: WT, wildtype

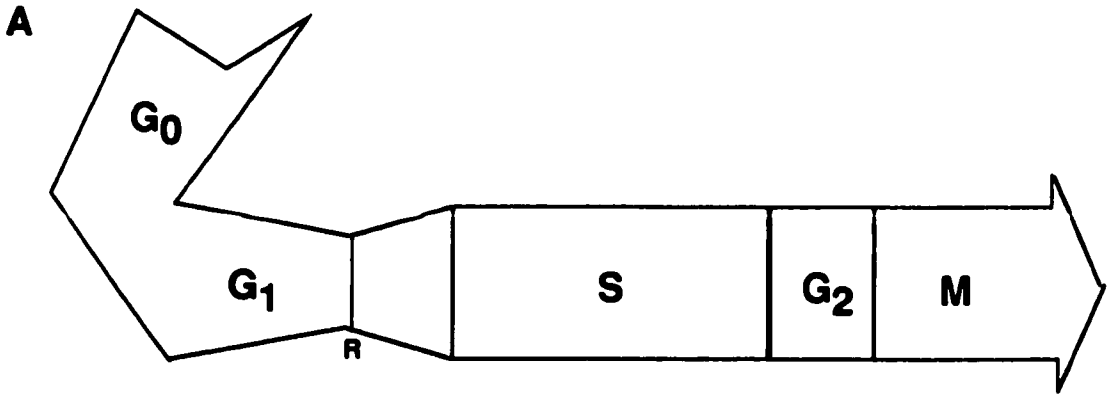
A
G0
G1
R
S
G2
M

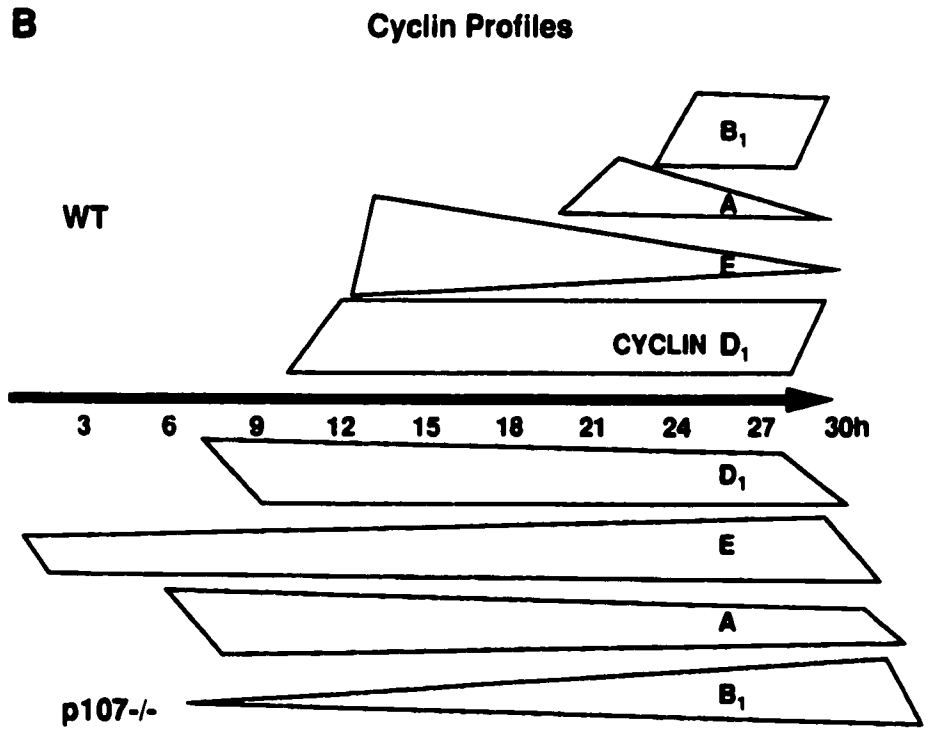
B
Cyclin Profiles
WT
B1
A
E
CYCLIN D1
3
6
9
12
15
18
21
24
27
30h
D1
E
A
B1
p107-/-

6.3. Discussion

The data is consistent with the assertion that p107 is a key player in mediating negative control of the E2F-family of transcription factors. Clearly, forced expression of E2F/DP is sufficient to induce expression of E2F-regulated genes and to drive growth arrested cells into S phase (reviewed in Dyson, 1998) . An analysis of E2F putative target genes, in addition to cyclins E and A, and analysis of E2F activity in the p107-deficient cells would greatly contribute to this study.

Constitutive expression of cyclin E is observed in Rb-deficient cells although the doubling time is unaltered (Herrara, *et al.*, 1996). The cyclin E promoter contains E2F binding sites that confer cell cycle regulated expression (Botz, *et al.*, 1996; Geng, *et al.*, 1996; Ohanti, *et al.*, 1995). Additionally, the cyclin A promoter is believed to be negatively regulated by p107. The cyclin A promoter has an E2F binding site that binds a complex containing E2F/p107 that is disrupted through interaction with cyclin E/cdk2 (Henglein, *et al.*, 1994; Huet, *et al.*, 1996; Schulze, *et al.*, 1995). Whereas the deregulated expression of cyclin A in $Rb^{-/-}$ EF cultures may be a result of the deregulated cyclin E expression, in the $p107^{-/-}$ cells the putative loss of repression by the p107/E2F complex may also contribute. The early induction of cyclin D1 expression in the $p107^{-/-}$ cells was intriguing, given that Ras, a central factor in mitogen signal-transduction, is known to increase cyclin D1 transcription (Leone, *et al.*, 1997; Peeper, *et al.*, 1997). Additionally, p107 may not be expressed for several hours after serum-restimulation of the EF cells. Recently though, characterization of the cyclin D1 promoter revealed that overexpression of Rb activated reporter transcription, and that p107 repressed transcription (Watanabe, *et al.*, 1998). Future immunoblot experiments may incorporate ^{125}I-labeled secondary antibodies to quantitate levels of cyclins for more direct comparisons. Taken together, the data strongly support the hypothesis that p107

functions as a key negative regulator acting to attenuate cellular proliferation. Also p107 may have a more extensive role than previously appreciated in regulating the expression of G_1 cyclins.

In addition to an E2F site, an Sp1 site is also present in the promoter of the cyclin D1 gene. Actually, several cell cycle-regulated genes, including cyclin E, thymidine kinase and c-myc, contain Sp1 and E2F-binding sites in their promoters (Azizhan, *et al.*, 1993). An analysis of Sp1 activity using a reporter system may reveal increases in the mutant EF compared to wildtype. Also, p107, distinct among the Rb proteins in that it interacts directly with Sp1, uses discrete domains to interact with Sp1 versus E2F (Datta, *et al.*, 1995). One prediction from this data is that p107 bound to the promoter could simultaneously inhibit Sp1- and E2F-mediated transcription.

A comprehensive analysis of several, potentially E2F-regulated genes in $Rb^{-/-}$, $p107^{-/-}$ and $p130^{-/-}$ EF cells was performed by Hurford *et al* . (1997). These cells were derived from embryos in a hybrid C57Bl/6J;129Sv genetic background. $p107^{-/-}$ EF cells in these experiments did not exhibit any perturbed expression of the genes examined. The compound $p107^{-/-}$;$p130^{-/-}$ mutant EF exhibited deregulated expression of myb, cdc2, rrm2 and cyclin A2. This data indicated a significant degree of functional compensation between p107 and p130 in the context of fibroblasts, specifically in the hybrid genetic background. This is perhaps not surprising, given that no phenotypes were exhibited by embryos or mice generated in this hybrid background. The variable phenotypes are again attributable to genetic strain effects. An equivalent analysis, as described in this chapter, for cells derived from the $p107^{-/-}$ C57Bl/6 backcrossed strain would directly test this assumption.

CHAPTER 7

Enhanced Proliferation, Regeneration and Perturbed Differentiation of p107$^{-/-}$ Skeletal Myoblasts.

7.1. Introduction

During vertebrate development, skeletal muscle is derived from cells in the prechordal and somitic mesoderm. These precursors give rise to committed myogenic cells which become the skeletal muscle of the head, trunk and limbs (reviewed Buckingham, 1994; Cossu, *et al.*, 1996; Hauschka, 1994; Miller, 1990). In the mouse, the first skeletal myofibres develop at E8.5. Satellite cells, named for their unique locations beneath the basal lamina, are the myogenic precursor cells of postnatal and adult skeletal muscle. Satellite cells are first detected late in embryogenesis (E17) coincident with the formation of a distinct basement membrane around the muscle fiber (reviewed Bischoff, 1994; Yablonka-Reuveni, 1995). In normal adult skeletal muscle, satellite cells are mitotically quiescent. Furthermore, there is a stable pool of these cells maintained in the adult. Although satellite cells are committed myogenic precursors, expression of any of the four myogenic regulatory factors is not detected. Following trauma, these cells are activated, through the release of factors (mitogens) from the damaged fibres and potentially secondary to immune responses (Bischoff, 1986; Bischoff, 1990; Mezzogiorno, *et al.*, 1993). The satellite cells peripheral to the damaged site are responsible for regeneration (reviewed Grounds and Yablonka-Reuveni, 1993).

Activation initiates a cascade of changes in gene expression which appear to somewhat recapitulate embryonic skeletal muscle development.

Interplay between the myogenic regulatory factors (MRFs) and members of the Rb family is implicated in the irreversible exit from the cell cycle and elaboration and maintenance of late skeletal muscle differentiation. Particularly, Rb has been implicated in interfacing cell cycle arrest and terminal differentiation in skeletal muscle (Gu, *et al.*, 1993a; Schneider, *et al.*, 1994; Zacksenhaus, *et al.*, 1996; reviewed in Lassar, *et al.*, 1994). In $Rb^{-/-}$ muscle cell cultures, although early markers were properly induced and cells fuse and resemble differentiated derivatives, re-stimulation of the cultures induced ectopic S phases (Schneider, *et al.*, 1994). Interestingly, in the Rb mutant myotubes, p107 was up-regulated in contrast to the down-regulation which normally accompanies terminal differentiation. p107 could not fully substitute for Rb in this context, and indicated that p107 exerts its function during myoblast proliferation and not maintenance of cell cycle arrest in wildtype muscle cells. In agreement with this, *in vitro* studies in myoblast cell lines revealed p107/E2F complexes in the proliferative phase (Corbeil, *et al.*, 1995; Kiess, *et al.*, 1995; Shin, *et al.*, 1995). The data does not exclude the possibility that p107 functions to initiate cell cycle arrest in differentiating myoblasts.

The reasons for investigating the satellite cell phenotype in the p107 mutants were four-fold. Primarily, I wanted to investigate that the altered cell growth observed in EF was not restricted to this cell type. Secondly, we took advantage of this population of quiescent cells to assess the growth and differentiation properties of adult tissue that can be assessed both *in situ* following injury; and in cell culture. Primary myoblasts are technically amicable to isolate and culture, and can be induced to differentiate in the presence of low mitogen media. Finally, given the numerous previous studies that have implicated the Rb family in differentiation, specifically focused on skeletal muscle,

analyses of the *in vivo* and primary cells in the context of the *p107* null mutation was an extension of this work.

p107$^{-/-}$ skeletal muscle regeneration was enhanced as assessed at 4.5 days post-injury, and the damaged sites contained 2-fold higher percentages of BrdU-positive nuclei. Analyses of *in vitro* growth and differentiation revealed enhanced proliferation and perturbed cell-cycle exit and expression of several differentiation-specific genes. The data indicate that *p107*$^{-/-}$ skeletal myoblasts are enhanced in their ability to proliferate and are slightly perturbed in cell cycle exit and progress of their differentiation programme.

7.2. Results

7.2.i. Enhanced regeneration in *p107*$^{-/-}$ skeletal muscle

Satellite cells are the source of myogenic stem cells in adult muscle. These cells remain quiescent in adult muscle until activated by trauma such as crush or ischemia. To investigate the function of p107 during the *in vivo* proliferation and subsequent differentiation of activated satellite cells, mechanical damage was induced in the *tibialus anterior* muscle and the number of BrdU-incorporating cells was assessed 4.5 days later. The *tibialus anterior* muscle was chosen because of its surface location and easily identified landmarks. At 4.5 days post-injury, the crushed regions of wildtype muscles (n=2) contained 12% BrdU-positive cells, whereas the *p107*$^{-/-}$ crushed muscle (n=3) contained approximately 25% BrdU-positive nuclei throughout the damaged region (Figure 7.1). As well, the more intact architecture at the damaged site suggested that muscle repair was accelerated in the *p107*$^{-/-}$ muscle. Taken together, the data suggest that either there is a larger pool of satellite cells in the mutant muscle, or that *p107*$^{-/-}$ activated satellite cells exhibit unique proliferative or differentiation capabilities. A further possibility is that *p107*$^{-/-}$ satellite cells display an enhanced ability to migrate to the site of injury.

7.2.ii. Characterization of *p107*$^{-/-}$ myoblast cultures

To assess whether the relative proportions and growth of satellite cells was equivalent in wildtype versus p107$^{-/-}$, primary mixed cultures were established from the lower hind limbs. After 4.5 days, the primary cultures were immunostained with anti-desmin antibody which recognizes a muscle-specific intermediate filament. The *p107*$^{-/-}$ cultures contained 1900 desmin-positive cells / mg wet weight, whereas the wildtype cultures contained approximately 100 desmin-positive cells (Table 7.1, Figure 7.2). This

indicated that there were greater numbers of satellite cells resident in the muscle or that the *p107*$^{-/-}$ activated satellite cells exhibited enhanced proliferation.

To further examine the role of p107 in satellite cell proliferation and differentiation, low passage and pure primary cultures from p107-deficient and littermate muscles were generated. The purity of the primary cultures was assessed with desmin-specific antibody. More than 97% of cells in wildtype and mutant cultures were desmin-expressing, and the level of expression appeared equivalent indicating that these essentially pure cell populations also represented homogeneous pools of satellite cells. The cell cultures used in these experiments were of low passage (P3-6).

To determine if the level of proliferation was equivalent in mutant myoblasts compared to wildtype, 10^5 cells were replica cultured and counted over a 1-week period. The wildtype cultures (n=2) doubled every 35 hours, versus 17 hours in mutant cultures (n=2). Similarly, ^{3}H-thymidine incorporation revealed about a 2-fold higher growth rate for the *p107*$^{-/-}$ cells in growth conditions, normalized to cell number (Figure 7.3). Therefore, under growth conditions, *p107*$^{-/-}$ myogenic cells exhibited an accelerated cell cycle, reminiscent of the mutant EF cells (Chapter 6). FACS analysis was also performed with cells from growing cultures. The percentages of cells in the G_1 phase for wildtype cells was 70%, S 15%, G_2 12% in comparison to *p107*$^{-/-}$ cells which were distributed 64% G_1, 22% S, 13% G_2 (Figure 7.2). The apparent shift to a greater proportion of wildtype cells in $G_{1/0}$ can be attributed to the higher spontaneous rate of differentiation in these cultures. As described previously (Chapter 6), cells isolated from *p107*$^{-/-}$ embryos displayed altered cell-cycle kinetics and doubled in approximately half the time of wildtype cells. Taken together, the data indicate that a 2-fold difference in desmin-positive cells derived from the muscle would exist, if all other parameters such as proportion of resident satellite cells and differentiation potential were equivalent.

Interestingly, a significant proportion of wildtype cells in growth conditions appeared to be differentiated, as judged by the spindle-like morphology of the cells compared to the majority of cells that appeared highly refractive and had a small compact cytoplasm. Immunostaining with MF-20, a pan-myosin heavy chain antibody, revealed that approximately 12% of wildtype cells versus 2.5% of p107$^{-/-}$ cells expressed this differentiation-specific marker (Figure 7.4). This indicated that the inherent rate of spontaneous differentiation was significantly reduced, and suggested that in p107-deficient cells, cell cycle arrest was compromised.

The rate of cell cycle arrest following mitogen withdrawal and induction of differentiation was assessed by measuring the ^{3}H-thymidine incorporated on 1-day intervals of a differentiation time-course experiment. *p107*$^{-/-}$ cells continued to synthesize DNA in mitogen-poor media whereas wildtype cells rapidly withdrew from the cell cycle (Figure 7.4). These results represent two independently-derived myoblast populations for each genotype. The data indicate that loss-of-function of p107 in myogenic cells resulted in an increased propensity for continued proliferation under differentiation conditions. The results suggest that p107 is partly required for appropriate exit from the cell cycle. Additionally, *p107*$^{-/-}$ myogenic cells appear to have enhanced proliferative capacity.

7.2.iii. *In vitro* differentiation

In order to examine the differentiation capabilities of primary myoblasts, cultures were treated with low mitogen conditions, 5% horse serum in DMEM. The progress of differentiation was investigated by fixing cells at 1-day intervals and immunostaining with the pan-myosin specific antibody, MF20 (Figure 7.4). As previously described, in growth media, $p107^{-/-}$ cells exhibited about 8-fold lower frequency of spontaneous differentiation. Consistent with this, $p107^{-/-}$ cultures exhibited a deficit in their propensity to differentiate in low-mitogen conditions. By 24 hours, approximately 58% of wildtype cultures expressed MHC, indicating a progression to the terminally differentiated state. Over subsequent days in differentiation media, the percentage of wildtype cells expressing MHC increased to reach approximately 97%. In contrast, 24h following mitogen-withdraw, the percentage of differentiated cells in $p107^{-/-}$ cultures was only 15%. By the second day, the percent of MF20-positive cells approached 40% in the mutant cultures, although cells continued to incorporate ^{3}H-thymidine. Although the number of differentiated $p107^{-/-}$ myocytes increased over the next 4 days, the percentage of differentiated cells only approached 60%. The fusion index of the differentiating cultures was obtained by counting differentiated myocytes containing 2 or more nuclei. The fusion index of differentiated wildtype cultures approached 90% by the fifth day of the treatment, and myocytes contained 4 nuclei on average. In $p107^{-/-}$ cultures, myotubes contained an average of 48 nuclei. The data suggest that $p107^{-/-}$ cells exhibit enhanced proliferation under differentiation conditions resulting in delayed differentiation kinetics. However, there is an enhanced ability to form large, multi-nucleated myotubes. This may be a result of nuclei continuing to divide in myotubes, as the density of cells induced to differentiation did not affect this phenotype. Immunostaining of BrdU treated cultures would confirm or exclude this possibility.

To investigate the progress of differentiation in p107-deficient cultures at the molecular level, total RNA was prepared from both wildtype and *p107*$^{-/-}$ cultures in growth media, and during a 5-day time-course following the induction of differentiation. RNA isolated from the induced cultures was subjected to Northern analysis with a panel of differentiation-specific cDNAs. Actin isoform switching from an initial expression of cardiac α-actin to skeletal α-actin was analyzed. Cardiac α-actin expression peaked at day 1 in wildtype and *p107*$^{-/-}$ myoblasts, however the downregulation of the mRNA following day 1 did not progress to the same extent for the subsequent four days in culture (Figure 7.5.A, B). Skeletal α-actin mRNA expression was also markedly induced within the first 24 h in both wildtype and mutant cultures, although the levels were slightly reduced in the *p107*$^{-/-}$ cells (Figure 7.5.C, D). Additionally, expression of skeletal α-actin in growing cultures was high in wildtype cells, but at very low levels in mutant cultures. This data is consistent with the finding that the rate of spontaneous differentiation is very low in *p107*$^{-/-}$ myoblast cultures. Overall, the expression patterns of these early markers of skeletal muscle differentiation are not greatly affected in mutant myoblasts.

Skeletal muscle determination and differentiation pathways depend on the action of the MRF family of basic helix-loop-helix transcription factors. The expression patterns of late markers of differentiation, including the two muscle regulatory factors, myogenin and MRF4, were also examined by Northern analyses (Figure 7.6). As previously described, the expression of MHC isoforms appeared strikingly reduced in the *p107*$^{-/-}$ muscle cells compared to wildtype (Figure 7.4). Myogenin was detected throughout the differentiation time course, including growing myoblasts at day 0 which was surprising, considering that myogenin is not detected in established myoblast cell lines, i.e. C2C12, 10T^{1}/2. Other work in the lab has revealed that although the myogenin protein is not detected in growing myoblasts, the mRNA is abundant (A. Girgis-Garbaldo

and L. Sabourin). Work is ongoing to explain whether myogenin expression is regulated at the translational or post-translational level. Myogenin mRNA levels appeared slightly higher in *p107*$^{-/-}$ cultures at days 4 and 5 of differentiation (Figure 7.5A, B). MRF4 mRNA, the last muscle regulatory factor to be expressed, was induced to low levels at day 3 of differentiation of wildtype cultures, increasing to a peak at day 4. By contrast, in *p107*$^{-/-}$ muscle cultures the expression of this late marker of differentiation was not strongly up-regulated (Figure 7.6C, D). Equivalent loading of RNA was confirmed by probing the same blots with 18S cDNA (example Figure 7.6E, F). Interestingly, *Rb*$^{-/-}$ cells induced to differentiate into skeletal muscle in culture also exhibit reduced, or absent expression of late markers (Novitch, *et al.*, 1996). Also, in MRF4 deficient mice, normal skeletal muscle develops but myogenin expression is increased four-fold (Zhang, *et al.*, 1995). The apparent increase in myogenin expression in the *p107*$^{-/-}$ muscle cells is intriguing, and may explain why the expression patterns of several muscle-specific genes are not greatly perturbed, and that *p107*$^{-/-}$ mice exhibit histologically normal skeletal muscle.

A fundamental aspect of skeletal muscle terminal differentiation is the irreversible withdrawal from the cell cycle that accompanies this cellular differentiation programme. The presence of serum growth factors, the overexpression of cell cycle promoting factors or expression of viral or nuclear oncoproteins has been demonstrated to inhibit myogenesis (Guo and Walsh, 1997; Massague, *et al.*, 1986; Rao, *et al.*, 1994; Skapek, *et al.*, 1996; Skapek, *et al.*, 1995; Tiainen, *et al.*, 1996; Wang, *et al.*, 1995; Webster, *et al.*, 1988). One of the initial events associated with loss of the myogenic phenotype in the cells overexpressing these factors is activation of cdk activity. As well, overexpression of the cdk inhibitors, p21, p27 or p57, have been shown to enhance *in vitro* myogenesis (Gu, *et al.*, 1993b; Guo and Walsh, 1997; Guo, *et al.*, 1995; Wang and Walsh, 1996). During the first 24 hours of differentiation in culture, myoblasts exit the cell cycle. This exit is

accompanied by the increased expression of the cyclin-dependent kinase inhibitor p21. p21 expression was analyzed by Northern blot analysis of total RNA from the wildtype and *p107*$^{-/-}$ cultures (Figure 7.7A, B). In wildtype cells, there was a strong induction of p21 expression at day 1 in contrast to a more prolonged and sustained induction in p107$^{-/-}$ cultures, initiated at day 1 of differentiation. Interestingly, p21 induction is sustained in differentiated myocytes that are exposed to high concentrations of mitogen (Guo, *et al.*, 1995). This data supports the delayed and generally deficient terminal differentiation exhibited by the mutant muscle cells in culture.

Rb mRNA and protein expression are induced 10-fold in some muscle cell lines following induced differentiation (i.e. C2, P19) (Garriga, *et al.*, 1998; Slack, *et al.*, 1995). Preliminary immunoblot analysis revealed a peak in Rb expression during the first 2 days of differentiation in wildtype, but not *p107*$^{-/-}$ cultures (Figure7.7C, D). This is consistent with delayed or asynchronous cell cycle exit.

Continued cell cycling in differentiation-induced cultures and the expression patterns of cell-cycle negative regulatory factors, including p21 and Rb, suggest an uncoupling of cell cycle arrest and terminal differentiation. The expression pattern of the muscle-specific mRNAs indicated that *p107*$^{-/-}$ cells were asynchronously being induced to differentiate, or alternatively that the proper induction and subsequent down-regulation of specific factors was perturbed following the loss of p107.

Figure 7.1 *In vivo* regeneration is enhanced in p107$^{-/-}$ skeletal muscle

BrdU incorporation in 4.5 day post-injury skeletal muscle. The damaged *tibialis anterior* muscle in (A) wildtype mice contained 12% of nuclei that stained positive for BrdU compared to 25% in p107$^{-/-}$ mice (B). Panels were photographed at 100X magnification. Arrows indicate BrdU-positive cells.

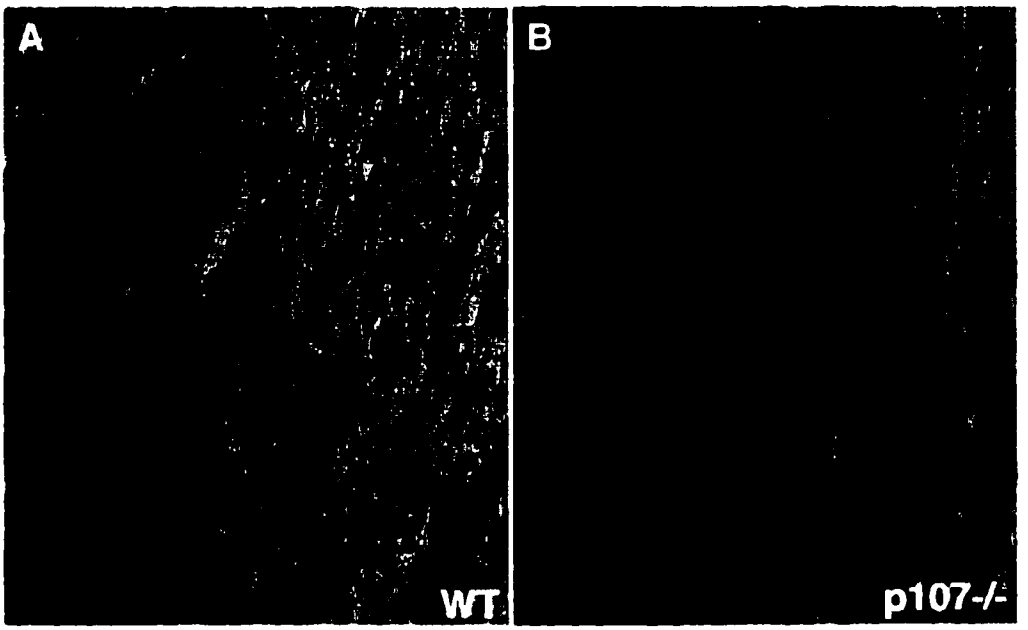
A
WT
B
p107-/-

Table 7.1. *p107*$^{-/-}$ muscle cultures contain elevated numbers of myogenic cells [a].

Genotype	Total number cells / mg wet weight	Percent desmin-positive cells	Total number myoblasts / mg wet weight
Wildtype	2168	5.4	114
	1791	4.8	86
	2334	3.3	77
Mean [b]	$2097^{+/-}278$	$4.5^{+/-}1.1$	$92^{+/-}19.3$
p107$^{-/-}$	8674	23.3	2021
	10380	15.4	1599
	13764	16.5	2271
Mean [b]	$10937^{+/-}2591$	$18.4^{+/-}4.3$	$1963^{+/-}339.6$

[a] Myogenic cells were assessed with desmin antibody.

[b] Errors are presented as standard deviations.

Figure 7.2 Increased numbers of desmin-positive cells from *p107*$^{-/-}$ muscle

Immunocytochemistry of 4.5 day mixed cultures from (A) wildtype and (B) *p107*$^{-/-}$ skeletal muscle stained with anti-desmin antibody indicated a dramatic increase in the number of myoblasts cultured from *p107*$^{-/-}$ mice. Note, the intensity of staining in both wildtype and *p107*$^{-/-}$ cultures appears uniform indicating that the myoblast population is homogeneous. Arrowheads indicate desmin-positive, myogenic cells.

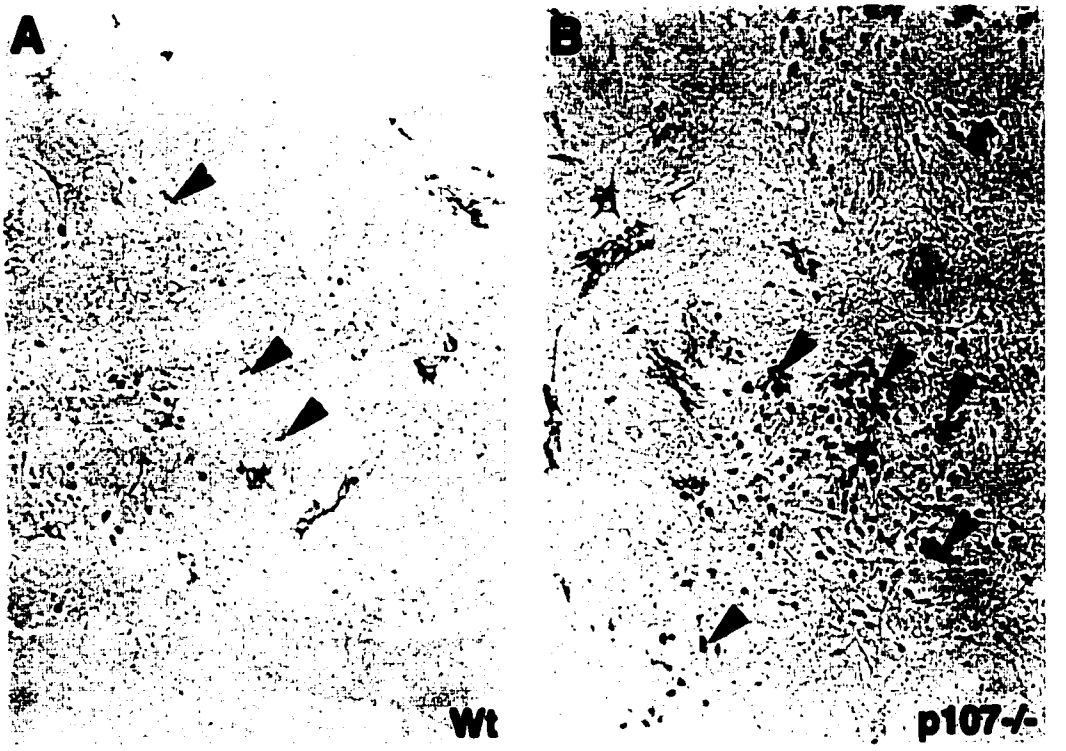
A
Wt
B
p107-/-

Figure 7.3 Two-fold acceleration in cell-cycle kinetics in *p107*$^{-/-}$ myoblasts

(A) Growth curves for cultured wildtype and *p107*$^{-/-}$ myoblasts (n=2 for each genotype). Growth of *p107*$^{-/-}$ myoblasts plotted in red. (B) Flow cytometry of myoblasts in growth conditions indicated an increase in the G_0/G_1 compartment in wildtype cultures relative to *p107*$^{-/-}$ (n=2), which corresponded to the higher frequency of spontaneous differentiation exhibited by the wildtype cells in culture. (C) ^{3}H-Thymidine incorporation was performed in asynchronous purified cultures from WT (129Sv;Balb/c), *p107*$^{-/-}$ (129Sv;Balb/c), WT (C57Bl/6 B2) and *p107*$^{-/-}$N (C57Bl/6 B2, normal appearance at weaning). Note that the genetic background significantly influenced the growth phenotype.

A

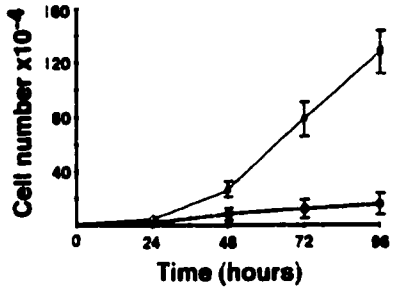
Cell number x10⁻⁴
160
120
80
40
0
24
48
72
96
Time (hours)

B

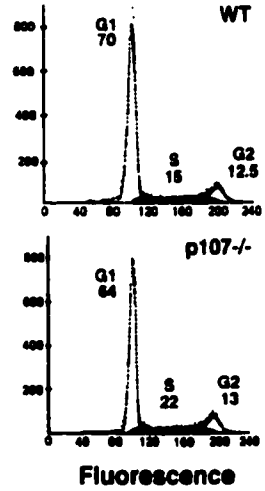
WT
G1
70
S
15
G2
12.5
p107-/-
G1
64
S
22
G2
13
Fluorescence

C

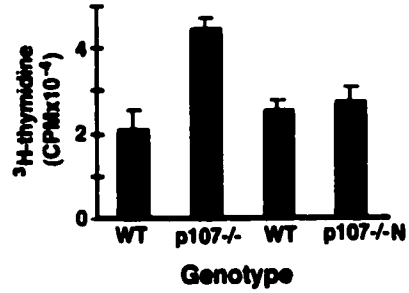
³H-thymidine
(CPMx10⁻⁴)
4
2
0
WT
p107-/-
WT
p107-/-N
Genotype

Figure 7.4. *In vitro* differentiation deficit in *p107*$^{-/-}$ myoblast cultures

(A) Wildtype and *p107*$^{-/-}$ primary cultures were immunostained with anti-panMHC antibody at day 0 (WT 12.5 versus 2.5%), day 1 (WT 57.6 versus 14.8%) and day 4 of differentiation (WT 96%). At day 4, a significant proportion of p107-deficient myotubes contained strikingly increased numbers of nuclei. (B) Although there was a large reduction in ^{3}H-thymidine incorporation in *p107*$^{-/-}$ cultures (red line) by day 2 of differentiation these mutant cultures continued to synthesize DNA. Note, at day 0 the incorporation in wildtype cultures (blue line) was approximately half that of *p107*$^{-/-}$ cultures (normalized to protein).

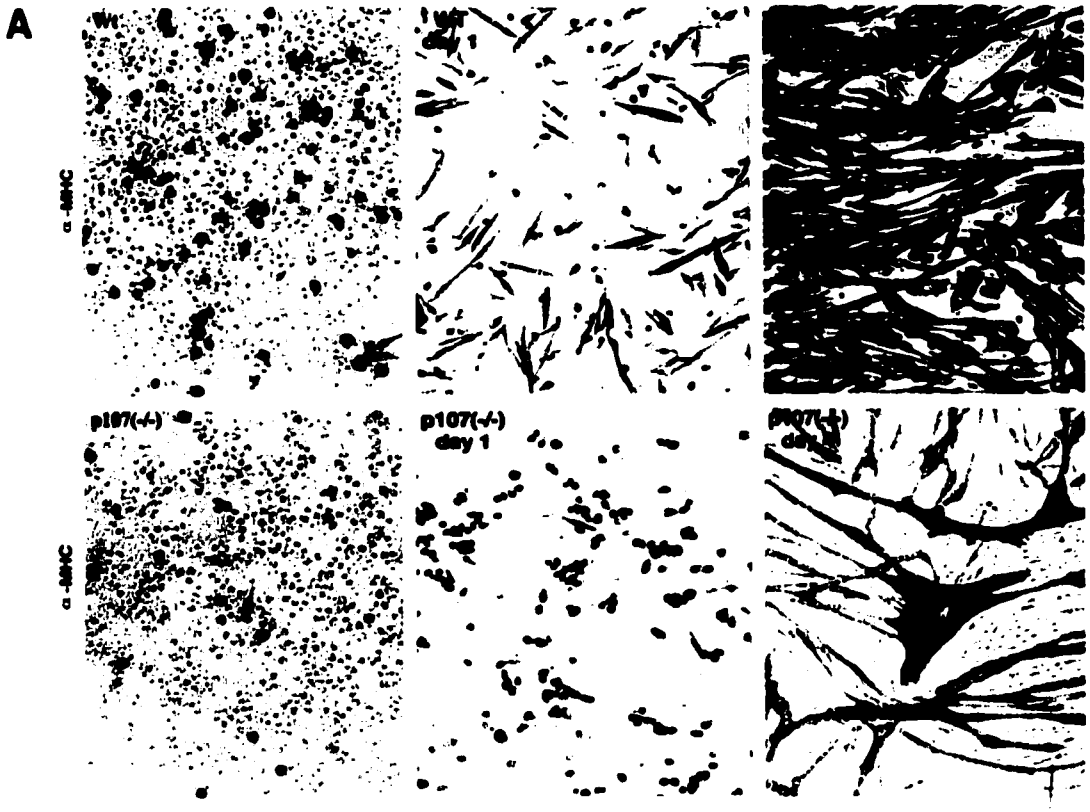
A
α -MHC
p107(-/-)
day 1

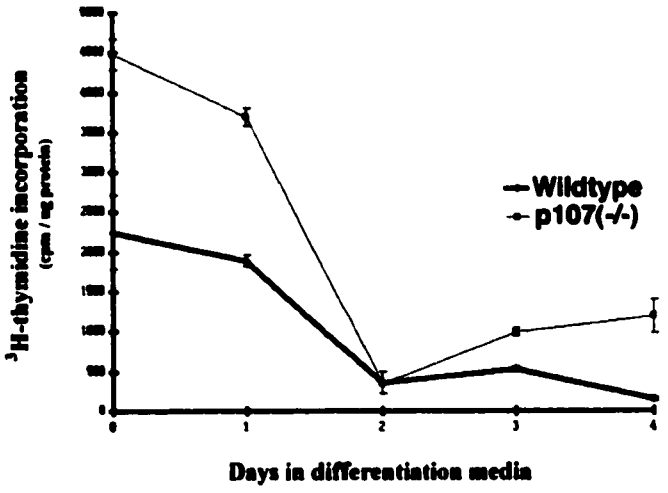
B
^{3}H-thymidine incorporation
(cpm / ug protein)
Wildtype
p107(-/-)
0
1
2
3
4
Days in differentiation media

Figure 7.5. Northern analysis of muscle actin isoforms

10ug of total RNA, isolated from differentiating primary cultures was probed with the specific cDNAs for (A) cardiac and (B) skeletal α-actins. In wildtype cultures, cardiac and skeletal α-actins were induced at day 1. Cardiac α-actin expression was thereafter reduced in wildtype cultures, whereas it was sustained although to a lower level in mutant cultures. Skeletal α-actin expression was detected for all wildtype time points, yet expression was very low in mutant day 0 cultures, corresponding to low level spontaneous differentiation. Expression increased to a plateau following day 1 in the mutant cultures. Ribosomal RNA size (kb) is indicated at the left.

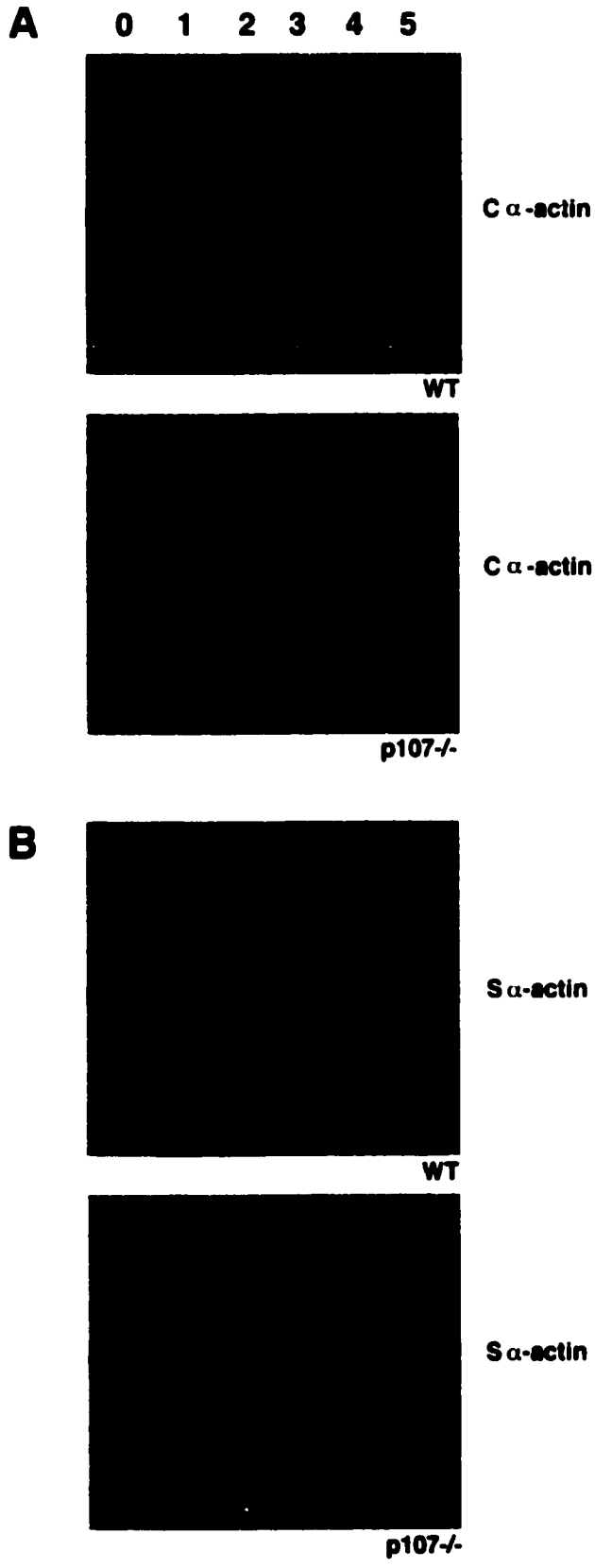
A
0 1 2 3 4 5
C α-actin
WT
C α-actin
p107-/-
B
S α-actin
WT
S α-actin
p107-/-

Figure 7.6. Northern analysis of secondary myogenic regulatory factors

10ug of total RNA was probed with cDNAs corresponding to the muscle regulatory factors, myogenin and MRF4. Myogenin expression was detected throughout the time-course, and appeared higher in *p107*$^{-/-}$ day 4 and 5 cultures (compare A and B). MRF4 induction was strikingly absent in *p107*$^{-/-}$ cultures (D) in contrast to its appearance beyond day 3 in wildtype cultures (C). (E, F) An 18S ribosomal probe confirmed equivalent loading. Ribosomal RNA size (kb) is indicated at the left.

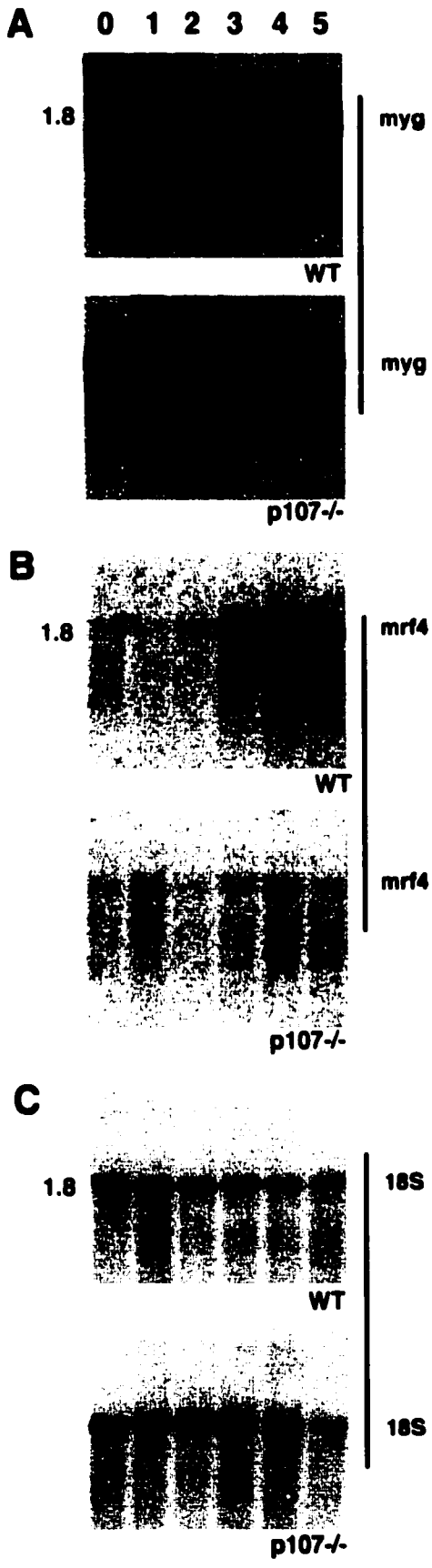
A
0 1 2 3 4 5
1.8
myg
WT
myg
p107-/-
B
1.8
mrf4
WT
mrf4
p107-/-
C
1.8
18S
WT
18S
p107-/-

Figure 7.7 Analysis of the induction of cdk inhibitor p21 and Rb

(A) 10 μg of total RNA was probed with the cDNA corresponding to human p21. p21 expression was highly induced at day 1 in wildtype cultures in contrast to *p107*$^{-/-}$ cultured where p21 was induced to lower levels and expression was sustained. Size in kb is indicated at the left. (B) 50 μg of protein lysates from a differentiation time-course were subjected to SDS-PAGE. Rb antisera reactive to the C-terminal revealed an induction and peak in expression at days 1 and 2. In *p107*$^{-/-}$ cultures, the extent of induction was greatly reduced, although the level of expression at day 3 was higher relative to wildtype at day 3. M^r represents apparent relative mobility in kD.

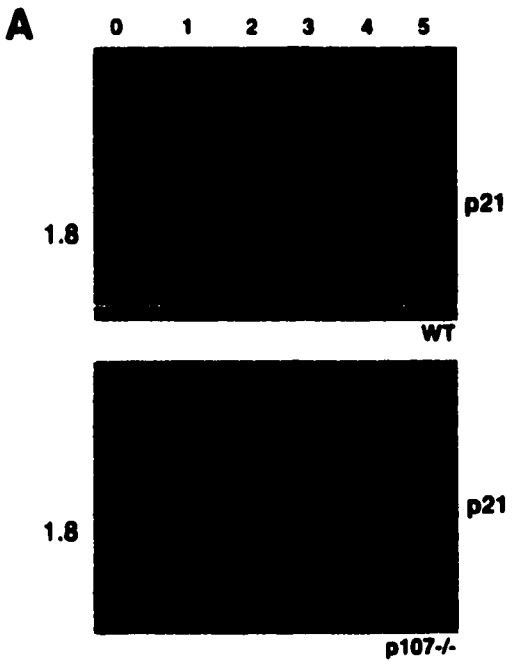
A
0
1
2
3
4
5
1.8
p21
WT
1.8
p21
p107-/-

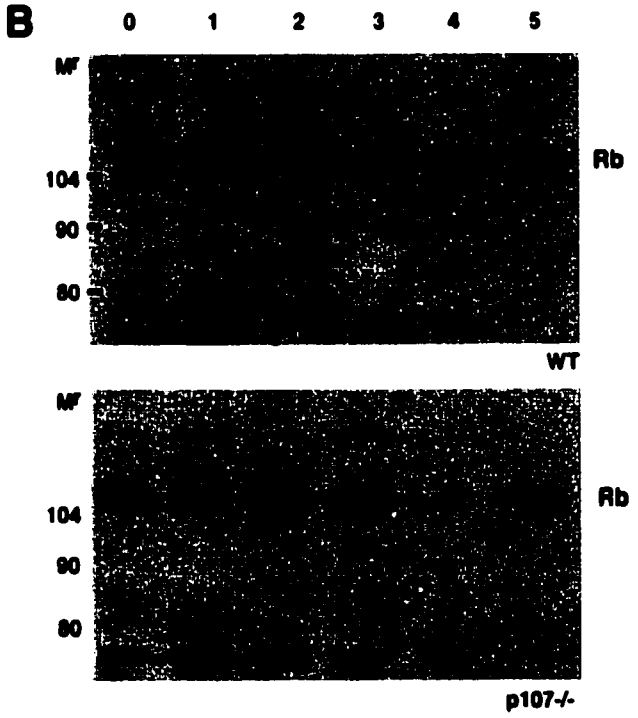
B
0
1
2
3
4
5
MF
104
90
80
Rb
WT
MF
104
90
80
Rb
p107-/-

7.3 Discussion

The embryonic development of p107-deficient skeletal muscle was not directly assessed, but newborn or adult muscle generally appeared histologically normal and was obviously functional. Satellite cell activation and proliferation are believed to recapitulate the processes that comprise embryonic skeletal muscle development. To specifically address subtle disturbances in activation and proliferation of p107 mutant myoblasts, satellite cell proliferation was monitored following injury *in vivo*, or differentiation induced in cultures of purified myoblast populations.

Regenerating *p107*$^{-/-}$ skeletal muscle contained a greater percentage of BrdU-incorporating cells compared to wildtype cells, 4.5 days following injury. The myoblast culture experiments indicated that increased proliferation of the mutant satellite cells would account for this discrepancy. Future experiments may involve a more in-depth evaluation of the *in vivo* response to damage. By assessing the numbers of cells that are immunoreactive for both c-met, a newly-defined marker for satellite cells, and BrdU, the exact identity of the proliferating cells can be determined. As well, a time course of the *in vivo* response following damage, from 36 hours when satellite cells invade the site and proliferate, to a period when the wildtype muscle would be regenerated (by 2 weeks), could also be informative in the analysis of this subtle phenotype (reviewed Grounds and Yablonka-Reuveni, 1993). Additionally, by quantitating levels of creatine kinase, a muscle injury marker, homogenates of the entire damaged muscle can be assessed throughout the course of regeneration (Bischoff, 1994; McArdle, *et al.*, 1994).

There does appear to be a deficit p107 myoblasts to exit from the cell cycle, indicated by the lower frequency of spontaneous differentiation, the high proportion of mutant cells that did not up-regulate MHC expression at day 1 post-induction, and continued DNA synthesis as revealed by ^{3}H-thymidine incorporation. Cultured *Rb*$^{-/-}$ 'myocytes' are not considered terminally differentiated since these can be induced into S

phase. Rb-deficient fibroblasts transduced with MyoD proceeded to an atypical skeletal muscle differentiation, and expressed early markers, but late differentiation markers were perturbed (Novitch, *et al.*, 1996). This work also reported that DNA synthesis was not inhibited in the Rb-deficient 'myocytes' and most cells arrested in S and G_2 phases of the cell cycle. p107 or p130-deficient fibroblasts did not exhibit a phenotype distinguishable from wildtype fibroblasts in this analysis. Future experiments should address whether differentiated wildtype and *p107*$^{-/-}$ myocytes are resistant to mitogenic stimulation. Preliminary results (data not shown) indicate that a portion of p107-deficient as well as wildtype differentiated cells incorporate ^{3}H-thymidine after an overnight incubation in 10% FCS DMEM.

Potentially *p107*$^{-/-}$ myoblasts initiate differentiation and express early markers of skeletal muscle, but subsequently do not survive. This would explain the apparent mis-expression or low induction of differentiation markers, for example the pattern of MRF4 expression. During *in vitro* myogenesis, a fraction of myoblasts usually undergo apoptosis, whereas most cells complete the differentiation programme and form myotubes that are resistant to apoptosis. Work by others has demonstrated that expression of the cdk inhibitors p21 or p16, and Rb correlates with enhanced survival of myocytes (Guo and Walsh, 1997; Wang, *et al.*, 1997; Wang and Walsh, 1996). As well, an *Rb*$^{-/-}$ myoblast cell line does undergo higher frequencies of apoptosis following low-mitogen induced differentiation. Overexpression of these molecules, which normally function to negatively regulate cell-cycle progression, does confer a degree of resistance to programmed cell death. The survival of *p107*$^{-/-}$ differentiated cells may be compromised by inappropriate cell cycle progression or perturbed expression of cdk inhibitors or Rb.

The expression of several cdk inhibitors including p16, p18, p21, p27 and p57 are correlated with skeletal myogenesis. However, gene disruption studies in which p18,

p21 or p27 have been mutated in mice demonstrated that these factors are not required for skeletal muscle development. However, it is highly possible that these results reflect functional overlap among members of the two families of inhibitors. Cdk activity can be assessed in *p107*$^{-/-}$ cultures in an attempt to correlate this activity with inappropriate regulation of cdk inhibitors and perturbed cell cycle withdrawal during differentiation.

In *p107*$^{-/-}$ differentiating myoblasts, the expression profiles of p21 and Rb are not fully comparable to those of wildtype cultures. At 1 day post-induction, p21 and Rb levels are markedly increased in wildtype cultures, in contrast to p107 mutant cultures. The viability of cells in the *p107*$^{-/-}$ cultures induced to differentiate can be assessed. Approaches to determine the frequency of apoptosis in the cultured cells include TUNEL assay, anti-Annexin-V reactivity in non-permeabilized cells, and FACS analysis if differentiation is induced in conditions that inhibit fusion (i.e. low calcium media).

Although subtle differences apparently exist between p107-deficient and wildtype cells, functional compensation by p107-related factors may be invoked to result in normal development and function of skeletal muscle and satellite cells *in vivo*. As described in Chapter 6 of this thesis, *p107* can be specifically mutated in experiments by generating mice with homozygous *p107* 'floxed' alleles and skeletal muscle-specific Cre recombinase transgenes. Our laboratory has access to Rb 'floxed' mice as well. Therefore, both Rb and p107 can be specifically mutated in the skeletal muscle of Cre transgenic mice, or primary satellite cells in culture expressing exogenously-supplied Cre recombinase. Work is ongoing to generate p130 'floxed' alleles. These future studies will further elucidate the individual and concerted roles of this protein family in skeletal muscle growth and differentiation, by addressing the functional overlap between these related factors.

CHAPTER 8

Summary and Conclusions

8.1. Specific and overlapping roles for p130 and p107 in growth and development.

The expression and functional patterns, and structural and functional relatedness of the Rb, p107 and p130 proteins suggest that there are overlapping as well as unique roles for these factors during growth, quiescence and differentiation. During embryonic development, Rb, p107 and p130 appear to be expressed in temporally or spatially distinct cells and tissues, although a degree of overlap exists, for example in the liver, CNS, and bone. As well in adult tissue, or in proliferating versus arrested or differentiating cells, the expression or activity of these factors is relatively distinct. p130 is prominent in differentiated and quiescent cells, and consequently is highly expressed in all adult tissues (Chen, *et al.*, 1996a; Chittenden, *et al.*, 1993; Cobrinik, *et al.*, 1993; Pertile, *et al.*, 1995; Smith, *et al.*, 1998; Chapter 3). By contrast, p107 is not expressed in quiescent cells and is virtually undetectable in the adult (Jiang, *et al.*, 1997; Kim, *et al.*, 1995). Together, the expression data is consistent with specific requirements for each of these factors during growth and differentiation.

The ability of the Rb proteins to interact with similar or identical proteins permit the coordinate regulation of at least some cellular functions, such as E2F transcriptional activity, and cell cycle transitions (review in Dyson, 1998). This activity has been extensively studied and indeed may be central to the coordinated exit from the cell cycle

for which Rb, p107 and p130 are implicated. However, these proteins diverge in several regions of sequence, and unique interactions with cellular factors have been revealed. For example, p107 is capable of interacting with c-Myc and Sp1 transcription factors, and repressing their activities (Beijersbergen, *et al.*, 1994a; Datta, *et al.*, 1995; Gu, *et al.*, 1994b). Additionally, p107 and p130 interact with cyclin proteins distinct from Rb-associated cyclins (Ewen, *et al.*, 1992; Faha, *et al.*, 1992; Hannon, *et al.*, 1993; Li, *et al.*, 1993). Also, it is reasonable to hypothesize that although Rb, p130 and p107 are capable of associating with a specific factor and regulating its activity, these interactions may not be relevant beyond the scope of the experimental system (*in vitro*, yeast screens, etc.). In many cases, the concurrent expression and activities of these factors, in a cell context consistent with them interacting, are not addressed.

8.1.i Cell-type specific requirements

That specific tissues are affected, or more severely so, in p107 mice and p130 embryos raises several points. If there are specific factors in a cell type-specific context that interact with the p107 and p130 proteins, then given that these interacting factors have an important role in the tissue's development or function, a phenotype will manifest in this specific tissue. For example, Wiggan *et al* (1998) refer to the ability of the Rb proteins to interact with homeodomain-containing factors. In the previously reported p107/p130 compound mutants, endochondral bone development was perturbed. Potentially, p107 and p130 regulate Cart-1 in determined chondrocytes. Alternatively, proper negative regulation of a factor by the p130 or p107/E2F complex may be crucial in a specific tissue context. For example, evidence was provided by Hurford *et. al* (1997) that distinct, putative E2F-target genes are specific for Rb- versus p107 and p130-mediated regulation.

Although p130 is ubiquitously expressed, like Rb, the $p130^{-/-}$ embryos displayed tissue-specific affects. In p130 mutant embryos, growth and development were generally

delayed, however, neuronal cell survival and cardiogenesis were severely compromised. This result may be due to the timing of cell cycle exit and subsequent differentiation of specific tissues during embryogenesis. The marked degree of apoptosis exhibited by neuronal cell types could be classified in this category. Alternatively, cell specific pathways or specific molecules may exist that absolutely require p130 as an effector or for appropriate control, respectively. For instance, the cardiac phenotype is interesting in this respect. If this phenotype is cell autonomous, there may be myocardial-specific molecules that directly or indirectly require p130 during myocardial differentiation.

The similarity between the p130 and Rb neuronal phenotypes leads to the suggestion that these factors are absolutely required for enforcing terminal differentiation and survival of this cell type. Further analysis of the p130-deficient neural cells may incorporate primary neuronal cell culture to analyze if this phenotype is cell autonomous. Analogous studies were performed for Rb-deficient neurons to assess growth, differentiation and survival (Lee, *et al.*, 1994; Slack, *et al.*, 1998). Inactivation of the Rb family, via expression of adenovirus E1A, during *in vitro* neuronal differentiation leads to loss of these cells. This data indicated that Rb proteins are required for the induction and survival of post-mitotic neurons. Also recently reported, loss of Rb and p107 resulted in retinoblastoma in chimeric mice, demonstrating the concerted roles of these proteins in tumour suppression (Robanus-Maandag, *et al.*, 1998). The overlapping functions of these factors may be addressed in future experiments that target these proteins for tissue-specific disruption.

8.1.ii Functional compensation and overlap

The generation of viable and fertile $p107^{-/-}$ mice testifies to functional compensation. Clearly, there is genetic evidence supporting that functional compensation exists within this gene family. Functional compensation is the ability of a factor to fulfill

the entire or part of the role normally occupied by a related factor. In the *p107*$^{-/-}$ embryos and mice, generally other factors must be compensating to accomplish proper development. Increased expression of Rb in the mutant embryos suggests that this protein ensures the proper development of some tissues. The p107-deficient mice developed a myeloid proliferative disorder. Therefore, requirements for p107 for the normal development of specific cell types were also revealed in the mutants. The mechanism underlying the metaplasia exhibited by the p107 mutants is unresolved at present. Undeniably though, this work supports the existence of functionally overlapping factors. Future *in vivo* experiments with compound, conditional Rb, p107 and p130 mutations will definitely assist in elucidating the functional overlap within this protein family.

One ES cell line harbouring homozygous mutations in all the Rb proteins has been produced (G. Mulligan, personal communication). ES cells can be aggregated to form embryoid bodies in which many cell types will be represented as the ES cells differentiate (robertson, 1987). In the triple gene-disrupted embryoid bodies, the efficiency of neuronal differentiation is markedly reduced. If the ES cells are introduced into B-cell recombination deficient mice, immature B cells are found in the periphery indicating that the Rb proteins are required for B cell terminal differentiation. Low percentage chimeras were derived from these triple mutant ES cells, however they had a very short lifespan, living an average of $4^1/2$ months. All 15 mice examined exhibited hyperplasias with an average of four tumours per animals. The spectrum of tissues with tumours included choroid plexus, adrenal gland, smooth muscle, ovary, testis, stomach and intestines. These results support that there is a concerted tumour suppression function of the Rb gene family in mice. This concerted function is further indicated by the development of retinoblastomas in compound mutant *Rb* and *p107* chimeras

(Robanus-Maandag, *et al.*, 1998). The chimeric mouse analysis will of course benefit by the generation of control ES lines harbouring double, homozygous disruptions. However, these studies are limited by the chimeric animal approach.

The data presented in this thesis and by other groups that have genetically examined the functions of the Rb, p107 and p130 proteins clearly indicate tissue-specific requirements for these factors; and suggest functional overlap and compensation within this protein family. The genetic and biochemical studies suggest that p107 functions during cellular proliferation along with Rb. p107-deficient myoblasts exhibited a deficit in withdrawing from the cell cycle, and the expression of p107 in differentiating cells has been demonstrated to be extinguished in G_0 over time (Chapter 7, Cobrinik, *et al.*, 1993). These findings are consistent with p107 functioning to regulate cell proliferation and the final cell division of differentiating cells, thereby contributing to permanent withdrawal from the cycle. Data presented in chapter 5 suggest that in most cell types, p107 function is compensated, potentially by Rb and possibly by p130 although its expression has not been notably affected. However, to demonstrate functional compensation, activity of p107 targets (cyclinE/A/cdk2, E2F-4, myc, Sp1) should be assessed in a variety of cell types from the p107 mutants. Consequently, these rescued activities should be isolated along with Rb or p130 in the appropriately functioning complex. As compound mutants are non-viable, family members must be compensating for the loss of p107 (Cobrinik, *et al.*, 1996; Lee, *et al.*, 1996, chapter 5).

p130 appears to function during or for the maintenance of the post-mitotic state, and subsequently the survival of cells in this compartment. Again these activities appear to overlap Rb function as assessed by genetic and biochemical approaches. The cell autonomy of the p130 phenotypes must be addressed, especially as cardiac insufficient is suggested to be the cause of lethality. An approach to rescue the cardiac phenotype, as discussed in chapter 4, is expression of p130 in the heart. A second avenue to investigate

cell autonomy of the phenotypes is to derive ES cells from the *p130*$^{-/-}$ embryos for use in chimeric mouse experiments. Lastly, work is ongoing to develop a p130 conditional mutant allele using loxP sites and CRE expression. This stain of mice will be bred with Rb and/or p107 conditional mutant mice to generate the strain required for mutating combinations of these genes in specific tissues, at distinct stages of development. The intrinsic loss-of-function mutations of these genes will be dependent on CRE transgene expression. Expressing the Rb, p107 and p130 proteins or chimeric proteins from the transcriptional control of the related factors would be an elegant approach, albeit a considerable undertaking, to assess the degree of overlap and assign distinct functions to the Rb family members.

Results of the genetic studies presented in this thesis have further indicated that unique and overlapping roles exist within the Rb family. The abiltiy of Rb, p130 and p107 to interact with and apparently functionally substitute for each other indicates that concerted or overlapping functions exist. The Rb proteins appear to function in a concerted manner to regulate cell proliferation and to accommodate cell transitions, from quiescence to S phase, and to the post-mitotic state of differentiated cells.

8.2. Strain-dependence and modifier loci

Gene targeting experiments to derive null mutations *in vivo* and reveal the functions of the gene product are confounded by compensatory mechanisms and secondary phenotypic changes. Clearly a null-mutant might not only lack the product of a single gene but might also have invoked any number or manner of compensatory mechanisms during development to counteract the affect of the null mutation. Therefore, the resulting phenotype may be complex and not directly related to the function of the gene of interest.

Also important and particularly relevant to the work described within this thesis, is that the same mutation in one gene can have slightly variant, or markedly different phenotypes when placed on different genetic backgrounds. The *p130* and *p107* mutant alleles that we generated were bred onto C57Bl/6J and Balb/cJ genetic backgrounds (specifically, the worked described assessed phenotypes on 129Sv hybrid strains), and the mice were housed in a specific-pathogen free facility. Therefore, both allelic (mutant allele) variation and environmental modifiers are essentially excluded as factors that cause the variation in phenotypes of the mutant mice. However, the genetic variation, between these inbred strains of mice, provided modifier genes that dramatically affected the phenotypes of the *p130* and *p107* mutations. Given that the C57Bl/6 strain of mice diverged from the Balb/C strain around the year 1905, it is not unexpected that a great deal of polymorphism exists between the two strains used in the experiments described in this thesis (Hogan, *et al.*, 1986). Additionally, genetic contribution by the 129Sv ES cells is present. Ignoring genetic background effects can lead to misinterpretation of results (Erickson, 1996; Gerlai, 1996). There are numerous inbred mouse strains and logically, some strains are more closely related than others.

One approach that may seem attractive is to avoid analyzing phenotypes on hybrid genetic backgrounds. This may be accomplished by backcrossing the mutant hybrid animals several times to the strain of choice, i.e. Balb/c, to create a congenic strain. Although each generation will be enriched for the Balb/c genotype, eliminating linked genes is a considerable undertaking, as even after 12 backcrossed generations, 1% of the 129 genome could still be represented (Gerlai, 1996). There are methods and services that make it easier to arrive at a congenic mouse strain. By assessing mice with a set of dense molecular markers, microsatellites, the time needed to generate the congenic strain can be significantly reduced (Markel, *et al.*, 1997). Alternatively, investigators may choose to avoid using hybrid mice completely. For this, chimeras can be bred to the

genetic strain from which the ES cells originate. 129Sv mice are quite difficult to breed, however C57Bl/6 ES cell lines can be derived and will likely come into common use given that this mouse strain is so widely applied in genetic studies (Simpson,*et al.*, 1997).

Although avoiding hybrid strains may simplify the analysis, this approach also seriously limits the information that can be derived from animal experiments. Rather, researchers are looking to hybrid mouse strains as an approach to elucidate variable disease progression or penetrance in humans. Although environmental or genetic factors or both contribute to this variability, modifying loci can be assessed most efficiently in hybrid mouse strains. As well, the extensive genetic map of the mouse, in addition to the short gestational period, large litter sizes, availability of inbred strains, and the ability to perform controlled matings, makes it an ideal genetic model. By characterizing novel modifier genes, additional insights into molecular pathways or (human) pathogenesis can be provided. These approaches have been successfully used to identify genes or loci that modify mouse models of complex human traits including susceptibility to tumourigenesis (Fineman, *et al.*, 1998). That strain-dependent differences exist are not only relevant to 'knock-out' studies, but also to classic transgenic analysis in mice and essentially any studies conducted in animals.

Genetic analyses of modifiers can reveal components of the pathways within which the gene products of interest function. Therefore, by assessing the modifier loci in the p107 and p130 mutant mice, genes with epistatic relations to these factors may be found. However, modifying genes do not necessarily directly interact, or act in similar pathways to the gene being modified. Essentially, very indirect actions of the modifiers of the p130 and p107 phenotypes can be also be expected. The modifier genes may include Rb and genes that function to regulate Rb expression or activity, for example cdk inhibitors; however, the identification of the modifiers will depend upon future genetic analysis.

8.2.i Mapping modifier genes

Simple sequence length polymorphisms (SSLPs or microsatellites) are highly variable among inbred mouse strains. Microsatellites are the most abundant class of marker of the mouse genetic map and consequently, have greatly contributed to the extent of mapping in the mouse. SSLPs, including di- tri- and tetranucleotide repeats, were developed as markers for genetic analysis in humans, and subsequently applied in the mouse. These repeats are very abundant in most mammalian genomes, with the most frequent being $(CA)_n$ repeats which are present in about 10^5 dispersed locations and are essentially evenly dispersed along the chromosomes. The polymorphism of microsatellites is due to the variable length of the repeat among individuals in a species, ascribed to slippage during DNA replication. The mutation rate is estimated to be approximately 10^{-4} per generation (Dietrich, *et al.*, 1996). The microsatellites are anonymous sequences that make it possible to trace inheritance in any genetic cross, which permits the genetic analysis of otherwise complex, polygenic and quantitative traits. Significantly, microsatellites are even informative in crosses between closely related strains.

The advantages of microsatellite analysis are that they are easy to genotype by PCR and show a polymorphism rate of about 50% among inbred mouse strains. Very efficient genotyping of large crosses or populations are accomplished with fluorescence-conjugated PCR primers and multiplexing of the primers in PCR reactions (Esposito *et al.*, 1998; Mansfield et al., 1994; Miller and Yuan, 1997; Rhodes *et al.*, 1997). The extent of multiplexing is limited though, as most of the published and applied PCR primers designed for specific microsatellites amplify products in the 130-150 range (Dietrich, 1996).

The majority of mouse microsatellite markers were developed at the Whitehead Institute/MIT Center for Genome Research from random genomic clones and public databases. This initiative generated 6580 microsatellites, all of which have been mapped and analyzed for polymorphism on a panel of 12 common laboratory mouse strains, including C57Bl/6, Balb/c and 129Sv. An integrated mouse map was presented by combining gene-based and microsatellite-based maps. This map contains a microsatellite marker approximately every 1 cM (or an average spacing between all markers of 0.2 centimorgans or about 400 kilobases) (Dietrich *et al.*, 1996). Therefore, the extent of the mouse map makes it invaluable for locating, identifying and cloning candidate genes.

Research Genetics Inc. has chosen 410 of the MIT microsatellite markers, and provide an analysis referred to as a genome-wide screen. In the case of the *p107* modifying genes, genomic DNA samples from affected and revertant (normal appearance) B2 C57Bl/6 mice can be genotyped by PCR for the 410 microsatellites. Modifying loci can then be distinguished by the genotype correlated to phenotypically normal versus mutant mice. The studies, described in this thesis, employed mice or ES cells from 3 inbred (homogenous) strains, so only 3 parental microsatellite alleles are segregating in the B2 C57Bl/6 population. The majority of the microsatellites applied by Research Genetics will distinguish 129Sv alleles. An example of the microsatellites on mouse chromosome 2 and their appropriate sizes in the three genetic strains used in our laboratory are presented in figure 8.1. Further genetic analysis of modifying genes indicated by the microsatellite genotypes can be accomplished by continuing with breeding to generate congenic lines and generating recombinant (informative) chromosomes across the regions highlighted by the microsatellite analysis in breeding experiments. Finally, progeny testing can be employed to deduce the distinct allele carried on the recombinant chromosome(s) (Dietrich *et al.*, 1996; reviewed in Copeland *et al.*, 1993). The breeding experiments initiated and described in this thesis have

provided the material to analyze the modifier genes that impinge upon the mutant phenotype.

Figure 8.1 Schematic representation of the chromosome 2 microsatellite linkage map.

(A) 20 microsatellite marker loci are arranged (not by scale here) for the chromosome 2 specific set applied by Research Genetics for genome-wide linkage screening in the mouse (Dietrich *et al.*, 1996; Research Genetics Web Page). (B) This table presents and compares the allele sizes for all the chromosome 2 microsatellites applied. Light yellow represents informative microsatellites and allele sizes that reveal a distinct allele, and vibrant yellow indicates microsatellites that can distinguish each of the 3 parental alleles. Differences of less than 4 bp can only be distinguished using optimized protocols that reduce overlapping stutter pattern.

A Chromosome 2

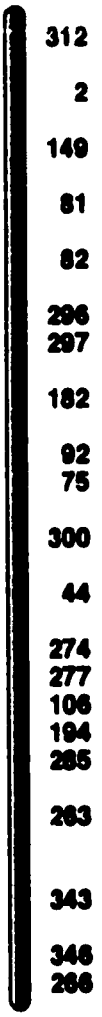

B

Locus	Allele sizes (bp)		
	C57	Balb	129Sv
2	129	129	
44	150	148	
75	112	106	
81	150	150	
82	196	196	
92	148	148	
106	150	150	154
149	213	195	195
182	147	151	151
194	116	132	130
263	134	136	134
266	136	138	132
274	138	138	134
277	303	303	299
296	136	152	162
296	144	144	154
297	147	147	147
300	124	106	106
304	120	186	136
312	126	126	116
323	114	110	126
343	173	173	173
346	99	99	116

CHAPTER 9

References

Adra, C.N., N.A. Ellis and M.W. McBurney. 1988. The family of mouse phosphoglycerate kinase genes and pseudogenes. Som Cell Mol Genet 14: 69-81.

Almasan A., Y. Yin, R. E. Kelly, E. Y. Lee, A. Bradley, W. Li, J.R. Bertino and G.M Wahl. 1995. Deficiency of retinoblastoma protein leads to inappropriate S-phase entry, activation of E2F-responsive genes, and apoptosis. Proc Natl Acad Sci 92: 5436-5440.

Ang, S.L and J. Rossant. 1994. HNF-3 beta is essential for node and notochord formation in mouse development. Cell 78: 561-574.

Asimakopoulos, F.A., N.J. White, E. Nacheva and A.R. Greene. 1994. Molecular analysis of chromosome 20q deletions associated with myeloproliferative disorders and myelodysplastic syndromes. Blood 84: 3086-3094.

Auffray, C. and R. Rougeon. 1980. Purification of mouse immunoglobulin heavy-chain messenger RNAs from total myeloma tumor RNA. Eur J Biochem 107: 303-314.

Azizhan, C.J.., E.D. Jensen, J.A. Pierce and M. Wade. 1993. Transcription from TATA-less promoters: dohydrofolate reductase as a model. Crit Rev Eukaryotic Gene Expression 3: 229-254.

Bagchi, S., R. Weinmann and P. Raychaudhuri. 1991. The retinoblastoma protein copurifies with E2F-1, an E1A-regulated inhibitor of the transciption factor E2F. cell 65: 1063-1072.

Bai, C., R. Richman and S.J. Elledge. 1994. Human cyclin F. EMBO J 13: 6087-6098.

Baker, J., J.-P. Liu, E.J. Robertson and A. Efstradiadis. 1993. Role of insulin-like growth factors in embryonic development and post-natal growth. Cell 75: 73-82.

Bandara, L.R., V.M. Buck, M. Zamanian, L.H. Johnston and N.B. LaThangue. 1993. Functional synergy between DP-1 and E2F-1 in the cell cycle-regulating transcription factor DRTF1/E2F. embo j 12: 4317-4324.

Bandara, L.R. and N.B. LaThangue. 1991. Adenovirus E1A prevents the retinoblastoma gene product from complexing with a cellular transcription factor. Nature 351: 494-497.

Bang, O.S., F.W. Ruscetti, M.H. Lee, S.J. Kim and M.C. Birchenall-Roberts. 1996. Transforming growth factor-b1 modulates p107 function in myeloid cell: correlation with cell cycle progression. J Biol Chem 271: 7811-7819.

Beijersbergen, R.L., L. Carlee, R.M. Kerkhoven and R. Bernards. 1995. Regulation of the retinoblastoma protein-related p107 by G1 cyclin complexes. Genes Dev 9: 1340-1353.

Beijersbergen, R.L., E.M. Hijmans, L. Zhu and R. Bernards. 1994a. Interaction of c-Myc with the Rb-related protein p107 results in inhibition of c-Myc-mediated transactivation. EMBO J 13: 4080-4086.

Beijersbergen, R.L., R.M. Zhu, L. Carlee, P.M. Voorhoeve and R. Bernards. 1994b. E2F-4, a new member of the E2F gene family, has oncogenic activity and associates with p107 in vivo. Genes Dev 8: 2680-2690.

Benezra, R., R.L. Davis, D. Lockshon, D.L. Turner and H. Weintraub. 1990. The protein Id: a negative regulator of helix-loop-helix DNA binding proteins. Cell 61: 49-59.

Bernards, R. 1997. E2F: a nodal point in cell cycle regulation. Biochem Biophys Acta 1333: M33-M40.

Bernards, R., G M Schackleford, M R Berber, J M Horowitz, S H Friend M Schartl, E Bogenmann, J M Rapaport, T Mcgee, T P Dryja, *et al.* 1989. Structure and function of the murine retinoblastoma gene and characterization of its encoded protein. Proc Natl Acad Sci 86:6474-6478.

Bignon, Y., Y. Chen, C.-Y. Chang, D.J. Riley, J.J. Windle, P.L. Mellon and W.-H. Lee. 1993. Expression of a retinoblastoma transgene results in dwarf mice. Genes Dev 7: 1654-1662.

Birnboim, H.C. 1988. rapid extraction of high molecular weight RNA from cultured cells and granulocytes for Northern analysis. Nucleic acids research 16: 1487-1497.

Bischoff, R. 1986. A satellite cell mitogen from crushed adult muscle. Dev Biol 115: 140-147.

Bischoff, R. 1990. Interactions between satellite cells and skeletal muscle fibers. Development 109: 943-952.

Bischoff, R. 1994. The satellite cell and muscle regeneration. In Myogenesis Vol. 2 A.G. Engel and C. Franszini-Armstrong, ed. McGraw-Hill, New York. pp97-118.

Blake, M.C. and J.C. Azizkhan. 1989. Transcription factor E2F is required for efficient expression of the hamster dihydrofolate reductase gene in vitro and in vivo. Mol Cell Biol 11: 4994-5002.

Bonyadi, M., S.A. Rusholme, F.M. Cousins, H.C. Su, C.A. Biron, M. Farall and R.J. Akhurst. 1997. Mapping of a major genetic modifier of embryonic lethality in TGFβ1 knockout mice. Nature Genetics 15: 207-211.

Bookstein, R., J.-Y. Shew, P.-Y. Chen, Y. Scully and W.-H. Lee. 1990. Suppression of tumorigenicity of human prostate carcinoma cells by replacing a mutated RB gene. 247 712-715:

Botz, J., K. Zerfass-Thome, D. Spitkovsky, H. Delius, B. Vogt, M. Eilers, A. Hatzigeorgiou and P. Jansen-Durr. 1996. Cell cycle regulation of the murine cyclin E gene depends on an E2F binding site in the promoter. Mol Cell Biol 16: 3401-3409.
Bouchard, C., P. Staller and M. Eilers. 1998. Control of cell proliferation by Myc. Trends Cell Biol 8: 202-206.

Braun, T., E. Bober and H.H. Arnold. 1992. Inhibition of muscle differentiation by the adenovirus E1A protein: repression of the transcriptional activating function of the HLH protein Myf-5. Genes Dev 6: 888-902.

Braun, T., E. Bober, G. Buschhausen-Denker, S. Kohtz, K.H. Grzeschik and H.H. Arnold. 1989. Differential expression of myogenic determination genes in muscle cells: possible autoactivation by the Myf gene products. EMBO J 8: 3617-3625.

Braun, T., M.A. Rudnicki, H.-H. Arnold and R. Jaenisch. 1992. Targeted inactivation of the muscle regulatory gene Myf-5 results in abnormal rib development and perinatal death. Cell 71: 369-382.

Brehm, A., E.A. Miska, D.J. McCance, J.L. Reid, A.J. Bannister and T. Kouzarides. 1998. Retinoblastoma protein recruits histone deacetylase to repress transcription. Nature 391: 597-601.

Bremner, R., B.L. Cohen, M. Sopta, P.A. Hamel, C.H. Ingles, B.L. Gallie and R.A. Phillips. 1995. Direct transcriptional repression by pRb and its reversal by specific cyclins. Mol Cell Biol 15: 3256-3265.

Buchkovich, K., L.A. Duffy and E. Harlow. 1989. The retinoblastoma protein is phosphorylated during specific phases of the cell cycle. Cell 58: 1097-1105.

Buckingham, M. 1994. Molecular biology of muscle development. Cell 78: 15-21.

Cao, L., B. Faha, M. Dembski, L.-H. Tsai, E. Harlow and N. Dyson. 1992. Independent binding of the retinoblastoma protein and p107 to the transcription factor E2F. Nature 355: 176-179.

Capecchi, M.R. 1989. Altering the genome by homologous recombination. Science 244: 1288-1292.

Cardoso, M.C., H. Leonhardt and B. Nadal-Ginard. 1993. Reversal of terminal differentiation and control of DNA replication: cyclin A and cdk2 specifically localize at subnuclear sites of DNA replication. Cell 74: 979-992.

Caruso, M., F. Martelli, A. Giordano and A. Felsani. 1993. Regulation of the MyoD gene transcription and protein function by the transforming domains of the adenovirus E1A oncoprotein. Oncogene 8: 267-278.

Castano, E., Y. Kleyner and B.D. Dynlacht. 1998. Dual cyclin-binding domains are required for p107 to function as a kinase inhibitor. Mol Cell Biol 18: 5380-5391.

Cavanaugh, A.H., W.M. Hempel, L.J. Taylor, V. Rogalsky, G. Todorov and L.I. Rothblum. 1995. Activity of RNA polymerase I transcription factor UBF blocked by Rb gene product. Nature 374: 177-180.

Chellappan, S., S. Hiebert, M. Mudryj, J. Horowitz and J. Nevins. 1991. The E2F transcription factor is a cellular target for the Rb protein. Cell 65: 1053-1061.

Chelleppan, S., V.B. Kraus, B. Kroger, K. Munger, P.M. Howley, W.C. Phelps and J.R. Nevins. 1992. Adenovirus E1A, simian virus 40 tumor antigen, and human papillomavirus E7 protein share the capacity to disrupt the interaction between transcription factor E2F and the retinoblatoma gene product. Proc Natl Acad Sci USA 89: 4549-4553.

Chen, G., C.T. Guy, H.-W. Chen, N. Hu, E.Y.-H.P. Lee and W.-H. Lee. 1996a. Molecular cloning and developmental expression of mouse *p130*, a member of the *retinoblastoma* gene family. J Biol Chem 271: 9567-9572.

Chen, L.I., K. Nishinaka, K. Kwan, I. Kitabayashi, Y. Yokoyama, y.H. Fu, S. Grunwald and R. Chiu. 1994. The retinoblastoma gene product Rb stimulates Sp1-mediated transcription by liberating Sp1 from a negative regulator. Mol Cell Biol 14: 4380-4389.

Chen, P.-L., D.J. Riley, Y. Chen and W.-H. Lee. 1996b. Retinoblastoma protein positively regulates terminal adipocyte differentiation through interaction with C/EBPs. Genes Dev 10: 2794-2804.

Chen, P.L., P. Scully, J.Y. Shew, J.Y. Wang and W.-H. Lee. 1989. Phosphorylation of the retinoblastoma gene product is modulated during the cell cycle and cellular differentiaion. Cell 58: 1193-1198.

Chittenden, T., D.M. Livingston and J. DeCaprio. 1993. Cell-cycle analysis of E2F in primary human T cells reveals novel E2F complexes and biochemically distinct forms of E2F. Mol Cell Biol 13: 3975-3983.

Chittenden, T., D.M. Livingston and W.G.J. Kaelin. 1991. The T/E1A-binding domain of the retinoblastoma product can interact selectively with a sequence-specific DNA-binding protein. Cell 65: 1073-1082.

Chow, K.N. and D.C. Dean. 1996. Domains A and B in the Rb pocket interact to form a transcriptional repressor motif. Mol Cell Biol 16: 4862-4868.

Chu, W.M., Z. Wang, R.G. Roeder and C.W. Schmid. 1997. RNA polymerase III transcription repressed by Rb through its interactions with TFIIIB and TFIIIC2. J Biol Chem 272: 4755-4761.

Clarke, A.R., E.R. Maandag, M. van Roon, N.M.T.v.d. Lugt, M.van der Valk, M.L. Hooper, A. Berns and H. te Riele. 1992. Requirement for a functional Rb-1 gene in murine development. Nature 359: 328-330.

Clarke, S. and S. Gordon. 1998. Myeloid-specific gene expression. J Leuk Biol 63: 153-164.

Claudio, P. P., C. M. Horward, A. Baldi, A. De Luca, Y. Fu, G. Condorelli, Y. Sun, N. Colburn, B. Calabretta and A. Giordano. 1994. p130/pRb2 has growth suppressive properties similar to yet distinctive from those of retinoblastoma family members pRb and p107. Cancer Res 54: 5556-5560.

Clegg, C.H., T.A. Linkhart, B.B. Olwin and S.D. Hauschka. 1987. Growth factor control of skeletal muscle differentiation: commitment to terminal differentiation occurs in G_1 phase and is repressed by fibroblast growth factor. J Cell Biol 105: 949-956.

Cobrinik, D. 1996. Regulatory interactions among E2F's and cell cycle control proteins. Cur Top Micro Immunol 208: 31-61.

Cobrinik, D., M. H. Lee, G. Hannon, G. Mulligan, R. T. Bronson, N. Dyson, E. Harlow, D. Beach, R. A. Weinberg and T. Jacks. 1996. Shared role of the pRb-related p130 and p107 proteins in limb development. Genes Dev 10:1633-1644.

Cobrinik, D., P. Whyte, D.S. Peeper, T. Jacks and R.A. Weinberg. 1993. Cell cycle-specific association of E2F with the p130 E1A-binding protein. Genes Dev 7: 2392-2404.

Copeland, N.G., N.A. Jenkins, D.J. Gilbert, J.T. Eppig, L.J. Maltais *et al.* 1993. A genetic linkage map of the mouse: current applications and future prospects. Science 262:57-66.

Corbeil, H.B., P. Whyte and P.E. Branton. 1995. Characterization of transcription factor E2F complexes during muscle and neuronal differentiation. Oncogene 11: 909-920.

Cossu, G., S. Tajbakhsh and M. Buckingham. 1996. How is myogenesis initiated in the embryo? Trends Genet 12: 218-223.

Cress, W.D., D.G. Johnson and J.R. Nevins. 1993. A genetic analysis of the E2F1 gene distinguishes regulation by Rb, p107 and adenovirus E4. Mol Cell Biol 13: 6314-6325.

Dagnino, L., C.J. Fry, S.M. Bartley, P. Farnham, B.L. Gallie and R.A. Phillips. 1997a. Expression patterns of the E2F family of transcription factors during mouse nervous system development. Mech Dev 66: 13-25.

Dagnino, L., C.J. Fry, S.M. Bartley, P. Farnham, B.L. Gallie and R.A. Phillips. 1997b. Expression patterns of the E2F family of transcription factors during murine epithelial development. Cell Growth Diff 8: 553-563.

Dalton, S. 1992. Cell cycle regulation of the human cdc2 gene. EMBO J 11: 1797-1807.

Datta, P.K., P. Raychaudhuri and S. Bagchi. 1995. Association of p107 with Sp1: Genetically separableregions of p107 are involved in regulation of E2F- and Sp1-dependent transcription. Mol Cell Biol 15: 5444-5452.

Davie, J.R. 1998. Covalent modifications of histones: expression from chromatin templates. Curr Opin Genet Dev 8: 173-178.

Davies, R., R. Hicks, T. Crook, J. Morris and K. Vousden. 1993. Human papillomavirus type 16 E7 associates with a histone H1 kinase and with p107 through sequences necessary for transformation. J Virol 67: 2521-2528.

Davis, M.P., G.W. Dewald, R.V. Pierre and H.C. Hoagland. 1984. Hematologic manifestations associated with deletions of the long arm of chromosome 20. Cancer Genet Cytogenet 12: 63-71.

Davis, R.L., H. Weintraub and A.B. Lassar. 1987. Expression of a single transfected cDNA converts fibroblasts to myoblasts. Cell 51: 987-1000.

Decaprio, J.A., J.W. Ludlow, J. Figge, J.Y. Shew, C.M. Huang, W.-H. Lee, E. Marsilio, E. Paucha and D.M. Livingston. 1988. SV40 large tumor antigen forms a specific complex with the product of the retinoblastoma susceptibility gene. Cell 54: 275-283.

Decaprio, J.A., J.W. Ludlow, D. Lynch, Y. Furukawa, J. Griffin, H. Pwinica-Worms, C.-M. Huang and D.M. Livingston. 1989. The product of the retinoblastoma susceptibility gene has properties of a cell cycle regulatory element. Cell 58: 1085-1095.

Deed, R.W., E. Hara, G.T. Atherton, G. Peters and J.D. Norton. 1997. Regulation of Id3 cell cycle function by Cdk-2-dependent phosphorylation. Mol Cell Biol 17: 6815-6821.

DeGregori, J., T. Kowalik and J.R. Nevins. 1995. Cellular targets for activation by the E2F1 transcription factor include DNA synthesis- and G1/S-regulatory genes. Mol Cell Biol 15: 4215-4224.

DeLuca, A., T.K. Maclachlan, L. Bagella, C. Dean, C.M. Howard, P.P. Claudio, A. Baldi, K. Khalili and A. Giordano. 1997. A unique domain of pRb2/p130 acts as an inhibitor of Cdk2 kinase activity. J Biol Chem 272: 20971-20974.

Deng, C., P. Zhang, J.W. Harper, S.J. Elledge and P. Leder. 1995. Mice lacking p21CIP1/WZF1 undergo normal development, but are defective in G1 checkpoint control. Cell 82: 675-684.

de Stanchina, E., M. E. Mccurrach, F. Zindy, S. Y. Shieh, G. Ferbeyre, A. V. Samuelson, C. Prives, M. F. Roussel, C. J. Sherr, and S. W. Lowe. 1998. E1A signaling to p53 involves the p19(ARF) tumor suppressor. Genes Dev 12:2434-2442.

Dieffenbach, C.W. and G.S. Dveksler. 1995. PCR primer: a laboratory manual. Cold Spring Harbor Laboratory Press. Cold Spring Harbor, N.Y.

Dietrich, S., F.R. Schubert and A. Lumsden. 1997. Control of dorsoventral pattern in the chick paraxial mesoderm. Development 124: 3895-3908.

Dietrich, W.F., J. Miller, R. Steen, M.A. Merchant, D. Damron-Boles *et al.* 1996. A comprehensive genetic map of the mouse genome. Nature 14:149-159.

Dowdy, S.F., P.W. Hinds, K. Louie, S.I. Reed, A. Arnold and R.A. Weinberg. 1993. Physical interaction of the retinoblastoma protein with human D cyclins. Cell 73: 499-511.

Downward, J. 1997. Cell cycle: routine role for Ras. Curr Biol 7: R258-260.

Draetta, G.F. 1994. Mammalian G1 cyclins. Curr Opin Cell Biol 6:842-846.

Dudov, K.P. and R.P. Perry. 1984. The gene family encoding the mouse ribosomal protein L32 contains a uniquely expressed intron-containing gene and an unmutated processed gene. Cell 37: 457-468.

Dunaief, J.L., B.E. Strober, S. Guha, P.A. Khavari, K. Alin, J. Luban, M. Begemann, G.R. Crabtree and S.P. Goff. 1994. The retinoblastoma protein and BRG1 form a complex and cooperate to induce cell cycle arrest. Cell 79: 119-130.

Dynlacht, B.D., O. Flores, J.A. Lees and E. Harlow. 1994. Differential regulation of E2F trans-activation by cyclin/cdk2 complexes. Genes Dev 8: 1772-1786.

Dyson, N. 1998. The regulation of E2F by pRb-family proteins. Genes Dev 12: 2245-2262.

Dyson, N., P. Guida, K. Munger and E. Harlow. 1992. Homologous sequences in adenovirus E1A and human papillomavirus E7 proteins mediate interaction with the same set of cellular proteins. J Virol 66: 6893-6902.

Dyson, N., P. Mhowley, K. Munger and E. Harlow. 1989. The human papilloma virus-16 E7 oncoprotein is able to bind to the retinoblastoma gene product. Science 242: 934-937.

Edmondson, D.G. and E.N. Olson. 1989. A gene with homology to the myc similarity region of MyoD1 is expressed during myogenesis and is sufficient to activate the muscle differentiation program. Genes Dev 3: 628-640.

Erickson, R.P. 1996. Mouse models of human genetic disease: which mouse is more like a man? BioEssays 18: 993-998.

Ericson, J., S. Morton, A. Kawakami, H. Roelink and T.M. Jessell. 1996. Two critical periods of Sonic hedgehog signaling required for the specification of motor neuron identity. Cell 87: 661-673.

Ericson, J., S. Thor, T. Edlund, T.M. Jessell and T. Yamada. 1992. Early stages of motor neuron differentiation revealed by expression of homeobox gene Islet-1. Science 256: 1555-1560.

Evans, M.J. and M.H. Kaufman. 1981. Establishment in culture of pluripotent cells from mouse embryos. Nature 292: 154-156.

Ewen, M.E., B. Faha, E. Harlow and D.M. Livingston. 1992. Interaction of p107 with cyclin A independent of complex formation with viral oncoproteins. Science 255: 85.

Ewen, M.E., H.K. Sluss, C.J. Sherr, H. Matsushime, J. Kato and D.M. Livingston. 1993. Functional interactions of the retinoblastoma protein with mammalian D-type cyclins. Cell 73: 487.

Ewen, M.E., Y. Xing, J.B. Lawrence and D.M. Livingston. 1991. Molecular cloning, chromosomal mapping, and expression of the cDNA for p107, a retinoblastoma gene product-related protein. Cell 66: 1155-1164.

Fagan, R., K.J. Flint and N. Jones. 1994. Phosphorylation of E2F-1 modulates its interaction with the retinoblastoma gene product and the adenoviral E4 P19 kDa protein. Cell 78: 799-811.

Faha, B., M.E. Ewen, L.-H. Tsai, D.M. Livingston and E. Harlow. 1992. Interactions between human cyclin A and adenovirus E1A-associated p107 protein. Science 255: 87.

Fantl, V., G. Stamp, A. andrews, I. Rosewell and C. Dickson. 1995. Mice lacking cyclin D1 are small and show defects in eye and mammary gland development. Genes Dev 9: 2364-2372.

Fero, M.L., M. Rivkin, M. Tasch, *et al.* 1996. A syndrome of multiorgan hyperplasia with features of gigantism, tumorigenesis, and female sterility in p27(Kip1)-deficient mice. Cell 85: 733-744.

Ferreira, R., L. Magnaghi-jaulin, P. Robin, a. Harel-Bellan and d. Trouche. 1998. The three members of the pocket proteins family share the ability to repress E2F activity through recruitment of a histone deacetylase. Proc Natl Acad Sci 95: 10493-10498.

Field, S.J., F.-Y. Tsai, F. Kuo, A.M. Zubiaga, W.G.J. Kaelin, D.M. Livingston, S.H. Orkin and M.E. Greenberg. 1996. e2F-1 functions in mice to promote apoptosis and suppress proliferation. Cell 85: 549-561.

Fimia, G.M., V. Gottifredi, B. Bellei, M.R. Ricciardi, A. Tafuri, P. Amati and R. Maione. 1998. The activity of differentiation factors induces apoptosis in polyomavirus large T-exrpessing myoblasts. Mol Cell Biol 9: 1449-1463.

Fineman, R.J., R.C. Jansen, M.A.V.D. Valk and P. Demant. 1998. High frequency of interactions between lung cancer susceptibility genes in the mouse: mapping of Sluc5 to Sluc14. Cancer Res 58: 4794-4798.

Fisher, P.R. and D.O. Morgan. 1993. A novel cyclin associates with MOI5/cdk7 to form the cdk-activating kinase. Cell 78: 713-724.

Fishman, M.C. and K.R. Chien. 1997. Fashioning the vertebrate heart: earliest embryonic decisions. Development 124: 2099-2117.

Flemington, E.K., S.H. Speck and W.G.J. Kaelin. 1993. E2F-1 mediated transactivation is inhibited by complex formation with the retinoblastoma susceptibility gene product. Proc Natl Acad Sci 90: 6914.

Flink, I.L., S. Oana, N. Maitra, J.J. Bahl and E. Morkin. 1998. Changes in E2F complexes containing retinoblastoma family members and increased cyclin-dependent kinase inhibitor activities during terminal differentiation of cardiomyocytes. J Mol Cell Cardiol 30: 563-578.

Franklin, D.S., V.L. Godfrey, H. Lee, G.I. Kovalev, R. Schoonhoven, S. Chen-Kiang, L. Su and Y. Xiong. 1998. CDK inhibitors p18(INK4c) and p27(Kip1) mediate two separate pathways to collaboratively suppress pituitary tumorigenesis. Genes Dev 12: 2899-2911.

Friend, S.H., R. Bernards, S. Rogelj, R.A. Weinberg, J.M. Rapaport, D.M. Albert and T.P. Dryja. 1986. A human DNA segment with properties of the gene that predisposes to retinoblastoma and ostersarcoma. Nature 323: 643-646.

Friend, S.H., J.M. Horowitz, M.R. Gerber, X.-F. Wang, E. Bogemann, F.P. Li and R.A. Weinberg. 1987. Deletions of a DNA sequence in retinoblastomas and mesenchymal tumors: Organization of the sequence and its encoded protein. Proc Natl Acad Sci USA 84: 1563-1566.

Fung, Y.K.T., A.L. Murphy, A. T'Ang, J. Qian, S.H. Hinrichs and W.F. Benedict. 1987. Structural evidence for the authenticity of the human retinoblastoma gene. Science 236: 1657-1661.

Furukawa, Y., J.A. Decaprio, A. Freedman, Y. Kanakura, M. Nakamura, T.J. Ernst, D.M. Livingston and J.D. Griffin. 1990. Expression and state of phosphorylation of the retinoblastoma susceptibility gene product in cycling and noncycling human hematopoietic cells. Proc Natl Acad Sci 87: 2770-2774.

Garriga, J., A. Limon, X. mayol, S.G. Rane, J.H. Albrecht, E.P. Reddy, B. andres and X. Grana. 1998. Differential regulation of the retinoblastoma family of proteins during cell proliferation and differentiation. Biochem J 333: 645-654.

Gavrieli, Y., Y. Sherman and S.A. Ben-Sasson. 1992. Identification of programmed cell death in situ via specific labeling of nuclear DNA fragmentation. J Cell Biol 119: 493-501.

Geng, Y., E.N. Eaton, M. Picon, J.M. Roberts, A.S. Lundberg, A. Gifford, C. Sardet and R.A. Weinberg. 1996. Regulation of cyclin E transcription by E2Fs and retinoblastoma protein. Oncogene 12: 1173-1180.

Gerlai, R. 1996. Gene-targeting studies of mammalian behavior: is it the mutation or the background genotype? Trends Neurosci 19: 177-181.

Gilbert, S.F. 1994. Developmental Biology, Fourth Edition. Sinauer Associates, Inc. Sunderland, Massachusetts.

Ginsberg, D., G. Vairo, T. Chittendent, Z.-X. Xiao, G. Xu, K.L. Wydner, J.A. DeCaprio, J.B. Lawrence and D.M. Livingston. 1994. E2F-4, a new member of the E2F transcription factor family, interacts with p107. Genes Dev 8: 2665-2679.

Giordano, A., C. Mccall, P. Whyte and B.R. Franza. 1991. Human cyclin A and the retinoblastoma protein interact with similar but distinguishable sequences in the adenovirus E1A gene product. Oncogene 6: 481-485.

Girard, F., U. Strausfeld, A. Fernandez and N.J.C. Lamb. 1991. Cyclin A is required for the onset of DNA replication in mammalian fibroblasts. Cell 67: 1169-1179.

Girling, R., J.F. Partridge, L.R. Bandara, N. Burden, N.F. Totty, J.J. Hsuan and N.B. LaThangue. 1993. A new component of the transcription factor DRTF1/E2F. Nature 362: 83-87.

Goodnow, C.C. 1992. B cell tolerance. Curr Opin Immunol 4: 703-710.

Goodrich, D.W. and W.-H. Lee. 1993. Molecular characterization of the retinoblastoma susceptibility gene. Biochem Biophys Acta 1155: 43-61.

Gossler, A., T. Doetschman, R. Korn, E. Derfling and R. Kemler. 1986. Transgenesis by means of blastocyst-derived embryonic stem cell lines. Proc Natl Acad Sci USA 83: 9065-9069.

Grana, X. and E.P. Reddy. 1995. Cell cycle control in mammalian cells: role of cyclins, cyclin dependent kinases (CDKs), growth suppressor genes and cyclin-dependent kinase inhibitors (CKIs). Oncogene 11: 211-219.

Green, A.R. 1996. Deletions of chromosome 20q and the pathogenesis of myeloproliferative disorders. Brit J Haemat 95: 219-226.

Gregory, P.D. and W. Horz. 1998. Chromatin remodelling in gene regulation. Curr Opin Cell Biol 10: 339-345.

Grounds, M.D. and Z. Yablonka-Reuveni. 1993. Molecular and cell biology of skeletal muscle regeneration. Mol Cell Biol Hum Dis Ser 3: 210-256.

Gu, H., J.A. Marth, P.C. Orban, H. Mossman and K. Rahewsky. 1994a. Deletion of a polymerase b gene segment in T cells using cell type-specific gene targeting. Science 265: 103-106.

Gu, W., K. Bhatia, I.T. Magrath, C.B. Dang and R. Dalla-Favera. 1994b. Binding and suppression of the Myc transcriptional activation domain by p107. Science 264: 251-254.

Gu, W., J.W. Schneider, G. Condorelli, S. Kaushal, V. Mahdavi and B. Nadal-Ginard. 1993a. Interaction of myogenic factors and the retinoblastoma protein mediates muscle cell commitment and differentiation. Cell 72: 309-324.

Gu, Y., C.W. Tirci and D.O. Morgan. 1993b. Inhibition of cdk2 activity in vivo by an associated 20K regulatory subunit. Nature 366: 707-710.

Guan, K.-L., C.W. Jenkins, Y. Li, M.A. Nichols, X. Wu, C.L. O'keefe, A.G. Matera and Y. Xiong. 1994. Growth suppression by p18, a p16INK4/MTS1 and

p14INK4/MTS2-related cdk6 inhibitor, correlates with wild-type pRb function. Genes Dev 8: 2939-2952.

Guo, K. and K. Walsh. 1997. Inhibition of myogenesis by multiple cyclin-Cdk complexes. Coordinate regulation of myogenesis and cell cycle activity at the level of E2F. J Biol Chem 272: 791-797.

Guo, K., J. Wang, V. andres, R.C. Smith and K. Walsh. 1995. MyoD-induced expression o fp21 inhibits cyclin-dependent kinase activity upon myocyte terminal differentiation. Mol Cell Biol 15: 3823-3829.

Haetboer, G., R.M. Kerkhoven, A. Shvarts, R. Bernards and R.L. Beijersbergen. 1996. Degradation of E2F by the ubiquitin-proteosome pathway: regulation by retinoblastoma family proteins and adenovirus transforming proteins. Genes Dev 10: 2960-2970.

Hagemeier, C., A. Cook and T. Kouzarides. 1993. The retinoblastoma protein binds E2F residues required for activation in vivo and TBP binding in vitro. Nucleic Acids Res 21: 4998-5004.

Halevy, O., B.G. Novitch, D.B. Spicer, S.X. Skapek, J. Rhee, G.J. Hannon, D. Beach and A.B. Lassar. 1995. Correlation of terminal cell cycle arrest of skeletal muscle with induction of p21 by MyoD. Science 267: 1018-1024.

Hamel, P.A., R.M. Gill, R.A. Phillips and B.L. Gallie. 1992. Transcriptional repression of the E2-containing promoters EIIaE, c-mcy, and RB1 by the product of the RB1 gene. Mol Cell Biol 12: 3431-3438.

Hampsey, M. 1998. Molecular genetics of RNA pol II general transcriptional machinery. Microbiol Mol Biol Rev 62: 465-503.

Han, V.K.M. and D.J. Hill. 1992. The involvement of insulin-like growth factors in embryonic and fetal development. In The Insulin-like Growth Factors: Structure and Biological Functions, P N Scholfield, ed. (Oxford, England; Oxford University Press) pp. 178-219.

Hanks, M., W. Wurst, L. Anson-Cartwright, A.B. Auerbach and A.L. Joyner. 1995. Rescue of the En-1 mutant phenotype by replacement of En-1 with En-2. Science 269: 679-682.

Hannon, G.J. and D. Beach. 1994. p15INK4B is a potential effector of TGF-b-induced cell cycle arrest. Nature 371: 257-261.

Hannon, G.J., D. Demetrick and D. Beach. 1993. Isolation of the Rb-related p130 through its interaction with cdk2 and cyclins. Genes Dev 7: 2378-2381.

Hara, E., M. Hall and G. Peters. 1997. Cdk2-dependent phosphorylation of Id2 modulates activity of E2A-related transcription factors. EMBO J 16: 332-342.

Harbour, J.W., S.-H. Lai, J. Whang-Peng, A.F. Gazdar, J.P. Minna and F.J. Kaye. 1988. Abnormalities in structure and expression of the human retinoblastoma gene in SCLC. Science 241: 353-357.

Harlow, E. 1992. For our eyes only. Nature 359: 270.

Harlow, E. and D. Lane. 1988. Antibodies: a laboratory manual. Cold Spring Harbor Laborartory. Cold Spring Harbor, New York

Harlow, E., P. Whyte, B.R. Franza and C. Schley. 1986. Association of adenovirus early-region 1A proteins with cellular polypeptides. Mol Cell Biol 6: 1579.

Harper, J.W., G.R. Adami, N. Wei, K. Keyomarsi and S.J. Elledge. 1993. The p21 Cdk-interacting protein Cip1 is a potent inhibitor of G1 cyclin-dependent kinases. Cell 75: 805-816.

Harper, J. W., S. J. Elledge, K. Keyomarsi, B. Dynlacht, L. H. Trai, P. Zhang, S. Dobrowolski, C. Bai, L .Sonnell-Crowley, E. Swindle *et al.* 1995. Inhibition of cyclin dependent kinases by p21. Mol Cell Biol 6:387-400.

Hasty, P., A. Bradlely, J.H. Morris, D.G. Edmondson, J.M. Venuti, E.N. Olson and W.H. Klein. 1993. Muscle deficiency and neonatal death in mice with a targeted mutation in the myogenin gene. Nature 364: 501-506.

Hauschka, S.D. 1994. The Embryonic Origin of Muscle. In Myology 2nd ed. (eds A. G. Engel and C. Franzini-Armstrong) New York: McGraw-Hill. pp 3-73.

Hauser, P.J., D. Agrawal, B. Chu and W.J. Pledger. 1997. p107 and p130 associated cyclin A has altered substrate specificity. J Biol Chem 272: 22954-22959.

Helin, K. 1998. Regulation of cell proliferation by the E2F transcription factors. Curr Opin Genet Devel 8: 28-35.

Helin, K., E. Harlow and A. Fattaey. 1993. Inhibition of E2F-1 transactivation by direct binding of the retinoblastoma protein. Mol Cell Biol 13: 6501.

Helin, K., K. Holm, A. Niebuhr, H. Eiberg, N. Tommerup, S. Hougaard, H.S. Poulsen, M. Spang-Thomsen and P. Norgaard. 1997. Loss of the retinoblastoma protein-related p130 protein in small cell lung carcinoma. Proc Natl Acad Sci 94: 6933-6938.

Helin, K., J.A. Lees, M. Vidal, N. Dyson, E. Harlow and A. Fattaey. 1992. A cDNA encoding a pRb-binding protein with properties of the transcription factor E2F. Cell 70: 337-350.

Helin, K., C.-L. Wu, A.R. Fattaey, J. Lees, B.D. Dynlacht, C. Ngwu and E. Harlow. 1993. Heterodimerization of the transcription factors E2F-1 and DP-1 leads to co-operative trans-activation. Genes Dev 7: 1850-1861.

Henglein, B., X. Cchenivesse, J. Wang, D. Eick and C. Brechot. 1994. Structure and cell cycle-regulated transcription of the human cyclin A gene. Proc Natl Acad Sci 91: 5490-5494.

Herrara, R.E., V.P. Sah, B.O. Williams, T.P. Makela, R.A. Weinberg and T. Jacks. 1996. Altered cell cycle kinetics, gene expression and G1 restriction point regulation in Rb-deficient fibroblasts. Mol Cell Biol 16: 2402-2407.

Hiebert, S.W. 1993. Regions of the retinoblastoma gene product required for its interaction with the E2F transcription factor are necessary for E2 promoter repression and pRb-mediated growth suppression. Mol Cell Biol 13: 3384-3391.

Hiebert, S.W., S.P. Chellapan, J.M. Horowitz and J.R. Nevins. 1992. The interaction of Rb with E2F coincides with an inhibition of the transcriptional activity of E2F. Genes Dev 6: 177-185.

Hiebert, S.W., M. Lipp and J.R. Nevins. 1989. E1A-dependent trans-activation of the uman MYC promoter is mediated by the E2F factor. Proc Natl Acad Sci 86: 3594-3598.

Hiebert, S.W., G. Packham, D.K. Strom, R. Hafffner, M. Oren, G. Zambetti and J.L. Cleveland. 1995. E2F-1:DP-1 induces p53 and overrides survival factors to trigger apoptosis. mol cell biol 15: 6864-6874.

Hijmans, E.M., P.M. Voorhoeve, R.L. Beijersbergen, L.J.V. Veer and R. Bernards. 1995. E2F-5, a new E2F family member that interacts with p130 in vivo. mol cell biol 15: 3082.

Hinds, P.W., S. Mittnacht, V. Dulic, A. Arnold, S.L. Reed and R.A. Weinberg. 1992. Regulation of retinoblastoma functions by ectopic expression of human cyclins. Cell 70: 993.

Hirsinger, E., D. Duprez, C. Jouve, P. Malapert, J. Cooke and O. Pourquie. 1997. Noggin acts downstream of Wnt and Sonic Hedgehog to antagonize avian somite patterning. Development 124: 4605-4614.

Hoang, A.T., B. Lutterbach, B.C. Lewis, T. Yano, T.Y. Chou, J.F. Barret, M. Raffeld, S.R. Hann and C.V. Dang. 1995. A link between increased transforming activity of lymphoma-derived MYC mutant alleles, their defective reulation by p107, and altered phosphorylation of the c-Myc transactivation domain. Mol Cell Biol 15: 4031-4042.

Hofmann, F., F. Martelli, D.M. Livingston and Z. Wang. 1996. The retinoblastoma gene product protects E2F-1 from degradation by the ubiquitin-proteosome pathway. Genes Dev 10: 2949-2959.

Hogan, B., F. Costantini and E. Lacy. 1986. Manipulating the Mouse Embryo: A Laboratory Manual pp. 2-12.

Horowitz, J.M., D.W. Yandell, S.-H. Park, S. Canning, P. Whyte, K. Buchkovich, E. Harlow, R.A. Weinberg and T.P. Dryja. 1989. Point mutational inactivation of the retinoblastoma antioncogene. Science 243: 936-940.

Hosokawa, Y. and A. Arnold. 1998. Mechanism of cyclin D1 (CCND1, PRAD1) overexpression in human cancer cells: analysis of allele-specific expression. Genes Chromosomes Cancer 22: 66-71.

Howard, C.M., P.P. Claudio, G.L. Gallia, J. Gordon, G.G. Giordano, W.W. Hauck, K. Khalili and A. Giordano. 1998. Retinoblastoma-related protein pRb2/p130 and suppression of tumor growth in vivo. J Natl Cancer Inst 90: 1451-1460.

Hu, N., M.L. Gulley, J.T. Kung and E.Y. Lee. 1997. Retinoblastoma gene deficiency has mitogenic but not tumorigenic effects on erythropoiesis. cancer res 57: 4123-4129.

Hu, N., A. Gutsmann, D.C. Herbert, A. Bradley, W.-H. Lee and E.Y.P. Lee. 1994. Heterozygous Rb-1 delta 20/+ mice are predisposed to tumors of the pituitary gland with a nearly complete penetrance. Oncogene 9: 1021-1027.

Hu, Q., N. Dyson and E. Harlow. 1990. The regions of the retinoblastoma protein needed for binding to adenovirus E1A or SV40 large T antigen are common sites for mutations. EMBO J 9: 1147-1155.

Hu, Q., J.A. Lees, K.J. Buchkovich and E. Harlow. 1992. The retinoblastoma protein physically associates with the human cdc2 kinase. Mol Cell Biol 12: 971-980.

Huang, S., N. Wang, B.Y. Tseng, W.-H. Lee and E.Y.-H.P. Lee. 1990. Two distinct and frequently mutated regions of retinoblastoma protein are required for binding to SV40 T antigen. EMBO J 9: 1815-1822.

Huber, H.E., G. Edwards, G.J. Goodhart, D.R. Patrick, P.S. Juang, M. Ivey-Hoyle, S.F. Barnett, A. Oliff and D.C. Heimbrook. 1993. Transcription factor E2F binds DNA as a heterodimer. Proc Natl Acad Sci 90: 3525-2529.

Huet, X., J. Rech, A. Plet, A. Vie and J.M. Blanchard. 1996. Cyclin A expression is under negative transcriptional control during the cell cycle. Mol Cell Biol 16: 3789-3798.

Hurford, J.R.K., D. Cobrinik, M.-H. Lee and N. Dyson. 1997. pRb and p107/p130 are required for the regulated expression of different sets of E2F responsive genes. genes Dev 11: 1447-1463.

Hutchins, J.B. and S.W. Barger. 1998. Why neurons die: cell death in the nervous system. Anat Rec 253: 79-90.

Ivey-Hoyle, M., R. Conroy, H. Huber, P.J. Goodhart, A. Oliff and D.C. Heimbrook. 1993. Cloning and characterization of E2F-2, a novel protein with the biochemical properties of transcription factor E2F. Mol Cell Biol 13: 7802.

Jacks, T., A. Fazeli, E.M. Schmitt, R.T. Bronson, M.A. Goodell and R.A. Weinberg. 1992. Effects of an Rb mutation in the mouse. Nature 359: 295-300.

Jiang, Z., E. Zackenhaus, B.L. Gallie and R.A. Phillips. 1997. The retinoblastoma gene family is differentially expressed during embryogenesis. Oncogene 14: 1789-1797.

Johnson, D.G. 1995. Regulation of E2F-1 gene expression by p130 (Rb2) and D-type cyclin kinase activity. Oncogene 11: 1685-1692.

Johnson, D.G., K. Ohanti and J.R. Nevins. 1994. Autoregulatory control of E2F1 expression in response to positive and negative regulators of cell cycle progression. Genes Dev 8: 1514-1525.

Johnson, D.G., J.K. Schwartz, W.D. Cress and J.R. Nevins. 1993. Expression of transcription factor E2F1 induces quiescent cells to enter S phase. nature 365: 349-352.

Jones-Villeneuve, E.M., M.W. Mcburney, K.A. Rogers and V.I. Kalnins. 1982. Retinoic acid induces embryonal carcinoma cells to differentiate into neurons and glial cells. J Cell Biol 94: 253-262.

Kaelin Jr., W.G., M.E. Ewen and D.M. Livingston. 1990. Definition of the minimal simian virus 40 large T antigen- and adenovirus E1A-binding domain in the retinoblastoma gene product. Mol Cell Biol 10: 3761.

Kaelin, W. G. Jr., W. Krek, W. R. Sellers, J. A. Decaprio, F. Ajchenbaum, C. S. Fuchs, T. Chittenden, Y. Li, P. J. Farnham, M. A. Blanar, *et al.* Expression cloning of a cDNA encoding a retinoblastoma-binding protein with E2F-like properties. Cell 70:351-364.

Kaufman, M.H. 1992. The atlas of mouse development. (Academic Press) London U.K.

Kiess, M., R.M. Gill and P.A. Hamel. 1995. Expression and activity of the retinoblastoma protein (pRb)-family proteins, p107 and p130, during L6 myoblast differentiation. Cell Growth Diff 6: 1287-1298.

Kiess, M., R.M. Gill and P.A. Hamel. 1995. Expression of the positive regulator of cell cycle progression, cyclin D3, is induced during differentiation of myoblasts into quiescent myotubes. Oncogene 10: 159-166.

Kim, K.K., M.H. Soonpaa, A.I. Daud, G.Y. Koh, J.S. Kim and L.J. Field. 1994. Tumor suppressor gene expression during normal and pathologic myocardial growth. J Biol Chem 269: 22607-22613.

Kim, K.K., M.H. Soonpaa, H. Wang and L.J. Field. 1995. Developmental expression of p107 mRNA and evidence for alternative splicing of the p107 (RBL1) gene product. Genomics 28: 520-529.

Kiyokawa, H., R. D. Kineman, K. O. Manova-Todorova, V. C. Soares, E. S. Hoffman, M. Ono, D. Khanam, A. C. Hayday, L. A. Frohman and A. Kiff. Enhanced growth of mice lacking the cyclin-dependent kinase inhibitor function of p27(Kip1). Cell 85:721-732.

Kobayashi, M., Y. Yamauchi and A. Tanaka. 1998. Stable expression of antisense Rb-1 RNA inhibits terminal differentiation of mouse myoblast C2 cells. Exp Cell Res 239: 40-49.

Kovesdi, I., R. Reichel and J.R. Nevins. 1986a. E1A transcription induction: enhanced binding of a factor to upstream promoter sequences. Science 231: 719-722.

Kovesdi, I., R. Reichel and J.R. Nevins. 1986b. Identification of a cellular transcriprion factor involved in E1A trans-activation. Cell 45: 219-225.

Kozak, M. 1986. Point mutations define a sequence flanking the AUG initiator codon that modulates translation by eukaryotic ribosomes. Cell 44: 283-292.

Krek, W., D. Livingston and S. Shirodkar. 1993. Binding to DNA and the retinoblastoma gene product promoted by complex formation of different E2F family members. Science 262: 15577-1569.

Lacy, S. and P. Whyte. 1997. Identification of a p130 domain mediating interactions with cyclinA/cdk2 and cyclin E/cdk2 complexes. Oncogene 14: 2395-2406.

Laird, P.W., A. Zijderveld, A. Linders, M.A. Rudnicki, R. Jaenisch and A. Berns. 1991. Simplified mammalian DNA isolation procedure. Nuc Acids Res 19: 4293.

Lassar, A.B., S.X. Skapek and B. Novitch. 1994. Regulatory mechanisms that coordinate skeletal muscle differentiation and cell cycle withdrawal. Curr Opin Cell Biol 6: 788-794.

Lavender, P., L. Vandel, A.J. Bannister and T. Kouzarides. 1997. The HMG-box transcription factor HBP1 is targeted by the pocket proteins and E1A. Oncogene 14: 2721-2728.

Lazaro, J.B., M. Kitzmann, M.A. Poul, M. Vandromme, N.J. Lamb and A. Fernandez. 1997. Cyclin dependent kinase 5, cdk5, is a positive regulator of myogenesis in mouse C2 cells. J Cell Sci 110: 1251-1260.

Lee, E.Y.-H.P., N. Hu, S.-S.F. Yuan, L. Cox, A. Bradley, W.-H. Lee and K. Herrup. 1994. Dual roles of the retinoblastoma protein in cell cycle regulation and differentiatoin. Genes Dev 8: 2008-2021.

Lee, M.H., B.O. Williams, G. Mulligan, S. Mukai, R.T. Bronson, N. Dyson, E. Harlow and T. Jacks. 1996. Targeted disruption of p107: functional overlap between p107 and Rb. Genes Dev 10: 1621-1632.

Lee, W.-H., R. Bookstein, F. Hong, L.-J. Young, J.-Y. Shew and E.Y.-H.P. Lee. 1987. Human retinoblastoma susceptibility gene: cloning, identification, and sequence. Science 235: 1394-1399.

Lee, W.Y.-H.P., C.Y. Chang, N. Hu, Y.-C.J. Yang, C.-C. Lai, K. Herrup, W.-H. Lee and A. Bradley. 1992. Mice deficient for Rb are nonviable and show defects in neurogenesis and haematopoiesis. Nature 359: 288-294.

Lees, E., B.F. Faha, V. Dulic, S.I. Reed and E. Harlow. 1992. CyclinE/cdk2 and cyclinA/cdk2 kinases associate with p107 and E2F in a temporally distinct manner. Genes Dev 6: 1874-1885.

Lees, J.A., M. Aito, M. Vidal, M. Valentine, T. Look, E. Harlow, N. Dyson and K. Helin. 1993. The retinoblastoma protein binds to a family of E2F transcription factors. Mol Cell Biol 13: 7813.

Lees, J.A., K.J. Buchkovich, D.R. Marshak, C.W. anderson and E. Harlow. 1991. The retinoblatoma protein is phosphorylated on multiple sites by human cdc2. EMBO J 10: 4279.

Leone, G., J. Degregori, R. Sears, L. Jakoi and J.R. Nevins. 1997. Myc and Ras collaborate in inducing accumulation of active cyclinE/Cdk2 and E2F. nature 387: 422-426.

Li, E., T.H. Bestor and R. Jaenisch. 1992. Targeted mutation of the DNA methyltransferase gene results in embryonic lethality. cell 69: 915-926.

Li, Y., C. Graham, S. Lacy, A.M.V. Duncan and P. Whyte. 1993. The adenovirus E1a-associated 130-kDa protein is encoded by a member of the retinoblastoma gene family and physically interacts with cyclins A and E. Genes Dev 7: 2366-2377.

Lifsted, T., T. Levoyer, M. Williams, W. Muller, A. Klein-Szanto, K.H. Buetow and K.W. Hunter. 1998. Identification of inbred mouse strains harboring genetic modifiers of mammary tumor age of onset and metastatic progression. Int J Cancer 77: 640-644.

Lin, B.T.-Y., S. Gruenwals, A.O. Morla, W.-H. Lee and J.Y.J. Wang. 1991. Retinoblastoma cancer suppressor gene product is a substrate of the cell cycle regulator cdc2 kinase. EMBO J 10: 857-864.

Lindeman, G.J., S. Gaubatz, D.M. Livingston and D. Ginsberg. 1997. The subcellular localization of E2F-4 is cell-cycle dependent. Proc Natl Acad Sci 94: 5095-5100.

Litvin, J., M. Montgomery, A. Gonzalez-Sanchez, J.G. Bisaha and D. Bader. 1992. Commitment and differentiation of cardiac myocytes. Trends Cardiovasc Med 2: 27-32.

liu, j., j. baker, a.s. perkins, e.j. robertson and a. efstradiatis. 1993. Mice carrying null mutations of the genes encoding insulin-like growth factor (Igf-1) and type 1 IGF receptor (Igf1r). Cell 75: 59-72.

Liu, Y. and R.N. Kitsis. 1996. Induction of DNA synthesis and apoptosis in cardiac myocytes by E1A oncoprotein. J Cell Biol 133: 325-333.

Lloyd, A.C. 1998. Ras versus cyclin-dependent kinase inhibitors. Curr Opin Genet Dev 8: 43-48.

Ludlow, J.W., J. Decaprio, C.M. Huang, W. Lee, E. Paucha and D.M. Livingston. 1989. SV40 large T antigen binds preferentially to an underphosphorylated member of the retinoblastoma susceptibility gene product family. cell 56: 57.

Luo, X.L., A.A. Postigo and D.C. Dean. 1998. Rb interacts with histone deacetylase to repress transcription. Cell 92: 463-473.

Maandag, E.C., M.V.D. Valk, M. Vlaar, C. Feltkamp, J. O'brien, M.V. Roon, N.V.D. Lugt, A. Berns and H. teRiele. 1994. Developmental rescue of an embryonic-lethal mutation in the retinoblastoma gene in chimeric mice. EMBO J 13: 4260-4268.

MacLeod, K.F., Y. Hu and T. Jacks. 1996. Loss of Rb activates both p53-dependent and independent cell death pathways in the developing mouse nervous system. EMBO J 15: 6178-6188.

Magaghi-Jaulin, L., R. Groisman, I. Naguibneva, P. Robin, S. Lorain, J.P.L. Villain, F. Troalin, D. Trouche and A. Harel-Bellan. 1998. Retinoblastoma protein represses transcription by recruiting a histone deacetylase. Nature 391: 601-605.

Mainone, R. and P. Amati. 1997. Interdependence between muscle differentiation and cell-cycle control. Biochem Biophys Acta 1332: M19-M30.

Maione, R., G.M. Fimia, P. Holman, B. Schaffhausen and P. Amati. 1994. Retinoblastoma antioncogene is involved in the inhibition of myogenesis by polyomavirus large T antigen. Cell Growth Differ 5: 231-237.

Mansfield, D.C., A.F. Brown, D.K. Green, A.D. Carothers, S.W. Morris, H.J. Evans and A.F. Wright. 1994. Automation of genetic linkage analysis using fluorescent microsatellite markers. Genomics 15:225-233.

Mansour, S.L.R. and M.R. Capecchi. 1988. Disruption of the proto-oncogene *int-2* in mouse embryonic-derived stem cells: a general strategy for targeting mutations to non-selectable genes. Nature 336: 348-352.

Marcelle, C., M.R. Stark and M. Bronner-Fraser. 1997. Coordinate action of BMPs, Wnts, Shh, and Noggin mediate patterning of the dorsal somite. Dev 124: 3955-3863.

Markel, P., P. Shu, C. Ebeling, G.A. Carson, D.L. Nagle, J.S. Smutko and K.J. Moore. 1997. Theoretical and empirical issues for marker-assisted breeding of congenic mouse strains. 17 280-284:

Marti, E., D.A. Bumcrot, R. Takada and A.P. Mcmahon. 1995. Requirement of 19K form of Sonic hedgehog peptide for induction of distinct ventral cell types in CNS explants. Nature 375: 322-325.

Martin, G.R. 1981. Isolation of a pluripotent cell line from early mouse embryos cultured in medium conditioned by teratocarcinoma stem cells. Proc Natl Acad Sci 78: 7634-7638.

Massague, J., S. Cheifetz, T. Endo and B. Nadal-Ginard. 1986. Type beta transforming growth factor is an inhibitor of myogenic differentiation. Proc Natl Acad Sci 83: 8206-8210.

Matsushime, H., M.E. Ewen, D.K. Strom, J.Y.D.K. Hands, M.F. Roussel and C.J. Sherr. 1992. Identification and properties of an atypical catalytic subunit (p34PSK-J3/cdk4) for mammalian D type G1 cyclins. Cell 71: 323.

Mayol, X., J. Garriga and X. Grana. 1995. Cell cycle-dependent phosphorylation of the retinoblastoma -related protein p130. Oncogene 11: 801-808.

Mayol, X. and X. Grana. 1998. The p130 pocket protein: keeping order at cell cycle exit/re-entrance transitions. Front Biosci 3: D11-24.

Mayol, X., X. Grana, A. Baldi, N. Sang, Q. Hu and A. Giordano. 1993. Cloning of a new member of the retinoblastoma gene family (pRb2) that binds to the E1A transforming domain. Oncogene 8: 2561-2566.

McArdle, A., R.H. Edwards and M.J. Jackson. 1994. Release of creatine kinase and prostaglandin E2 from regenerating skeletal muscle fibers. J Appl Physiol 76: 1274-1278.

McMahon, J.A., S. Takada, L.B. Zimmerman, C.-M. Fan, R.M. Harland and A.P. McMahon. 1998. Noggin-mediated antagonism of BMP signaling is required for growth and patterning of the neural tube and somite. Genes Dev 12: 1438-1452.

Megeney, L.A., B. Kablar, K. Garrett, J.E. anderson and M.A. Rudnicki. 1996. MyoD is required for myogenic stem cell function in adult skeletal muscle. Genes Dev 10: 1173-1183.

Mendoza, A.E., J.-Y. Shew, E.Y.-H.P. Lee, R. Bookstein and W.-H. Lee. 1988. A case of synovial sarcoma with abnormal expression of the human retinoblastoma susceptibility gene. Hum Pathol 487-489:

Mezzogiorno, A., M. Coletta, B.M. Zani, G. Cossu and M. Molinaro. 1993. Paracrine stimulation of senescent satellite cell proliferation by factors released by muscle or myotubes from young mice. Mech Ageing Dev 70: 35-44.

Mihara, K., X. Cao, A. Uen, S. Chandler, B. Driscoll, A.L. Murphree, A. Tang and Y.K. Fung. 1989. Cell cycle-dependent regulation of phosphorylation of the human retinoblastoma gene product. Science 246: 1300.

Miller, J.B. 1990. Myogenic programs of mouse muscle cell lines: expression of myosin heavy chain isoforms, MyoD1 and myogenin. J Cell Biol 111: 1149-1159.

Miller, M.J. and B.Z. Yuan. 1997. Semiautomated resolution of overlapping stutter patterns in genomic microsatellite analysis. Anal Biochem 15:50-56.
Moberg, K., M.A. Starz and J.A. Lees. 1996. E2F-4 switches from p130 to p107 and pRb in response to cell cycle entry. Mol cell biol 16: 1436.

Morgan, D.O. 1997. Cyclin-dependent kinases: engines, clocks and microprocessors. Annu Rev Cell Dev Biol 13: 261-292.

Morgenbesser, S.D., B.O. Williams, T. Jacks and R.A. Depinho. 1994. p53-dependent apoptosis produced by Rb-deficiency in the developing mouse lens. Nature 371: 72-74.

Morkel, M., J. Wenkle, A.J. Bannister, T. Kouzarides and C. Hagemeier. 1997. An E2F-like repressor of transcription. Nature 390: 567-568.

Mudryj, M., S.W. Hiebert and J.R. Nevins. 1990. A role for the adenovirus inducible E2F transcription factor in a proliferation dependent signal transduction pathway. EMBO J 9: 2179.

Muller, R. 1995. Transcriptional regulation during the mammalian cell cycle. Trends Genet 11: 173-178.

Mulligan, G.J., J. Wong and T. Jacks. 1998. p130 is dispensable in peripheral T lymphocytes: evidence for functional compensation by p107 and pRb. Mol Cell Biol 18: 206-220.

Munsterberg, A.E., J. Kitajewski, D.A. Bumcrot, A.P. McMahon and A.B. Lassar. 1995. Combinatorial signaling by Sonic hedgehog and Wnt family members induces myogenic bHLH gene expression in the somite. Genes Dev 9: 2911-2922.

Murre, C., P.S. Mccaw, H. Vaessin, *Et Al.* 1989. Interactions between heterologous helix-loop-helix proteins generate complexes that bind specifically to a common DNA sequence. Cell 58: 537-544.

Nabashima, Y., K. Hanaoka, M. Hayasaka, E. Esumi, S. Li, I. Nonaka and Y. Nabeshima. 1993. Myogenin gene disruption results in perinatal lethality because of severe muscle defects. Nature 364: 532-535.

Nakamura, T., R. Sanokawa, Y.G. Saski, D. Ayusawa, M. Oishi and N. Mori. 1995. Cyclin I: a new cyclin encoded by a gene isolated from human brain. Exp Cell Res 221: 534-542.

Nakayama, K., N. Ishida, M. Shirane, A. Inomata, T. Inoue, N. Shishido, I. Horii, K.Y. Loh and K. Nakayama. 1996. Mice lacking p21(Kip1) display increased body size, multiple organ hyperplasia, retinal dysplasia, and pituitary tumors. Cell 85: 707-720.

Neuman, E., E.K. Flemington, W.R. Sellers and W.G. Kaelin Jr. 1994. Transcription of the E2F-1 gene is rendered cell cycle dependent by E2F DNA-binding sites within its promoter. mol cell biol 4: 6607-6615.

Nevins, J.R. 1992. E2F: A link between the Rb tumor suppressor protein and viral oncoproteins. Science 258: 424-429.

Nevins, J.R., G. Leone, J. Degregori and L. Jakoi. 1997. Role of the Rb/E2F pathway in cell growth control. J cell Physiol 173: 233-236.

Nigg, E.A. 1995. Cyclin-dependent protein kinases: key regulators of the eukaryotic cell cycle. Bioessays 17: 471-480.

Norton, J.D., R.W. Deed, G. Craggs and F. Sablitzky. 1998. Id helix-loop-helix proteins in cell growth and differentiation. Trends Cell Biol 8: 58-65.

Novitch, B.G., G.J. Mulligan, T. Jacks and A.B. Lassar. 1996. Skeletal muscle cells lacking the retinoblastoma protein display defects in muscle gene expression and accumulate in S and G2 phases of the cell cycle. J Cell Biol 135: 441-456.

Ohanti, K., J. Degregori and J.R. Nevins. 1995. Regulation of the cyclin E gene by transcription factor E2F. Proc Nat Acad Sci 92: 12146-12150.

Ohtsubo, M., A.M. Theodoras, J. Schumacher, J.M. Roberts and M. Pagano. 1995. Human cyclin E, a nuclear protein essential for the G1-to -S transition. Mol Cell Biol 15: 2612-2624.

Olson, E.N. 1992. Interplay between proliferation and differentiation within the myogenic lineage. Dev Biol 154: 261-272.

Olson, E.N., E. Sternberg, J.S. Hu, G. Spizz and C. Wilcox. 1986. Regulation of myogenic differentiation by type beta transforming growth factor. J Cell Biol 105: 1799-1805.

Oswald, F., H. Lovec, T. Moroy and M. Lipp. 1994. E2F-dependent regulation of hyman MYC; trans-activation by cyclins D1 and A overrides tumour suppressor protein functions. Oncogene 9:2029-2036.

Pagano, M., R. Peppercock, C. Verde, W. Ansorge and G. Draetta. 1992. Cyclin A is required at two points in the human cell cycle. EMBO J 11: 961-971.

Pan, H. and A.E. Griep. 1994. Altered cell cycle regulation in the lens of HPV-16 E6 or E7 transgenic mice: implications for tumor suppressor gene function in development. Genes dev 8: 1285-1299.

Pardee, A.B. 1974. A restriction point for control of normal animal cell proliferation. Proc Natl Acad Sci 71: 1286-1290.

Pardee, A.B. 1989. G1 events and regulation of cell proliferation. Science246 603-608:

Parker, S.B., G. Eichele, P. Zhang, A. Rawls, A.T. Sands, A. Bradley, E.N. Olson, J.W. Harper and S.J. Elledge. 1995. p53-independent expression of $p21^{Cip1}$ in muscle and other terminally differentiating cells. Science 267: 1024-1027.

Pearson, B.E., H.P. Nasheuer and T.S.F. Wang. 1991. Human DNA polymerase alpha gene: sequences controlling expression of cycling and serum-stimulated cells. Mol Cell Biol 11: 2081-2095.

Peeper, D.S., P. Keblusek, K. Helin, M. Toebes, A.J.V.D. Eb and A. Zantema. 1995. Phosphorylation of a specific cdk site in E2F-1 affects its eletrophoretic ability and promotes pRb-binding in vitro. Oncogene 10: 39-48.

Peeper, D.S., T.M. Upton, M.H. Ladha, E. Neuman, J. Zalvide, R. Bernards, J.A. Decaprio and M.E. Ewen. 1997. Ras signaling linked to the cell-cycle machinery by the retinoblastoma protein. Nature 386: 177-181.

Pertile, P., A. Baldi, A.D. Luca, L. Bagella, L. Virgilio, M.M. Pisano and A. Giordano. 1995. Molecular cloning, expression and developmental characterization of the murine retinoblastoma-related gene Rb2/p130. Cell Growth Dev 6: 1695-1664.

Phillips, A.C., S. Bates, K.M. Ryan, K. Helin and K.H. Vousden. 1997. Induction of DNA synthesis and apoptosis are separable functions of E2F-1. Genes dev 11: 1853-1863.

Pines, J. 1995. Cyclins and cyclin-dependenet kinases: themes and variations. Advan Can Res 66: 181-212.

Pines, J. and T. Hunter. 1989. Isolation of a human cyclin cDNA: evidence for cyclin mRNA and protein regulation in the cell cycle and for interaction with p34cdc2. Cell 58: 833-846.

Pines, J. and T. Hunter. 1991. Human cyclin A and B1 are differentially located in the cell and undergo cell cycle-dependent nuclear transport. J Cell Biol 115: 1-17.

Placzek, M. 1995. The role of the notochord and floor plate in inductive interactions. Curr Opin Gene Dev 5: 499-506.

Placzek, M. and A. Furley. 1996. Neural development: Patterning cascades in the neural tube. Curr Biol 6: 526-529.

Placzek, M., T.M. Jessel and J. Dodd. 1993. Induction of floor plate differentiation by contact-dependent, homeogenetic signals. Development 117: 205-218.

Polyak, K., M.-H. Lee, H. Erdjument-Bromage, A. Koff, J.M. Roberts, P. Tempst and J. Massague. 1994. p27kip1, a cyclin -dependent kinase inhibitor and a potential mediator of extracellular antimitogenic signals. Cell 78: 59-66.

Puri, P.L., C. Balsano, V.L. Burgio, P. Chirillo, G. Natoli, L. Ricci, E. Mattei, A. Graessmann and M. Levrero. 1997. MyoD prevents cyclinA/cdk2 containing E2F complexes formation in terminally differentiated myocytes. Oncogene 14: 1171-1184.

Qin, X.-Q., T. Chittenden, D.M. Livingston and W.G.J. Kaelin. 1992. Identification of a growth suppression domain within the retinoblastoma gene product. Genes Dev 9: 953-964.

Qin, X.Q., D.M. Livingston, W.G.J. Kaelin and P.D. Adams. 1994. Deregulated transcription factor E2F-1 expression leads to S-phase entry and p53-mediated apoptosis. Proc Natl Acad Sci USA 91: 10918-10922.

Quell, D.E., R.A. Ashmun, S.A. Shurtleff, J.-Y. Kato, D. Bar-Sagi, M.F. Roussel and C.J. Sherr. 1993. Overexpression of mouse D-type cyclin accelerates G1 phase in rodent fibroblasts. Genes Dev 7: 1559-1571.

Rabbitts, P.H., J.V. Watson, A. Lamond, A. Forster, M.A. Stinson, G. Evan, E. Atherton, R. Sheppard and T.H. Rabbitts. 1985. Metabolism of c-myc gene products: c-myc mRNA and protein expression in the cell cycle. EMBO J 4: 2009.

Rando, T.A. and H.M. Blau. 1994. Primary mouse myoblast purification, characterization, and transplantation for cell-mediated gene therapy. J cell biol 125: 1275-1287.

Rao, S.S., C. Chu and D.S. Kohtz. 1994. Ectopic expression of cyclin D1 prevents activation of gene transcription by myogenic basic helix-loop-helix regulators. Mol Cell Biol 14: 5259-5267.

Raschella, G., B. Tanno, F. Bonetto, T. Battista, A.D. Luca and A. Giordano. 1997. Retinoblastoma-related protein pRb2/p130 and its binding to the B-myb promoter increase during neuroblastoma differentiation. J Cell Biochem 67: 297-303.

Raychaudhuri, P., S. Bagshi, S.H. Devoto, V.B. Kraus, E. Moran and J.R. Nevins. 1991. Domains of the adenovirus E1A protein required for oncogenic activity are also required for dissociation of E2F transcription factor complexes. Genes Dev 5: 1200-1211.

Reshef, R., M. Maroto and A.B. Lassar. 1998. Regulation of dorsal somitic cell fates: BMPs and Noggin control the timing and patterning of myogenesis. Genes Dev 12: 290-303.

Resnitzky, D., L. Hengst and S.I. Reed. 1995. Cyclin A- associated kinse activity is rate limiting for entrance into S phase and is negatively regulated in G1 by p27kip1. Mol Cell Biol 15: 4347.

Resnitzky, D. and S. Reed. 1995. Different roles for cyclins D1 and E in regulation of the G1-to-S transition. Mol Cell Biol 15: 3463.

Rhodes, M., A. Dearlove, R. Straw, S. Fernando, A., Evans, M. Greener, T. Lacey, M. Kelly, K. Gibson, S.D. Brown and C. Mundy. 1997. High-thoughput microsatellite analysis using flourescent dUTPs for high-resolution genetic mapping of the mouse genome. Genome Res 7:81-86.

Richon, V.M., R.A. Rifkind and P.A. Marks. 1992. Expression and phosphorylation of the retinoblastoma protein during induced differentiation of murine erythroleukemia cells. Cell Growth Diff 3: 413-420.

Riley, D.J., C.Y. Liu and W.-H. Lee. 1997. Mutations of N-terminal regions render the retinoblastoma protein insufficient for functions in development and tumour suppression. Mol Cell Biol 17: 7342-7352.

Robanus-Maandag, E., M. Dekkler, M.v.d. Valk, M.-L. Carrozza, J.-C. Jeanny, J.-H. Dannenberg, A. Berns and H. teRiele. 1998. p107 is a suppressor of retinoblastoma development in pRb-deficient mice. Genes Dev 12: 1599-1609.

Robertson, E.J. 1987. Embryo-derived stem cells. In Teratomas and embryonic stem cells: a practical approach (ed. E.J. Robertson), chap. 4. IRL Press, Oxford.

Rodewald, H.R. and H.J. Fehling. 1998. Molecular and cellular events in early thymocyte development. Adv Immunol 69: 1-112.

Roelink, H., A. Augsburger, J. Heemskerk, V. Korzh, S. Norlin, A. Ruiz i Altaba, Y. Tanabe, M. Placzek, T. Edlund, T. M. Jessell, *et al.* 1994. Floor plate and motor neuron induction by vhh-1, a vertebrate homolog of hedgehog expressed by the notochord. Cell 76:761-775.

Roelink, H., J.A. Proter, C. Chiang, Y. Tanaabe, D.T. Chang, P.A. Beachy and T.M. Jessell. 1995. Floor plate and motor neuron induction by different concentrations of the amino-terminal cleavage product of sonic hedgehog autoproteolysis. Cell 81: 445-455.

Rohrer, D.K., K.H. Desai, J.R. Jasper, M.E. Stevens, D.P.J. Regula, G.S. Barsh, D. Berenstein and B.K. Kobilka. 1996. Targeted disruption of the mouse b1-adrenergic receptor gene:developmental and cardiovascular effects. Proc Nat Acad Sci 93: 7375-7380.

Rong, P.M., M.-A. Teillet, C. Ziller and N.M. LeDouarin. 1992. The neural tube/notochord complex is necessary for vertebral but not limb and body wall striated muscle differentiation. Development 657-672:

Rossant, J. 1996. Mouse mutants and cardiac development: New molecular insights into cardiogenesis. Circulation Res 78: 349-353.

Rozmahel, R. 1996. Modulation of disease severity in cyctic gibrosis transmembrane conductance regulator deficient mice by a secondary genetic factor. Nature Genet 12: 280-287.

Ruas, M. and G. Peters. 1998. The p16INK4a/CDKN2A tumor suppressor and its relative. Biochem Biophys Acta 1378: F115-177.

Rudnicki, M.A., T. Braun, S. Hinuma and R. Jaenisch. 1992. inactivation of MyoD in mice leads to up-regulation of the myogenic HLH gene myf-5 and results in apparently normal muscle development. Cell 71: 383-390.

Rudnicki, M.A. and R. Jaenisch. 1995. The MyoD family of transcription factors and skeletal myogenesis. Bioessays 17: 203-209.

Rudnicki, M.A. and M.W. McBurney. 1987a. Teratocarcinomas and Embryonic Stem Cells (E Robertson ed). IRL Press: Oxford, UK pp.32-36.

Rudnicki, M.A., P.N.J. Schnegelsberg, R.H. Stead, T. Braun, H.-H. Arnold and R. Jaenisch. 1993. MyoD or myf-5 is required for the formation of skeletal muscle. Cell 75: 1-20.

Sala, A., A.D. Luca, A. Giordano and C. Peschle. 1996. The retinoblastoma family member p107 binds to B-Myb and suppresses its autoregulatory activity. j Biol Chem 271: 28738-28740.

Sambrook, J., E.F. Fritsch and T. Maniatus. 1989. Molecular cloning: A laboratory manual , 2 ed. (Cold Spring Harbor Laboratory Press) Cold Spring Harbor, N.Y.

Sardet, C., M. Vidal, D. Cobrinik, Y. Geng, C. Onufryk, A. Chen and R.A. Weinberg. 1995. E2F-4 and E2F-5, two members of the E2F family, are expressed in the early phases of the cell cycle. Proc Natl Acad Sci 92: 2403.

Savatier, P., S. Hong, L. Szekely, K.G. Wiman and J. Samarut. 1994. Contrasting patterns of retinoblastoma protein expression in mouse embryonic stem cells and embryonic fibroblasts. Oncogene 9: 809-818.

Schneider, J.W., W. Gu, L. Zhu, V. Mahdavi and B. Nadal-Ginard. 1994. Reversal of terminal differentiation mediated by p107 in $Rb^{-/-}$ muscle cells. Science 264: 1467-1471.

Schulze, A., K. Zerfass, D. Spitkovsky, S. Middendorp, J. Berges, K. Helin, P. Jansen-Durr and B. Henglein. 1995. Cell cycle regulation of the cyclin A gene promoter is mediated by a variant E2F site. Proc Nat Acad Sci 92: 11264-11268.

Schwarz, J.K., S.H. Devoto, E.J. Smith, S.P. Chellappan, L. Jakoi and J.R. Nevins. 1993. Interactions of the p107 and Rb proteins with E2F during the cell proliferation response. EMBO J 12: 1013.

Serrano, M., G.J. Hannon and D. Beach. 1993. A new regulatory motif in cell cycle control causing specific inhibition of cyclin D/cdk4. Nature 366: 704-707.

Sewing, A., C. Burger, S. Brusselbach, C. Schalk, F.C. Luciibello and R. Muller. 1993. Human cyclin D1 encodes a labile nuclear protein whose synthesis is directly induced by growth factors and suppressed by cyclic AMP. J Cell Sci 104: 545-555.

Shan, B. and W.-H. Lee. 1994. Deregulated expression of E2F-1 induces S-phase entry and leads to apoptosis. Mol Cell Biol 14: 8166-8173.

Shan, B., X. Zhu, P.L. Chen, T. Durfee, Y. Yang, D. Sharp and W.-H. Lee. 1992. Molecular cloning of cellular genes encoding retinoblastoma-associated proteins: identification of a gene with properties of the transcription factor E2F. Mol Cell Biol 12: 5602-5631.

Shao, Z., S. Ruppert and P.D. Robbins. 1995. The retinoblastoma-susceptibility gene product binds directly to the human TATA-binding protein-associated factor TAFII250. Proc Natl Acad Sci 92: 3115.

Sherr, C.J. 1993. Mammalian G1 cyclins. Cell 73: 1059-1065.

Sherr, C.J. 1994. G1 phase progression: cycling on cue. Cell 4: 551-555.

Sherr, C.J. 1996. Cancer cell cycle. Science 27: 1672-1677.

Sherr, C.J. and J.M. Roberts. 1995. Inhibitors of mammalian G1 cyclin-dependent kinases. Genes Dev 9: 1149.

Sherr, C.J. 1998. Tumor surveillance via the ARF-p53 pathway. Genes Dev 12: 2984-2991.

Shin, E.K., A. Shin, C. Paulding, B. Schaffhausen and A.S. Yee. 1995. Multiple changes in E2F function and regulation occur upon muscle differentiation. Mol Cell Biol 15: 2252-2262.

Shirodkar, S., M. Ewen, J.A. Decaprio, J. Morgan, D.M. Livingston and T. Chittenden. 1992. The transcription factor E2F interacts with the retinoblastoma product and a p107-cyclin A complex in a cell cycle regulated manner. cell 68: 157-166.

Sibilia, M. and E.F. Wagner. 1995. Strain-dependent epithelial defects in mice lacking the EGF receptor. Science 269: 234-238.

Sidle, A., C. Palaty, P. Dirks, O. Wiggan, M. Kiess, R.M. Gill, A.K. Wong and P.A. Hamel. 1996. Activity of the retinoblastoma family proteins, Rb, p107 and p130, during cellular proliferation and differentiation. Crit Rev Biochem Mol Biol 31: 237-271.

Simpson, E. M., C.C. Linder, E. E. Sargent, M. T. Davisson, L. E. Mobraaten and J. J. Sharp. 1997. Genetic variation among 129 substrains and its importance for targeted mutagenesis in mice. Nature Genetics 16: 19-27.

Skapek, S.X., J. Rhee, P.S. Kim, B.G. Novitch and A.B. Lassar. 1996. Cyclin-mediated inhibition of muscle gene expression via a mechanism that is independent of pRb hyperphosphorylation. Mol Cell Biol 16: 7043-7053.

Skapek, S. X., J. Rhee, D. B. Spicer and A. B. Lassar. 1995. Inhibition of myogenic differentiation in proliferating myoblasts by cyclin D1-dependent kinase. Science 267: 1022-1024.

Slack, J. M. W. 1992. From Egg to Embryo (eds. P.W. Barlow, P. Bray, P.B. Green, and J.M.W. Slack), 2nd ed. pp. 171-277. Cambridge, Cambridge University Press.

Slack, R. S., H. El-Bizri, J. Wong, D. J. Belliveu and F. D. Miller. 1998. A critical temporal requirement for the retinoblastoma protein family during neuronal determination. J Cell Biol 140: 1497-1509.

Slack, R.S., P.A. Hamel, T.S. Badon, R.M. Gill and M.W. Mcburney. 1993. Regulated expressionof hte retinoblastoma gene in differentiating embryonal carcinoma cells. Oncogene 8: 1585-1591.

Slack, R.S., I.S. Skerjanc, B. Lach, J. Craig, K. Jardine and M.W. McBurney. 1995. Cells differentiating into neuroectoderm undergo apoptosis in the absence of functional retinoblastoma family proteins. J Cell Biol 129: 779-788.

Slansky, J.E., Y. Li, W.G.J. Kaelin and P.J. Farnham. 1993. A protein synthesis-dependent increase in E2F1 mRNA correlates with growth regulation of the dihydrofolate reductase promoter. Mol Cell Biol 13: 1610-1618.

Smith, E.J., G. Leone and J.R. Nevins. 1998. Distinct mechanisms control the accumulation of the Rb-related p107 and p130 proteins during cell growth. Cell Growth Diff 9: 297-303.

Smith, E.J. and J. Nevins. 1995. the Rb-related p107 protein can suppress E2F function independently of binding to cyclinA/cdk2. mol cell biol 15: 338.

Starostik, P., K.N. Chow and D.C. Dean. 1996. Transcriptional repression and growth suppression by the p107 pocket protein. Mol Cell Biol 16: 3606-3614.

Stiegler, P., A. DeLuca, L. Bagella and A. Giordano. 1998. The COOH-terminal region of pRb2/p130 binds to histone deacetylase 1 (HDAC1), enhancing transcriptional repression of the E2F-dependent cyclin A promoter. Cancer Res 58: 5049-5052.

Strober, B.E., J.L. Dunaief and S.P. Goff. 1996. Functional interactions between the hBRM/hBRG1 transcriptional activators and the Rb family of proteins. Mol Cell Biol 16: 1576-1583.

Szekely, L., W. Jiang, F. Bulichakus, A. Rosen, N. Ringertz, G. Klein and K.G. Wiman. 1992. Cell type and differentiation dependent heterogeneity in retinoblastoma protein expression in SCID mouse fetuses. Cell Growth Diff 3: 139-156.

T'Ang, A., J.M. Varley, S. Chakroborty, A.L. Murphree and Y.K.T. Fung. 1988. Structural rearrangement of hte retinoblastoma gene in human breast carcinoma. Science 242: 263-266.

Tamira, K., Y. Kanaoka, S. Jinno, A. Nagata, Y. Ogiso, K. Shimizzu, T. Hayakawa, H. Nojima and H. Okayama. 1993. Cyclin G: a new mammalian cyclin with homology to fission yeast Cig1. Oncogene 8: 2113-2118.

Tanabe, Y., H. Roelnik and T.M. Jessel. 1995. Induction of motor neurons by Sonic hedgehog is independent of floor plate differentiation. Curr Biol 5: 651-658.

Tedesco, D., M. Caruso, L. Fischer-Fantuzi and C. Vesco. 1995. The inhibition of cultured myoblast differentiation by the simian virus 40 large T antigen occurs after myogenin expression and Rb up-regulation and is not exerted by transformation-competent cytoplasmic mutants. J Virol 69: 6947-6957.

Teillet, M.-A., Y. Watanabe, P. Jeffs, D. Duprez, F. Lapointe and N.M. Ledouarin. 1998. Sonic hedgehog is required for survival of both myogenic and chondrogenic somitic lineages. Development 125: 2019-2030.

Templeton, D., S.H. Park, L. Lanier and R.A. Weinberg. 1991. Nonfunctional mutants of the retinoblastoma protein are characterized by defects in phosphorylation, viral oncoprotein association and nuclear tethering. Proc Natl Acad Sci 88: 3033-3037.

Tevosian, S.G., H.H. Shin, K.G. Mendelson, K.A. Sheppard, K.E. Paulson and A.S. Yee. 1997. HBP1: a HMG box transcription repressor that is targeted by the retinoblastoma family. Genes Dev 11: 383-396.

Thalmeiere, K., H. Snovzik, R. Mertz, E.L. Winnacker and M. Lipp. 1989. Nuclear factor E2F mediates basic transcription and transactivation by E1A of the human MYC promoter. Genes Dev 3: 527-536.

Thayer, M.J., S.J. Tapscott, R.L. Davis, W.E. Wright, A.B. Lassar and H. Weintraub. 1989. Positive autoregulation of the myogenic determination gene MyoD1. Cell 58: 241-248.

Thomas, K.R. and M.R. Capecchi. 1987. Site-directed mutagenesis by gene targeting in embryo-derived stem cells. Cell 51: 503-512.

Threadgill, D.W., A.A. Dlugosz, L.A. Hansen, *et al.* 1995. Targeted disruption of mouse EGF receptor: effect of genetic backgroumd on mutant phenotype. Science 269: 230-234.

Tiainen, M., D. Spitkovsky, P. Jansen-Durr, A. Sacchi and M. Crescenzi. 1996. Expression of E1A in terminally differentiated muscle cells reactivates the cell cycle and suppresses tissue-specific genes by separably mechanisms. mol cell biol 16: 5302-5312.

Tijan, R. and T. Maniatus. 1994. Transcriptional activation: a complex puzzle with few easy pieces. Cell 77: 5-8.

Toguchida, J., K. Ishizaki, M.S. Sasaki, M. Ikenaga, M. Sugimoto, Y. Kotoura and T. Yamamuro. 1988. Chromosomal reorganization for the expression of recessive mutation of retinoblastoma susceptibility gene in the development of osteosarcoma. Can Res 48: 3939-3943.

Tommasi, S. and G.P. Pfeifer. 1995. In vivo structure of the human cdc2 promoter: release of a p130-E2F-4 complex from sequences immediately upstream of the transcription initiation site coincides with induction of cdc2 expression. Mol Cell Biol 15: 6901-6913.

Toyoshima, H. and T. Hunter. 194. p27, a novel inhibitor of G1 cyclin-cdk protein kinase activity, is related to p21. Cell 78: 67-74.

Trimarchi, J.M. 1998. E2F-6, a member of the E2F family that can behave as a transcriptional repressor. Proc Natl Acad Sci 95: 2850-2855.

Tsai, K.Y., Y. Hu, D. Crowley, L. Yamasaki and T. Jacks. 1998. Mutation of E2F-1 suppresses apoptosis and inappropriate S phase entry and extends survival of Rb-deficient mouse embryos. Mol Cell 2: 293-304.

Tsuchida, T., M. Ensini, B. Morton, M. Baldassare, T. Edlund, T.M. Jessel and S.L. Pfaff. 1994. Topographic organization of embryonic motor neurons defined by expression of LIM homeobox genes. cell 79: 957-970.

Vairo, G., D.M. Livingston and D. Ginsberg. 1995. Functional interaction between E2F-4 and p130: evidence for distinct mechanisms underlying growth suppression by different retinoblastoma protein family members. Genes Dev 9: 869-881.

Vandeneijnde, S.M., A.J. Luijsterburg, L. Boshart, C.I. Dezeeuw, J.H. Vandierendonck, C.P. Reutelingsperger and C. Vermeij-Keers. 1997. in situ detection of apoptosis during embryogenesis with Annexin V: from whole mount to ultrastructure. Cytometry 29: 313-320.

Verona, R., K. Moberg, S. Estes, M. Starz, J.P. Vernon and J.A. Lees. 1997. E2F activity is regulated by cell cycle-dependent changes in subcellular localization. Mol Cell Biol 17: 7268-7282.

Voit, R., K. Schafer and I. Grummt. 1997. Mechanism of repression of RNA polymerase I transcription by the retinoblastoma protein. Mol Cell Biol 17: 4230-4237.

Vonboehmer, H. 1992. Thymic selection: a matter of life and death. Immunol Today 13: 454-456.

Wang, J., K. Guo, K.N. Wils and K. Walsh. 1997. Rb functions to inhibit apoptosis during myocyte differentiation. Cancer Res 57: 351-354.

Wang, J., K. Helin, P. Jin and B. Nadal-Ginard. 1995. Inhibition of in vitro myogenic differentiation by cellular transcription factor E2F1. Cell Growth Diff 6: 1299-1306.

Wang, J. and K. Walsh. 1996. Resistance to apoptosis conferred by Cdk inhibitors during myocyte differentiation. Science 273: 359-361.

Watanabe, G., C. Albanese, R.J. Lee, A. Reutens, G. Vairo, B. Henglein and R.G. Pestell. 1998. Inhibition of cyclin D1 kinase activity is associated with E2F-mediated inhibition of cyclin D1 promoter activity through E2F and Sp1. Mol Cell Biol 18: 3212-3222.

Watanabe, S., S. Ishida, K. Koike and K. Arai. 1995. Characterization of cis-regulatory elements of the c-myc promoter responding to human GM-CSF or mouse interleukin 3 in mouse proB cell line BA/F3 cells expressing the human GM-CSF receptor. Mol Cell Biol 6: 627-636.

Webster, K.A., G.E. Muscat and L. Kedes. 1988. Adenovirus E1a products suppress myogenic differentiation and inhibit transcription from muscle-specific promoters. Nature 332: 553-557.

Weichselbaum, R.R., M. Beckett and A. Diamond. 1988. Some retinoblastomas, osteosarcomas and soft tissue sarcomas may share a common etiology. Proc Natl Acad Sci 85: 2106-2109.

Weinberg, R.A. 1995a. The molecular basis of oncogenes and tumor suppressor genes. Ann N Y Acad Sci 758: 331-338.

Weinberg, R.A. 1995b. The retinoblastoma protein and cell cycle control. Cell 81: 323-330.

Weinstein, D.C., I. Ruiz, A. Altaba, W.S. Chen, P. Hoodless, V.R. Prezioso, T.M. Jessel and J.E.J. Darnell. 1994. The winged-helix transcription factor HNF-3 beta is required for notochord development in the mouse embryo. Cell 78: 575-588.

Weintraub, H. 1993. The Myod family and myogenesis: redundancy, networks and thresholds. cell 75: 1241-1244.

Weintraub, H., R. Davis, S. Tapscott, M. Thayer, M. Krause, R. Benezra, T. K. Blackwell, D. Turner, R. Rupp, S. Hollenberg *et al.* 1991. MyoD functions as a nodal point. Science 251:761-766.

Weintraub, S.J., K.N.B. Chow, R.X. Luo, S.H. Zhang and S.H.D.C. Dean. 1995. Mechanism of active transcriptional repression by the retinoblastoma protein. Nature 375: 812.

Weintraub, S.J., C.A. Prater and D.C. Dean. 1992. Retinoblastoma protein switches the E2F site from positive to negative element. Nature 358: 259.

Welsh, P.J. and J.Y.J. Wang. 1995. Disruption of retinoblastoma protein function by coexpression of its C pocket fragment. Genes Dev 9: 31-46.

White, R.J., D. Trouche, K. Martin, S.P. Jackson and T. Kouzarides. 1996. Repression of RNA polymerase III transcription by the retinoblastoma protein. Nature 382: 88-90.

Whyte, P. 1995. The retinoblastoma product and its relatives. Sem Cancer Biol 6: 83-90.

Whyte, P., K.J. Buchkovich, J.M. Horowitz, S.H. Friend, M. Raybuck, R.A. Weinberg and E. Harlow. 1988a. Association between an oncogene and an anti-oncogene: the adenovirus E1A proteins bind to the retinoblastoma gene product. Nature 334: 124.

Whyte, P., H.E. Ruley and E. Harlow. 1988b. Two regions of the adenovirus early region 1A proteins are required for transformation. J Virol 62: 257-265.

Whyte, P., N.M. Williamson and E. Harlow. 1989. Cellular targets for transformation by the adenovirus E1A proteins. Cell 56: 67-75.

Wiggan, O., A. Taniguchi-Sidle and P.A. Hamel. 1997. Interaction of the pRb-family proteins with factors containing paired-like homeodomains. Oncogene 16: 227-236.

Williams, B.O., E.M. Schmitt, L. Remington, R.T. Bronson, D.M. Albert, R.A. Weinberg and T. Jacks. 1994. Extensive contribution of Rb-deficient cells to adult chimeric mice with limited histopathological consequences. EMBO J 13: 4251-4259.

Wiman, K.G. 1993. The retinoblastoma gene: role in cell cycle control and cell differentiation. FASEB J 7: 841-845.

Windle, J.J., D.M. Albert, J.M. O'brien, D.M. Marcus, C.M. Disteche, R. Bernards and R.L. Mellon. 1990. Retinoblastoma in transgenic mice. Nature 343: 665-669.

Winston, T.J. and W.J. Pledger. 1993. Growth factor regulation of cyclin D1 mRNA expression through protein synthesis-dependent and -independent mechanisms. Mol Biol Cell 4: 1133-1144.

Wolf, D.A., H. Hermeking, T. Albert, T. Herzinger, P. Kind and D. Eick. 1995. A complex between E2F and the pRb-related protein p130 is specifically targeted by the simian virus 40 large T antigen during transformation. Oncogene 10: 2067-2078.

Won, K.-A., Y. Xiong, D. Beach and M.Z. Gilman. 1992. Growth-regulated expression of D-type cyclin genes in human diploid fibroblasts. Proc Natl Acad Sci 89: 9910-9914.

Woo, M.S.-A., I. Sanchez and B.D. Dynlacht. 1997. p130 and p107 use a conserved domain to inhibit cellular cyclin-dependent kinase activity. Mol Cell Biol 17: 3566-3579.

Wu, C.L., L.R. Zukerberg, C. Ngwu, E. Harlow and J.A. Lees. 1995. In vivo association of E2F and DP family proteins. Mol Cell Biol 15: 2536-2546.

Wu, X. and A.J. Levine. 1994. p53 and E2F-1 cooperate to mediate apoptosis. Proc Natl Acad Sci USA 91: 3602-3606.

Yablonka-Reuveni, Z. 1995. Development and postnatal regulation of adult myoblasts. Microsc Res Tech 30: 366-380.

Yamada, T., S.L. Pfaff, T. Edlund and T.M. Jessel. 1993. Control of cell pattern in the neural tube: motor neuron induction by diffusible factors from notchord and floor plate. Cell 73: 673-686.

Yamada, T., M. Placzek, H. Tanaka, J. Dodd and T.M. Jessel. 1991. Control of cell pattern in the developing nervous system: polarizing activity of the floor plate and notochord. Cell 64: 635-647.

Yamasaki, L., T. Jacks, R. Bronson, E. Goillet, E. Harlow and N. Dyson. 1996. Tumor induction and tissue atrophy in mice lacking E2F-1. Cell 85: 537-548.

Yee, S.P. and P.E. Branton. 1985. Detection of cellular proteins associated with human adenovirus type 5 early region 1A polypeptides. Virology 147: 142.

Zabludoff, S.D., M. Csete, R. Wagner, X. Yu and B.J. Wold. 1998. p27Kip1 is expressed transiently in developing myotomes and enhances myogenesis. Cell Growth Differ 9: 1-11.

Zacksenhaus, E., R.M. Gill, R.A. Phillips and B.L. Gallie. 1993. Molecular cloning and characterization of the mouse Rb1 promoter. Oncogene 8: 2343-2351.

Zacksenhaus, E., Z. Jiang, D. Chung, J.D. Marth, R.A. Phillips and B.L. Gallie. 1996. pRb controls proliferation, differentiation and death of skeletal muscle cells and other lineages during embryogenesis. Genes Dev 10: 3051-3064.

Zamanian, M. and N.B.L. Thangue. 1992. Adenovirus E1a prevents the retinoblastoma gene product from repressing the activity of a cellular transcription factor. EMBO J 11: 2603.

Zamanian, M. and N.B.L. Thangue. 1993. Transcriptional repression by the Rb-related protein p107. Mol Cell Biol 4: 389.

Zhang, W., R.R. Behringer and E.N. Olson. 1995. Inactivation of the myogenic bHLH gene MRF4 results in up-regulation of myogenin and rib abnormalities. Genes Dev 9: 1388-1399.

Zhang, Y. and S.P. Chellapan. 1995. Cloning and characterization of human DP2, a novel dimerization partner of E2F. Oncogene 10: 2085.

Zhang, Y., Y. Xiong and W.G. yarbrough. 1998. ARF promotes MDM2 degradation and stabilizes p53: ARF-INK4a locus deletion impairs both the Rb and p53 tumour suppressor pathways. Cell 92: 725-734.

Zhu, L., G. Enders, J.A. Lees, R.L. Beijersbergen, R. Bernards and E. Harlow. 1995a. The pRb-related protein p107 contains two growth suppression domains: independent interactions with E2F and cyclin/cdk complexes. EMBO J 14: 1904-1913.

Zhu, L., E. Harlow and B.D. Dynlatch. 1995b. p107 uses a p21CIP1-related domain to bind cyclin/cdk2 and regulate interactions with E2F. Genes Dev 9: 1740-1752.

Zhu, L., S. van der. Heuvel, K. Helin, A. Fattaey, M. Ewen, D.M. Livingston, N. Dyson and E. Harlow. 1993. Inhibition of cell proliferation by p107, a relative of the retinoblastoma protein. Genes Dev 6: 1111-1125.

Zhu, L., L. Zhu, E. Xie and L.-S. Chang. 1995c. Differential roles of two tandem E2F sites in repression of the human p107 promoter by retinoblastoma and p107 proteins. Mol Cell Biol 15: 3552-3562.

Zou, X., Y. Lin, S. Rudchenko and K. Calame. 1997. Positive and negatibe regulation of c-Myc transcription. Curr Top Microbiol Immunol 224: 57-66.

Zuniga-Pflucker, J.C. and M.J. Lenardo. 1998. Regulation of thymocyte development from immature progenitors. Curr Opin Immunol 8: 215-224.